

# INVESTIGATION OF THE TRANSCRIPTOME OF THE RUMEN FLUKE FISCHOEDERIUS ELONGATUS

 $\mathbf{BY}$ 

#### MISS PICHANEE WATTHANASIRI

# A DISSERTATION SUBMITTED IN PARTIAL FULFILLMENT OF THE REQUIREMENTS FOR THE DEGREE OF THE DOCTOR OF PHILOSOPHY (BIOMEDICAL SCIENCES)

# GRADUATE PROGRAM IN BIOMEDICAL SCIENCES FACULTY OF ALLIED HEALTH SCIENCES THAMMASAT UNIVERSITY ACADEMIC YEAR 2020

**COPYRIGHT OF THAMMASAT UNIVERSITY** 

# INVESTIGATION OF THE TRANSCRIPTOME OF THE RUMEN FLUKE FISCHOEDERIUS ELONGATUS

BY

#### MISS PICHANEE WATTHANASIRI

# A DISSERTATION SUBMITTED IN PARTIAL FULFILLMENT OF THE REQUIREMENTS FOR THE DEGREE OF THE DOCTOR OF PHILOSOPHY (BIOMEDICAL SCIENCES)

# GRADUATE PROGRAM IN BIOMEDICAL SCIENCES FACULTY OF ALLIED HEALTH SCIENCES THAMMASAT UNIVERSITY ACADEMIC YEAR 2020

COPYRIGHT OF THAMMASAT UNIVERSITY

# THAMMASAT UNIVERSITY FACULTY OF ALLIED HEALTH SCIENCES

#### **DISSERTATION**

BY

#### MISS PICHANEE WATTHANASIRI

#### **ENTITLED**

# INVESTIGATION OF THE TRANSCRIPTOME OF THE RUMEN FLUKE $FISCHOEDERIUS\ ELONGATUS$

was approved as partial fulfillment of the requirements for the degree of the Doctor Philosophy (Biomedical Sciences)

on July 22, 2020

Chairman

(Associate Professor Poom Adisakwattana, Ph.D.)

Member and Advisor

(Associate Professor Hans Rudi Grams, Dr. rer. nat.)

Member and Co-advisor

(Professor Peter Smooker, Ph.D.)

Member

(Assistant Professor Chollanot Kaset, Ph.D.)

Member

(Pongsakorn Martviset, Ph.D.)

Dean

(Associate Professor Plaiwan Suttanon, Ph.D.)

Dissertation Title INVESTIGATION OF THE TRANSCRIPTOME

OF THE RUMEN FLUKE

FISCHOEDERIUS ELONGATUS

Author Miss Pichanee Watthanasiri

Degree Doctor of Philosophy in Biomedical Sciences

Department/Faculty/University Graduate Program in Biomedical Sciences

Faculty of Allied Health Sciences

Thammasat University

Dissertation Advisor Associate Professor Hans Rudi Grams, Dr. rer. nat.

Dissertation Co-Advisor Professor Peter Smooker, Ph.D.

Dissertation Co-Advisor Associate Professor Suksiri Vichasri Grams,

Dr. rer. nat.

Dissertation Co-Advisor Associate Professor Ratchaneewan Aunpad, Ph.D.

Dissertation Co-Advisor Assistant Professor Amornrat Geadkaew-Krenc,

Ph.D.

Academic Years 2020

#### ABSTRACT

Fischoederius elongatus, a pouched amphistomes in the family Gastrothylacidae, is a neglected food-borne parasite that infects a large number of cattle in Thailand. The fluke causes economic losses by massive infection in the rumen of ruminants. This causes obstruction of food absorption and results in decreased milk and meat production. Also, acute infection with the fluke causes severe mucosal damage and significantly increases mortality in young animals. Importantly, Fischoederius elongatus was reported as a case of zoonosis trematode in a woman who had severe vomiting in Guangdong, China (1991). At present, routine diagnosis of the fluke infection is based on microscopic examination by using fecal egg count and morphological egg identification. It is difficult to distinguish Fischoederius elongatus from other amphistomes by egg morphology. In addition, the rumen fluke eggs are similar to eggs of the liver fluke Fasciola spp. Misdiagnosis may lead to incorrect drug treatment and development of resistance. The aim of the present study was to

characterize *Fischoederius elongatus* in Thailand by observing the fluke morphology, and by analysis of molecular biology, taxonomy, physiology and pathology using mitochondrial genome characterization and transcriptomics. The morphology of Fischoederius specimens collected in this study was found following the classic literature description of Fischoederius elongatus by Sey (1991). Fischoederius specimens collected in this study during the years 2014–2019 had either large or small testes. Specimens with large testes were mature and contained often intrauterine eggs. Specimens with small testes were immature and also had an undeveloped ovary and only a small number of vitellaria. The developmental stage was confirmed by transcriptome data which lacked for example vitelline protein encoding transcripts. Moreover, molecular studies of Fischoederius will provide basic knowledge usable for diagnosis. A PCR-amplified fragment of ribosomal ITS2 originating from one of the collected specimens showed significant identity (99%, E-value: 0.0) to closely related trematodes in the database; however, this region has high sequence conservation making it not suitable for species identification. For this reason, mtCOX1, a universal marker for species identification, was investigated. PCR products of mtCOX1 from 48 single flukes were used for restriction analysis with *MseI*. Surprisingly, nine restriction pattern (A-I) were observed and sequence analysis of mtCOX1 pattern A-I showed 0.7–9.3% sequence difference. Together with a phylogenetic analysis these findings suggested that the collected specimens represented five distinct species A, [BEG], [CFH], D, and I. Hence, Fischoederius elongatus might represent a cryptic species, a complex of morphologically indistinguishable species. Furthermore, the mitochondrial genome of Fischoederius mtCOX1 MseI pattern A was characterized. The complete genome with 14,780 bp in length contains twelve protein-coding genes (cox3 > cytb >nad4L > nad4 > atp6 > nad2 > nad1 > nad3 > cox1 > cox2 > nad6 > nad5), 23 tRNA genes, two rRNA genes (rrnS and rrnL), and two non-coding regions (SNR and LNR). All genes are transcribed in the same direction. Interestingly, inverted repeats causing hairpin-like structures were detected in the mitochondrial genomes of Fischoederius mtCOX1 MseI pattern A, [BE], C, D, and I that might have originated from transposable elements and possibly affect DNA recombination, replication and transcription. Moreover, the obtained transcriptome data of Fischoederious mtCOX1 MseI pattern A, C, and E showed similar expression profiles. Highly abundant genes

with complete sequence and known function included cathepsin-like cysteine protease (B, C, L), fatty acid-binding protein, thioredoxin, and tegumental calcium-binding protein. Polyclonal mouse *Fischoederius* anti-ES antibody detected a predominant 35 kDa antigen in an immunoblot of *Fischoederius* antigens. This antigen might be *Fischoederius* cathepsin B by its molecular weight in accordance with the high abundance of cathepsin B transcripts in the transcriptome data. Cysteine proteases play important roles in parasite feeding, host tissue invasion, and immune evasion. These proteins should be further investigated for application in diagnosis and vaccine innovation.

**Keywords:** *Fischoederius elongatus*, amphistomes, cryptic species, gross morphology, mitochondrial genome, restriction analysis, transcriptome, ribosomal ITS2, cytochrome c oxidase subunit I, cathepsin B

#### **ACKNOWLEDGEMENTS**

This dissertation could not have been successfully achieved without the strong support and collaborative efforts of several people and institutes. First of all, I would like to express my deep gratitude to my major advisor, Assoc. Prof. Dr. Hans Rudi Grams, who always provided effective advice and practical suggestions to solve problems through my Ph.D. study. He inspired and motivated me with an impressive guideline and made my research challenging. Without his support, my dissertation would be impossible.

Following with all of my co-advisors, I would like to express my deep appreciation and gratefulness to Assoc. Prof. Dr. Suksiri Vichasri-Grams who encouraged and contributed valuable guidances, suggestions and comments. I am very thankful to Assoc. Prof. Dr. Ratchaneewan Aunpad for her qualified support and contribution. Likewise, I would like to offer my thankfulness to Asst. Prof. Dr. Amornrat Geadkaew-Krenc for her observant support and suggestion in my laboratory work.

I am very grateful to Prof. Peter Smooker who provided the memorable opportunity to conduct research in his laboratory at the School of Science, RMIT University, VIC, Australia for his kind encouragement, strong help and support during my visit. Also, I am very thankful to Dr. Bronwyn Campbell, Dr. Thi Thu Hao Van, Dr. Andrew Guy, Dr. Thomas McLean, and Dr. Luke Norbury for practical and useful suggestions in high-throughput sequencing, bioinformatics applications, and laboratory instruction. Equally, many thanks to all students and staff members who gave me a sincerely friendship, especially Ms. Debolina Majumdar, Mrs. Marta Bustos, and Mrs. Syeda Umme Habiba Wahid.

My deep appreciation to Ms. Phatcharaporn Chiawwit and her friend, Ms. Nitchanun Sinsongsaeng from the Faculty of Veterinary Technology, Kasetsart University, who provided experienced advice and skillful knowledge in the rumen fluke morphology. I am very grateful to Mr. Rangsan Praevanich, Faculty of Tropical Medicine, Mahidol University for his expert help in whole mount staining techniques. I would like to give my deep thankfulness to Asst. Prof. Dr. Potjanee Srimanote, Molecular Immunology and Microbiology Unit, Graduate Program in Biomedical

Sciences, Faculty of Allied Health Sciences, Thammasat University for her attentive and valuable suggestions and kindly providing opportunity to use her laboratory facilities to complete my research work. Equally, I am sincerely grateful to Mr. Sompoat Prachan, Mrs. Mudtika Fungkrajai, and Mrs. Benja Norapong, the scientists from the Department of Medical Technology, Faculty of Allied Health Sciences, Thammasat University, for their kind help and support of my laboratory work at the department.

I would like to express my deeply gratitude to Assoc. Prof. Dr. Patcharee Isarankura-Na-Ayudhya, Asst. Prof. Pussadee Tobunluepop, and Asst. Prof. Dr. Anek Pootong, my undergraduate advisors and lecturer from Department of Medical Technology, Faculty of Allied Health Sciences, Thammasat University, who kindly introduced and suggested me to initiate my Ph.D. study. I am also thankful to all instructors and staff members of the Graduate Program in Biomedical Sciences, Faculty of Allied Health Sciences, Thammasat University for their active support during this dissertation. Especially, I would like to express my thanks to both past and present members of the Molecular Biology and Parasitology Unit, Dr. Wansika Phadungsil, Dr. Pongsakorn Martviset, Dr. Wanlapa Chaibangyang, Dr. Sinee Siricoon, Dr. Thwet Oo Lwin, Mr. Nanthawat Kosa, Ms. Kornkanok Nakudom, and Ms. Rosnanee Salang, who often provided kind help during the specimen collections and laboratory operation all day and all night at Thammasat University.

I would like to express thankfulness to my dissertation defense committee, my advisor, my co-advisor, Asst. Prof. Dr. Chollanot Kaset, from Department of Medical Technology, Faculty of Allied Health Sciences, Thammasat University, and Assoc. Prof. Dr. Poom Adisakwattana from Faculty of Tropical Medicine, Mahidol University for their acceptance to be my dissertation defense committee and kindness to approve my dissertation.

My dissertation would have not been achievable without the financial support from Thailand Science Research and Innovation (TSRI) through a Royal Golden Jubilee scholar (RGJ) under the supervision of Assoc. Prof. Dr. Hans Rudi Grams (PHD/0061/2556).

My special thanks to my beloved family, my parents and my both young brothers, and my friends, especially Dr. Wasine Churklam, Dr. Siriporn Kaewklom, Ms. Hatairat Sahachokpaiboon, Ms. Jinjuta Pinthong, Ms. Punnika Mongkolthong,

Mr. Kitipong Chuanboon, and Mr. Sataban Srisuriyatada who are always by my side. My dissertation would not be accomplished without all of the acknowledged persons and institutes. I am grateful to everyone for their kind support. Thank you.

Miss Pichanee Watthanasiri



### TABLE OF CONTENTS

	Page
ABSTRACT	(1)
ACKNOWLEDGEMENTS	(4)
LIST OF TABLES	(16)
LIST OF FIGURES	(18)
LIST OF ABBREVIATIONS	(26)
CHAPTER 1 INTRODUCTION	1
CHAPTER 2 OBJECTIVES	3
CHAPTER 3 REVIEW OF LITERATURE	4
3.1 The rumen fluke <i>Fischoederius elongatus</i>	4
	4
3.1.1 Taxonomic classification of <i>Fischoederius elongatus</i>	6
<ul><li>3.1.2 Morphology of <i>Fischoederius elongatus</i></li><li>3.1.2.1 Adult stage</li></ul>	6
3.1.2.1 Adult stage 3.1.2.2 Egg stage	14
3.1.2.2 Lgg stage 3.1.2.3 Miracidia stage	15
3.1.2.4 Redia stage	15
3.1.2.5 Cercaria stage	15
3.1.2.6 Metacercaria stage	16
3.1.3 Life cycle of the rumen fluke	16
3.1.4 Geographic distribution of <i>Fischoederius elongatus</i>	17
3.1.5 Pathogenesis of paramphistomiasis	19

	Pa	age
	3.1.6 Diagnosis of the rumen fluke	21
	3.1.6.1 Microscopic examination	21
	3.1.6.2 Molecular Diagnostics	21
	(1) High annealing temperature-random amplification of	21
	polymorphic DNA (HAT-RAPD) method	
	(2) Ribosomal internal transcribed spacer (ITS2) sequence	22
	(3) Mitochondrial cytochrome c subunit I (mtCOX1)	23
	sequence	
	3.1.6.3 Immunodiagnostics	24
	3.1.7 Control and treatment of the rumen fluke	24
3.2	Mitochondrial genome sequence of Fischoederius elongatus	26
	3.2.1 Complete mitochondrial genome sequence from Tianmen, China	26
	3.2.2 Complete mitochondrial genome sequence from Shanghai, China	28
3.3	Transcriptome study of trematode	30
	3.3.1 Definition of transcriptome	30
	3.3.2 Transcriptome Techniques	30
	3.3.2.1 Real-time quantitative polymerase chain reaction	30
	(1) Double-stranded DNA-binding dyes	30
	(2) Hybridization probes	31
	3.3.2.2 RNA-Seq	32
	(1) Illumina® next-generation sequencing (NGS) platform	32
	(2) Transcriptome Assembly	34
	3.3.3 Transcriptomes of trematodes	36
	3.3.3.1 Schistosoma mansoni	36
	3.3.3.2 Fasciola hepatica	37
	3.3.3.3 Fasciola gigantica	37
	3.3.3.4 Opisthorchis viverrini	38
	3.3.3.5 Clonorchis sinensis	39

	Page
3.3.3.6 Paramphistomum cervi	39
3.3.3.7 Calicophoron daubneyi	40
3.3.3.8 Fasciolopsis buski	41
3.4 Parasite excretion/secretion (ES) product	42
3.4.1 Definition of parasite excretion/secretion product	42
3.4.2 Parasite protease	42
3.4.3 Excretion/secretion product of Fischoederius elongatus	43
CHAPTER 4 RESEARCH METHODOLOGY	44
4.1 Morphology of Fischoederius elongatus	44
4.1.1 Collection of Fischoederius elongatus	44
4.1.2 Microscopic examination of whole fluke image	44
4.1.3 Semichon's carmine whole mount staining	44
4.1.4 Hematoxylin and eosin staining of parasite tissue section	44
4.1.4.1 Tissue embedding and tissue section	44
4.1.4.2 Hematoxylin and eosin staining	45
4.1.4.3 Image capture of tissue sections	45
4.2 Molecular identification of Fischoederius elongatus ribosomal ITS2	2 45
4.2.1 Isolation of Fischoederius elongatus total RNA extraction	45
4.2.2 DNase treatment of total RNA Fischoederius elongatus	46
4.2.3 Reverse Transcriptase Polymerase Chain Reaction (RT-PCR)	47
4.2.4 Agarose gel electrophoresis	48
4.2.5 DNA Extraction from agarose gels using Thermo Scientific	49
GeneJET Gel Extraction Kit	
4.2.6 Plasmid purification using Thermo Scientific GeneJET Plasmid	49
Miniprep Kit	
4.2.7 Ligation of PCR amplicon into the pGEM®-T Easy vector	50

		Page
	4.2.8 Preparation of competent E. coli XL1-Blue cells	51
	4.2.9 Chemical transformation of competent <i>E. coli</i> XL1-Blue with	51
	the recombinant pGEM®-T Easy vector	
	4.2.10 Screening for positive transformants by colony PCR	52
	4.2.11 Restriction analysis of recombinant pGEM®-T Easy vector	52
	4.2.12 DNA sequence analysis	53
	4.2.13 Long time storage of transformants bacteria	53
4.3	Molecular characterization of Fischoederius elongatus	54
	mitochondrial genome	
	4.3.1 Isolation of Fischoederius elongatus mitochondrial extracts	54
	4.3.2 Fischoederius elongatus mitochondrial DNA extraction	54
	4.3.3 Fischoederius elongatus genomic DNA extraction	54
	4.3.4 Amplification of mitochondrial DNA fragments	55
	4.3.5 Amplification of mitochondrial DNA NAD1 and NAD2	57
	4.3.6 Fischoederius elongatus mitochondrial genome sequence	58
	analysis	
	4.3.6.1 Fischoederius elongatus mitochondrial genome sequence	59
	assembly	
	4.3.6.2 Fischoederius elongatus mitochondrial genome sequence	59
	annotation	
	4.3.6.3 Multiple alignment of Fischoederius elongatus	60
	mitochondrial genome	
	4.3.6.4 Phylogenetic analysis of Fischoederius elongatus	60
	mitochondrial genome	
	4.3.7 Polymerase chain reaction-restriction fragment length	60
	polymorphism (PCR-RFLP) of Fischoederius spp. mtCOX1	

			Page
4.4	Transcri	iptome sequencing of adult stage Fischoederius elongatus	61
	4.4.1 Tota	al RNA extraction and purification for high-throughput	61
	sequ	uencing	
	4.4.2 Qua	dification and quantification measurement of total RNA	62
	4.4.3 Etha	anol precipitation of total RNA for shipment	62
	4.4.4 Tota	al RNA preparation for shipment at ambient temperature	62
	4.4.5 Illu	mina® Next generation sequencing	62
	4.4.5.1	cDNA library preparation for Illumina® Next generation	62
		sequencing	
	4.4.5.2	High-throughput sequencing	63
	4.4.5.3	Quantification measurement of high-throughput sequencing	63
	4.4.6 Bio	informatics analysis of adult Fischoederius elongatus	64
	tran	scriptome data	
	4.4.6.1	Sequence assembly and annotation	64
	4.4.6.2	Contaminating sequences	64
	4.4.6.3	Duplicated sequences	64
	4.4.6.4	Complete sequences analysis	64
	4.4.6.5	Prediction of protein function using InterProScan	65
	4.4.6.6	Gene ontology	65
4.5	Antigen	icity of Fischoederius elongatus	65
	4.5.1 Prep	paration of parasite antigen	65
	4.5.1.1	Crude worm extract of adult Fischoederius elongatus	65
	4.5.1.2	Excretion/secretion extract of adult Fischoederius	65
		elongatus	
	4.5.1.3	Measurement of protein concentration by Bradford assay	66
	4.5.1.4	Preparation of parasite antigens electrophoresis	66
	4.5.1.5	Analysis of parasite proteins by sodium dodecyl sulphate	66
		polyacrylamide gel electrophoresis (SDS-PAGE)	

	Page
4.5.1.6 Detection of parasite antigens in the polyacrylamide gel	67
using Coomassie Blue G-250 Staining	
4.5.2 Production of polyclonal mouse antibody	67
4.5.2.1 Antibody production in mice	67
4.5.2.2 Determination of antibody titer by indirect enzyme-linked	68
immunosorbent assay (ELISA)	
4.5.2.3 Determination of serum circulating antigen using Western	69
blot analysis	
CHAPTER 5 RESULTS	70
5.1 Morphology of Fischoederius spp.	70
5.1.1 Collection of Fischoederius specimens	70
5.1.2 Semichon's carmine whole mount staining	71
5.1.3 Histological examination of Fischoederius spp.	73
5.2 Molecular identification of <i>Fischoederius</i> spp. ribosomal ITS2 region	n 82
5.3 Restriction analysis of Fischoederius spp. mtCOX1	85
5.3.1 Fischoederius spp. mtCOX1	85
5.3.2 MseI restriction endonuclease analysis of Fischoederius spp.	85
mtCOX1	
5.3.3 Images of Fischoederius spp.	89
5.3.4 Genetic variation of Fischoederius spp. mtCOX1	92
5.4 Mitochondrial genome of Fischoederius spp.	95
5.4.1 General features of Fischoederius spp. mitochondrial genome	95
MseI pattern A	
5.4.1.1 Protein-coding genes of Fischoederius spp. mitochondrial	99
genome MseI pattern A	

				Page
	5.4	.1.2	Transfer RNA genes, ribosomal RNA genes and	127
		1	non-coding regions of Fischoederius spp. mitochondrial	
			genome <i>Mse</i> I pattern A	
	5.4.2	Gene	tic variation of 12 protein-coding genes of Fischoederius	130
	;	spp. r	mitochondrial genome MseI pattern A	
	5.4.3	Gene	tic relationship of Fischoederius mitochondrial genome	131
		MseI	pattern A to other trematodes	
	5.4.4	Secor	ndary structure in nad2-1-3-cox1 region of Fischoederius	134
		spp. r	mitochondrial genome MseI pattern A, B, C, D and I	
	5.4.5	Inves	tigation of trematode genetic relationship based on	141
		mitoc	chondrial nad1, nad2, nad3 sequences	
.5	Tran	scrip	tome analysis of Fischoederius spp.	145
	5.5.1	Fisch	oederius total RNA	145
	5.5.2	Chara	acterization of Fischoederius spp. transcriptome	146
	5.5.3	Anno	tation of Fischoederius spp. transcriptome	147
	5.5.4	Deve	lopment stage verification of Fischoederius spp.	150
	5.5.5	Gene	ontology of Fischoederius spp. transcriptome	152
	5.5.6	Trans	script abundance in the Fischoederius MseI A, C, and E	156
	1	transc	criptome	
	5.5.7	Highl	y abundant transcripts with complete coding sequence and	160
		poten	tial for application in the transcriptome data of	
	-	Fisch	oederius MseI A	
	5.5	.7.1 <b>(</b>	Cathepsin B-like cysteine proteinase	160
	5.5	.7.2	Cathepsin L-like cysteine proteinase	168
	5.5	.7.3	Cathepsin C-like cysteine proteinase	171
	5.5	.7.4 1	Fatty acid-binding protein	175
	5.5	.7.5	Thioredoxin	175
	5.5	.7.6	Calcium-binding protein	175

			Page
	5.6	Efficacy of polyclonal mouse Fischoederius spp. anti-ES antibody	180
		5.6.1 Fischoederius spp. excretion/secretion (ES) products	180
		5.6.2 Fischoederius spp. crude worm (CW) extracts	180
		5.6.3 Production of polyclonal mouse <i>Fischoederius</i> spp. anti-ES	180
		antibody	
		5.6.4 Western blot analysis of polyclonal mouse <i>Fischoederius</i> spp.	182
		anti-ES antibody against ES product	
		5.6.5 Cross reactivity of polyclonal mouse Fischoederius spp.	184
		anti-ES antibody against crude worm extracts of other	
		trematodes	
СНАР	TER	2 6 DISCUSSION	186
	6.1	Morphology and histology of Fischoederius spp.	186
	6.2	Molecular identification of Fischoederius spp. ribosomal ITS2	188
		region	
	6.3	Molecular characterization of Fischoederius spp. mtCOX1	189
	6.4	Mitochondrial genome of Fischoederius spp.	190
	6.5	Inverted repeat elements in Fischoederius spp. mitochondrial	192
		genome	
	6.6	Fischoederius spp. transcriptome	193
	6.7	Polyclonal mouse Fischoederius spp. anti-ES antibody	196
	6.8	Further research and application	197
СНАР	TER	7 CONCLUSIONS	199
REFE	REN	CES	203
	1	VLAI	∠(J.)

	Page
APPENDICES	220
APPENDIX A REAGENT PREPARATIONS	221
APPENDIX B DNA AND PROTEIN STANDARD	233
APPENDIX C VECTOR MAP	238
APPENDIX D ANIMAL ETHICAL PERMISSION	240
BIOGRAPHY	241

### LIST OF TABLES

Tables		Page
3.1	Synonymy of members in the genera Fischoederius and	6
	Velasquezotrema	
3.2	Key of the species of Fischoederius	7
3.3	Comparison of histological structure type of amphistome	10
5.1	Top 5 hits BLASTN result of 460 bp Fischoederius spp. ribosomal	82
	ITS2 search against nucleotide collection (nr/nt) database of limited	
	to Platyhelminthes (taxid:6157)	
5.2	Sequence identity values of mtCOX1 region between	93
	Fischoederius spp. in this study (A-I) and other trematodes	
5.3	Features of the mitochondrial genome of Fischoederius MseI A	98
5.4	Nucleotide contents of each protein coding gene within the	99
	mitochondrial genome of Fischoederius MseI pattern A	
5.5	Codon usage of 12 protein-coding genes of mitochondrial genome of	100
	Fischoederius MseI Pattern A	
5.6	Comparsion of sequence identity value between Fischoederius MseI	130
	pattern A and F. elongatus isolated from Tianmen, China,	
	F. elongatus isolated from Shanghai, China, F. cobboldi,	
	and G. crumenifer	
5.7	Length of PCR amplicons by using the indicated primer sets for the	134
	nad2-1-3-cox1 region of Fischoederius mitochondrial genome MseI	
	pattern A, B, C, D, and I	
5.8	Intraspecies and interspecies variation of NAD1, NAD2, NAD3	142
	proteins of F. elongatus, F. cobboldi, and G. crumenifer	
5.9	Summary of de novo transcriptome assembly for Fischoederius MseI	147
	pattern A, C, and E	
5.10	TBLASTN results of four proteins active in the reproductive system	151
	against transcriptome data of Fischoederius MseI pattern A, C, and E	

# LIST OF TABLES (Cont.)

Tables		Page
5.11	Sequence identity values of Fischoederius MseI A cathepsin B-like	164
	cysteine proteinase (TBIU011911) with other trematode cathepsin B	
	sequences	
5.12	Sequence identity values of Fischoederius MseI A cathepsin B-like	167
	cysteine proteinase (Comp1676_seq3) with other trematode	
	cathepsin B sequences	
5.13	Sequence identity values of Fischoederius MseI A cathepsin L-like	168
	cysteine proteinase (Comp422_seq1) with other trematode	
	cathepsin L sequences	
5.14	Sequence identity values of Fischoederius MseI A cathepsin C-like	171
	cysteine proteinase (TBIU021593) with other trematode	
	cathepsin C sequences	
5.15	Sequence identity values of Fischoederius MseI A fatty acid-binding	177
	protein (TBIU012177) with other fatty acid-binding protein sequences	
5.16	Sequence identity values of Fischoederius MseI A thioredoxin	178
	(Comp175_seq0) with other thioredoxin sequences	
5.17	Sequence identity values of Fischoederius MseI A tegumental	179
	calcium-binding protein (TBIU007768) with other calcium-binding	
	protein sequences	

#### LIST OF FIGURES

Figures		Page
3.1	Taxonomy classification of Fischoederius elongatus	5
3.2	Classification of Fischoederius elongatus and other amphistomes	5
3.3	Schematic drawing of Fischoederius elongatus	8
3.4	Dome to conical, non-ciliated papillae	8
3.5	Median sagittal section of adult Fischoederius elongatus	9
3.6	Carmine staining of adult stage amphistomes in Thailand	11
3.7	Morphology drawing of adult stage amphistome	12
3.8	Median sagittal section of Pharynx	13
3.9	Median sagittal section of Acetabulum	13
3.10	Median sagittal section of Terminal genitalium	14
3.11	Egg stage of Fischoederius elongatus	14
3.12	Cercaria indicae XXIX (Sewell, 1922) of Fischoederius elongatus	16
3.13	Generalized life cycle of the rumen fluke	17
3.14	Global distribution intestinal flukes studied by Chai et al., 2020	18
3.15	Global distribution of amphistomes studied by Sey (1991)	18
3.16	Geographic distribution of the rumen fluke and liver fluke	19
	in Suphanburi Province	
3.17	Pathogenesis of paramphistomiasis in sheep	20
3.18	Egg stage under microscopic examination	21
3.19	Arrangement of the mitochondrial genome of Fischoederius elongatus	27
	from Tianmen, China (GenBank: KM_397348)	
3.20	Arrangement of the mitochondrial genome of Fischoederius elongatus	29
	from Shanghai, China (GenBank: MN537973)	
3.21	TaqMan® hybridization probe method	31
3.22	Illumina® sequencing	33
3.23	Trinity assembling overview	35
3.24	Silver-stained polyacrylamide gel of resolved Fischoederius elongatus	43
	ES product	

Figures		Page
4.1	nad2-1-3-cox1 primer diagram	58
4.2	Timeline diagram of Fischoederius spp. anti-ES antisera production	68
	in BALB/c mice.	
5.1	Fischoederius spp. in the rumen of an infected cattle at a local	70
	slaughter house in 2019	
5.2	Fischoederius spp. maintained in PBS in a culture plate	71
	(collected in 2016)	
5.3	Semichon's carmine staining of Fischoederius spp., large testes	72
	flukes (collected in 2015 and 2019) and small testes flukes	
	(collected in 2016)	
5.4	Hematoxylin and eosin staining of Fischoederius spp. small testes	75
	cross-sections collected in 2016	
5.5	Hematoxylin and eosin staining of Fischoederius spp. large testes	76
	cross-sections collected in 2015–2016	
5.6	Hematoxylin and eosin staining of Fischoederius spp. cross-sections	80
	collected in the years 2014–2019	
5.7	Agarose gel electrophoresis of Fischoederius spp. ribosomal ITS2	83
5.8	Nucleotide sequences of the isolated Fischoederius spp. ribosomal	84
	ITS2 cDNA (515 bp) using SHOWSEQ in EMBOSS	
5.9	Agarose gel showing the Fischoederius spp. 1,536 bp mtCOX1 PCR	85
	products obtained from gDNA of four specimens	
5.10	Virtual MseI restriction map of mtCOX1 sequence Fischoederius	87
	MseI pattern A-I created in NEBcutter version 2.0	
5.11	Restriction analysis of Fischoederius spp. mtCOX1 with MseI	88
5.12	Micrographs of Fischoederius MseI pattern A, D, I	89
5.13	Micrographs of Fischoederius MseI pattern B, E, G	90
5.14	Micrographs of <i>Fischoederius Mse</i> I pattern C, F, H	91

Figures		Page
5.15	Phylogenetic analysis of Fischoederius spp. mtCOX1 pattern A–I	94
	and other trematodes	
5.16	Agarose gel electrophoresis of Fischoederius MseI pattern A	96
	mitochondrial genome fragments amplified by PCR	
5.17	Diagrams of the mitochondrial genome of Fischoederius MseI	97
	pattern A using Organellar Genome DRAW (OGDRAW)	
5.18	Nucleotide and deduced amino acid sequences of the isolated	101
	Fischoederius spp. cytochrome c oxidase subunit III (645 bp)	
	using SHOWSEQ in EMBOSS	
5.19	Multiple alignment of cytochrome c oxidase subunit III	102
5.20	Nucleotide and deduced amino acid sequences of the isolated	103
	Fischoederius spp. cytochrome b (1,100 bp) using SHOWSEQ	
	in EMBOSS	
5.21	Multiple alignment of cytochrome b	105
5.22	Nucleotide and deduced amino acid sequences of the isolated	106
	Fischoederius spp. NADH dehydrogenase subunit 4L (264 bp)	
	using SHOWSEQ in EMBOSS.	
5.23	Multiple alignment of NADH dehydrogenase subunit 4L	106
5.24	Nucleotide and deduced amino acid sequences of the isolated	107
	Fischoederius spp. NADH dehydrogenase subunit 4 (1,281 bp)	
	using SHOWSEQ in EMBOSS	
5.25	Multiple alignment of NADH dehydrogenase subunit 4	109
5.26	Nucleotide and deduced amino acid sequences of the isolated	110
	Fischoederius spp. ATP synthase subunit 6 (516 bp) using	
	SHOWSEQ in EMBOSS	
5.27	Multiple alignment of ATP synthase subunit 6	111

Figures		Page
5.28	Nucleotide and deduced amino acid sequences of the isolated	112
	Fischoederius spp. NADH dehydrogenase subunit 2 (876 bp)	
	using SHOWSEQ in EMBOSS	
5.29	Multiple alignment of NADH dehydrogenase subunit 2	113
5.30	Nucleotide and deduced amino acid sequences of the isolated	114
	Fischoederius spp. NADH dehydrogenase subunit 1 (897 bp)	
	using SHOWSEQ in EMBOSS	
5.31	Multiple alignment of NADH dehydrogenase subunit 1	115
5.32	Nucleotide and deduced amino acid sequences of the isolated	116
	Fischoederius spp. NADH dehydrogenase subunit 3 (357 bp)	
	using SHOWSEQ in EMBOSS	
5.33	Multiple alignment of NADH dehydrogenase subunit 3	116
5.34	Nucleotide and deduced amino acid sequences of the isolated	117
	Fischoederius spp. cytochrome c oxidase subunit I (1,542 bp)	
	using SHOWSEQ in EMBOSS	
5.35	Multiple alignment of cytochrome c oxidase subunit I	119
5.36	Nucleotide and deduced amino acid sequences of the isolated	120
	Fischoederius spp. cytochrome c oxidase subunit II (582 bp)	
	using SHOWSEQ in EMBOSS	
5.37	Multiple alignment of cytochrome c oxidase subunit II	121
5.38	Nucleotide and deduced amino acid sequences of the isolated	122
	Fischoederius spp. NADH dehydrogenase subunit 6 (452 bp)	
	using SHOWSEQ in EMBOSS	
5.39	Multiple alignment of NADH dehydrogenase subunit 6	123
5.40	Nucleotide and deduced amino acid sequences of the isolated	124
	Fischoederius spp. NADH dehydrogenase subunit 5 (1,581 bp)	
	using SHOWSEQ in EMBOSS	
5 41	Multiple alignment of NADH dehydrogenase subunit 5	126

Figures		Page
5.42	Prediction of mitochondrial tRNA of Fischoederius MseI	128
	pattern A	
5.43	Mitochondrial diagrams of Fischoederius mitochondrial genome	132
	MseI pattern A and other trematodes using OGDRAW	
5.44	Phylogenetic analysis of concatenated amino acid sequences of	133
	twelve protein-coding genes of Fischoederius mitochondrial	
	genome MseI pattern A with other trematodes	
5.45	Images of 0.7% [w/v] agarose gels of resolved PCR products of	135
	nad2-1-3-cox1 region in Fischoederius mitochondrial genome	
5.46	Example of substandard sequencing quality in the nad2/nad1	137
	problem area that had the secondary structure formation	
5.47	Image of 0.7% [w/v] agarose gel showing the re-amplification	138
	products of the nad2-nad1 fragment with primers HRG-625/623	
5.48	Diagrams of the nad2-1-3-cox1 region of Fischoederius MseI	139
	pattern A, B, C, D and I	
5.49	Inverted repeat sequences in the nad2-1-3-cox1 region of the	140
	mitochondrial genomes of Fischoederius MseI pattern A, B, C,	
	D and I detected by using EMBOSS einverted	
5.50	Phylogenetic analysis of NAD1, NAD2, NAD3 deduced amino	143
	acid sequences of Fischoederius MseI pattern A, B, C, D, I and	
	other trematodes	
5.51	Total RNA isolated from Fischoederius spp.	145
5.52	Electropherograms of Fischoederius spp. total RNA	146
5.53	Distribution of the contigs by length for Fischoederius MseI	147
	pattern A	
5.54	Distribution of database hits obtained by BLASTX with	148
	Fischoederius MseI pattern A transcriptome data (6 Gb)	

Figures		Page
5.55	BLASTX first hit species distribution in searches with	149
	Fischoederius MseI pattern A, C, and E transcriptome data	
5.56	Top 20 of gene ontology of Fischoederius MseI pattern A	153
	transcriptome in each major category	
5.57	Top 20 of gene ontology of Fischoederius MseI pattern C	154
	transcriptome in each major category	
5.58	Top 20 of gene ontology of Fischoederius MseI pattern E	155
	transcriptome in each major category	
5.59	Top 50 abundant known transcripts of Fischoederius MseI A	157
	transcriptome	
5.60	Top 50 abundant known transcripts of Fischoederius MseI C	158
	transcriptome	
5.61	Top 50 abundant known transcripts of Fischoederius MseI E	159
	transcriptome	
5.62	Nucleotide and deduced amino acid sequences of Fischoederius	162
	MseI A cathepsin B-like cysteine proteinase (TBIU011911) using	
	SHOWSEQ in EMBOSS	
5.63	Signal peptide prediction of Fischoederius MseI A cathepsin B-like	163
	cysteine proteinase (TBIU011911) using SignalP	
5.64	Transmembrane region prediction of Fischoederius MseI A	163
	cathepsin B-like cysteine proteinase (TBIU011911) using TMHMM	
5.65	Nucleotide and deduced amino acid sequences of Fischoederius	165
	MseI A cathepsin B-like cysteine proteinase (Comp1676_seq3)	
	using SHOWSEQ in EMBOSS	
5.66	Signal peptide prediction of Fischoederius MseI A cathepsin B-like	166
	cysteine proteinase (Comp1676 seq3) using SignalP	

Figures		Page
5.67	Transmembrane region prediction of Fischoederius MseI A	166
	cathepsin B-like cysteine proteinase (Comp1676_seq3)	
	using TMHMM	
5.68	Nucleotide and deduced amino acid sequences of Fischoederius	169
	MseI A cathepsin L-like cysteine proteinase (Comp422_seq1)	
	using SHOWSEQ in EMBOSS	
5.69	Signal peptide prediction of Fischoederius MseI A cathepsin	170
	L-like cysteine proteinase (Comp422_seq1) using SignalP	
5.70	Transmembrane region prediction of Fischoederius MseI A	170
	cathepsin L-like cysteine proteinase (Comp422_seq1) using	
	ТМНММ	
5.71	Nucleotide and deduced amino acid sequences of Fischoederius	172
	MseI A cathepsin C-like cysteine proteinase (TBIU021593)	
	using SHOWSEQ in EMBOSS	
5.72	Nucleotide and deduced amino acid sequences of Fischoederius	174
	MseI A cathepsin C-like cysteine proteinase (TBIU021593)	
	using SHOWSEQ in EMBOSS	
5.73	Transmembrane region prediction of Fischoederius MseI A	174
	cathepsin C-like cysteine proteinase (TBIU021593) using	
	ТМНММ	
5.74	Nucleotide and deduced amino acid sequences of Fischoederius	177
	MseI A thioredoxin (Comp175_seq0) using SHOWSEQ in	
	EMBOSS	
5.75	Nucleotide and deduced amino acid sequences of Fischoederius	178
	MseI A thioredoxin (Comp175_seq0) using SHOWSEQ in	
	EMBOSS	

Figures		Page
5.76	Nucleotide and deduced amino acid sequences of Fischoederius	179
	MseI A tegumental calcium-binding protein (TBIU007768) by	
	SHOWSEQ in EMBOSS	
5.77	Line graph of polyclonal antibody level of Fischoederius	181
	excretion/secretion (ES) product immunized Balb/c mice	
	determined by indirect ELISA (Dilution 1:25,600)	
5.78	SDS-PAGE (12.5% acrylamide gel) of parasite excretion/secretion	182
	(ES) products	
5.79	Western blot analysis of Fischoederius spp. anti-ES and ES product	183
5.80	SDS-PAGE (12.5% acrylamide gel) of parasite antigens	184
5.81	Cross-reactivity analysis of Fischoederius spp. anti-ES against	185
	parasite antigens at antibody dilution 1:3,000 from Mouse no. 1 and	
	Mouse no. 2	

#### LIST OF ABBREVIATIONS

#### Symbols/Abbreviations Terms

% Percent

% [v/v] Volume/volume percent
 % [w/v] Weight/volume percent
 ×g Gravitational acceleration

°C Celsius degree

μg Microgram μL Microliter μm Micrometer

μM Micromolar

AFA Alcohol-formal acetic acid

As Anterior sucker

atp6 ATP synthase membrane subunit 6atp8 ATP synthase membrane subunit 8

B. bubalis Bubalis

BCIP/NBT 5-Bromo-4-chloro-3-indolyl-phosphate/Nitro blue

tetrazolium

B. indicus Bos indicus

BLAST The Basic Local Alignment Search Tool

Bm Basement membrane

bp Base pair

BSA Bovine serum albumin

Ca Caeca

Cb Caecal bifurcation

Cc Cotylophoron cotylophorum

cDNA Complementary deoxyribonucleic acid

C. calicophorumCalicophorum calicophorumC. cotylophorumCotylophorum cotylophorum

#### **Symbols/Abbreviations** Terms

C. daubneyi Calicophoron daubneyi

C. hircus Capra hircus

cm Centimeter

C. microbothrioides Calicophoron microbothrioides

cox1 Cytochrome c oxidase subunit I
cox2 Cytochrome c oxidase subunit II
cox3 Cytochrome c oxidase subunit III

C. sinensis Clonorchis sinensis

Csp Carmyerius spatiosus

C. spatiosus Carmyerius spatiosus

Csy Carmyerius synethes

C. synethes Carmyerius synethes

C-terminus (COOH-terminus (Hydroxyl terminus)

CWE Crude worm extract

*cytb* Cytochrome b

D. annularis Diplodus annularis

DEPC Diethyl pyrocarbonate

DNA Deoxyribonucleic acid

DNase Deoxyribonuclease

dNTP Deoxynucleoside triphosphate

D. sargus
Diplodus sargus
D. vulgaris
Diplodus vulgaris
E. coli
Escherichia coli

EDTA Ethylene diamine tetraacetic acid

E. explanatum Explanatum explanatum

e.g. exempli gratia

Eg Eggs

#### Symbols/Abbreviations Terms

ELISA Enzyme-linked immunosorbent assay

EMBOSS The European molecular biology open software suite

Es Esophagus

ES Excretion/Secretion product

EST Express-sequence tag

et al. et alii

F-A Fischoederius spp. MseI pattern A

F. brevisaccus Fischoederius brevisaccus

F. buski Fasciolopsis buski

F. ceylonensis Fischoederius ceylonensis

Fc Fischoederius cobboldi

F. cobboldi Fischoederius cobboldi

Fcm Fischoederius compressus

F. compressus Fischoederius compressus

Fe Fischoederius elongatus

F. elongatus Fischoederius elongatus

FeT Fischoederius elongatus isolated from Tianmen, China

FeS Fischoederius elongatus isolated from Shanghai, China

F. emiljavieri Fischoederius emiljavieri

F. fischoederi Fischoederius fischoederi

F. gigantica Fasciola gigantica

Fj Fischoederius japonicas

F. japonicas Fischoederius japonicas

F. hepatica F. hepatica

F. magna Fascioloides magna

Fo Fischoederius ovatus

F. ovatus Fischoederius ovatus

#### **Symbols/Abbreviations** Terms

F. philippinensis Fischoederius philippinensis

F. siamensis
Fischoederius siamensis
Fischoederius skrjabini

F. skrjabini Fischoederius skrjabini

F-spp A Fischoederius spp. MseI pattern A
F-spp B Fischoederius spp. MseI pattern B

F-spp C Fischoederius spp. MseI pattern C
F-spp D Fischoederius spp. MseI pattern D
F-spp E Fischoederius spp. MseI pattern E

F-spp I Fischoederius spp. MseI pattern I

F. upiensis Fischoederius upiensis

g Gram

Gc Gastrothylax crumenifer
G. crumenifer Gastrothylax crumenifer

gDNA Genomic deoxyribonucleic acid

Gf Genital fold

GO Gene ontology

Gp Genital pore

Gpi Genital papilla

Gs Genital sphincter

HCl Hydrochloric acid

H. loi Hurleytrematoides loi

H. paloniae Homalogaster paloniae

hr Hour

HRP Horseradish peroxidase

H. sasali Hurleytrematoides sasali

i.e. id est

Symbols/Abbreviations Terms

Ig Immunoglobulin

ITS2 Internal transcribed spacer 2

kb Kilobase

kDa Kilodalton

KEGG Kyoto Encyclopedia of Genes and Genomes

kg Kilogram

LB Luria-Bertani
Lc Laurer's canal

L. luteola Littoraria luteola

LNR Long non-coding regions

M Molar

MALDI-TOF MS Matrix-Assisted Laser Desorption/Ionization-Time of

Flight Mass Spectrometry

mg Milligram

Mg Mehlis' gland

min Minute
mL Milliliter
mM Millimolar
mm Millimeter

Mo Mouth

mRNA Messenger ribonucleic acid

mt Mitochondria

mtCOX1 Mitochondrial cytochrome c subunit I

mtDNA Mitochondria genome

N Normal

NaCl Sodium chloride

nad1 NADH dehydrogenase subunit 1

#### Symbols/Abbreviations Terms

nad2
 nad4
 NADH dehydrogenase subunit 2
 nad4
 NADH dehydrogenase subunit 4
 nad4L
 NADH dehydrogenase subunit 4L
 nad5
 NADH dehydrogenase subunit 5
 nad6
 NADH dehydrogenase subunit 6

NCBI National Center for Biotechnology Information

NGS Next-generation sequencing

nm Nanometer

NSS Normal saline

N-terminus NH<sub>2</sub>-terminus (Amino terminus)
Od Orthocoelium dicranocoelium
O. dicranocoelium Orthocoelium dicranocoelium

OD Optical density

Op Orthocoelium parvipapillatum
O. parvipapillatum Orthocoelium parvipapillatum

OPD Ortho-Phenylenediamine

Os Orthocoelium streptocoelium
O. streptocoelium Orthocoelium streptocoelium

Ov Ovary

O. viverrini Opisthorchis viverrini

Ot Ootype

PBS Phosphate buffered saline
Pc Paramphistomum cervi
P. cervi Paramphistomum cervi

PCR Polymerase Chain Reaction
Pe Paramphistomum epiclitum
P. epiclitum Paramphistomum epiclitum

#### **Symbols/Abbreviations** Terms

Pg Paramphistomum gracile
P. gracile Paramphistomum gracile
PGM Personal Genome Machine

pH Potential of Hydrogen ion

Ph Pharynx

PMSF Phenylmethylsulfonyl fluoride

Ps Posterior sucker

Pt Parenchymal tissue

P. westermani Paragonimus westermani

qPCR Real-time quantitative polymerase chain reaction

RIN RNA integrity number

RNA Ribonucleic acid

RNase Ribonuclease

rRNA Ribosomal ribonucleic acid

rrnS Small subunit ribosomal ribonucleic acid
rrnL Large subunit ribosomal ribonucleic acid

RT-PCR Reverse transcriptase polymerase chain reaction

rpm Round per minute

RPMI Roswell Park Memorial Institute medium

rRNA Ribosomal ribonucleic acid

SAGE Serial analysis of gene expression

SDS Sodium dodecyl sulfate

SDS-PAGE Sodium dodecyl sulfate polyacrylamide gel

electrophoresis

sec Second

S. japonicum Schistosoma japonicum
S. mansoni Schistosoma mansoni

#### Symbols/Abbreviations Terms

SNR Short non-coding regions

Sr Seminal receptacle
SRA Short Read Archive

S. turkestanicum Schistosoma turkestanicum

TBE Tris/Borate/EDTA

TBS Tris buffered saline

Tc Tegumental cells

Te Testes

TEMED N,N,N',N'-tetramethylethylenediamine

Tg Tegument

Tge Terminal genitalium
TPM transcripts per million

Tris (hydroxymethyl) aminomethane

Triton X-100 Iso-octylphenoxypolyethoxyethanol

trn Transfer ribonucleic acid
tRNA Transfer ribonucleic acid

Tween 20 Polyoxyethylene-sorbitan monolaurate

UV Ultraviolet

Ut Uterus V Volt

Vb Velasquezotrema brevisaccus
V. brevisaccus Velasquezotrema brevisaccus

Vg Vitelline glands
Vp Ventral pouch

Vt Vitellaria

V. tripurensis Velasquezotrema tripurensis

# LIST OF ABBREVIATIONS (Cont.)

# Amino acid codes

Full name	1-letter abbreviation	3-letter abbreviation
Alanine	A	Ala
Arginine	R	Arg
Asparagine	N	Asn
Aspartic acid	D	Asp
Cysteine	C	Cys
Glutamic acid	Е	Glu
Glutamine	Q	Gln
Glycine	G	Gly
Histidine	Н	His
Isoleucine	I	Ile
Leucine	L	Leu
Lysine	K	Lys
Methionine	M	Met
Phenylalanine	F	Phe
Proline	P	Pro
Serine	S	Ser
Threonine	T	Thr
Tryptophan	W	Trp
Tyrosine	Y	Tyr
Valine	V	Val

# **CHAPTER 1**

# INTRODUCTION

Fischoederius elongatus (Trematoda, Digenea, Plagiorchiida) is a common gastrointestinal fluke that causes paramphistomiasis in ruminant, mainly in tropical and subtropical countries. F. elongatus is a member of pouched amphistomes. The adult stage of the fluke has a sword shape-like reddish body at approximate 6 mm body width and 20 mm body length. The flukes are food-borne trematodes which infect the definitive host through consumption of larva-infested water plants. The flukes are present in the rumen of the host and obstruct food absorption. Massive infection of the flukes causes severe mucosal damage in the host gastrointestinal tract. This leads to decreased milk and meat production and causes economic losses. Epidemiological surveys of Wongsawad (2000) indicated that ~90% of cattle in Chiang Mai province suffer from infection with Paramphistomum and/or Fischoederius spp.. Also Fischoederius infection has been reported from many countries, e.g. India, China, Philippines and Vietnam. Importantly, a Chinese woman from Guangdong Province was reported to be the first human infection case, but the route of infection is still unknown.

Identification of *F. elongatus* is based on microscopic examination, including the fecal egg counts and Semichon's carmine whole mount staining, but by these methods it is hard to distinguish *F. elongatus* from other amphistomes. Furthermore, the rumen fluke eggs are similar to eggs of the liver fluke *Fasciola* spp. Misdiagnosis may lead to incorrect drug treatment and development of resistance. Oxyclozanide has activity against immature and adult rumen flukes, but only effects adult liver flukes. Routine use of oxyclozanide against rumen flukes provides co-infecting immature liver flukes with an opportunity for development of resistance in adult worms. Microscopic examination of parasite tissue sections is necessary for analysis of morphological details and species identification; however this requires specialist knowledge and time. Thus, recent research has focused on molecular markers of the flukes. But only a small number of sequences is present in the biological databases, including ribosomal 28S, 18S, ITS2 and mitochondrial genome sequences.

Most of them are highly conserved among closely related species. Therefore, we need more information for species identification.

Recent next-generation sequencing technologies make it possible to identify transcriptome/genome sequences at large scale and to quickly find species-specific markers to improve diagnosis. In the present study, the transcriptome of *F. elongatus* will be characterized using a modern high-throughput sequencing platform and bioinformatics analysis of the sequence data. This technique is rapid and cost-effective for uncharacterized flukes. The obtained data will be analyzed to (1) reveal the taxonomic relationship between the species, to (2) learn how the flukes adapted to the conditions in the host rumen and (3) how they differ from the nearby species. Secreted proteins of the fluke will be predicted, possibly the most abundant secreted proteins have high potential as targets for diagnosis. Also, these proteins might have key regulatory roles in host-parasite interactions and pathogenesis.

Morphology and histology of the adult *F. elongatus* will be studied in addition to the analysis of the parasite transcriptome. This study will provide the basic knowledge for further molecular biology research and result in innovation on diagnosis and intervention.

# CHAPTER 2 OBJECTIVES

The objectives of the research are:

- 1. Morphological characterization of *Fischoederius elongatus* (Trematoda, Digenea, Plagiorchiida) using Semichon's carmine and hematoxylin and eosin staining
- 2. Molecular cloning and identification of cDNA encoding ribosomal internal transcribed spacer 2 (ITS2) region of *F. elongatus*
- 3. Molecular cloning and characterization of mitochondrial cytochrome c oxidase subunit I (mtCOX1) of *F. elongatus* 
  - 4. Restriction analysis of *F. elongatus* mtCOX1 and related species
  - 5. Molecular characterization of F. elongatus mitochondrial genome
- 6. Identification and annotation of mRNAs and encoded proteins expressed by the rumen fluke *F. elongatus* and related species by transcriptome analysis
- 7. Production of mouse polyclonal antibodies against *F. elongatus* excretion/secretion (ES) product
- 8. Identification of *F. elongatus* antigens using the anti-ES mouse serum on parasite extracts

# CHAPTER 3

# REVIEW OF LITERATURE

# 3.1 The rumen fluke Fischoederius elongatus

# 3.1.1 Taxonomic classification of Fischoederius elongatus

Fischoederius elongatus (Poirier, 1883) is a member of pouched amphistomes. The word 'Amphistoma' was defined by Rudolphi due to the fluke morphology. It refers to the trematodes that have an opening at both ends of the body. Nitzsch (1819) gave a more concise genetic term of the fluke, Amphistomum. They were characterized by the presence of an oral opening at the anterior end of the body and by a ventral sucker at the posteroterminal end. Amphistomes have a diverse body morphology including elongate, conical, cylindrical and fattened dorsoventrally shapes. They are also variable in size between 1.5–7.0 mm in width and 3.0–10.0 mm in length. Most living amphistomes have a light pink to red body color. The structure of the pharynx and its relationship to the length of the body is important in amphistome taxonomy. Arrangement of the circular muscle fibers in the ventral sucker as well as the position of male and female genitalia are important for fluke classification. Nasmark (1937) classified the paramphistomes based on histological structure including pharynx, ventral sucker, and terminal genitalium.

*F. elongatus* is a food-borne trematode that inhabits the rumen of ruminants. Massive infection of the flukes causes severe mucosal damage in the host gastrointestinal tract. The worm causes severe disease with significantly increased mortality rate during acute infection.<sup>5</sup>

*F. elongatus* is classified into the phylum: Platyhelminthes, class: Trematoda, subclass: Digenea superfamily: Paramphistomoidea, and family: Gastrothylacidae. Family Gastrothylacidae Stiles & Goldberger, 1910 is classified by the possession of a ventral pouch that is an internal sac with a single aperture on the ventral surface, starting closely to the anterior end of the body. Genus *Fischoederius* Stiles & Goldberger, 1910 is distinguished by the testes position. The testes lay tandem in mid-line, one anterodorsal to the other.<sup>3, 4, 6, 7</sup>

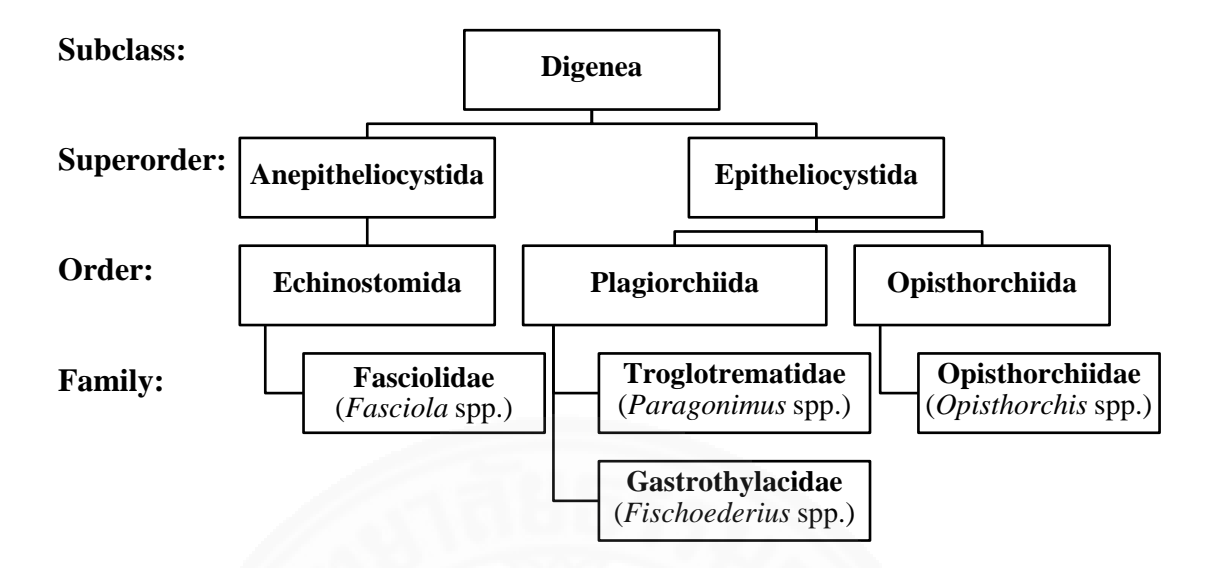


Figure 3.1 Taxonomy classification of Fischoederius elongatus.<sup>6</sup>

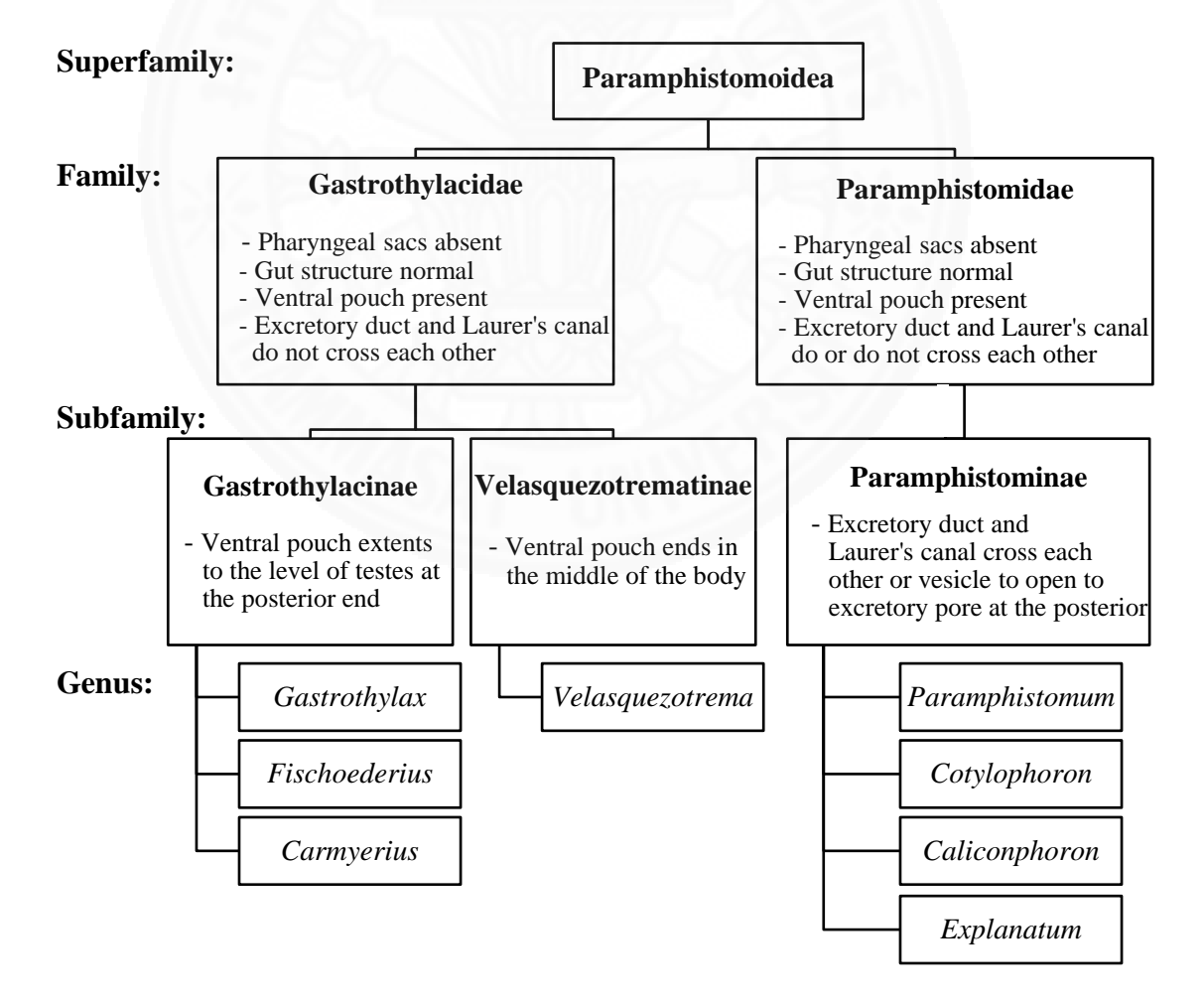


Figure 3.2 Classification of Fischoederius elongatus and other amphistomes.<sup>3,8</sup>

Genus *Fischoederius* currently contains 9 species including *F. elongatus* (Poirier, 1883 and Stiles & Goldberger, 1910) *F. cobboldi* (Poirier, 1883) Stiles & Goldberger, 1910, *F. japonicas* (Fukui, 1922) Yamaguti, 1939, *F. skrjabini* Kadenatsii, 1962, *F. ovatus* Wang, 1977, *F. compressus* Wang, 1979, *F. philippinensis* Eduardo, 1988, *F. upiensis* Eduardo, 2008, and *F. emiljavieri* Eduardo, 2009. Due to the mid-region body of a ventral pouch, *F. brevisaccus* Eduardo, 1981, was reclassified into Genus *Velasquezotrema* as *Velasquezotrema* brevisaccus. The synonyms of each member in the genera *Fischoederius* and *Velasquezotrema* are shown in **Table 3.1**.

Table 3.1 Synonymy of members in the genera Fischoederius and Velasquezotrema.8

11401	Synonyms	
F. elongatus	Gastrothylax elongatus Poirier, 1883	
	Fischoederius fischoederi Stiles & Goldberger, 1910	
	Fischoederius ceylonensis Stiles & Goldberger, 1910	
	Fischoederius siamensis Stiles & Goldberger, 1910	
F. cobboldi	Gastrothylax cobboldi Poirier, 1883	
F. japonicas	Fischoederius siamensis var. japonica Fukui, 1992	
	Gastrothylax elongatus var. japonica Fukui, 1992	
F. ovatus	Fischoederius ovis Zhang & Yang, 1986	
V. brevisaccus	Fischoederius brevisaccus Eduardo, 1981	

# 3.1.2 Morphology of Fischoederius elongatus

# **3.1.2.1 Adult stage**

Adult stage of *F. elongatus* has a reddish body with a sword-like shape, extremely elongated as shown in **Figure 3.3**. The body size is 3.70–20.8 mm in length and 1.80–3.70 mm in width. The ratio of body width to body length is 1:4. The tegument surface carries numerous papillae with dome to conical, non-ciliated papillae as shown in **Figure 3.4**. Acetabulum is 1.13–1.26 mm in diameter with *Fischoederius* type as shown in **Figure 3.5a**. Ventral pouch is present and usually triangular with ventrally directed apex. The internal surface of the ventral pouch usually

has a light brown color. Pharynx is *Paramphistomum* type as shown in **Figure 3.5b**. Esophagus is 0.63–0.84 mm in length and esophageal bulb is absent. The cecal bifurcation lays straight in lateral fields and terminates at the middle length of the body. Vitelline follicles are small in lateral fields, extending from level of ceca to testes. Lobed testes are positioned on the median and in vertical orientation which distinguishes the worm from other gastrointestinal flukes. Pars musculosa is moderately developed. Ovary is usually round. Terminal genitalium is located within the ventral pouch with *Elongatus* type as shown in **Figure 3.5c**. The key of species *Fischoederius* is shown in **Table 3.2**. <sup>3, 6-8, 16</sup>

Table 3.2 Key of the species of Fischoederius.<sup>8</sup>

	Key of the Species of Fischoederius				
1.	Ceca in lateral fields	2			
	Ceca in dorsal fields	4			
2.	Ceca extending to posterior testis	3			
	Ceca extending to middle part of body	F. skrjabini			
3.	Testes irregular in shape	F. cobboldi			
	Testes entire in shape				
4.	Ceca pre-equatorial	5			
	Ceca post-equatorial	F. japonicas			
5.	Testes overlap each other	F. elongatus			
	Testes separated by uterine coil	F. compressus			

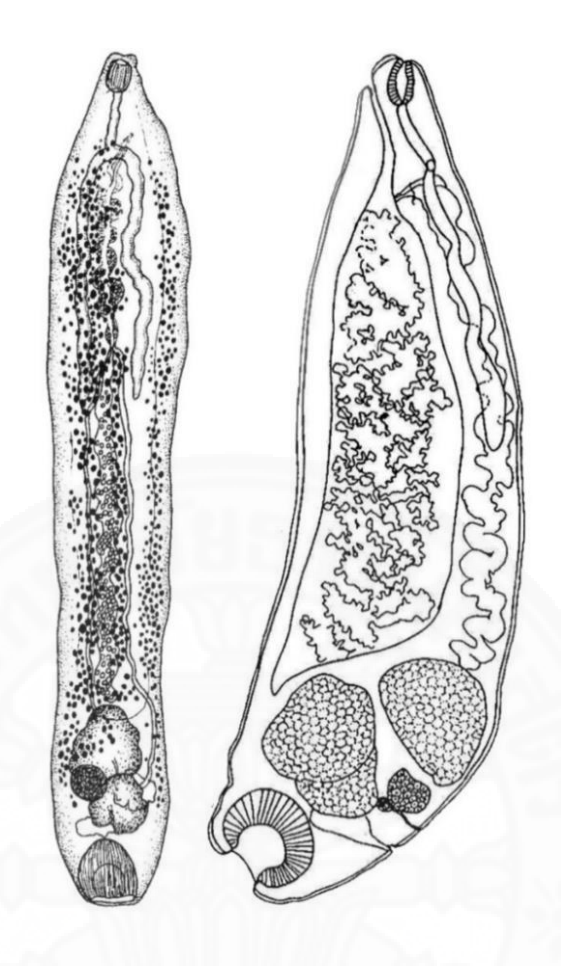


Figure 3.3 Schematic drawing of Fischoederius elongatus. 6,8

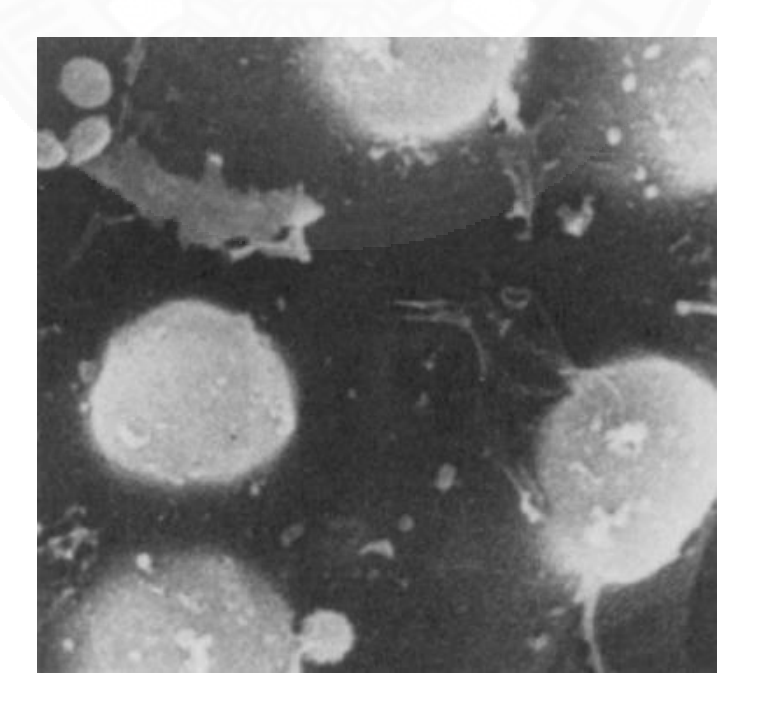
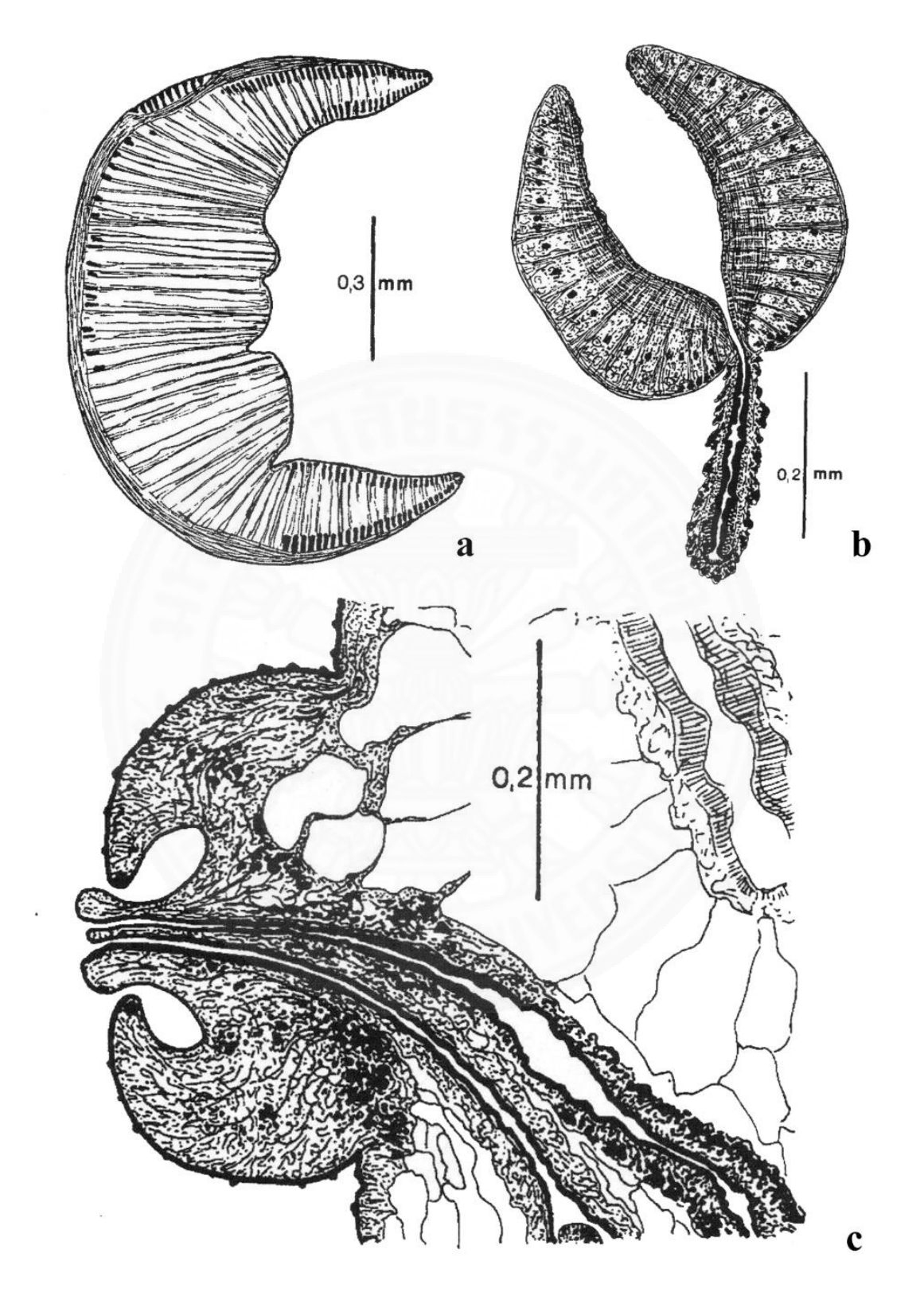


Figure 3.4 Dome to conical, non-ciliated papillae.8



**Figure 3.5** Median sagittal section of adult *Fischoederius elongatus*; (**a**) Acetabulum, *Fischoederius* type; (**b**) Pharynx, *Paramphistomum* type; (**c**) Terminal genitalium, *Elongatus* type.<sup>8</sup>

Following Nasmark (1937), a comparison of sagittal section of histological structure type, including acetabulum, pharynx, and terminal genitalium, of amphistomes commonly found in Thailand and nearby countries is shown in  ${\bf Table~3.3.}^4$ 

**Table 3.3** Comparison of histological structure type of amphistome.<sup>8</sup>

	Pharynx	Acetabulum	Terminal genitalium
	type	type	type
F. elongatus	Paramphistomum	Fischoederius	Elongatus
F. cobboldi	Paramphistomum	Gastrothylax	Microbothrium
F. japonicas	Paramphistomum	Carmyerius	Papillogenitalis
F. philippinensis	Calicophoron	Gastrothylax	Microbothrium
F. upiensis	Paramphistomum	Fischoederius	Leydeni
F. emiljavieri	Paramphistomum	Carmyerius	Bubalis
V. brevisaccus	Calicophoron	Gastrothylax	Brevisaccus
C. spatious	Paramphistomum	Gastrothylax	Gracile
G. crumenifer	Paramphistomum	Gastrothylax	Gracile
C. calicophorum	Calicophoron	Calicophoron	Calicophoron
P. cervi	Liorchis	Paramphistomum	Gracile
P. gracile	Calicophoron	Paramphistomum	Gracile
P. epiclitum	Calicophoron	Paramphistomum	Gracile



Figure 3.6 Carmine staining of adult stage amphistomes in Thailand.<sup>3</sup>

Fe: Fischoederius elongatus

Fc: Fischoederius cobboldi

Csp: Carmyerius spatiosus

Gc: Gastrothylax crumenifer

Cc: Cotylophoron cotylophorum

Os: Orthocoelium streptocoelium

Od: Orthocoelium dicranocoelium

Op: Orthocoelium parvipapillatum

Pg: Paramphistomum gracile

Pe: Paramphistomum epiclitum

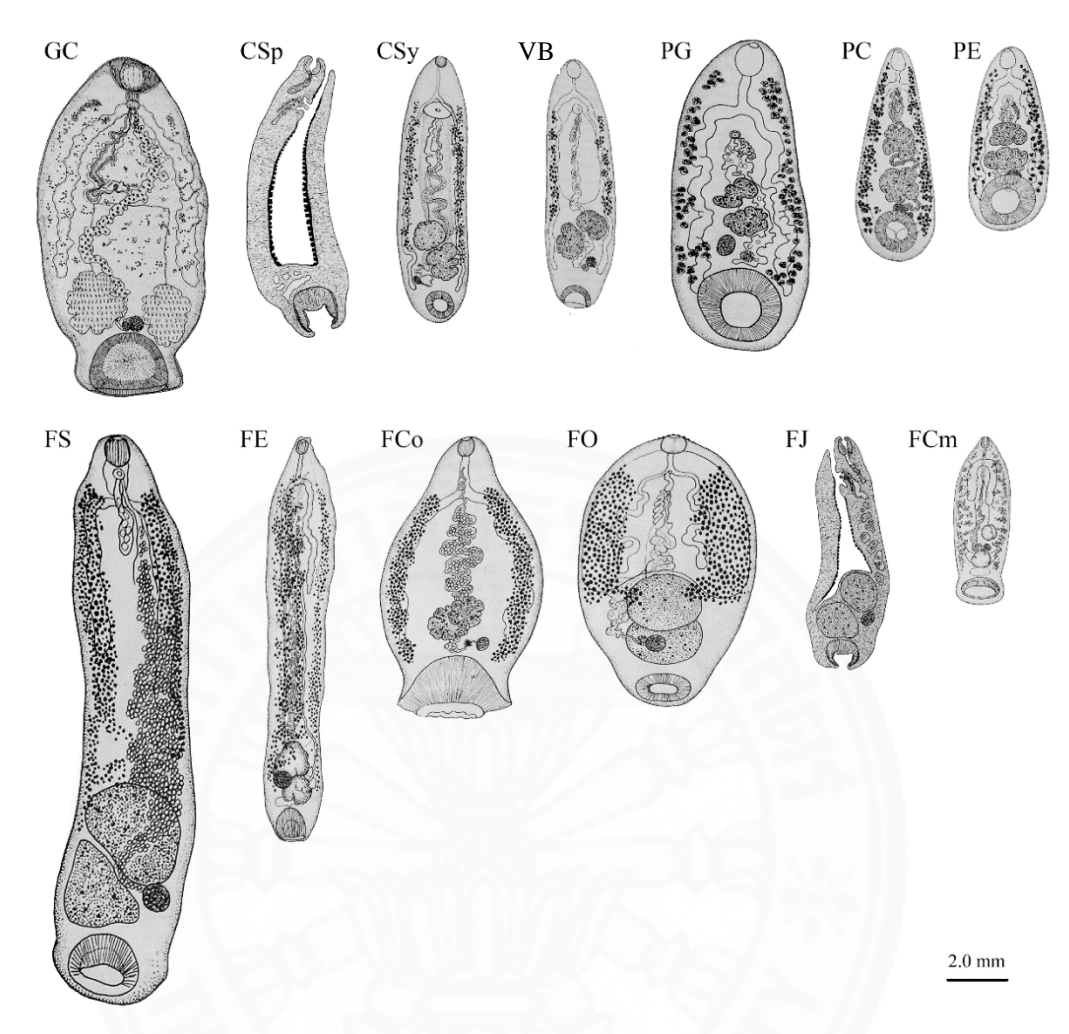


Figure 3.7 Morphology drawing of adult stage amphistome.<sup>8</sup>

GC: Gastrothylax crumenifer

CSp: Carmyerius spatiosus

CSy Carmyerius synethes

VB: Velasquezotrema brevisaccus

PG: Paramphistomum gracile

PC: Paramphistomum cervi

PE: Paramphistomum epiclitum

FS: Fischoederius skrjabini

FE: Fischoederius elongatus

FCo: Fischoederius cobboldi

FO: Fischoederius ovatus

FJ: Fischoederius japonicus

FCm: Fischoederius compressus

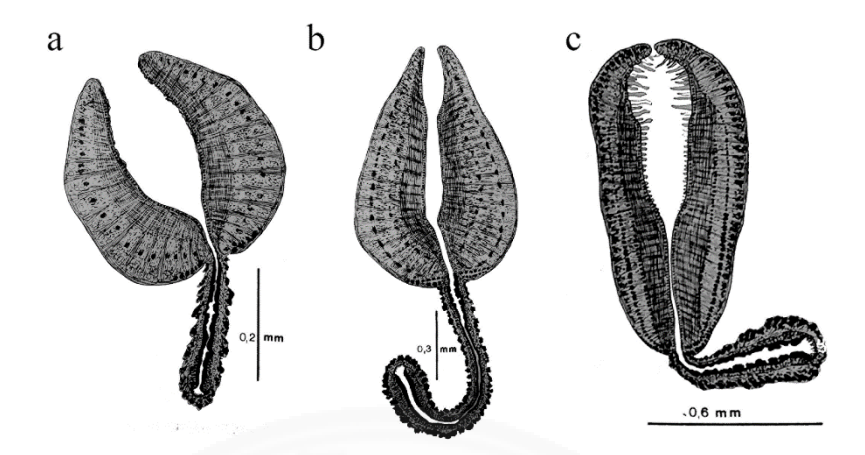


Figure 3.8 Median sagittal section of Pharynx.8

- (a) Paramphistomum type
- (b) Calicophoron type
- (c) Liorchis type

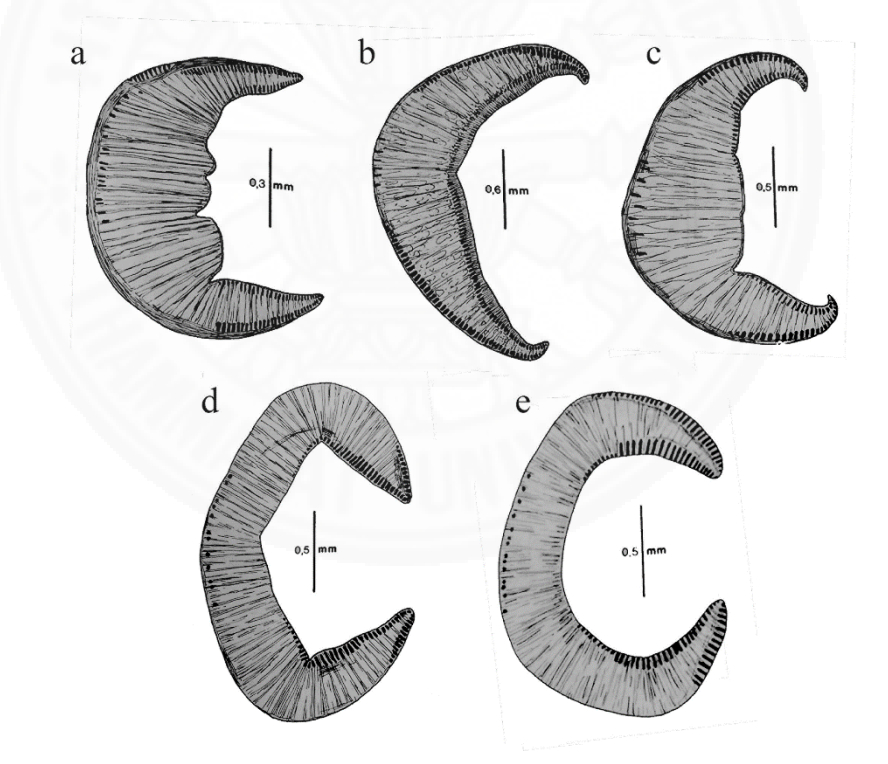


Figure 3.9 Median sagittal section of Acetabulum.<sup>8</sup>

- (a) Fischoederius type
- **(b)** *Gastrothylax* type
- (c) Carmyerius type
- (d) Calicophoron type
- (e) Paramphistomum type

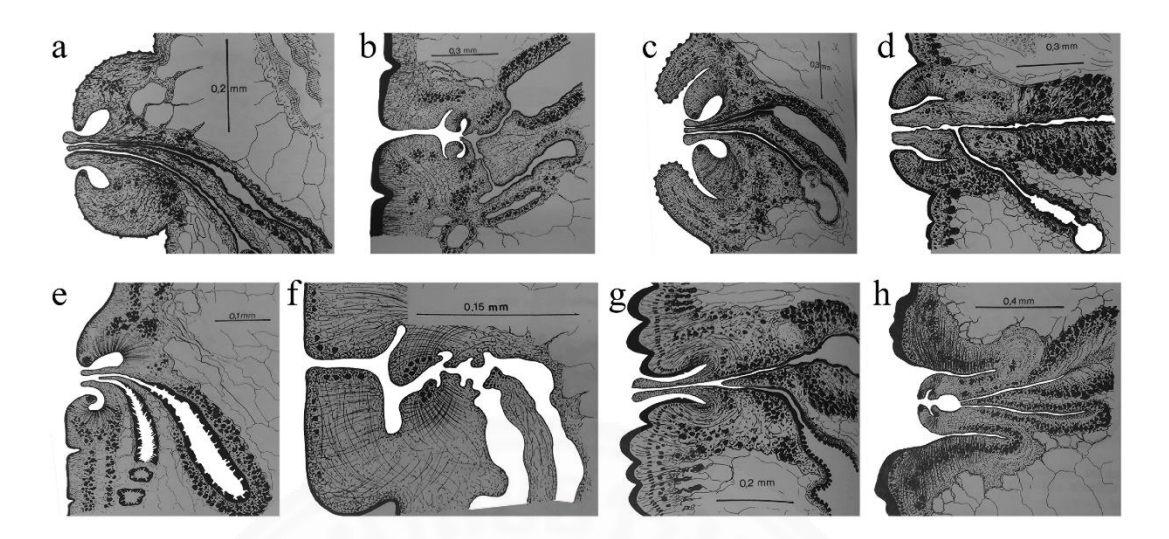


Figure 3.10 Median sagittal section of Terminal genitalium.<sup>8</sup>

- (a) Elongatus type
- **(b)** *Microbothrium* type
- (c) Papillogenitalis type
- (d) Leydeni type
- (e) Bubalis type
- (f) Brevisaccus type
- (g) Gracile type
- (h) Calicophoron type

# **3.1.2.2** Egg stage

The off-white eggs are oval shaped with uniform thin shell at the anti-opercular end. The anterior end of the egg has a distinct operculum. The deposited egg contains a zygote of 8-16 cells stage. The average size of the egg is around  $0.14\times0.08$  mm.  $^{8,\,17,\,18}$ 



Figure 3.11 Egg stage of Fischoederius elongatus. 19

# 3.1.2.3 Miracidia stage

The embryo is located in the middle of the egg and completes development in 7–8 days. The average size of the ovum is increasing from  $0.03\times0.03$  to  $0.16\times0.06$  mm within seven days. The miracidium will hatch on the eighth day of development. It usually swims in straight lines and rotates the body along the long axis. The body cilia are pyriform in shape. Twenty epithelial cells are arranged in four transverse rows in the ratio 6:8:4:2. The anterior part contains a conical apical papilla. The gut is located at the base of an apical papilla. There are two pairs of penetration glands beside the gut. The nervous system is located at the posterior of the gut. The miracidium contain a pair of flame cells and ducts forming the excretory system. They also contain germinal cells and germinal balls in different sizes. The measured size is around 0.17–0.06 mm. The snail intermediate hosts were indicated as *Lymnaea acuminate*, *Littoraria luteola*, *Gyraulus euphraticus*. 8, 17, 18

# 3.1.2.4 Redia stage

The redia is elongate in shape. The body size is  $0.80\times0.10$  mm. The body contains a small oral opening, a well-developed pharynx, saccular cecum, a mass of pyriform granular cells, and three pairs of flame cells. The redia contains the developing cercariae.<sup>8, 18, 20, 21</sup>

# 3.1.2.5 Cercaria stage

The cercaria of *F. elongatus* is identical with *Cercaria indicae* XXIX (Sewell, 1922) as shown in **Figure 3.12**. <sup>20</sup> The body pigment develops in the snail tissue and the body measures 0.26–0.69×0.35–0.15 mm, and the tail length is 0.75 mm. The body surface is covered with rod-like cytogenous cells. Conical eyespots are located near to the anterior end. Acetabulum is broader than long with a size of 0.09–0.12 mm. The pharynx is 0.07 mm in diameter, followed by the esophagus with a quarter of body length, and the ceca that terminate at the edge to the posterior half of the body. Esophagus and ceca contain rectangular granules. Main excretory canal is formed by cross-connecting tubes with antero-median diverticulum. Primordia of genital organs are rounded masses of cells. The reproductive organs are ovary and tandem testes placed anterior and posterior to the ovary. <sup>8, 18, 20, 21</sup>

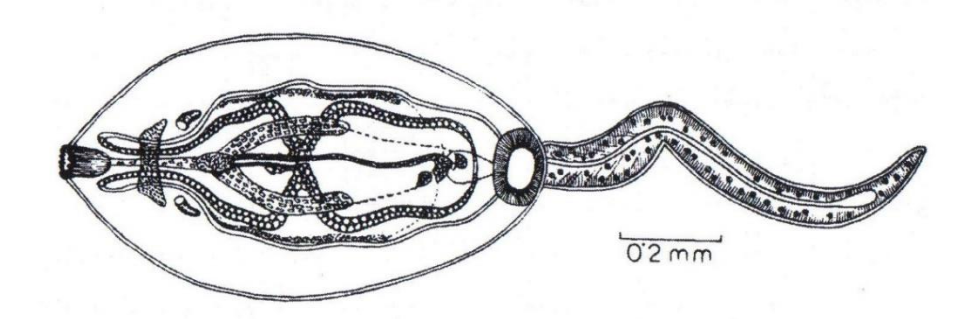


Figure 3.12 Cercaria indicae XXIX (Sewell, 1922) of Fischoederius elongatus. 18

# 3.1.2.6 Metacercaria stage

The metacercaria is hemispherical in shape. The body has a diameter of 0.30 mm and the cyst wall is 0.02 mm thick.  $^{8,\,18,\,20,\,21}$ 

# 3.1.3 Life cycle of the rumen fluke

Due to a lack of resolved details of the *F. elongatus* life cycle, a general life cycle of rumen flukes is shown in **Figure 3.13**. The rumen flukes develop into adult stage in the stomach of livestock and pass their immature eggs into the host feces. The next part of the life cycle occurs in freshwater and after completing embryogenesis the hatched miracidium infect an aquatic snail. The immature flukes develop through several stages in the aquatic snail. Then the cercariae shed in the water around the snail and form metacercarial cysts on water plants. Mammals acquire the infection by eating vegetation containing metacercariae. The metacercarial cyst wall is digested in the duodenum, releasing the larval fluke which attaches to the wall of the intestine and feeds on plugs bitten from the wall, causing severe fluid and blood loss. Then the larvae migrate to the rumen where they develop into adult flukes, and continue the life cycle.<sup>3, 22</sup>

In detail, Rao and Ayyar (1932) studied the development of *F. elongatus* in the definitive host. They have determined *Cercariae indicae* XXIX (Sewell, 1922) as *F. elongatus* larval stage, and the snail *L. luteola* (Lamarck, 1822) as an intermediate host. Eight weeks after the host were fed metacercaria cysts, some mature flukes were found in the rumen. The eggs were found in the host feces at eighteen weeks post-infection.<sup>21</sup> Kishore and Shoeb (2017) supported Rao and Ayyar (1932) by their studies in the encystment of *F. elongatus* in experimental animals.

Cercariae indicae XXIX (Sewell, 1922) was collected and identified from *L. luteola* (Lamarck, 1822). An infective stage metacercaria was excysted on peepal leaves and fed to the experimental animals including guinea-pig, rabbit, albino rat, kitten, kid, and lamb. Juveniles identified as *F. elongatus* were collected from some experimental animals, guinea-pig, kid, and lamb at 126 days after infection. This study clearly identified the larval stage and its aquatic snail host in the *F. elongatus* life cycle.<sup>23</sup> However, other details of the fluke's life-cycle are unresolved.

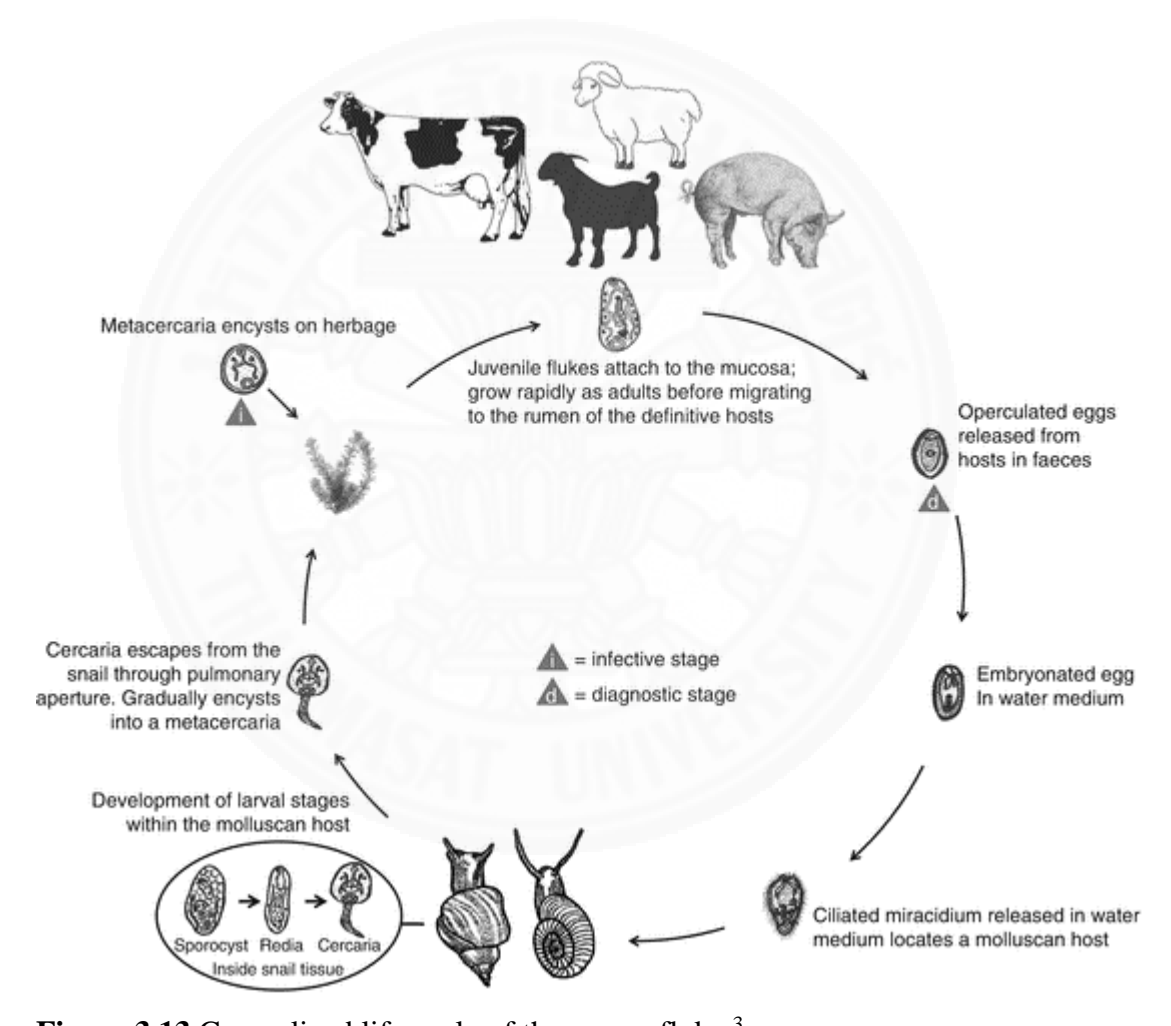


**Figure 3.13** Generalized life cycle of the rumen fluke.<sup>3</sup>

#### 3.1.4 Geographic distribution of Fischoederius elongatus

*F. elongatus* is widely distributed and common in Asia and Africa. The fluke infection in livestock has been reported in many countries, *e.g.* India, Sri Lanka, China, Taiwan, Indonesia, Japan, Korea, Philippines, Vietnam, Cambodia,

Borneo, Thailand, Java, Papua New Guinea, Nigeria, Senegal, Zambia, Egypt, Bulgaria, England, France, Poland, Hungary, Italy, Sardinia, Yugoslavia and Russia. 19, 24-31

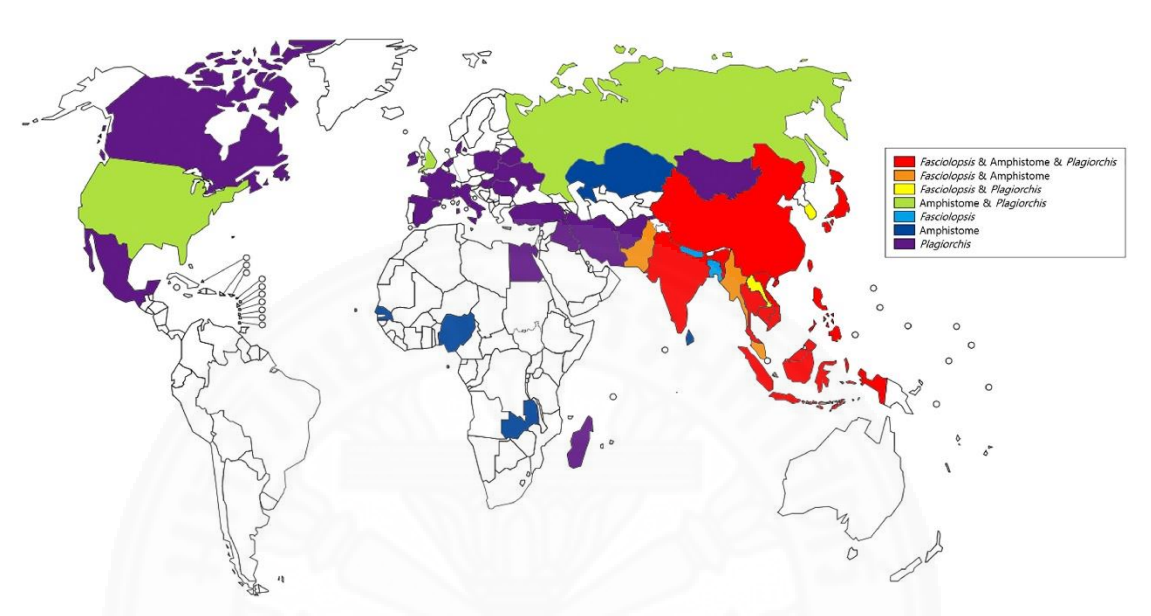


Figure 3.14 Global distribution intestinal flukes studied by Chai et al., 2020.<sup>29</sup>

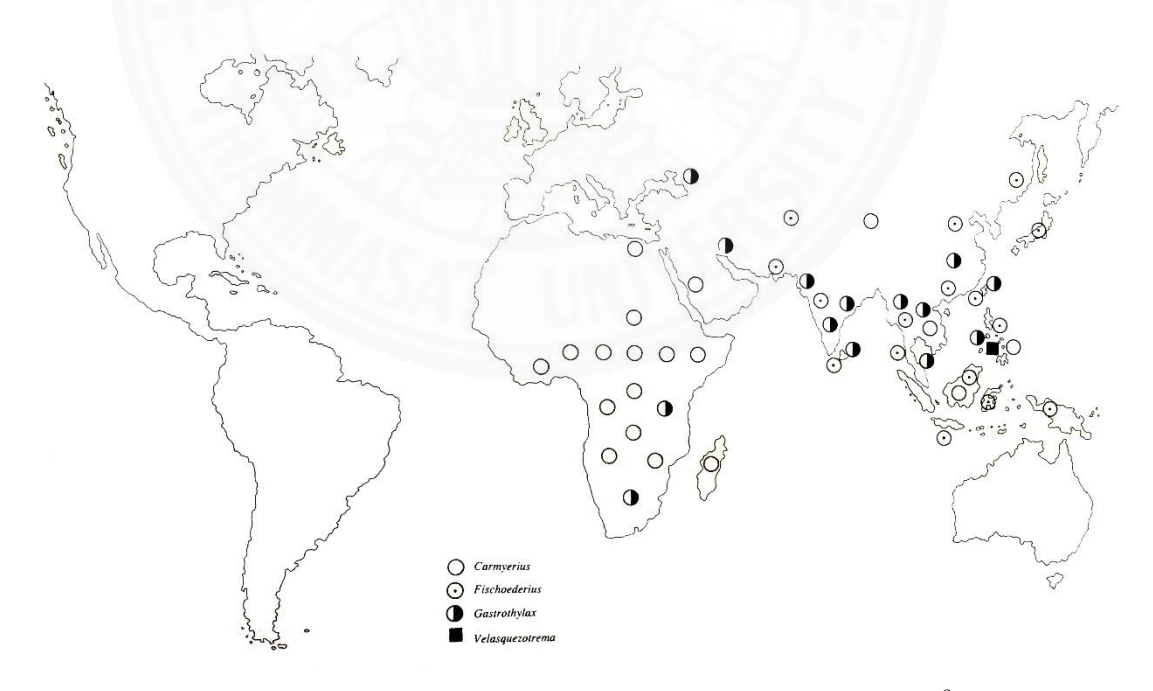
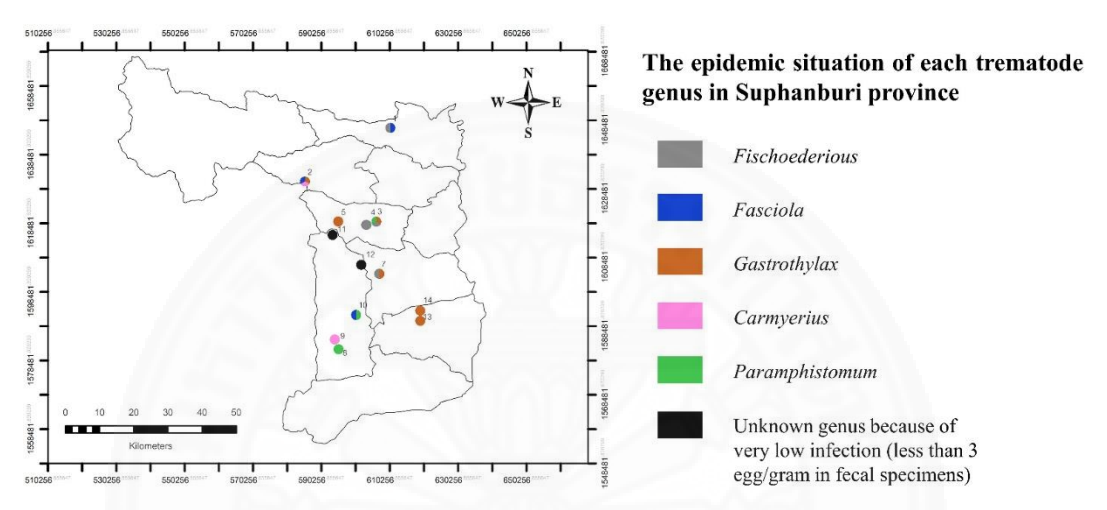


Figure 3.15 Global distribution of amphistomes studied by Sey (1991).8

In Thailand, epidemiological surveys of Wongsawad (2000) Chiang Mai University, North-Thailand are supportive of this finding and indicate that ~90%

of cattle in Chiang Mai province suffer from infection with *Paramphistomum* and/or *Fischoederius* spp..<sup>31</sup> An epidemiological survey in Suphanburi province, Thailand in 2020 reported 60.5% of the cattle infected with rumen flukes including *Fischoederius*, *Gastrothylax*, *Carmyerius*, and *Paramphistomum*, and also the liver fluke *F. gigantica*. The co-infection had two case reports.<sup>19</sup>



**Figure 3.16** Geographic distribution of the rumen fluke and liver fluke in Suphanburi Province.<sup>19</sup>

#### 3.1.5 Pathogenesis of paramphistomiasis

F. elongatus is a food-borne gastrointestinal fluke that causes paramphistomiasis, a common disease in livestock. They inhabit the rumen of ruminants and induce mucosal inflammation with associated mucoid diarrhea. The disease affects young animals with significantly increased mortality during acute infection. Many clinical reports demonstrated paramphistomiasis which is produced by various species of rumen flukes. The pathological changes are closely related to the number of flukes and the development of the flukes in the definitive host. The intensity of damage is associated with the number of metacercariae ingested. Newly excysted juveniles induce pathology in the small intestine. Most of them are located in the proximal region of the intestine. A large number of the parasites attaches to the mucosa of the host and causes hyperemia, thickening and hemorrhage. As shown in **Figure 3.17a** and **Figure 3.17b**, the immature flukes attach by their acetabulum at the villi of duodenum wall of the infected host. The flukes migrate through the submucosa of the

intestine which stimulates immune cells to surround and attack them and causes inflammation as shown in **Figure 3.17d**.<sup>32</sup> Adult flukes cause damage to the rumen by fibrotic inflammation. The host villi are shortened and thickened and even are destroyed in some areas in the late phase of paramphistomiasis.<sup>33, 34</sup> The clinical sign generally appears at 2–4 weeks postinfection with diarrhea in the host, mostly in 4–18 months old cattle infected with a massive number of immature flukes. The pathology of the disease stimulates a severe diarrhea in the host, and significantly increases mortality during acute infection.<sup>3, 5, 35, 36</sup> Importantly, a Chinese woman from Guangdong Province was reported to be the first human infection case, but it is still unknown how she was infected.<sup>37</sup>

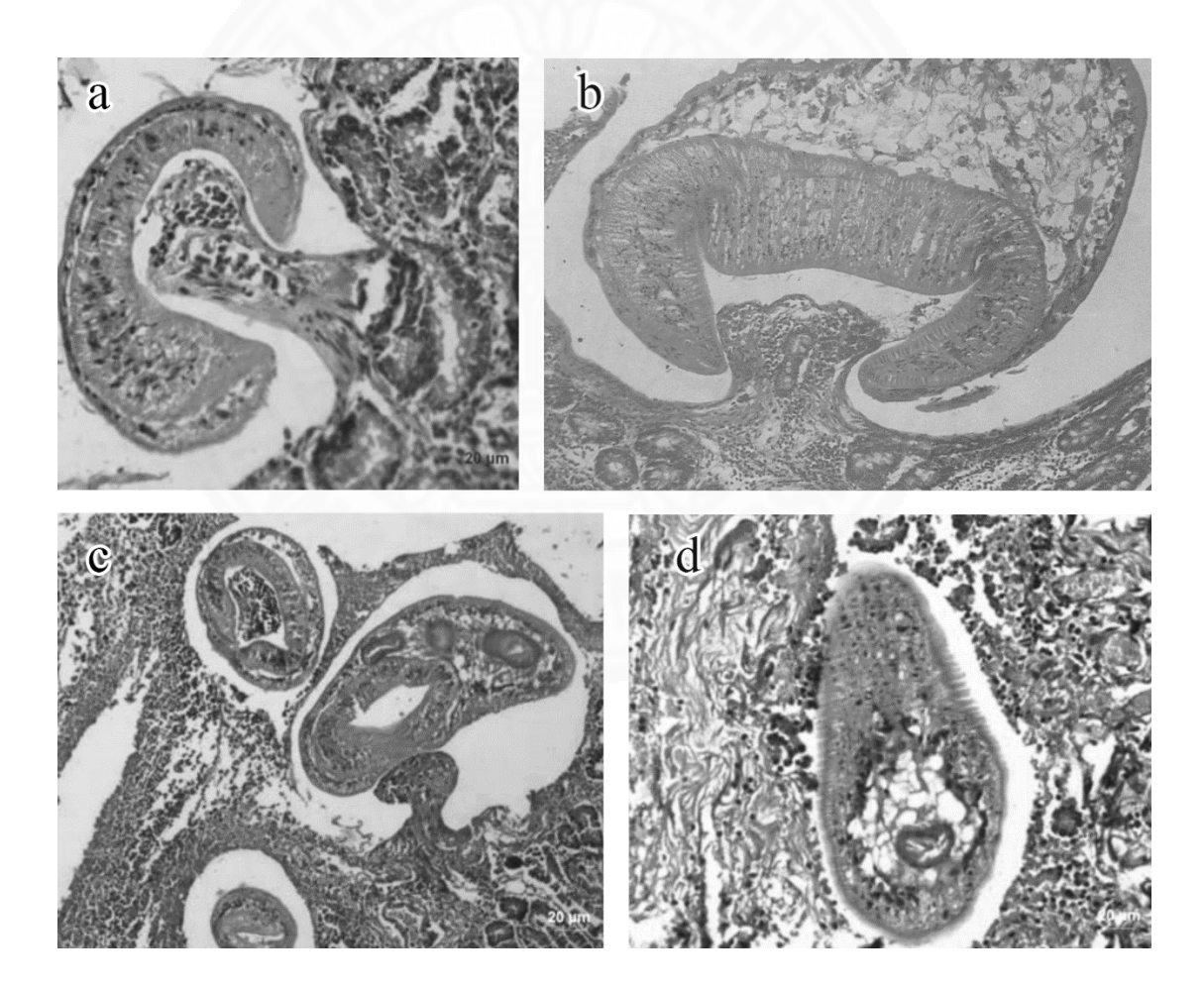


**Figure 3.17** Pathogenesis of paramphistomiasis in sheep. (a) Attachment of acetabulum of amphistome to the villi of duodenal wall of sheep; (b) *Paramphistomum epiclitum* attacked the duodenal wall; (c) Amphistome-sheep tissue section; (d) Amphistome surrounded by immune cells.<sup>32, 36</sup>

# 3.1.6 Diagnosis of the rumen fluke

# 3.1.6.1 Microscopic examination

The most common diagnostic method of *F. elongatus* is the microscopic examination. The routine protocol is based on fecal egg count by using sedimentation techniques. Common amphistome eggs are particularly heavy eggs that are 160–180 µm in size. Clear identification of the eggs requires contrast stains such as methylene blue or methyl green. However, the morphology of the rumen fluke is similar to the liver fluke. Both of them have a large oval operculated egg with a thin shell. The *Fasciola* eggs showed a more yellowish color than the *Fischoederius* eggs. <sup>38-40</sup> In research, Semichon's carmine whole mount staining method is used to identify the adult stage of the flukes. However, with this method it is hard to distinguish *F. elongatus* from other paramphistomes and the liver fluke *Fasciola gigantica*. A histological examination is necessary for clear identification, but it requires a specialist and is time-consuming. An alternative diagnostic method is requested. <sup>16</sup>

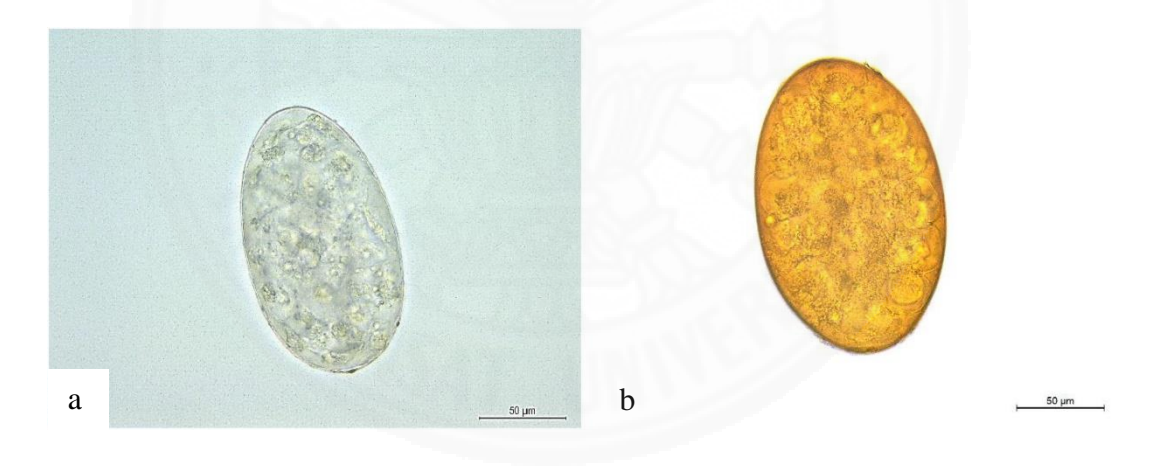


**Figure 3.18** Egg stage under microscopic examination (a) *Fischoederius elongatus*; (b) *Fasciola gigantica*. <sup>19</sup>

# 3.1.6.2 Molecular Diagnostics

# (1) High annealing temperature-random amplification of polymorphic DNA (HAT-RAPD) method

Wongsawad *et al.*, 2007 investigated the genetic diversity of trematodes by PCR-based HAT-RAPD method. Six arbitrary primers were designed and used to examine the polymorphic bands of DNA (OPA-02, OPA-05, OPA-7,

OPH-11, OPQ-14 and OPW-14). *F. elongatus* was one member of the investigated trematodes. The adult flukes were collected from the north of Thailand and thoroughly identified by their morphology. The agarose gel-determined DNA patterns of *F. elongatus* contained a total of 42 bands of DNA with sizes between 100–1,010 bp and were generated by using five primers (eight bands of 180–780 bp with OPA-02, six bands of 100–880 bp with OPA-07, thirteen bands of 190–1,010 bp with OPH-11, six bands of 200–900 bp with OPQ-14 and nine bands of 550–800 by with OPW-14). No band was observed in any investigated trematode by using OPA-05. The result showed that DNA bands of *F. elongatus* from different provinces were monomorphic bands that did not show variation between the samples.<sup>24, 41</sup>

Another six primers were designed to distinguish *F. elongatus* from other amphistomes including *P. epiclitum* and *Orthocoelium streptocoelium* (OPA-2, OPA-4, OPA-5, OPB-18, OPC-9 and OPH-11). DNA patterns of *F. elongatus* were generated using six primers, and the result showed following products, 760 bp with OPA-2, 670 and 1,159 bp with OPB-18, 670 and 950 with OPC-9, 260, 435 and 590 bp with OPH-11. No product was obtained with OPA-5. The similarity index based on HAT-RAPD patterns demonstrated that the index was 0.0645 between *P. epiclitum* and *F. elongatus*, and 0.0500 between *O. streptocoelium* and *F. elongatus*. The study demonstrated that DNA patterns from each primer might distinguish *F. elongatus* from *O. streptocoelium* and *P. epiclitum*. However, DNA patterns of nearby species (*e.g. Gastrothylax crumenifer, Carmyerius spatiosus* and *F. cobboldi*) need to be investigated in further studies. 41, 42

# (2) Ribosomal internal transcribed spacer (ITS2) sequence

Molecular phylogeny of rumen flukes was investigated by using the ribosomal internal transcribed spacer (ITS2) region. ITS2 is a molecular marker that showed variation among species. The phylogenetic resolution was improved with a secondary structure analysis using sequence-structure data combination. ITS2 region of *F. elongatus* was amplified using universal primers, designed on *Schistosoma* 5.8S and 28S sequences. The product size was 520 bp and the sequence could differentiate the fluke from other species (*F. cobboldi, G. crumenifer, C. spatiosus* and *Velasquezotrema tripurensis*). The sequence was submitted to NCBI databases with the accession number GU133062 and annotated as ITS2 sequence of

F. elongatus. However, ITS2 sequences are highly conserved among rumen flukes. The inferred ITS2 secondary structure of F. elongatus revealed a four-helix domain containing a UGGU motif and a U:U mismatch in the second helix with minimum free energy of -115.70 kcal/mol. Phylogenetic analysis based on rumen fluke ITS2 secondary structures showed high resolution and could differentiate family Gastrothylacidae from family Paramphistomidae by high bootstrap value. However, the amphistome clade between genus Fischoederius and genus Carmyerius was not clearly resolved with ~70% bootstrap value. F. elongatus ITS2 showed no intraspecies variation but high interspecies variation ranging from 0.4 to 4.7% with G. crumenifer and F. cobboldi. Accordingly, ITS2 might be somewhat useful as a DNA marker in distinguishing the amphistomes.<sup>43-45</sup>

# (3) Mitochondrial cytochrome c subunit I (mtCOX1) sequence

Gastrothylacid species identification was investigated by using the sequence of mitochondrial cytochrome c subunit I (mtCOX1). The mtCOX1 sequence was found highly conserved and useful for species-specific identification of *G. crumenifer*, *F. cobboldi and F. elongatus*. The rumen flukes were collected from different host species (*Bos indicus*, *Bubalus bubalis* and *Capra hircus*) and locations of Northeast India (Meghalaya, Tripura and Nagaland). The mtCOX1 sequences were submitted to NCBI databases with the accession numbers JQ806365, JX518952, and JX518953, respectively. Sequence analysis of a 394 bp mtCOX1 fragment showed no intraspecies variation of *F. elongatus* mtCOX1. Interspecies variation ranged from 5.6 to 11.9%. All mtCOX1 motifs of *F. elongatus* were species-specific motifs. The mtCOX1 region showed higher variation between the three species than the ITS2 region.<sup>45</sup>

The mtCOX1 region was used for discrimination of rumen fluke eggs from liver fluke eggs in Suphanburi Province, Thailand. The eggs of these flukes have slightly similar morphology and are difficult to distinguish from each other. Both of them have a large oval operculated egg with a thin shell. <sup>38-40</sup> The *Fasciola* eggs showed a more yellowish color than the *Fischoederius* eggs. The mtCOX1 was investigated as a molecular marker using PCR amplification. A 989 bp mtCOX1 fragment was used in this study. The positive rate of the method was about 72%.

Phylogenetic analysis of the 989 bp mtCOX1 sequences showed six clades *Fischoederius, Gastrothylax, Carmyerius, Paramphistomum, Explanatum*, and *Fasciola* spp.. The study showed that mtCOX1 was an effective marker for amphistome identification.<sup>19</sup>

# 3.1.6.3 Immunodiagnostics

Immunological studies of *F. elongatus* in the host were not found, thus this review focuses on data from the amphistome *P. epiclitum*. Hassan and Juyal (2006) investigated the immunodiagnosis of paramphistomiasis in domestic ruminants using dot-ELISA and Western blot analysis. Rabbit antiserum against adult *P. epiclitum* showed high titer at 1:40,000 dilution. Western blot profile revealed seven immunogenic bands at molecular weight range 32.5–94.4 kDa (32.5, 37.5, 42.2, 44.6, 53.08, 59.5 and 94.4 kDa). Cross-reactive band between *P. epiclitum* and *Cotylophoron cotylophorum* was 42.1 kDa, and the cross-reactive bands between *C. cotylophorum* and *G. crumenifer* were 50.1, 56.2 kDa.<sup>46</sup>

Salib *et al.*, 2015 evaluated indirect ELISA and western blotting for diagnosis of *Paramphistomum* spp. and *Carmyerius gergaerius* infected cattle and buffaloes in Egypt. Indirect ELISA from 84 collected samples showed high sensitivity, specificity, and accuracy at 74.0%, 82.4%, and 79.6%, respectively. Western blot analysis of a somatic antigen immunized rabbit antiserum and an infected animal serum represented six immunogenic bands at molecular weight range 27–87 kDa (27, 39, 58, 63, 71, and 87 kDa). The specific immunogenic band was found at 63 kDa reacting with *Paramphistomum* spp. and at 71 kDa reacting with *C. gergaerius*.<sup>47</sup>

A recent study on the excretion/secretion (ES) antigens of *F. elongatus* showed prominent protein bands at 14 kDa, 20 kDa, and 66 kDa. These prominent ES proteins are potential target antigens for further analysis.<sup>48</sup> These studies showed that there are immunodominant antigens of the fluke that can be developed as diagnosis tool.

#### 3.1.7 Control and treatment of the rumen fluke

The control program of the rumen fluke encourages the interruption of parasite life cycle which can be achieved through diagnosis, vaccine and drug treatment. The drug of choice for intestinal trematode treatment is praziquantel. The oral dose for human therapy is 25 mg/kg TID.<sup>49</sup> Bithionol sulfoxide, niclosamide,

hexachlorophene, fenbendazole, and oxyclozanide are effective anthelmintics against amphistomes in ruminants.<sup>50, 51</sup> Horak (1967) showed that the effective dose of bithionol sulfoxide against both immature and adult amphistomes in sheep is 25–100 mg/kg, but not against immature flukes in cattle.<sup>52</sup> Treatment with 40 mg/kg bithionol sulfoxide indicated 80–100% cure rate in ruminants.<sup>53</sup> Rolfe *et al.*, 1987 showed that a single dose (18.7 mg/kg) of oxyclozanide combination with levamisole had 94–98% effectivity against immature and adult amphistomes after 14 days treatment in cattle. Two doses three days apart of oxyclozanide showed 99–100% effectivity.<sup>51</sup> This drug also had high effectivity against *P. leydeni* in sheep at 99%.<sup>54</sup> However, Jeyathilakan *et al.*, 2003 reported only at 84% effectivity of oxyclozanide in sheep in Tamil Nadu, India.<sup>55</sup> Hexachlorophene also showed high effectivity against amphistome with a single dose of 20 mg/kg. However, the researcher found that some animals had neurological signs post-treatment.<sup>51</sup> However, due to the limited number of available drugs, the parasites might develop resistance against these drugs and the search for alternative treatment was encouraged.<sup>3,56</sup>

In Thailand, Prasitirat *et al.*, 1996 studied chemotherapy of naturally rumen fluke infected cattle. The result showed that bithionol sulfoxide was the most effective drug against the flukes with drug dosage at 80–90 mg/kg with a cure rate of 70% one week post treatment. The side effects of the drug were observed within 24 hours after drug administration *e.g.* diarrhea and anorexia.<sup>57, 58</sup>

Furthermore, misdiagnosis may lead to incorrect drug treatment and development of resistance. Oxyclozanide has activity against immature and adult rumen flukes, but only effects adult liver flukes. Routine use of oxyclozanide against rumen flukes provides co-infecting immature liver flukes with an opportunity for development of resistance in adult worms.<sup>59</sup> Nzalawahe *et al.*, 2018 reported a case of reduced effectiveness of anthelminthic drug in *F. gigantica* and amphistomes. This study showed that all five treatments including Albendazole, Nitroxynil, Oxyclozanide, Closantel and Triclabendazole were effective against *F. gigantica* at 14 days post-treatment in Iringa Rural and Arumeru Districts. However, Albendazole showed only 89% fecal egg count reduction (FECR) in Iringa Rural District and 49% FECR in Arumeru District. Only Oxyclozanide showed high effectivity against amphistomes with 99% FECR in both districts at 14 days post-treatment. Partial albendazole

resistance in *F. gigantica* might have been due to a too low dose of the drug. Mixed infection between *F. gigantica*, amphistomes, nematodes is commonly found in both districts. The liver fluke might have been exposed to an Albendazole dose below the recommended dose of 10 mg/kg because the recommended dose for amphistomes, nematodes is 7.5 mg/kg. Over time this might lead to resistance in *F. gigantica*.<sup>60</sup>

# 3.2 Mitochondrial genome sequence of Fischoederius elongatus

# 3.2.1 Complete mitochondrial genome sequence from Tianmen, China

Yang et al., 2015 researched the mitochondrial genome sequences of F. elongatus providing basic knowledge for phylogenetic and epidemiological studies. The conserved regions of F. elongatus mitochondria were amplified by using 12 oligonucleotide primers that were designed according to selected trematode mitochondrial sequences including cox3, cytb, nad4, cox1, rrnS and nad5. The mitochondrial fragments were manually assembled by comparison with other trematode mitochondrial genomes and then analyzed by bioinformatics. The results showed that the complete mitochondrial genome of F. elongatus is 14,120 bp in length (GenBank: KM\_397348). The mitochondrial genome contains 12 protein-coding genes, 22 tRNA genes, 2 rRNA genes and 2 non-coding regions that are transcribed in the same direction. The twelve protein-coding genes are encoded by 10,107 nucleotides. The most common initiation codon of the protein-coding genes is ATG, and the termination codons are TAG and TAA. Phenylalanine is the most frequently used amino acids of the protein-coding genes. The 22 tRNA genes range from 60–71 bp. The two rRNA genes consist of rrnS and rrnL. The two non-coding regions consist of one long non-coding region (LNR) and one short non-coding region (SNR). The organization of the mitochondrial genome is shown in Figure 3.19. Phylogenetic analysis of mitochondrial genomes showed that F. elongatus was closely related to P. cervi.<sup>61</sup>



**Figure 3.19** Arrangement of the mitochondrial genome of *Fischoederius elongatus* from Tianmen, China (GenBank: KM\_397348). The mitochondrial genome is 14,120 bp in length containing 12 protein-coding genes, 22 tRNA genes, 2 rRNA genes and 2 non-coding regions, encoded in the same direction. The 12 protein-coding genes are arranged in the following order; *cox*3, *cyt*b, *nad*4L, *nad*4, *atp*6, *nad*2, *nad*1, *nad*3, *cox*1, *cox*2, *nad*6 and *nad*5. *rrn*S rRNA gene is located between tRNA-Cys and *cox*2 and *rrn*L rRNA gene is located between tRNA-Thr and tRNA-Cys. Long non-coding region (LNR) is located between tRNA-Phe and *cox*3, and short non-coding region (SNR) is located between *cyt*b and *nad*4L.<sup>61</sup>

# 3.2.2 Complete mitochondrial genome sequence from Shanghai, China

Han et al., 2020 reported the mitochondrial genome extracted from F. elongatus in Shanghai, China (GenBank: MN537973). The genome length is 14,288 bp that contains 168 bp longer than the previously reported F. elongatus mitochondrial genome (GenBank: KM\_397348) due to the high mutation rate of mitochondrial genome. Mitochondrial genome MN537973 was assembled and annotated by using the programs DOGMA and MITOS. Twelve protein-contig genes were predicted including cox1-3, nad1-6, nad4L, atp6, and cytb that encoded a total of 3,284 amino acids. Gene atp8 was not present. All genes in MN537973 were arranged as in KM\_397348. Gene nad2 showed the highest level of nucleotide diversity, and gene nad6 showed the lowest level of nucleotide diversity using sliding window analysis. A total of 22 transfer RNAs and two noncoding regions were predicted in MN537973. The 22 tRNA genes ranged from 61–71 bp length. The two rRNAs were separated by tRNA-Thr and were located between cox1 and cox2. This genome also contained two AT-loops which were located between cytb and tRNA-Glu. The overall A+T content was 63.83%. The most frequent initiation codon was ATG, followed by GTG, and the most often present termination codon was TAA. The two F. elongatus mitochondrial genomes isolated from Tianmen and Shanghai China had 98.73% nucleotide identity. The organization of the mitochondrial genome is shown in **Figure 3.20**.<sup>62</sup>



**Figure 3.20** Arrangement of the mitochondrial genome of *Fischoederius elongatus* from Shanghai, China (GenBank: MN537973). The mitochondrial genome is 14,288 bp in length containing 12 protein-coding genes, 22 tRNA genes, 2 rRNA genes and 2 non-coding regions, encoded. The 12 protein-coding genes are arranged in the following order; *cox*3, *cyt*b, *nad*4L, *nad*4, *atp*6, *nad*2, *nad*1, *nad*3, *cox*1, *cox*2, *nad*6 and *nad*5. The two rRNAs are separated by tRNA-Thr and are located between *cox*1 and *cox*2. AT-loops are located between *cytb* and tRNA-Glu.<sup>62</sup>

# 3.3 Transcriptome study of trematode

#### 3.3.1 Definition of transcriptome

The transcriptome is defined as the complete set of all RNA molecules, including mRNA, rRNA, tRNA and other non-coding RNA transcribed in a cell or a population of cells. The quantity of each transcript can demonstrate the gene expression pattern in the analyzed tissue/cell and will show a wide range due to the required amounts for each product involved in various biological processes. It might also be indicative for healthy and disease state. Essential techniques for transcriptome analysis are real-time quantitative PCR (qPCR) and RNA-Seq. 63-66

# 3.3.2 Transcriptome Techniques

# 3.3.2.1 Real-time quantitative polymerase chain reaction

Real-time quantitative polymerase chain reaction (qPCR) analyzes gene expression by visualizing the abundance of the transcript in real time progression. The technique is highly quantitative and sensitive and is mostly used to explore a relatively small number of transcripts in a large set of samples. The general principle of real-time qPCR is based on polymerase chain reaction. The process consists of a series of temperature changes including the denaturing stage at 95°C to allow the separation of the double chain nucleic acid into single chains, the annealing stage at between 50–60°C to allow the binding of the primers with the template, and the extension stage at between 68–72°C to facilitate synthesis by DNA polymerase. During the thermal cycle of PCR, the fluorescence intensity of each target transcript is detected according to its amount in the sample. There are two types of real-time qPCR for generating the fluorescence emission; using (1) the double-stranded DNA-binding dyes and (2) the hybridization probes. <sup>67-69</sup>

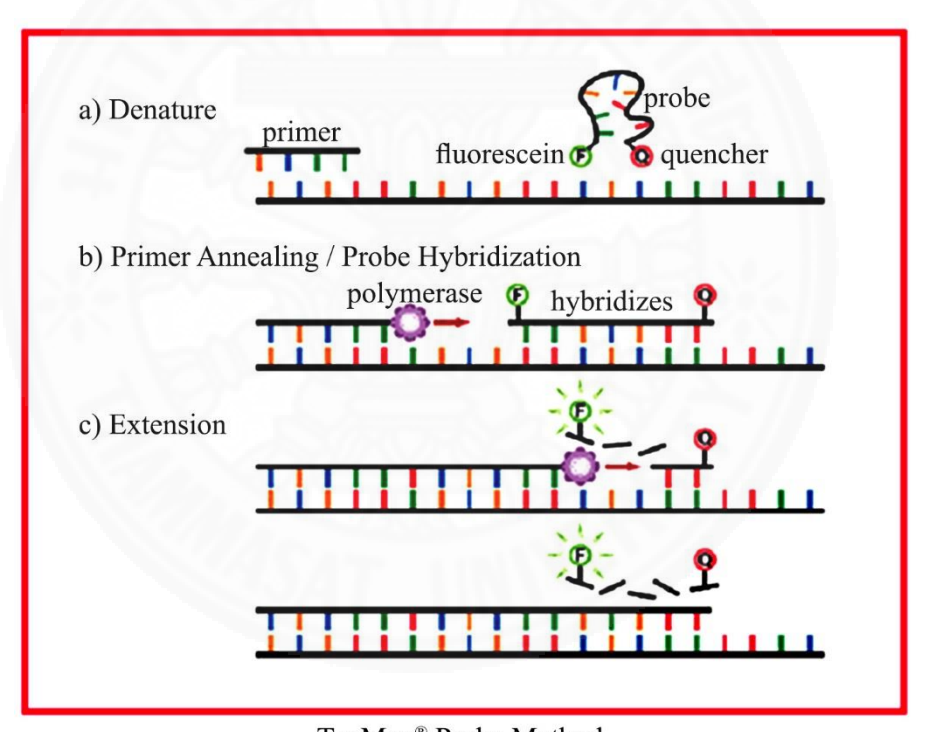
# (1) Double-stranded DNA-binding dyes

Real-time qPCR with non-specific double-stranded DNA-binding dyes that act as reporters. The dyes bind at the minor groove of all double-stranded DNA in extension stage, then the fluorescence is excited and emitted in denaturing stage. An increase of DNA product during PCR cycle leads to increase of the fluorescence intensity that is measured by a detector. The fluorescence level of target transcripts is usually normalized against a stable expressed gene to ensure

accuracy in the quantification. 67, 68

# (2) Hybridization probes

A hybridization reporter probe significantly increases specificity of real-time qPCR. Fluorescent dyes detect only the DNA containing the specific probe sequence that allows the detection of several genes in the same reaction. DNA-based probe is designed with a fluorescent reporter at 5' end and a quencher of fluorescence at 3' end of the probe. During the polymerization, *Taq* polymerase, containing 5' to 3' exonuclease activity, breaks the reporter-quencher proximity and allows the emission of fluorescence. An increase of target product in each thermal cycle causes a proportional increase in fluorescence. <sup>67, 68</sup>



TaqMan® Probe Method

**Figure 3.21** TaqMan® hybridization probe method; (**a**) Denaturing stage: An intact reporter fluorescence is quenched; (**b**) Annealing stage: Probes hybridized to the template and reporter fluorescence is still quenched; (**c**) Extension stage: During PCR, the probe is degraded by the *Taq* polymerase and the fluorescent reporter released.<sup>70</sup>

# 3.3.2.2 RNA-Seq

# (1) Illumina® next-generation sequencing (NGS) platform

Next-generation sequencing (NGS) has been developed for massively parallel analysis allowing for increased base coverage. NGS provides ability to look at gene expression level, gene fusion, gene mutations, transcription processes, post-transcriptional modifications and biological pathway changing. 71, 72 Illumina® dye sequencing is one technique of NGS, an invention of Solexa Company. This sequencing method is based on a clonal array formation and reversible dye-terminators enabling the identification of single bases that are introduced into DNA strands. The workflow of this techniques is in three basic steps: amplify, sequence and analyze as shown in Figure 3.22. The sequencing process begins with the ligation of DNA fragments to adapters at both ends. Then, the DNA templates are immobilized onto the flow cell surface and several million dense clusters of double-stranded DNA are generated by solid-phase bridge amplification. The sequencing is provided through sequencing by synthesis (SBS). During each sequencing cycle, four reversible dye-terminators bases are added and incorporated at the binding sites on the DNA template. After laser excitation, the fluorescent dye is captured to identify the base, and enzymatically cleaved out to allow competing of next nucleotide into the template. The sequencing cycles go on to determine the sequence, one base at a time. The sequence data are collected and aligned to references. This technique offers high accurate large-scale sequencing and gains actual sequencing data rapidly. 72-76 Illumina® sequencing is widely used in trematode transcriptome study, e.g. Schistosoma mansoni, 77 S. turkestanicum<sup>78</sup> and Fasciola gigantica.<sup>79</sup>

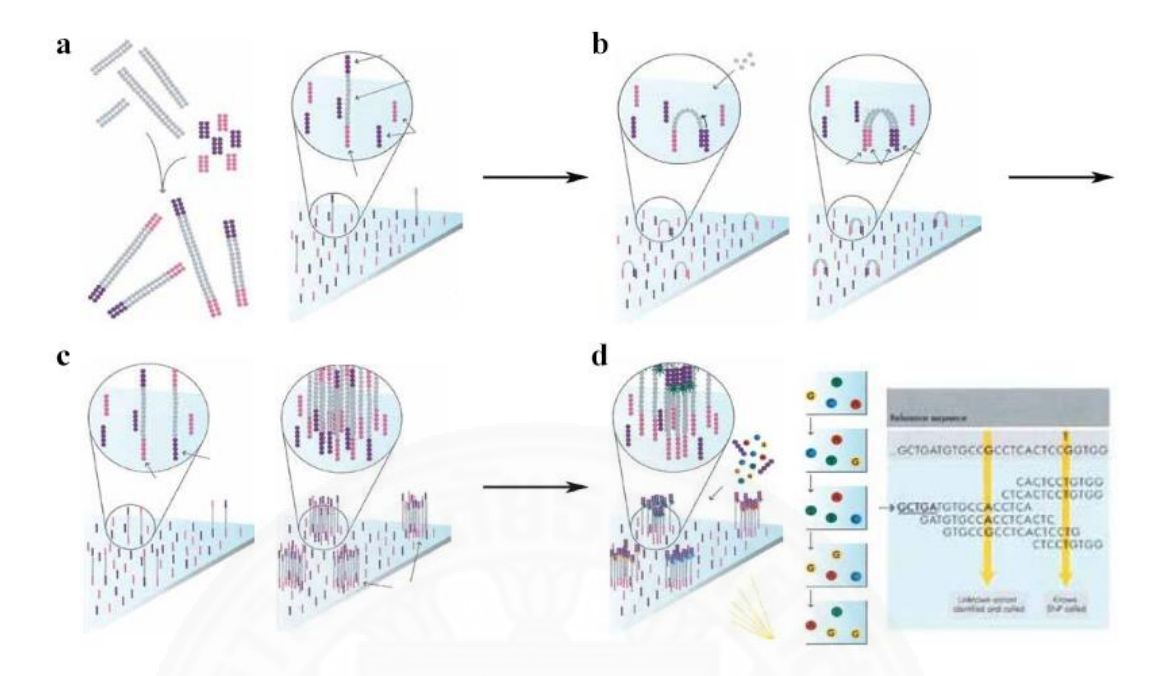


**Figure 3.22** Illumina<sup>®</sup> sequencing; (a) Randomly fragmented DNA is ligated into adapters and bound to the flow cell surface; (b) Unlabeled nucleotides and enzyme are added to initiate solid-phase bridge amplification and generated double-stranded DNA templates; (c) The double-stranded DNA templates are denatured to form single-stranded templates, and repeated amplification, resulting in several million dense clusters of double-stranded DNA on the flow cell surface; (d) Four labeled reversible terminators nucleotides are added and incorporated into DNA template, then the emitted fluorescent from each cluster is captured after laser excitation. The complementary base is identified, the sequence data is collected and aligned to a reference.<sup>74</sup>

# (2) Transcriptome Assembly

Transcriptome is generated from raw sequence reads by using assembly methods. A reference-based assembly is operated by mapping raw sequences on to a reference genome. The genome alignment reconstructs and characterizes the order of transcript sequences. However, this method is incapable for incidents of structural alterations of mRNA transcripts *e.g.* alternative splicing. In case a genome sequence is not available then *de novo* assembly is used for creating the transcriptome. The assembly is calculated by computer algorithms that determine and compile the overlaps between each pair of reads. The quality of *de novo* assembly is verified by aligning the assembled sequences of conserved genes to the sequences from closely related species. 80-82

For example, the program Trinity performs *de novo* assembly of transcriptome base on mapping-first approaches. Trinity has three steps including Inchworm, Chrysalis, and Butterfly. Inchworm reads the raw transcript data and tries to concatenate the single small reads. As a result a set of the longest paths possible for each k-mer appears. Then, Chrysalis merges all the paths in the set. In the end Butterfly cuts the unnecessary edges and extracts all possible sequences. The full-length assembly in all steps using de Brujin graphs as shown in **Figure 3.23**.<sup>80</sup>

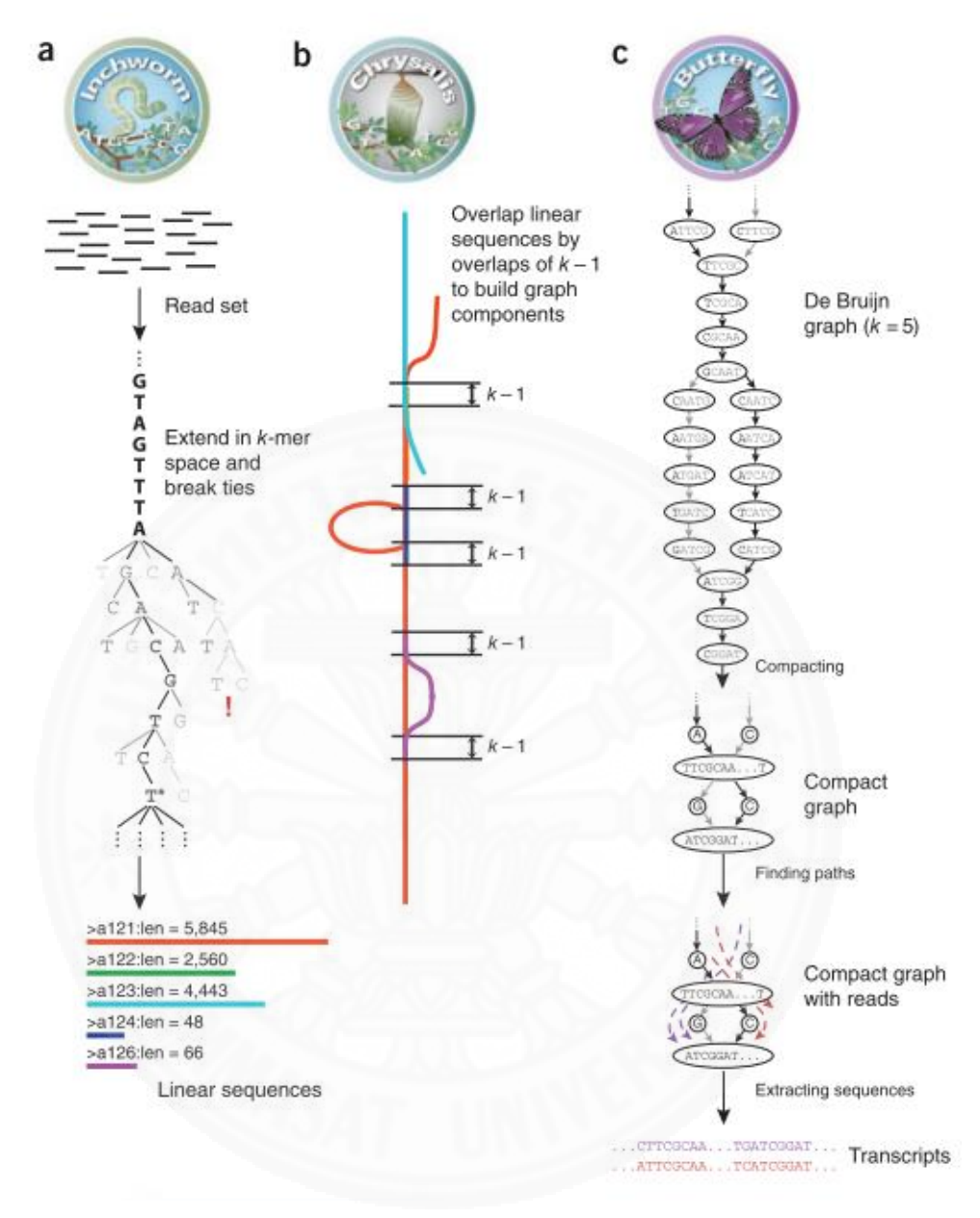


Figure 3.23 Trinity assembling overview (a) Inchworm; (b) Chrysalis; (c) Butterfly.<sup>80</sup>

### 3.3.3 Transcriptomes of trematodes

Some of the most neglected tropical diseases in mammals are caused by parasite flatworms including *Schistosoma mansoni*, *Fasciola hepatica*, *F. gigantica*, *Opisthorchis viverrini*, *Clonorchis sinensis*, *Paramphistomum cervi*, *Calicophoron daubneyi*, and *Fasciolopsis buski*. Currently, only a limited set of effective drugs and vaccines candidates are available. Hence, many researches focus on the investigation of the key targets for parasiticidal chemotherapy. By using next-generation sequencing (NGS) technologies such as 454-Roche and Illumina, the transcriptomes of the adult stage of trematodes were characterized and analyzed by bioinformatics platforms based on homology, gene ontology, and pathway mapping. The most abundant putative proteins might be the intervention targets that play regulatory roles in host-parasite interactions and pathogenesis. Understanding the present transcriptome data of trematodes provides fundamental knowledge for further investigation and development of novel treatment and control of these parasites.

### 3.3.3.1 Schistosoma mansoni

Six stages of Schistosoma mansoni were used to obtain 163,000 expressed-sequence tags (ESTs) from normalized cDNA libraries. ESTs were assembled and generated 31,000 sequences, representing 77% of putative new S. mansoni gene fragments. Fourteen thousand genes were predicted by using BLASTX searching against the Swiss-Prot dataset. Serial analysis of gene expression (SAGE) suggested that 50% of all genes were active in adult stage. Gene ontology classification of S. mansoni transcriptome showed that the most frequently identified biological process categories were protein metabolism, nucleic acid metabolism and transport. The metazoan-specific and eukarya-conserved sequences were characterized by comparison with known proteomes. The results showed that the metazoan-specific genes had essential role for eukaryotic cell function. S. mansoni transcriptome data also represented the alternative drug and vaccine targets. For example, L-type calcium channel alpha subunit gene that is a paralogous gene of calcium channel subunits, the target of praziquantel, might act as a new anthelminthic target; A group of homologs of *Plasmodium* circumsporozoite protein represented potential surface-exposed proteins of the parasite with potential as vaccine candidates. 83, 84

#### 3.3.3.2 Fasciola hepatica

The transcriptome of adult Fasciloa hepatica sampled from a sheep with naturally acquired infection was characterized by using 454-Roche next generation sequencing. More than 590,000 reads were generated and used for de novo assembly. A total of 135,645 unique sequences after assembly were searched against the present sequence database, including NCBI non-redundant sequence databases for both public nucleotide and protein sequences, SchistoDB for S. mansoni and the Shanghai Centre for Life Science & Biotechnology Information for S. japonicum. The result showed 82.4% of the sequences were novel sequences. ORFs were predicted from 73,180 of re-clustered sequences with 15,423 ORF-enriched contigs. Comparative genome analysis between F. hepatica and other organism showed that F. hepatica had the highest similarity with *Schistosoma* spp. at 40.1%, E-value < 1E<sup>-05</sup>. All predicted proteins were classified for potential molecular function and biological pathway which might lead to discovery of potential targets for drug and vaccine development. Examples of those were the excretion/secretion proteins that are involved in hostparasite interaction, e.g. protease, antioxidant, fatty acid-binding protein and prolylcarboxypeptidase-like proteins. Importantly, cysteine peptidases that are significant for trematode interventions were classified with similarity to known sequences, including cathepsin B, cathepsin L, and legumain, and novel sequences in the family Fasciolidae, including calpain and cathepsin F. 85, 86

### 3.3.3.3 Fasciola gigantica

The transcriptome of adult stage *Fasciloa gigantica* was characterized using Illumina high-throughput sequencing and bioinformatics platform. More than 20 million raw read sequences were generated and submitted to the NCBI databases with the accession number SRA024257. A total of 30,525 unique sequences was established after assembly. Sequence homology between *F. gigantica* and key eukaryotes were analyzed using BLASTX. The results showed that 91.0% of *F. gigantica* sequences matched with NCBI non-redundant sequence databases. The highest sequence similarity was found in *F. hepatica*. Comparative protein sequence analysis among the Trematoda showed that 38.3% of the sequences in family Fasciolidae (*F. gigantica* and *F. hepatica*) had highest conservation to sequences in the family Schistosomatidae followed by family Opisthorchiidae (26.8%). Only 253

protein sequences of *F. gigantica* were highest conserved in other trematodes but distinct in other eukaryotes, including proteases, membrane transporter protein and protein associated cellular signaling pathway. These proteins might represent key proteins in the host-parasite interaction. Based on gene ontology and KEGG pathway annotation, the most abundant transcripts of *F. gigantica* play important roles in the host immune modulation, including antioxidant molecules and proteases. For example, peroxiredoxin, thioredoxin and glutathione transferases interrupt the host-derived reactive oxygen species from the flukes. Cysteine proteases, catalytic enzymes, cleave host immunoglobulins. In conclusion, transcriptome study of *F. gigantica* provided biological knowledge of the flukes and essential information for development of novel trematode interventions.<sup>79</sup>

### 3.3.3.4 Opisthorchis viverrini

transcriptome of **Opisthorchis** viverrini was characterized by 454-Roche sequencing. More than 600,000 sequences were generated and assembled by an automated in silico assembly pipeline. A total of 162,487 sequences after assembly was collected, and 66.0% of those was predicted as ORF containing. Then the sequences with ORFs were re-assembled into supercontigs, resulting in 14,698 sequences of ORF-enriched supercontigs. Annotation of predicted proteins in transcriptome dataset revealed 33.3% of ORF-enriched sequences matched with available sequences in NCBI databases. About 70% of protein sequences from the transcriptome dataset were novel proteins. Predicted proteins of O. viverrini transcriptome shared greatest similarity to proteins of other trematodes (Clonorchis sinensis, S. mansoni, S. japonicum and F. hepatica) with 21.5% mean similarity. A total of 10,835 protein sequences showed high conservation with O. viverrini but no match with other trematodes. Protein functions were characterized based on gene ontology and KEGG pathway annotation. The results established 1,271 GO terms and 249 biology pathway terms. The protein functions of putative excretion/secretion proteins, which were identified by presence of a signal peptide and absence of a transmembrane domain, were predicted. ES products involved in metabolic pathways and the immune system were identified. These proteins were implicated in the development of O. viverrini induced cholangiocarcinoma. Thus, ES products are potential candidates for drug and vaccine strategies.<sup>87</sup>

#### 3.3.3.5 Clonorchis sinensis

The transcriptome of *Clonorchis sinensis* was characterized by using massive high-throughput sequencing. A total of 574,448 raw reads sequences were generated, assembled and searched for protein homology. 19,047 *C. sinensis* ORF-enriched sequences matched with known proteins in the NCBI databases. *C. sinensis* had the highest similarity with other trematodes, including *S. mansoni*, *S. japonicum*, *F. hepatica* and *O. viverrini*. 9,527 proteins were uniquely found in *C. sinensis*. Comparative genome analysis among *C. sinensis*, selected nematodes and mammals showed *C. sinensis* predicted proteins had greater similarity to mammals than nematodes. Base on gene ontology and KEGG pathway, the protein functions profiles of *C. sinensis* were similar with *O. viverrini*. A significant proportion of predicted proteins was associated with metabolic processes and immune system. For example, the peptidases in the parasite excretion/secretion product play a role in immune modulation by cleaving host immunoglobulin. These proteins are a virulent factor in the pathogenesis of cholangiocarcinoma. Further study of those proteins will provide knowledge for novel drug and vaccine development.<sup>87</sup>

### 3.3.3.6 Paramphistomum cervi

Transcriptome analysis of the rumen fluke *Paramphistomum cervi* from three different definitive hosts (sheep, goat and buffalo) provided a total of 7,433,721 raw reads in pooled data by using Ion Torrent PGM platform. The raw reads were assembled and filtered to remove contaminating sequences from *Bos taurus*, resulting in 3,272,893 total reads (43,753 transcript contigs). The assembled transcripts included a total of 7,003 full-length and open reading frame complete sequences. Parasite species identification was done by using bi-directional BLASTN against the complete *P. cervi* mitochondrion genome. The result showed high identity of *P. cervi* contig sequence with cytochrome oxidase subunit I. BLASTN alignment matched with the complete *P. cervi* mitochondrion genome sequence at E-value = 3.00e-70. Transcriptome annotation showed that 53.6% of the predicted proteins from *P. cervi* had similarity to proteins in NCBI databases. The proteins that had the highest percentage of top-hits were *C. sinensis* proteins. Comparison of transcript abundance among three different definitive hosts revealed the highest expression of transcripts was established in sheep. Proteins that play important roles in parasite living or in host-

parasite interaction were upregulated *e.g.* fatty acid binding proteins, cysteine proteases. T-cell epitope was predicted to serve as the potential targets for vaccine candidates. Cathepsin L was identified through the epitope GSISIAINA that was conserved in all transcriptome datasets of *P. cervi* isolated from three different definitive hosts. The presented data will provide the fundamental biological knowledge in this parasite and support identification of novel targets in vaccine development.<sup>88</sup>

### 3.3.3.7 *Calicophoron daubneyi*

The transcriptome of adult Calicophoron daubneyi from an individual specimen collected from a bovine host was performed on an Illumina HiSeq2500 platform. A total of 226,188,786 raw reads sequences were generated and then, 54,617 unique genes components were identified from the raw assembled sequences while 69.51% of gene components were observed without BLASTX/P annotation. Thirty eight of the 50 most highly expressed gene sequences showed significant conservation with the SRA files for P. cervi (accession no. SRA091604, SRA039814, SRA091607). All of those are unidentified components. Most of the highly expressed genes are involved in reproduction e.g. eggshell and vitelline protease, respiratory process, tubulin, and ferritin. Only 1.8% of the peptides encoded in the C. dauvbneyi transcriptome were predicted to contain a signal peptide. Other trematodes showed higher numbers of peptides with a signal peptide, e.g. 4.1% in Fascioloides magna and 5.1% in F. gigantica. Gene Ontology (GO) analysis showed that most of biological process terms were related to organic substance, primary and cellular metabolic processes. Most molecular function terms were related to binding activities. The cellular component terms were identified as intracellular and membrane component terms. Transcriptome data showed that all of phase I, II and III detoxification genes were obtained in the C. dauvbneyi transcriptome which might be related to their survival in the extreme environment of the cattle including CYP450s, GSTs and FABPs, respectively. CYP450 genes were identified as cytochrome P450 monooxygenase and NADPH-cytochrome P450 reductase with the key motifs. CYP450s are involved in parasite biology and xenobiotic detoxification. A total of 19 GST genes in 4 GST classes were identified in the transcriptome data. These proteins play roles as antigens and immunomodulators. FABPs were also found in the highest abundant proteins in proteome study including CdFABP IL1 and CdFABP IL2. FABPs might play an important role in survival in the rumen environment. The presence of FABPs and peptidase proteins in the *C. dauvbneyi* transcriptome is comparable to nearby trematodes, *e.g. F. magna* and *F. hepatica*. This study supports further analysis of host-parasite interaction at rumen stage.<sup>89</sup>

### 3.3.3.8 Fasciolopsis buski

The Illumina HiSeq1000 platform was transcriptome analysis of Fasciolopsis buski. A total of 32.01 million paired end reads were generated with high quality raw reads. 12,380 annotated genes of 30,677 unigenes were found by searching against NCBI non-redundant (nr), Uniprot/Swissport, and Uniprot/trEMBL databases. 6,752 unigenes were detected in all three databases. NCBI BLAST analysis showed that F. buski sequences had significant matches with C. sinensis, S. mansoni, and S. japonicum, and less with Fasciola spp. A total of 1,406 putative ES proteins were predicted based on the presence of signal peptides. Based on Clusters of Orthologous (COG) analysis most unigenes were mapped to General function partion. A total of 6,658 unigenes were matched with 36,433 gene ontology terms. Most of them were involved with cellular component organization and multicellular organism process. By comparison with other trematode transcriptome datasets including F. hepatica, F. gigantica, C. sinensis, O. viverrini, S. mansoni, and S. japonicum, 54% of the unigenes were found in any individual trematode and 19% of the unigenes were found in all trematodes. Venn diagram of homologous proteins showed that F. buski was related to Fasciolidae supported by strong bootstrap. Highly expressed genes of F. buski transcriptome were linked to translation process. A total of 478 peptidase proteins were identified classified into six catalytic types and 138 protease inhibitors by searching against MEROPS databases. Serine protease was the highest expressed protease, followed by protease inhibitor and cysteine protease. This expression pattern is different from other trematodes. Those proteases play important roles in host-parasite interaction, e.g. immune evasion. Moreover, the most highly expressed genes represented functions in metabolic process and reproductive process. For example, cytoskeleton protein plays a role in glycogen storage in adult parasite. FABP has functions in lipid transport and storage. Globin genes might be involved in oxygen transport and scavenger in parasite. F. buski transcriptome contained transposable elements and expressed genes involved in RNAi pathway. These

transcriptome data provided biological knowledge for parasite diagnosis and vaccine innovation.  $^{90}$ 

### 3.4 Parasite excretion/secretion (ES) product

### 3.4.1 Definition of parasite excretion/secretion product

Flukes release excretory/secretory products through the excretory system and cellular secretory pathways especially tegumental layer, digestive tract and reproductive tract epithelia. Parasites also adapt these secretory proteins for key roles in host-parasite interactions. Parasite excretory/secretory products act as antigens which induce inflammation processes and immunoregulation. The major proteins of parasite excretory/secretory product are proteases which for example show activity in parasite invasion and degradation of host chemokines, in addition they stimulate host immune responses. <sup>91</sup>

### 3.4.2 Parasite protease

Proteolytic enzymes or proteases are enzymes which break down proteins into peptides or amino acids by hydrolysis of the peptide bonds. Proteases are categorized as exopeptidases and endopeptidases depending on their site of action. Exopeptidases catalyze the hydrolysis of the terminal amino acid of a peptide chain, while endopeptidases catalyze the cleavage of internal peptide bonds in polypeptides or proteins. Proteases are involved in a large number of regulatory processes, e.g. nutrient digestion, protein activation and inflammation. 92 Parasites migrate through the host tissue by the release of proteolytic enzymes that degrade tissue barriers. This action stimulates host tissue inflammation. For example, parasite larvae secret serine proteases or metalloproteases into the ES product for migration through the intestinal wall or through skin or subcutaneous tissue. Parasite proteases also help parasites evade the immune response by host immunoglobulin degradation. Schistosoma mansoni releases an elastase-like serine protease activity that degrades IgE from both humans and rodents. Therefore, parasite proteases are major virulence factors in the pathogenesis of parasite diseases via parasite-host interactions. They are recruited as the key target for developing control programs for parasitic diseases.<sup>93</sup>

### 3.4.3 Excretion/secretion product of Fischoederius elongatus

Arunkumar and Krupakaran (2016) studied the polypeptide profile in the excretion/secretion product of *F. elongatus* collected from cattle. The ES product of the flukes was collected after 16 hours culture in RPMI-1640 medium. Protein concentration was 1.20 μg/μL and the proteins were separated by SDS-PAGE. Silver staining revealed bands ranging from 14 to 66 kDa molecular weight. Prominent protein bands were observed at 14, 20, and 66 kDa. Minor protein bands were observed at 35, 40, and 95 kDa. The polyacrylamide gel of *F. elongatus* ES product is shown in **Figure** 3.24. The prominent proteins might be suitable antigens for further studies in immunodiagnosis.<sup>48</sup>

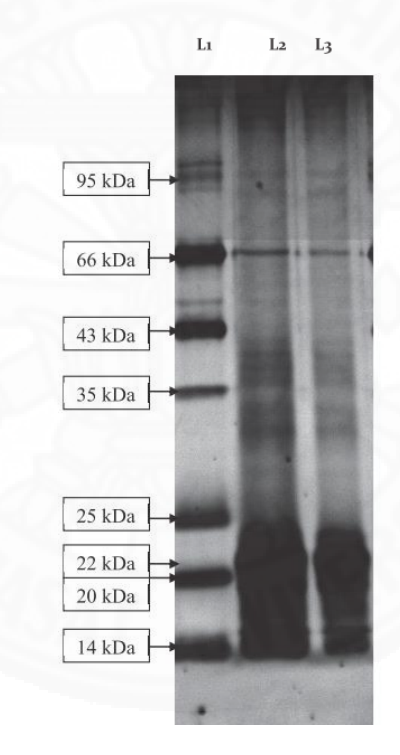


**Figure 3.24** Silver-stained polyacrylamide gel of resolved *Fischoederius elongatus* ES product.<sup>48</sup>

Lane 1: Mid range protein marker

Lane 2: F. elongatus ES product (12 µg)

Lane 3: F. elongatus ES product (6 µg)

# CHAPTER 4 RESEARCH METHODOLOGY

### 4.1 Morphology of Fischoederius elongatus

### 4.1.1 Collection of Fischoederius elongatus

Fischoederius elongatus specimens were collected from the rumen of naturally infected cattle sacrificed at a local slaughterhouse. The flukes were washed several times in PBS pH 7.2, and then cultured in RPMI-1640 for 2 hours to allow the flukes to regurgitate cecal contents. The flukes were stored in liquid nitrogen until used in further experiments.

### 4.1.2 Microscopic examination of whole fluke image

A single *F. elongatus* specimen was flattened between two glass slides to examine it morphology using a Nikon SMZ445 stereo microscope with a C-LEDS Hybrid LED Stand (Nikon Corporatation, Tokyo, Japan) at 0.8X objective magnification. Whole fluke image was taken using an iPhone 7 (Apple Inc., CA, USA) with an iDu LabCam microscope adapter for 80 iPhone 7/8 with multi-fit wide field 10× ocular (iDu Optics LLC, NY, USA). Due to the large size of some specimens two overlapping images had to be merged to obtain a whole image.

#### 4.1.3 Semichon's carmine whole mount staining

Single *F. elongatus* specimens were flattened between two glass slides and fixed in alcohol-formal acetic acid (AFA) fixative. The fixed flukes were dehydrated in 70% [v/v] ethanol for 30 minutes and immersed in Semichon's carmine overnight at room temperature. The stained flukes were dehydrated in 80% to 95% [v/v] serial ethanol, each step for 30 minutes, and counter-stained with fast green for 2–3 seconds. The stained flukes were dehydrated in absolute ethanol for 30 minutes and cleared with xylene for 1 hour. The flukes were mounted with Permount (Thermo Fisher Scientific, MA, USA) and examined under a light microscope.

### 4.1.4 Hematoxylin and eosin staining of parasite tissue section

### 4.1.4.1 Tissue embedding and tissue section

Freshly collected F. elongatus specimens were fixed in

Bouin's fixative solution (Sigma, MO, USA) overnight at room temperature. The fixed flukes were gradually dehydrated in 70%, 80%, 95%, and 100% [v/v] ethanol with each step repeated 3 times, 20 minutes each step. Absolute ethanol was replaced with xylene three times, 10 minutes each to clear the parasites. The parasites were then incubated in xylene:paraplast mixed at ratios 2:1, 1:1, 1:2 at 60°C, 1 hour each step. Then the parasites were incubated in pure paraplast at 60°C, three times, 1 hour each step. Finally, the tissue was embedded in paraplast. The embedded tissue was cut into 8-μm cross serial-sections on a microtome. The sections were placed on gelatin coated microscopic glass slides and processed for further analysis.

### 4.1.4.2 Hematoxylin and eosin staining

The serial-sections were dewaxed in xylene for 20 minutes and rehydrated in graded ethanol series from 100%, 95%, 80%, 70% [v/v], 5 minutes each step. The hydrated sections were washed with tap water. Basophilic substances of the tissue were stained with progressive hematoxylin. Nuclear coloration was converted from reddish purple to a crisp blue by bluing solution. The tissue was counter-stained with eosin which binds to acidophilic substances in a tissue. The stained tissue was dehydrated in graded ethanol series from 95% to 100% [v/v], 1 minute each step, and preserved in xylene, 10 minutes. The tissue was mounted in xylene based mounting medium and observed under a light microscope.

### 4.1.4.3 Image capture of tissue sections

Tissue histology was examined using a Olympus BX51 microscope (Olympus Corporation, Tokyo, Japan) at 4.0×, 10.0×, and 20.0× objective magnification. Images were recorded using a PixeLINK PL-B623 3MP microscopy digital camera (Aegis Electronic Group, Gilbert, AZ) and PixeLINK Capture Software. Merged images of whole specimens were created by using the function 'Photomerge' with setting 'Reposition and Blend Images Together' in the program Adobe Photoshop CS6 version 13.0 (Adobe Systems, CA, USA).

### 4.2 Molecular identification of *Fischoederius elongatus* ribosomal ITS2

### 4.2.1 Isolation of *Fischoederius elongatus* total RNA extraction

A single F. elongatus specimen from Section 4.1.1 was

homogenized in TRIzol® reagent (Ambion™ Life Technologies, MA, USA) using a tissue homogenizer (1 mL of TRIzol® reagent per 50-100 mg of tissue). The homogenate was centrifuged at 12,000×g for 10 minutes at 4°C. The clear supernatant was transferred into a new tube, and then incubated for 5 minutes at room temperature before 0.2 mL of chloroform per 1 mL of TRIzol® reagent was added. The tube was capped and shaken vigorously by hand for 15 seconds, and then incubated for 2-3 minutes at room temperature. After that, the sample was centrifuged at 12,000×g for 15 minutes at 4°C. The colorless upper aqueous phase was carefully transferred to a fresh tube. 0.5 mL of isopropyl alcohol per 1 mL of TRIzol® reagent was added, and then incubated for 10 minutes at room temperature. The sample was centrifuged at 12,000×g for 10 minutes at 4°C. The supernatant was removed. The pellet was washed with 75% ethanol, and then centrifuged at <7,500×g for 5 minutes at 4°C. The RNA pellet was dried and then redissolved in RNase-free water. The RNA quality was analyzed by 1.2% denaturing agarose gel electrophoresis. The concentration of RNA was measured on a NanoDrop ND-2000 UV-Vis Spectrophotometer (Thermo Fisher Scientific, MA, USA). The ratio of absorbance at 260 nm and 280 nm was used to assess the purity of RNA. Total RNA was kept at -80°C.

### 4.2.2 DNase treatment of total RNA Fischoederius elongatus

F. elongatus total RNA was treated with DNase I (Promega<sup>TM</sup>, WI, USA). The reaction samples contained the following components;

Components	Volume (µL)
Total RNA from each stage (1 µg)	X
DNase I (1U/µL)	1.0
10× DNase reaction buffer	2.0
Oligo(dT)20 primer (10 µM)	1.0
DEPC-treated distilled water	to 20.0
Total volume	20.0

The reaction sample was incubated for 30 minutes at 37°C. The reaction was stopped by adding DNase stop solution (20 mM EGTA, pH 8.0) and by incubation at 65°C for 10 minutes. DNase-treated RNA was kept at –80°C.

### **4.2.3** Reverse Transcriptase Polymerase Chain Reaction (RT-PCR)

The *F. elongatus* ribosomal ITS2 cDNA was generated and amplified by reverse transcriptase polymerase chain reaction (RT-PCR) using RevertAid<sup>TM</sup> RT Reverse Transcription Kit (Thermo Fisher Scientific, MA, USA). *F. elongatus* total RNA was used as template to generate first standard cDNA by using the following components;

Components	Volume (µL)
Total RNA (100 ng)	X
Oligo(dT) <sub>20</sub> primer (10 $\mu$ M)	1.0
DEPC-treated distilled water	to 12.5
Total volume	12.5

The reaction mixture was gently mixed and incubated for 5 minutes at 65°C due to a GC-rich RNA template. Then, the following components were added into the reaction.

Components	Volume (µL)
5× RevertAid <sup>TM</sup> reaction buffer	4.0
RiboLock <sup>TM</sup> RNase Inhibitor (20U/ $\mu$ L)	1.0
10 mM mixed dNTPs (2.5 mM each)	2.0
RevertAid <sup>TM</sup> Transcriptase (200U/ $\mu$ L)	1.0
Total volume	20.0

The reaction mixture was gently mixed and the cDNA was synthesized at  $42^{\circ}$ C for 60 minutes. The reaction was terminated by incubation at  $70^{\circ}$ C for 10 minutes. The first strand cDNA was stored at  $-20^{\circ}$ C.

The *F. elongatus* ribosomal ITS2 cDNA was generated and amplified by reverse transcriptase polymerase chain reaction (RT-PCR) using;

AG40 ribosomal ITS2 FW: 5'- GGTACCGGTGGATCACTCGGCTCGTG -3'
AG41 ribosomal ITS2 RV: 5'- GGGATCCTGGTTAGTTTCTTTTCCTCCGC -3'

The PCR reaction was prepared with the components below;

Components	Volume (µL)
Template	2.0
Forward primer (10µM)	1.0
Reverse primer (10µM)	1.0
10× KCl buffer	5.0
MgCl <sub>2</sub> (25mM)	3.0
Mixed dNTPs (2.5 mM each)	1.0
Taq DNA polymerase $(5U/\mu L)$	0.5
Distilled water	37.5
Total volume	50.0

The amplification of cDNA encoding ribosomal ITS2 was carried out on a thermocycler: pre-denaturation at 95°C for 5 minutes, 35 cycles of denaturation at 95°C for 1 minute, annealing at appropriate temperature for 1 minute, extension at 72°C for 1 minute and final extension at 72°C for 10 minutes. The PCR product was resolved on a 0.7% [w/v] agarose gel. PCR amplicons with the expected size were used for sequencing and cloning.

#### 4.2.4 Agarose gel electrophoresis

F. elongatus DNA and RNA integrity were determined by non-denaturing agarose gel electrophoresis in 0.7% [w/v] and 1.2% [w/v] agarose gels, respectively. Ultrapure™ agarose powder (Invitrogen, Carlsbad, CA, USA) was weighted to the final concentration requirement. The powder was dissolved in 0.5× TBE electrophoresis buffer (22.5 mM Tris-base, 22.5 mM boric acid, 1 mM EDTA, pH 8.0) in a microwave oven until fully homogeneous. The 10000× ViSafe Green Gel Stain (Vivantis Technologies Sdn. Bhd., Selangor Darul Ehsan, Malaysia) was added to a 1× final concentration and the solution was poured into a gasketed UV transmissible gel tray with an appropriate comb. The gel was left to harden for 60 minutes. After the gel had set, it was submersed in 0.5× TBE electrophoresis buffer in a gel electrophoresis chamber (Horizon®, Gibco-BRL, USA). Each sample was mixed with 10× sample nucleic acid electrophoresis loading buffer (0.25% [w/v] bromophenol

blue, 0.25% [w/v] xylene cyanol FF, and 50% [v/v] glycerol) to a 1× final concentration and loaded into a well of the agarose gel. An appropriate DNA ladder (Thermo Fisher Scientific, MA, USA) was loaded as a marker to estimate the size of nucleic acid bands in a lane. Gel electrophoresis was performed at 80V (PowerPac Basic Power Supply, Biorad, CA, USA) for 1–2 hours or until the bromophenol blue dye front had migrated about 2/3 of the gel length. Nucleic acid bands were visualized and recorded on a UV transilluminator gel documentation system (Major Science, CA, USA).

### 4.2.5 DNA Extraction from agarose gels using Thermo Scientific GeneJET Gel Extraction Kit

DNA fragments were extracted by using Thermo Scientific GeneJET Gel Extraction Kit (Thermo Fisher Scientific, MA, USA) according to the manufacturer protocol. An agarose block containing the DNA fragment was excised from the agarose gel using a clean scalpel and transferred into a microtube. The weight of the agarose block was measured and 1.0 vol of Binding buffer was added. The mixture was incubated at 50-60°C for 10 minutes and mixed by tube inversion every 2–3 minutes to allow the agarose to fully dissolve. In a case that the DNA fragment was less than 500 bp in size, 1 vol absolute isopropanol was added. The solution was transferred into a GeneJET purification column and centrifuged at 10,000×g, room temperature for 1 minute. The flow-through was discarded. Additional 100 µL of Binding Buffer was added to the column, followed by centrifugation as above and the flow-through was discarded. 700 µL of Wash Buffer with ethanol was added to the column and centrifuged as above. The empty purification column was again centrifuged as above to allow complete removal of wash buffer. Then the column was put into a new microcentrifuge tube, 30-50 µL Elution buffer was added to the column and the column was again centrifuged as above. The eluted DNA was stored at -20°C for further analysis.

## 4.2.6 Plasmid purification using Thermo Scientific GeneJET Plasmid Miniprep Kit

Plasmid DNA was extracted by using Thermo Scientific GeneJET Plasmid Miniprep Kit (Thermo Fisher Scientific, MA, USA) according to the manufacturer protocol. A positive transformant colony of *Escherichia coli* XL1-Blue containing recombinant pGEM®-T Easy was inoculated in 5 ml LB broth supplemented

with 100 µg/ml ampicillin and incubated at 37°C, 240 rpm for 12–16 hours. Bacterial cells were harvested by centrifugation at 4000 rpm, room temperature for 5 minutes. The remaining medium was removed and the pelleted cells were resuspended in 250 μL of resuspension solution and transferred into a microcentrifuge tube. 250 μL of lysis solution was added and mixed by tube inversion for a few times until the mixture became slightly clear. 350 µL of neutralization solution was added and mixed immediately by tube inversion for a few times. The neutralized bacterial lysate was cloudy with small white particles. The mixture was centrifuged at 10,000×g, room temperature for 5 minutes to pellet bacterial cell debris and chromosomal DNA. The cleared supernatant was transferred into a GeneJET spin column carefully avoiding transfer of white particles. The column was centrifuged at 10,000×g, room temperature for 1 minute and the flow-through was discarded. 500 µL of wash buffer with ethanol was added into the column and centrifuged at 10,000×g, room temperature for 1 minute and the flow-through was discarded. This step was repeated and the empty purification column was then centrifuged again as before to allow complete removal of wash buffer. The column was then put into a fresh microcentrifuge tube. 50 µL of distilled water was added onto the column membrane. The column was incubated at room temperature for 2 minutes and centrifuged at 10,000×g, room temperature for 2 minutes. The purified plasmid DNA was stored at -20°C for further analysis.

### 4.2.7 Ligation of PCR amplicon into the pGEM®-T Easy vector

Gel-extracts PCR amplicon was inserted into the pGEM®-T Easy vector (Promega<sup>TM</sup>, WI, USA) according to the manufacturer protocol. Ligation reaction was set up with optimized insert:vector molar ratios at 3:1 using the standard reaction as described below;

Pagation Component	Standard	
Reaction Component	Reaction (µL)	
2× Rapid Ligation Buffer, T4 DNA Ligase	5.0	
pGEM®-T Easy Vector (50ng)	1.0	
PCR product	3.0	
T4 DNA Ligase (3 Weiss units/μL)	1.0	
Total volume	10.0	

The solution was gently mixed by pipetting and incubated at 4°C overnight for the maximum number of transformants.

### 4.2.8 Preparation of competent *E. coli* XL1-Blue cells

Competent E. coli XL1-Blue cells were prepared for use in transformation reactions. Bacteria were grown on LB agar plate containing 15 µg/mL of tetracycline at 37°C for 16-18 hours. A single isolated colony was picked and inoculated in 5 mL LB broth. The culture was incubated at 37°C, 240 rpm overnight and used as starter in the next step. An amount of 1 µL of bacterial starter culture was added into 100 mL LB broth and incubated at 37°C, 240 rpm until its absorbance at OD<sub>600</sub> had reached a value of 0.5. The bacterial culture was quickly cooled down to 0°C in a salt-ice water bath. The cells were collected by centrifugation at 6,000×g, 4°C for 8 minutes. The bacterial cells were gently resuspended in 20 mL ice-cold 0.1 M MgCl<sub>2</sub> by agitation and centrifuged at 6,000×g, 4°C for 8 minutes. The supernatant was discarded and the bacterial cells were gently resuspended in 20 mL ice-cold 0.1 M CaCl<sub>2</sub>. The suspension was kept on ice for 20 minutes and centrifuged at 6,000×g, 4°C for 8 minutes. The supernatant was discarded and the bacterial cell pellet was gently resuspended in 4.3 ml 0.1 M CaCl<sub>2</sub> mixed with 0.7 ml glycerol. The competent E. coli XL1-Blue cells were aliquoted into 100 µL per microcentrifuge tube. The bacterial cells were shock frozen in liquid nitrogen for 5 minutes, and stored at -80°C until further use.

## 4.2.9 Chemical transformation of competent *E. coli* XL1-Blue with the recombinant pGEM®-T Easy vector

Recombinant pGEM®-T Easy DNA was introduced into *E. coli* XL1-Blue competent cells using a chemical transformation method. The ligation reaction was added into a 100 μL suspension of on-ice thawed competent *E. coli* XL1-blue cells and gently mixed by pipetting. The transformation sample was incubated on ice for 20 minutes. The transformation reaction was stopped by heat-shock at 42°C for 45 seconds. The sample was immediately placed on ice and left for 2 minutes. 900 μL of LB broth was added to the transformation reaction and incubated at 37°C, 240 rpm for 1 hour. Volumes of 10 μL and 100 μL of the sample were spread on LB agar containing 100 μg/ml ampicillin and incubated at 37°C overnight. Positive transformants bacteria were identified by using colony PCR.

### 4.2.10 Screening for positive transformants by colony PCR

Colony PCR was used to identify positive clones that carried the recombinant plasmid. A single transformant bacterial colony was picked from LB agar and suspended in  $100~\mu L$  distilled water. The suspension was heated for 5 minutes at  $95^{\circ}C$  and was used as a template for PCR amplification. The inserted DNA fragment in the recombinant plasmid was amplified using specific primers. The PCR reaction mixture contained the following components;

Components	Volume (µL)
Template	1.0
Forward primer (10 µM)	1.0
Reverse primer (10 µM)	1.0
10× KCl buffer	5.0
MgCl <sub>2</sub> (25 mM)	3.0
10 mM mixed dNTPs (2.5 mM each)	1.0
Taq DNA polymerase (5U/μL)	0.5
Distilled water	37.5
Total volume	50.0

The PCR reaction was performed as follows: pre-denaturation at 95°C for 5 minutes, 35 cycles of denaturation at 95°C for 1 minute, annealing at appropriate temperature for 1 minute, extension at 72°C for 1 minute and final extension at 72°C for 10 minutes. The PCR product was analyzed by 0.7% [w/v] agarose gel electrophoresis. Identified positive transformant bacteria were maintained as glycerol stocks.

### 4.2.11 Restriction analysis of recombinant pGEM®-T Easy vector

Purified recombinant pGEM®-T Easy DNA was digested with a restriction endonuclease recognizing a restriction site next to the inserted DNA fragment. *Eco*RI restriction endonuclease (Thermo Fisher Scientific, MA, USA) with the recognition site G^AATTC sites was used in this reaction. The restriction reaction contained the following components as shown next page.

Components	Volume (µL)
Plasmid DNA	1.0
EcoRI buffer (10×)	2.0
<i>Eco</i> RI (10 U/μL)	1.0
Distilled water	16.0
Total volume	20.0

The reaction mixture was gently mixed and incubated at 37°C for 1 hour. The restriction endonuclease was inactivated for 20 minutes at 65°C. The reaction product was analyzed by 0.7% [w/v] agarose gel electrophoresis. DNA sequencing of both strands was used to determine the sequence of the cloned region using pGEM®-T Easy vector specific SP6 and T7.

### 4.2.12 DNA sequence analysis

Sanger dideoxy sequencing was performed using commercial services (SolGent, Daejeon, South Korea). The difficult template sequencing for an unusual structure DNA was performed using commercial services (Macrogen, Seoul, South Korea). The sequence quality was checked by using the program FinchTV version 1.4.0 (Geospiza, Inc.; Seattle, WA, USA; http://www.geospiza.com). Then, the sequence was analyzed by bioinformatics tools, *e.g.* EMBOSS version 1.5 (http://emboss.open-bio.org). Plasmid sequences were removed from the insert sequence by using EMBOSS-CUTSEQ94 and EMBOSS-REVSEQ94 were used to obtain the reverse complementary sequence of the lagging-strand DNA for alignment with the leading-strand DNA sequence. Alignment and comparison of both DNA strands was done to confirm the full sequence of the DNA insert. Basic information of the full insert sequence, including sequence length and percent GC content, was determined using EMBOSS-INFOSEQ.94 Annotation of the insert sequence was determined by searching against non-redundant nucleotide database (nr/nt) using BLASTN (https://blast.ncbi.nlm.nih.gov/Blast.cgi).95

### 4.2.13 Long time storage of transformants bacteria

A single colony of transformant bacteria that contained the sequenced plasmid was inoculated in 5 mL of LB broth containing 100 µg/ml ampicillin and incubated at 37°C overnight. The bacterial culture was thoroughly mixed with

 $\frac{1}{2}$  vol of 60% [v/v] glycerol, frozen in liquid nitrogen and stored at  $-80^{\circ}$ C for further application.

### 4.3 Molecular characterization of *Fischoederius elongatus* mitochondrial genome

### 4.3.1 Isolation of *Fischoederius elongatus* mitochondrial extracts

Fluke mitochondria were extracted by using a sucrose gradient separation protocol. Frozen worm was homogenized in cold isolation medium (0.25 M sucrose, 10 mM Tris-HCl pH 7.4, 2 mM EDTA, 0.5 [w/v] BSA) using a chilled Potter-Elvehjem homogenizer. The homogenate was transferred into a new tube, and then centrifuged at 800×g at 4°C for 5 minutes to remove cellular debris. The supernatant was transferred into a new tube. The crude mitochondrial pellet was prepared by centrifugation at 18,000×g at 4°C for 10 minutes. The fluffy upper phase was removed by shaking gently with isolation medium. The mitochondrial extract was resuspended in isolation medium, and stored at –80°C

### 4.3.2 Fischoederius elongatus mitochondrial DNA extraction

The mitochondrial pellet was dispersed in mitochondrial lysis buffer (150 mM NaCl, 50 mM Na<sub>2</sub>EDTA, 10 mM Tris-HCl, pH 8.0). Proteinase K (Fermentas, MA, USA) and RNase A (Thermo Fisher Scientific, MA, USA) were added and incubated at appropriate conditions. The mitochondria were lysed by adding 2% SDS/0.4 M NaOH and incubated on ice for 5 minutes. KOAc/acetic acid solution was added, and the contents of the tube gently mixed. After 5 minutes incubation on ice, the mixture was centrifuged at 12,000×g, 4°C for 5 minutes. The resulting supernatant was transferred into a new tube. The mitochondrial DNA was extracted by using phenol/chloroform extraction protocol. The mitochondrial DNA was stored at –20°C for further analysis.

### 4.3.3 Fischoederius elongatus genomic DNA extraction

Single frozen *F. elongatus* specimens were thoroughly grinded in a cold tissue grinder. The tissue was resuspended in 500  $\mu$ L of homogenization buffer (30 mM Tris-HCl pH 8.0, 0.1 M NaCl, 10 mM EDTA, 0.5% Triton X-100). The mixture was briefly centrifuged at 5000×g, room temperature for 5 minutes. The pellet

was resuspended in 500  $\mu$ L extraction buffer (0.1 M Tris HCl pH 8.0, 0.1 M NaCl, 20 mM EDTA). The mixture was briefly centrifuged at 5000×g at room temperature for 2 minutes. The pellet was resuspended in 300  $\mu$ L extraction buffer. Then, 3  $\mu$ L of 10 mg/mL proteinase K (Fermentas, MA, USA) and 15  $\mu$ L of 20% SDS were added and incubated at 50°C for 1 hour to digest the proteins in the homogenate. Degraded proteins were removed by phenol/chloroform extraction. Then, 10  $\mu$ L of 10 mg/mL RNase A (Thermo Fisher Scientific, MA, USA) was added and incubated at 40°C for 1 hour. RNase A was removed by phenol/chloroform extraction and the genomic DNA was precipitated by 2.5 vol of absolute ethanol and 0.1 vol of 3 M sodium acetate pH 5.3. The DNA pellet was washed with 70% ethanol, dried for 10 minutes and resuspended in 10  $\mu$ L of distilled water. The DNA was stored at -20°C.

### 4.3.4 Amplification of mitochondrial DNA fragments

The mitochondrial DNA (mtDNA) of the flukes was isolated and purified as described in **Section 4.3.2**. Then, specific mitochondrial genome regions were amplified by PCR using the following primers;

	1/2/	k	Primers	y	Annealing temperature
1.	HRG-565	FW	5'- ATGGTGTCTCTGGTACGT -3'		50°C
	HRG-566	RV	5'- AAACACTTTCAACCTTCC -3'		
2.	HRG-567	FW	5'- GTGAGAAAGGTGGTCGTT -3'		55°C
	HRG-568	RV	5'- CACCGATTAGAACCACTCA -3'	or	
	HRG-651	FW	5'- GTGAGAAAGGTGGTCGTTTG -3'		55°C
	HRG-568	RV	5'- CACCGATTAGAACCACTCA -3'		
3.	HRG-594	FW	5'- TGGCGTTTTTGAGGTTATCAC -3'		55°C
	HRG-595	RV	5'- CGCAAAACCTTTCACACC -3'		
4.	HRG-596	FW	5'- TATGTGGTGATGAGATGGTG -3'		50°C
	HRG-623	RV	5'- CCAAGACAACCAACTACG -3'	or	
	HRG-625	FW	5'- GGTTAAGTTTGTAATAGGA -3'		42°C
	HRG-623	RV	5'- CCAAGACAACCAACTACG -3'		
5.	HRG-598	FW	5'- TTACTATGGTGCATGCTG -3'		55°C
	HRG-599	RV	5'- AACCAACACGCTTGTGATC -3'		

			Primers	Annealing
				temperature
6.	HRG-600	FW	5'- ATGTTGTTGTGGCTGCTTG -3'	50°C
	HRG-601	RV	5'- GCAATCCTTTCGTACTAAC -3'	
7.	HRG-602	FW	5'- TCGAGAGAGTATCTTTGTAG -3'	50°C
	HRG-603	RV	5'- GCCAACCAAACCTACACATC -3'	
8.	HRG-604	FW	5'- GATGGTGTTGTGATGTGG -3'	45°C
	HRG-605	RV	5'- CCTAACAACTTCCATAAG -3'	

The components of the PCR reaction mixture are shown below;

Component	Volume (µL)
mtDNA (25 ng)	5.0
Forward primer (10 μM)	1.0
Reverse primer (10 μM)	1.0
$10 \times Taq$ buffer with KCl and without MgCl <sub>2</sub>	5.0
MgCl <sub>2</sub> (25 mM)	3.0
Mixed dNTPs (2.5 mM each)	1.0
Taq DNA polymerase (5U/μL)	0.5
Distilled water	33.5
Total volume	50.0

The amplification reaction was carried out in a thermocycler using following conditions; pre-denaturation at 95°C for 5 minutes, 35 cycles of denaturation at 95°C for 1 minute, annealing at appropriate temperature for 1 minute, and extension at 72°C for 1 minute, then final-extension at 72°C for 10 minutes, and hold at 4°C. The PCR products was resolved by 0.7% [w/v] denaturing agarose gel electrophoresis.

PCR products were purified by GeneJET Gel Extraction Kit (Thermo Fisher Scientific, MA, USA) and directly sequenced. The mitochondrial DNA fragments were manually assembled compared with other trematode mtDNA, and then analyzed by bioinformatics programs.

### 4.3.5 Amplification of mitochondrial DNA NAD1 and NAD2

The *nad*1 and *nad*2 genes were amplified by standard PCR as described in **Section 4.3.4**. using designed primers binding to internal and external regions of the genes at appropriate conditions.

PCR primers for nad2-nad1 region are shown below;

Primers		Annealing	
		temperature	
FW	5'- TATGTGGTGATGAGATGGTG -3'	50°C	
RV	5'- GACAACCAACTACGAACCTC -3'		
FW	5'- TATGTGGTGATGAGATGGTG -3'	50°C	
RV	5'- CCAAGACAACTACG -3'		
FW	5'- GGTTAAGTTTGTAATAGGA -3'	42°C	
RV	5'- CCAAGACAACTACG -3'		
FW	5'- TGCTCTGCAAGTACGAGGTGAGTGT -3'	45°C	
RV	5'- GACAACCAACTACGAACCTC -3'		
FW	5'- TGCTCTGCAAGTACGAGGTGAGTGT -3'	45°C	
RV	5'- CCAAGACAACCAACTACG -3'		
FW	5'- TATGTGGTGATGAGATGGTG -3'	60°C	
RV	5'- ACACTCACCTCGTACTTGCAGAGCA -3'		
FW	5'- GGTTAAGTTTGTAATAGGA -3'	45°C	
RV	5'- ACACTCACCTCGTACTTGCAGAGCA -3'		
	RV FW RV FW RV FW	FW 5'- TATGTGGTGATGAGATGGTG -3' RV 5'- GACAACCAACTACGAACCTC -3' FW 5'- TATGTGGTGATGAGATGGTG -3' RV 5'- CCAAGACAACCAACTACG -3' FW 5'- GGTTAAGTTTGTAATAGGA -3' RV 5'- CCAAGACAACCAACTACG -3' FW 5'- TGCTCTGCAAGTACGAGGTGAGTGT -3' RV 5'- GACAACCAACTACGAACCTC -3' FW 5'- TGCTCTGCAAGTACGAGGTGAGTGT -3' RV 5'- TGCTCTGCAAGTACGAGGTGAGTGT -3' RV 5'- TATGTGGTGATGAGATGGTG -3' RV 5'- ACACTCACCTCGTACTTGCAGAGCA -3' FW 5'- GGTTAAGTTTGTAATAGGA -3'	

<sup>\*</sup>HRG669 and HRG670 are internal primers for repeat region.

PCR primers for nad2-nad1 terminal region are shown below;

Primers	Annealing
Timers	temperature
nad2 HRG-671 FW 5'- GTGCGTGGTTATTTTGTTTCTTGGTTGAG	-3' 60°C
HRG-670 RV 5'- ACACTCACCTCGTACTTGCAGAGCA -3'	
nad1 HRG-672 FW 5'- ATGTTGTTGACGGGAGTA -3'	45°C
HRG-673 RV 5'- AACAGCATGCACCATAGT -3'	

PCR products were purified and directly sequenced. Sequencing quality was verified in FinchTV version 1.4.0. The obtained *nad*1 and *nad*2 sequences were used to design additional primers to amplify and sequence neighboring overlapping fragments of the mitochondrial genome. The obtained overlapping sequences were assembled to get the full mitochondrial genome sequence from the start of *nad*2 to the end of *cox*1. Repeated DNA sequences were detected in EMBOSS-EINVERTED.<sup>94</sup>

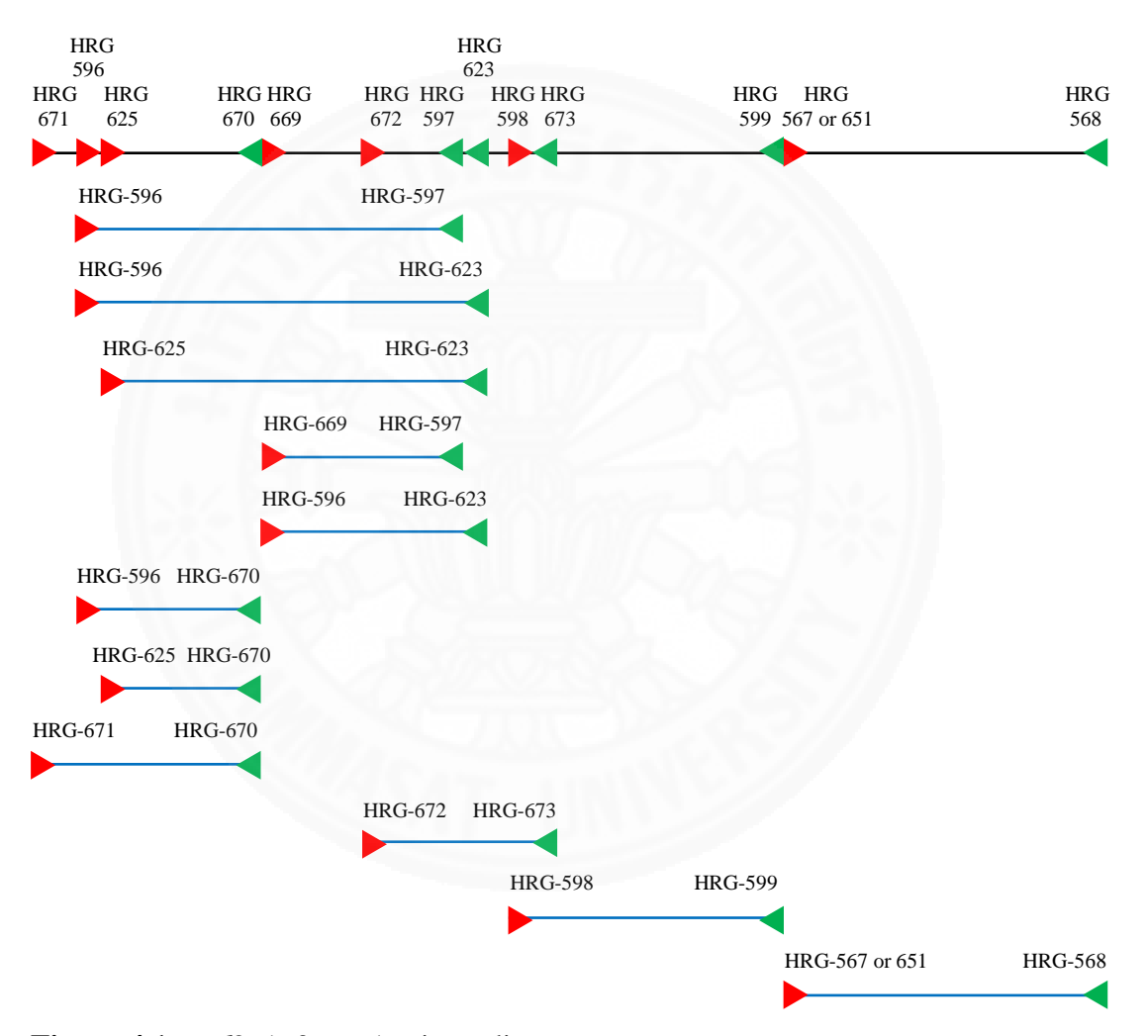


**Figure 4.1** *nad*2–1–3–*cox*1 primer diagram

## 4.3.6 Fischoederius elongatus mitochondrial genome sequence analysis

DNA sequencing was performed using commercial services for standard Sanger dideoxy sequencing (SolGent, Daejeon, South Korea) and Macrogen (Macrogen, Seoul, South Korea) for difficult Sanger dideoxy sequencing in case of secondary structure problems caused by inverted repeats. The DNA sequences were analyzed by bioinformatics tools including EMBOSS,<sup>94</sup> ClustalX version 2.1,<sup>96</sup> SeaView version 5.0.1,<sup>97</sup> and BLAST.<sup>95</sup>

### 4.3.6.1 *Fischoederius elongatus* mitochondrial genome sequence assembly

Mitochondrial genome sequences among the transcriptome data were identified by BLAST and aligned to the previously published mitochondrial genome sequence of *F. elongatus* (GenBank: NC\_028001). Specific oligonucleotide primers were designed to obtain missing regions of the mitochondrial genome by standard PCR. The PCR products were sequenced using Sanger dideoxy sequencing by commercial services. Mitochondrial genome sequences were aligned to amphistome mitochondrial genomes including *F. elongatus* (GenBank: NC\_028001), *F. cobboldi* (GenBank: NC\_030529), and *Paramphistomum cervi* (GenBank: NC\_023095) using the program Clustal X version 2.1. <sup>96</sup> The aligned sequences were manually adjusted and edited by using the program SeaView version 5.0.1. <sup>97</sup> The complete *F. elongatus* mitochondrial genome sequence of specimens with *Mse*I pattern A was assembled. <sup>95</sup>

### 4.3.6.2 Fischoederius elongatus mitochondrial genome sequence annotation

Mitochondrial genes were annotated based on the homologous genes in echinoderm and flatworm mitochondrial genomes (mitochondrial genetic code 9). The protein-coding genes were identified using MITOS (http://mitos2.bioinf.uni-leipzig.de/index.py)<sup>98</sup> in RefSeq 63 and RefSeq 81 Metazoa of RefSeq NCBI database (http://www.ncbi.nlm.nih.gov/refseq). Open reading frames were identified by ORF Finder (http://www.ncbi.nlm.nih.gov/gorf/gorf.html).<sup>99</sup> Annotation of the protein-coding genes was validated by searching the non-redundant protein sequences (nr) database for the homologous proteins by BLASTX (https://blast.ncbi.nlm.nih.gov/Blast.cgi).<sup>95</sup> Initiation and termination codons of the protein-coding genes were identified. Nucleotide codon usage of the protein-coding gene was analyzed using the program Codon Usage (http://www.bioinformatics.org/sms2/codon usage.html).<sup>100</sup> The tRNA gene of the mitochondrial genome were predicted in tRNAscan-SE version 2.0 (http://lowelab.ucsc.edu/tRNAscan-SE)<sup>101</sup> and in ARWEN (http://130.235.244.92/ARWEN/index.html)<sup>102</sup> with default parameters

searching for Metazoan mitochondrial tRNA genes. The large rRNA (rrnL) and small rRNA (rrnS) genes were predicted by comparison with *F. elongatus* (GenBank: NC\_028001). A *F. elongatus* circular mitochondrial genome map was drawn using Organellar Genome DRAW (OGDRAW) version 1.3.1 (https://chlorobox.mpimpgolm.mpg.de/OGDraw.html).<sup>103</sup>

## 4.3.6.3 Multiple alignment of *Fischoederius elongatus* mitochondrial genome

ClustalX version 2.1 was used to compare amphistome mitochondrial genomes. <sup>96</sup> Included in the multiple alignment were the mitochondrial genomes of *F. elongatus* (GenBank: NC\_028001), *F. cobboldi* (GenBank: NC\_030529), *G. crumenifer* (GenBank: NC\_027833), *Calicophoron microbothrioides* (GenBank: NC\_027271), and *Paramphistomum cervi* (GenBank: NC\_023095). ClustalX was used with the default parameters.

### 4.3.6.4 Phylogenetic analysis of *Fischoederius elongatus* mitochondrial genome

The phylogenetic relationship of *F. elongatus* and other trematode mitochondrial genomes was analyzed using the neighbor-joining method in MEGA X.<sup>104</sup> The 12 protein-coding genes were conceptually translated using the echinoderm and flatworm mitochondrial genetic code. Clustal X was used with default parameters to align the homologous sequences obtained from the mitochondrial genomes of *F. elongatus* (GenBank: NC\_028001), *F. cobboldi* (GenBank: NC\_030529), *G. crumenifer* (GenBank: NC\_027833), *C. microbothrioides* (GenBank: NC\_027271), *P. cervi* (GenBank: NC\_023095), *Explanatum explanatum* (GenBank: NC\_027958), *Homalogaster paloniae* (GenBank: NC\_030530), *Orthocoelium streptocoelium* (GenBank: NC\_028071), *Clonorchis sinensis* (GenBank: NC\_012147), and *Fasciola hepatica* (GenBank: NC\_002546).

## 4.3.7 Polymerase chain reaction-restriction fragment length polymorphism (PCR-RFLP) of *Fischoederius* spp. mtCOX1

F. elongatus mitochondrial cytochrome c oxidase subunit I (mtCOX1) sequences were amplified by PCR using the primers described in **Section 4.3.4**. PCR amplicon was resolved by 0.7% [w/v] agarose gel electrophoresis and purified by GeneJET Gel Extraction Kit (Thermo Fisher Scientific, MA, USA) as

described in **Section 4.2.5.** The purified fragment was cloned into pGEM-T Easy as described in **Section 4.3.6** for later sequencing. mtCOX1 gene amplification products were digested with 10U *Mse*I restriction enzyme (New England Biolabs, Ipswich, Massachusetts) according to the manufacturer's procedure. The restriction reaction was performed using the components below;

Components	Volume (µL)
mtCOX1 PCR product	10.0
MseI 10U	0.5
10× CutSmart® Buffer	2.5
Distilled water	12.0
Total Volume	25.0

The reaction was incubated at 37°C for 15 minutes and the enzyme inactivated at 65°C for 20 minutes. The digested fragments were separated by 3.0% agarose gel electrophoresis (80V for 3 hours). The PCR-RFLP patterns were recorded using a gel documentation system.

### 4.4 Transcriptome sequencing of adult stage Fischoederius elongatus

### 4.4.1 Total RNA extraction and purification for high-throughput sequencing

Total RNA of five frozen adult *F. elongatus* was isolated by using the TRIzol reagent extraction protocol as described in **Section 4.2.1**. The total RNA was purified with QIAgen RNeasy<sup>®</sup> Plus Mini Kit (QIAgen, Hilden, Germany) according to the optimized conditions to remove contaminated DNA. The flow-through containing purified RNA was collected. RNA was cleaned and reprecipitated by thefollowing steps. 0.1 vol of 2 M NaCl and 2.5 vol of ice-cold absolute ethanol was added to to the RNA solution and mixed by tube inverting. The sample was incubated for 1 hour at –20°C allowing it to precipitate. Then, the sample was centrifuged at 12,000×g for 20 minutes at 4°C. The supernatant was removed. The pellet was washed with 75% ethanol, and then centrifuged at <7,500×g for 5 minutes at 4°C. This washing

step was repeated for 3 times. The RNA pellet was dried and then dissolved in RNase-free water.

### 4.4.2 Qualification and quantification measurement of total RNA

The total RNA was resolved by 1.2% non-denaturing agarose gel electrophoresis to check its quality and its concentration was measured using a NanoDrop ND-2000 UV-Vis Spectrophotometer (Thermo Fisher Scientific, MA, USA). RNA integrity was determined on an Agilent 2100 BioAnalyzer (Agilent Technologies, Santa Clara, CA, USA) to obtain the RNA integrity number (RIN).

### 4.4.3 Ethanol precipitation of total RNA for shipment

The total RNA was kept precipitated in ethanol during dry ice shipment. The RNA was precipitated by the addition of 0.1 vol of 3.0 M NaOAc, pH 5.5 and 2.0 vol of absolute ethanol to the RNA solution. The precipitated RNA was kept at -80°C until dry ice shipment to the sequencing company.

### 4.4.4 Total RNA preparation for shipment at ambient temperature

The total RNA was was incubated and gently mixed with GenTegra® matrix in GenTegra®-RNA tube (GenTegra, Pleasanton, CA, USA), by pipetting. The RNA in the tube was dried with cap off using a vacuum desiccator for 4 hours. Following drying, the RNA was stored at ambient temperature until transportation for sequencing.

### 4.4.5 Illumina® Next generation sequencing

## 4.4.5.1 cDNA library preparation for Illumina® Next generation sequencing

cDNA library preparation was performed according to the manufacturers' instructions. The library was created by using NEBNext® Ultra RNA Library Prep Kit for Illumina® (New England Biolabs, Massachusetts, United States) to synthesize cDNA. Double-stranded cDNA was purified by AxyPrep Mag PCR Clean-up (Axygen Biosciences, CA, USA). End prep of the cDNA was performed and the cDNA processed immediately to T-A adaptor ligation at both ends. Following adaptor-ligation the cDNA was cleaned up by AxyPrep Mag PCR Clean-up (Axygen Biosciences, CA, USA) and then amplified for 11 cycles of PCR using P5 and P7 random primers containing an adapter sequence to allow the cDNA to bind to the flow cell and generate multiplexing that a specific adapter was added into cDNA for sample

identification. The PCR product was cleaned up again and sequenced on an Illumina<sup>®</sup> Hiseq2500 150 pair-ends (40 GB) platform (Illumina<sup>®</sup>, San Diego, CA, USA), according to the manufacturers' instructions. Demultiplexing of the obtained data was done in Illumina<sup>®</sup> bcl2fastq version 2.17. A quality score was calculated. The raw sequence data was used for bioinformatics analysis.

P7 adapter (read 1): 5'- AGATCGGAAGAGCACACGTCTGAACTCCAGTCA -3'
P5 adapter (read2): 5'- AGATCGGAAGAGCGTCGTGTAGGGAAAGAGTGT -3'

### 4.4.5.2 High-throughput sequencing

Purified *F. elongatus* total RNA with a RIN score > 7 was processed for library construction and sequenced on an Illumina<sup>®</sup> Hiseq2500 and Novaseq6000 150 pair-ends platform (Illumina<sup>®</sup>, San Diego, CA, USA), according to the manufacturers' instructions. First time sequencing was performed at 6 Gb using the commercial service of Theragen Etex (Theragen BioInstitute, Suwon-Si, South Korea) and second time sequencing was done at 40 Gb using the service of Vishuo Biomedical (Vishuo Biomedical, Bangkok, Thailand). The sequenced paired-end reads that were generated from the *F. elongatus* cDNA library were assembled and remapped using software based on a De Bruijn-graph. All nucleotide sequences of *F. elongatus* were aligned with BLASTN and BLASTX analyses searching the non-redundant databases.<sup>95</sup> Contaminating sequences including from bacteria, virus, fungi, plants and the bovine host was excluded. Protein-coding sequences was classified according to their predicted function using the program InterProScan version 5.0,<sup>105</sup> and used for further analysis.

### 4.4.5.3 Quantification measurement of high-throughput sequencing

The quality of raw sequences from high-throughput sequencing was examined using FastQC. 106 FastQC was performed by a series of analysis modules including basic statistics, per base sequence quality, per sequence quality scores, GC content, N content, sequence length distribution, duplicate sequences, and k-mers.

## 4.4.6 Bioinformatics analysis of adult *Fischoederius elongatus* transcriptome data

### 4.4.6.1 Sequence assembly and annotation

Raw sequences of high quality were assembled in Trinity<sup>80</sup> for the 6 Gb transcriptome data and in Bridger assembler<sup>107</sup> for 40 Gb transcriptome data. The completeness of the assembled sequences was checked using the program BUSCO.<sup>108</sup> The assembled transcript sequences from *F. elongatus* were used for BLASTX<sup>95</sup> searches in UniProtKB and NCBI non-redundant protein database to identify known homologous sequences in other species. All open reading frames (ORFs) were predicted against the NCBI Conserved Domains Database (CDD).

### **4.4.6.2** Contaminating sequences

The transcriptome data was searched for contaminating sequences including from bacteria, fungi, virus, plants, bovine host and human using BLASTN and BLASTX. The sequences were compared with Platyhelminthes (taxid: 6157) and contaminating organisms, *e.g.* Bacteria (taxid: 2), Fungi (taxid: 4751), Viruses (taxid: 10239), Plants (taxid: 3193), Bovinae (taxid: 27592) and *Homo sapiens* (taxid: 9606). Then the % query cover, % identity and % similarity of aligned sequences were analyzed at cut-off = 95%. Sequences with higher similarity to contaminating microorganisms or mammalians sequences than the Platyhelminthes sequences were removed.

### 4.4.6.3 Duplicated sequences

The transcriptome sequences were checked for duplicates using multiple alignment programs, *e.g.* ClustalX. <sup>96</sup> Slightly different sequences might represent polymorphisms, close isoforms, or erroneous sequences.

### 4.4.6.4 Complete sequences analysis

The top 100 abundant transcripts were further analyzed. Conceptual translations were generated in EMBOSS-TRANSEQ.<sup>94</sup> Putative ORFs were identified in EMBOSS-SHOWORF and EMBOSS-PLOTORF,<sup>94</sup> respectively. The selected ORFs were compared with alignment results from BLASTX,<sup>95</sup> then the sequences were searched for protein motifs. Signal peptides were predicted using SignalP version 5.0 (http://www.cbs.dtu.dk/services/SignalP).<sup>109</sup> Transmembrane domains were predicted using TMHMM version 2.0 (http://www.cbs.dtu.dk/services/TMHMM).<sup>110</sup>

#### 4.4.6.5 Prediction of protein function using InterProScan

Protein-coding sequences were functional classified using InterProScan version 5.0.<sup>105</sup> The selected sequences from transcriptome data were conceptually translated and searched against the protein database. Conserved protein domains were identified by signature predictive models and the obtained results were used to predict the protein function.

### 4.4.6.6 Gene ontology

Gene ontology (GO) was used for further classification of the obtained protein-coding sequences. The sequences were classified into three related domains including cellular component, molecular function, and biological process. All *F. elongatus* sequences were searched with Blast2GO to obtain their ontologies and annotation data. *F. elongatus* proteins that can be identified as homologous to known proteins in other organisms which have potential as diagnostic tools were selected for further analysis.

### 4.5 Antigenicity of Fischoederius elongatus

### 4.5.1 Preparation of parasite antigen

#### 4.5.1.1 Crude worm extract of adult Fischoederius elongatus

Frozen adult *F. elongatus* was homogenized on ice in homogenization buffer (150 mM NaCl, 10 mM Tris-HCl, pH 7.2, 1 mM EDTA pH 8.0, 1 mM PMSF, 0.5% [v/v] Triton-X 100) at a ratio 1 g tissue per 2 mL buffer by using a tissue homogenizer. The homogenate was rotated for 1 hour at 4°C, and then centrifuged at 12,000×g for 15 minutes at 4°C to remove insoluble material. The supernatant was collected as soluble crude worm extract. The concentration of protein was measured using a Bradford assay. The protein quality was analyzed by SDS-PAGE. Crude worm extract was aliquoted and stored at –20°C for further experiments.

## 4.5.1.2 Excretion/secretion extract of adult *Fischoederius* elongatus

Adult *F. elongatus* was washed several times with 10 mM PBS pH 7.2. The worms were incubated in 10 mM PBS pH 6.0, 7.2, and 8.0 for 4 hours at  $37^{\circ}$ C. The medium was collected and centrifuged at  $5000 \times g$  for 20 minutes at  $4^{\circ}$ C to

remove the insoluble materials and worm eggs. The supernatant was transferred into a new tube, and then concentrated using 3,000 MWCO centrifugal concentrator. The concentrated proteins were collected as excretion/secretion product. The concentration of protein was measured using a Bradford assay. The protein quality was analyzed by SDS-PAGE. Excretion/secretion product was aliquoted and stored at –20°C for further experiments.

### 4.5.1.3 Measurement of protein concentration by Bradford assay

Protein concentration of all extracts were measured by a Bradford assay (Bio-Rad, Hercules, CA, USA). The dye solution reagent was prepared by diluting 1:4 with distilled de-ionized water. The protein standard curve was prepared using six concentrations of bovine serum albumin (BSA) at 0.05, 0.1, 0.2, 0.3, 0.4, 0.5 mg/mL. The protein standards were assayed in duplicate. 10 μL of each protein sample was added into separate wells of a 96-well microtiter plate. 200 μL of diluted dye reagent was added into each well and mixed by pipetting thoroughly. The reaction mixtures were incubated for 5 minutes at room temperature. The absorbance was measured at 595 nm.

### 4.5.1.4 Preparation of parasite antigens electrophoresis

Parasite protein extracts were mixed with an equal volume of 2× sample protein electrophoresis loading buffer (0.125 M Tris-HCl, pH 6.8, 4% [w/v] SDS, 20% [v/v] glycerol, 0.2 M DTT, 0.02% [w/v] bromophenol blue). The samples were heated for 5 minutes at 95°C to denature the protein. The denatured protein samples were loaded into the wells of a polyacrylamide gel set up in a electrophoresis chamber (Amersham Biosciences, Little Chalfont, United State). Broad range molecular weight standard (Bio-Rad, CA, USA) was loaded in the first lane. Protein electrophoresis was performed at 20 mA per gel (Electrophoresis Power Supply EPS 301, Amersham Biosciences, United State) for 1–2 hours or until the front dye marker had reached the bottom of the gel. After gel electrophoresis, the polyacrylamide gel was carefully removed from the two-glass plates. The gel was stained with 0.008% [w/v] Coommassie Blue G-250 (Brilliant Blue G-250, USB Corporation, OH, USA).

## 4.5.1.5 Analysis of parasite proteins by sodium dodecyl sulphate polyacrylamide gel electrophoresis (SDS-PAGE)

SDS-PAGE was used for separation of proteins according to

their molecular masses. Polyacrylamide gel was prepared using a modified protocol from the Hoeffer manual (Amersham Biosciences, Little Chalfont, United State). Trisglycine polyacrylamide gel was used in this study. 12.5% separating gel was prepared from 6 mL mixture of 2.5 mL of 30% [w/v] acrylamide stock, 1.5 mL of 1.5 M Tris-HCl, pH 8.8, 0.06 mL of 10% [w/v] SDS, and 1.88 mL of distilled de-ionized water. Polymerization was initiated by adding 60 μL of 10% [w/v] APS and 2.5 μL of TEMED to the mixture. 4% stacking gel was prepared from 2 mL mixture of 270 µL of 30% [w/v] acrylamide stock, 0.5 mL of 0.5 M Tris-HCl pH 6.8, 0.02 mL of 10% [w/v] SDS, and 1.18 mL of distilled de-ionized water. Polymerization was initiated by adding 20 μL of 10% [w/v] APS and 2 μL of TEMED to the mixture. First the separating gel mix was added into a gel cassette followed by the stacking gel mix. The gel cassette was assembled into the gel apparatus and glycine electrophoresis buffer was filled into the buffer chambers. Protein samples were prepared and loaded into the wells. The electrophoresis proceeded at 20 mA per gel until the front dye has reached the bottom of the gel. The gel was removed from the cassette, and then stained in 0.008% [w/v] Coomassie blue G-250 dye solution for visualization of the protein bands or used for Western blotting.

## 4.5.1.6 Detection of parasite antigens in the polyacrylamide gel using Coomassie Blue G-250 Staining

The polyacrylamide gel was rinsed with water to remove excess SDS. It was stained in Coomassie blue staining solution (0.008% [w/v] Coomassie Brilliant Blue G-250, 35 mM HCl) and heated in a microwave oven for 30 seconds. Then, the gel was incubated at room temperature, 140 rpm for 1 hour or until the bands of the standard protein marker were observed. After staining, the gel was rinsed with water for destaining. Parasite antigens bands were visualized directly and the gel was scanned using a Canon scanner (Canon, Tokyo, Japan).

### 4.5.2 Production of polyclonal mouse antibody

### 4.5.2.1 Antibody production in mice

6–8 weeks old female BALB/c mice were separately immunized three times with *F. elongatus* excretion/secretion product. The pre-immune serum was collected one week before immunization and was used as negative control serum. The antigen was prepared by mixing equal volumes of parasite antigen and

Freund's adjuvant. The mice were intraperitoneally injected with 25  $\mu g/100~\mu L$  prepared antigen, three times in a 3-weeks interval. Then the mice were bled every two weeks after immunization. The collected blood was centrifuged at  $10,000\times g$ , room temperature for 5 minutes. The separated serum was kept at  $-20^{\circ}C$  for further analysis. This animal experiment was ethically approved by Thammasat University Animal Care and Use Committee (Protocol Number: 012/2560).

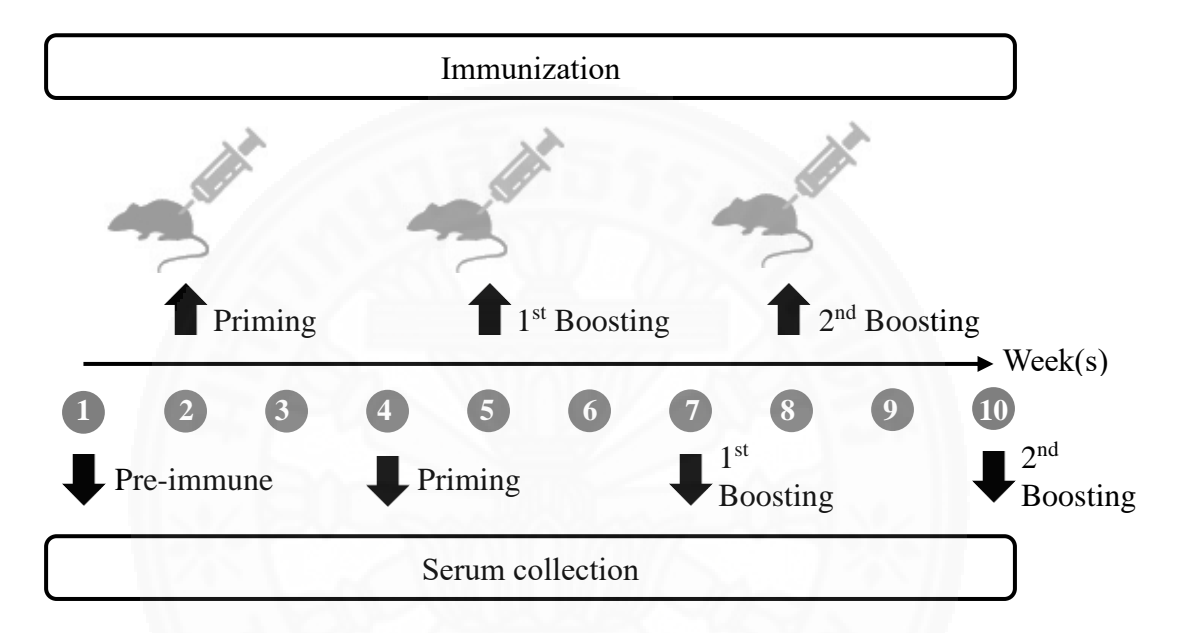


**Figure 4.2** Timeline diagram of *Fischoederius* spp. anti-ES antisera production in BALB/c mice.

### 4.5.2.2 Determination of antibody titer by indirect enzyme-linked immunosorbent assay (ELISA)

Parasite antigens were prepared as described in **Section 4.5.1**.

A 96-well microtiter plate was coated with parasite antigens in carbonate buffer, pH 9.6, and then incubated overnight at 4°C. The coated antigens were washed several times with distilled de-ionized water. 0.25% [w/v] BSA blocking solution was added into the well and incubated for 30 minutes at room temperature, and then washed several times with distilled de-ionized water. Pre-immune serum, priming serum, 1<sup>st</sup> boost serum, and 2<sup>nd</sup> boost serum was stepwise 2-fold diluted starting from 1:100, and all dilutions were assayed in duplicate. The plate was incubated at 37°C for 1 hour, and then washed several times. Horseradish peroxidase (HRP) conjugated Goat anti-

mouse IgG (Invitrogen, Carlsbad, CA, USA) at dilution 1:3,000 with antibody diluent was added and incubated at 37°C for 1 hour. The well was washed and then 100  $\mu$ L of OPD substrate solution (Sigma, MO, USA) was added and incubated for 30 minutes at room temperature in a dark place. The reaction was stopped by adding 25  $\mu$ L of 3 M H<sub>2</sub>SO<sub>4</sub>. The absorbance was measured at 492 nm.

## 4.5.2.3 Determination of serum circulating antigen using Western blot analysis

Parasite antigen was prepared as described in **Section 4.5.1**.

The proteins were size-separated by Tris-Glycine SDS-PAGE and transferred onto a 0.45 µm nitrocellulose membrane by semi-dry blotting. After blotting, the membrane was washed and equilibrated in Tris-buffered saline (TBS) for 5 minutes. Unspecific binding sites on the membrane were blocked by gentle shaking in 5% [w/v] skimmed milk in TBS for 1 hour at room temperature. Polyclonal mouse antiserum and pre-immune serum was added at optimal dilutions with 1% [w/v] skimmed milk in TBS at 4°C overnight. The membrane was washed and immersed in 1:30,000 dilution alkaline phosphatase (AP) conjugated goat anti-mouse IgG (Sigma, MO, USA), and incubated for 1 hour at room temperature with shaking. Then the membrane was equilibrated in detection buffer (100 mM Tris-HCl, pH 9.5, 100 mM NaCl, 5 mM MgCl<sub>2</sub>). The immune complex was detected using chromogenic substrates BCIP/NBT (Ameresco, MA, USA) in a dark place. The reaction was stopped with distilled de-ionized water.

# CHAPTER 5 RESULTS

### 5.1 Morphology of Fischoederius spp.

### **5.1.1** Collection of *Fischoederius* specimens

Flukes were collected from the rumen of naturally infected cattle at local slaughterhouses, Pathumthani Province, Thailand during the years 2014–2019 as described in **Section 4.1.1**. The local origins of the cattle were not specified. The flukes attached to the rumen villi were gathered in several spots with each spot containing more than 100 worms as shown in **Figure 5.1**. The flukes were classified as members of the genus *Fischoederius* by their morphology (shape, color, and size) as described in **Section 4.1.2** by observation under a stereomicroscope.



**Figure 5.1** *Fischoederius* spp. in the rumen of an infected cattle at a local slaughterhouse in 2019.

The flukes had a sword-like shape with reddish body color. The alive flukes showed body contraction and extension in phosphate buffered saline and some specimens reached a body length of more than 2 cm. The body size was very different between the specimens with a range from <1 cm to >2 cm. The reproductive organs, testes and ovary were also sometimes vary small suggesting immature flukes. The flukes had a pharynx at the anterior end of the body and a large sucker at the posterior end of the body. The ventral pouch, an inner cavity, was observed initiating from the pharynx extending to the region of the reproductive organs. The cecal bifurcation close to the esophagus extended to the middle of body length. Occasionally, the ceca still contained turbid artifacts even though the flukes had been incubated at 37°C for 2 hours to allow them to regurgitate the cecal content. The lobed testes were located in the median and vertical orientation. The alive flukes were cultured in PBS are shown in **Figure 5.2**.

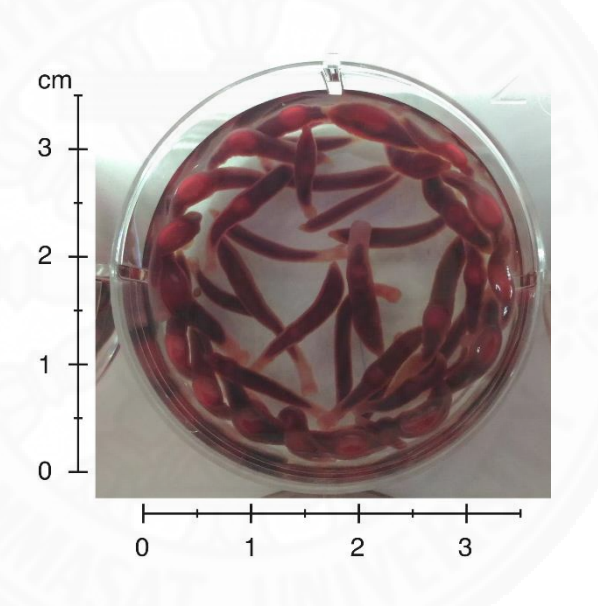


**Figure 5.2** *Fischoederius* spp. maintained in PBS in a culture plate (collected in 2016).

### 5.1.2 Semichon's carmine whole mount staining

Fixed *Fischoederius* specimens were subjected to carmine staining as described in **Section 4.1.3**. *Fischoederius* whole mounts had 15.5–16.2 mm body length and 2.0–4.2 mm body width (**Figure 5.3**). The flukes had a sword-like shape and were covered with a thick tegument without ciliated papilla. The anterior opening close to the pharynx was visible. The pharynx was small with a size of 0.2–0.5×0.5–0.7 mm. The esophagus without muscular bulb continued from pharynx and joined with the ceca in a Y-shape in the dorsal field of the body. The two ceca had a tubular structure with a diameter of 0.1–0.2 mm and extended to the middle length of the body. The fluke had

a large ventral pouch, an internal sac, with ovoid shape along the body overlapping the testes. Vitellaria were present in the lateral field of the body with 0.01–0.05 mm in diameter. The lobed testes positioned in the median and vertical orientation with 1.0–1.1 mm in diameter. The ovary was located beside the testes with 0.3–0.4 in diameter. The uterus reached from the oviduct up to the genital pore located at the anterior end. Eggs were ovoid in shape with a size of 0.10–0.11×0.01–0.05 mm. The posterior sucker had ovoid shape with a size of 0.5–1.7×0.4–0.8 mm.

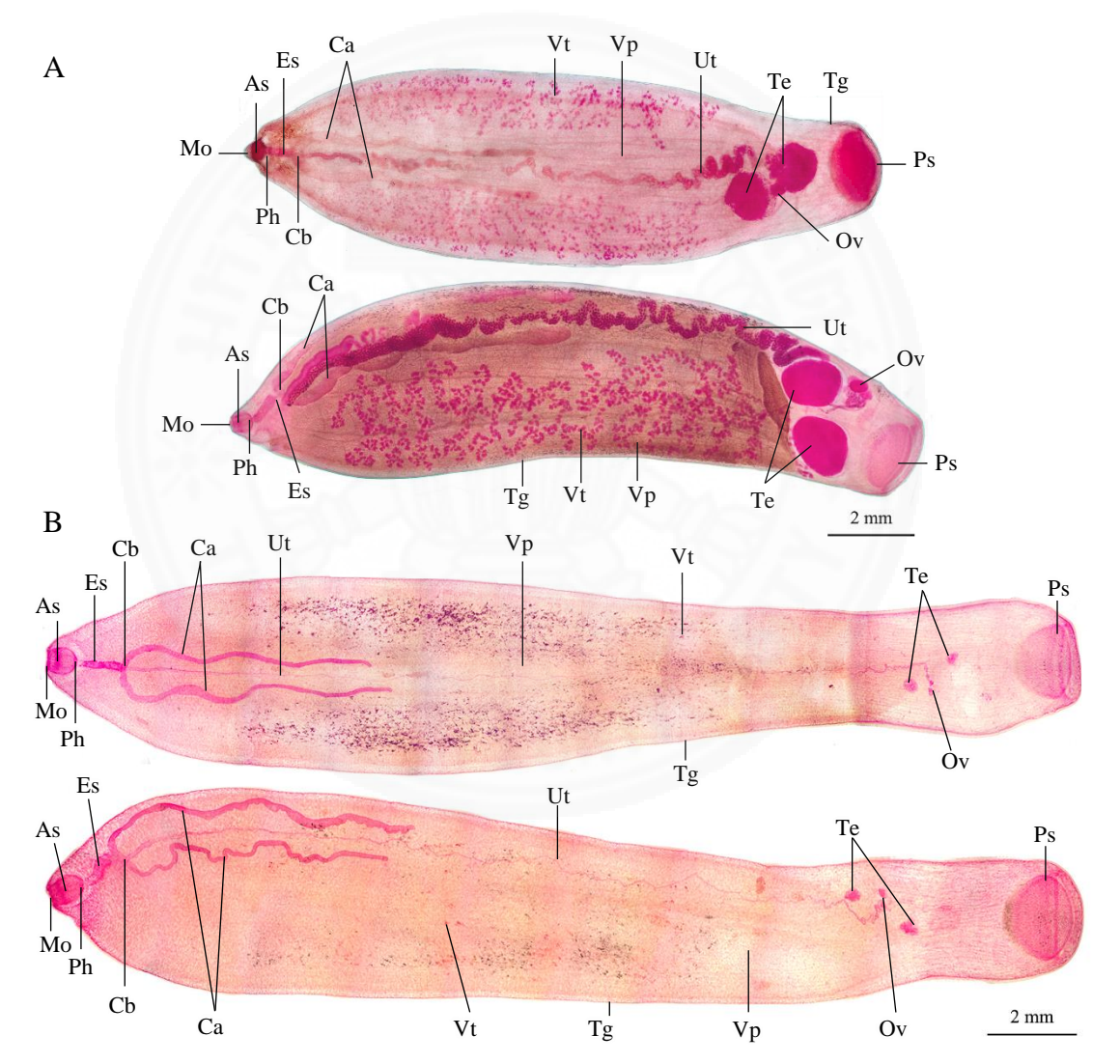


**Figure 5.3** Semichon's carmine staining of *Fischoederius* spp. (**A**) large testes flukes (collected in 2015 and 2019); (**B**) small testes flukes (collected in 2016); Mo: Mouth; As: Anterior sucker; Ph: Pharynx; Es: Esophagus; Cb: Cecal bifurcation; Ca: Ceca; Ut: Uterus; Vp: Ventral pouch; Tg: Tegument; Te: Testes; Ov: Ovary; Vt: Vitellaria; Ps: Posterior sucker.

The reproductive organs were not always developed in the collected flukes. Mature flukes with developed reproductive organs are shown in **Figure 5.3A** and immature flukes with small testes (0.2–0.3 mm in diameter) are shown in **Figure 5.3B**. The specimens with small testes were collected in 2016 and had a large body size, 22.8–23.0 mm in length and 2.2–4.2 mm in width. The full reproductive system was poorly developed including uterus and vitellaria and eggs were not observed.

#### 5.1.3 Histological examination of *Fischoederius* spp.

A detailed histological study of *Fischoederius* spp. was performed using hematoxylin and eosin staining as described in **Section 4.1.4**. Serial cross-sections of the fluke from the anterior to the posterior end are shown in **Figure 5.4** (small testes fluke) and **Figures 5.5 I–IV** (large testes flukes).

All regions of the fluke were covered with a thick acidophilic tegument with nonciliated papillae. The two layers of circular muscles below the basement membrane of the tegument had a layer of longitudinal muscles batched between them. Tegumental cells were located deep in the muscle layers (**Figure 5.6a**). Parenchymal tissue filled the interior of the fluke. Vitellaria appeared in form of basophilic particle in the lateral field of the body. The anterior part of the fluke contained the digestive organs and genital pore, while the posterior part contained the reproductive organs.

In the anterior part, anterior sucker had small circular structure covered with fine thick layer muscle. Below the thick layer was thin circular muscle and radial elongated layer. The inner surface of anterior sucker was circular muscle and then longitudinal muscle and arranged muscle fiber without papillae (Figures 5.4a, 5.5a, 5.6b). The anterior part of the fluke contained the digestive tract, while the posterior part was reproductive system. The esophagus anteriorly extended from pharynx without muscular bulb. The tube was covered with dense basophilic glandular cells, the lumen was star-like shaped (Figures 5.4b, 5.5-Ic-e, 5.5-IIc-f, 5.5-IIId-f, 5.5-IVd, 5.6c). The cecal bifurcation had a straight tubular structure and reached from the basal of esophagus to the mid-length of body in the dorsal field (Figures 5.4b-g, 5.5-Ic-i, 5.5-IIc-l, 5.5-IIIc-k, 5.5-IVb-i, 5.6c). The ceca had two muscle layers, the outer longitudinal and inner circular muscles with numerous glandular cells around them (Figure 5.6c). A terminal genitalium opening to the ventral pouch and without

cirrus sac was present near the cecal bifurcation (**Figures 5.4c–e**, **5.5-Id–e**, **5.5-IId–f**, **5.5-IIIc–f**, **5.5-IVc–d**, **Figure 5.6c**). The genital pore was surrounded by genital papillae with papillae in the outer surface. Enormously developed genital fold was present with poorly developed genital sphincter with radial fiber (**Figure 5.6c**). Ventral pouch laid behind the oral opening and reached to the posterior testes in the posterior end. The internal sac was along the ventral field with cross-triangular shape (**Figures 5.4a–l**, **5.5-Ia–n**, **5.5-IIb–p**, **5.5-IIIb–q**, **5.5-IVa–o**).

In the posterior region, the reproductive organs were poorly developed in the small testes flukes (Figure 5.4). Histology of cross-section presented only the basophilic organ behind the end of the ventral pouch that might be the two vertical arranged testes (Figures 5.4k, 5.4l, 5.4p, 5.6d). In flukes with large testes male and female reproductive organs were fully developed. The testes were tandem lobed with globular bodies. The anterior testis was located dorsal to the ventral pouch, and the posterior testis located at the end of ventral pouch ended close to the posterior sucker. Testes were surrounded with connective tissues (Figures 5.5-Ik-r, 5.5-IIn-q, 5.5-IIIm-r, 5.5-IVm-q, 5.6e). The seminal receptacle with spermatozoa had an ovoid shape and was located in a lateral position to testes and ovary (Figures 5.6e, 5.6g). The ovary had ovoid shape and was located between anterior and posterior testis. Ovary contained various basophilic germ cells and was surrounded by connective tissue (Figures 5.5-Io-q, 5.5-IIp-q, 5.5-IIIs, 5.5-IVo-p, 5.6e). The ovoid ootype was located in the center of the Mehlis' gland as a basophilic layer duct. The Mehlis' gland consisted of cells with large nuclei and basophilic cytoplasm. Laurer's canal was connected with the ootype and located in the dorsal field. Vitelline follicle contained basophilic granules (Figures 5.6f, 5.6g). The uterus was filled with eggs and extended from the ootype to the genital pore in the anterior end in the dorsal field (Figures 5.4f-j, 5.5-If-n, 5.5-IIh-n, 5.5-IIIf-p, 5.5-IVe-q, 5.6h). Eggs had ovoid shape with thin shell (Figure **5.6h**). The posterior sucker had arranged strong muscle fibers covered with fine circular and thick longitudinal muscles, and then radial elongated layer which stretched below the posterior testis (**Figures 5.4r–t**, **5.5-Iq–t**, **5.5-IIr–t**, **5.5-IIIs–t**, **5.5-IVr–t**, **5.6i**).

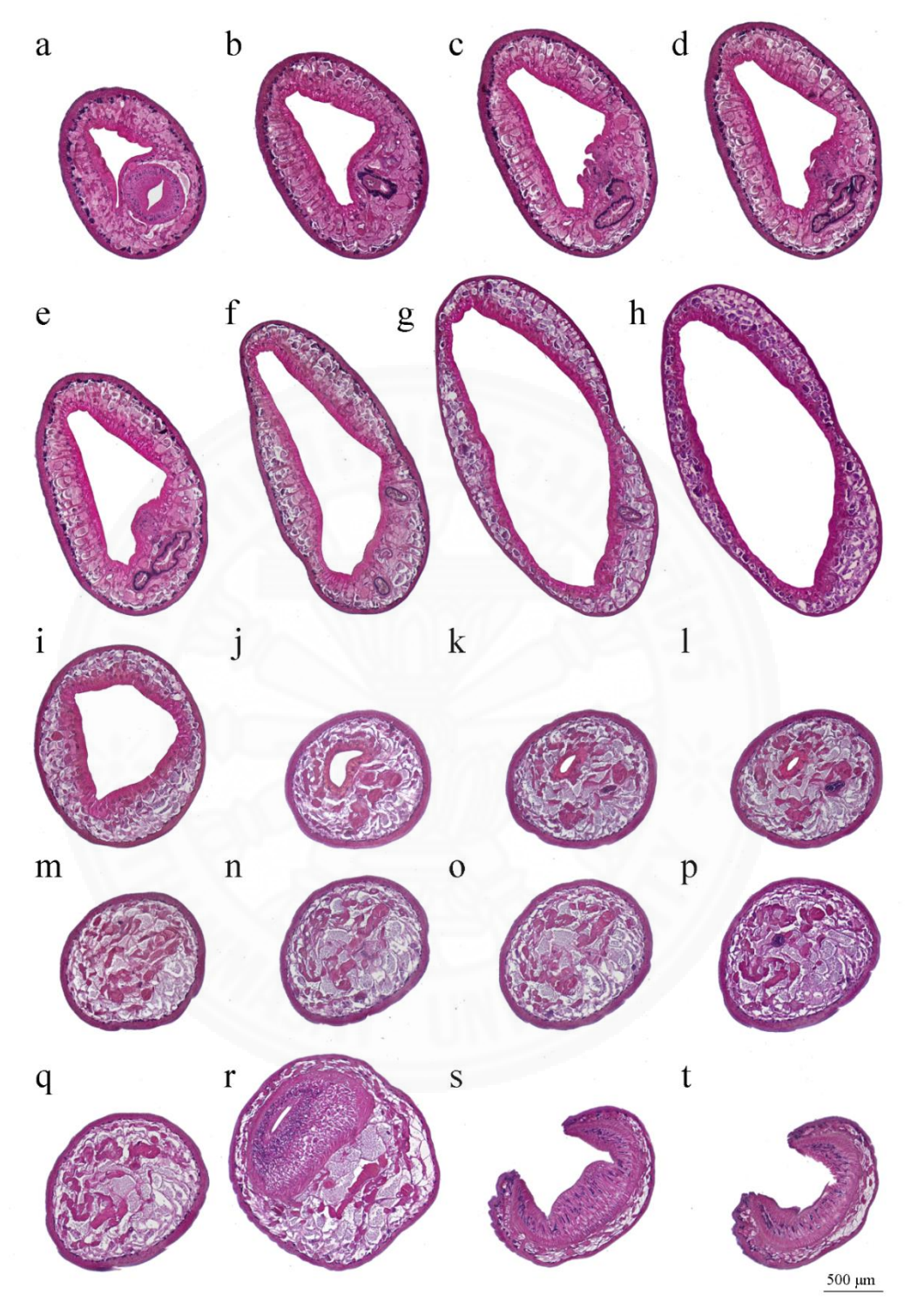


**Figure 5.4** Hematoxylin and eosin staining of *Fischoederius* spp. small testes crosssections collected in 2016. (**a–t**) serial cross-sections of the fluke from the anterior to the posterior end.

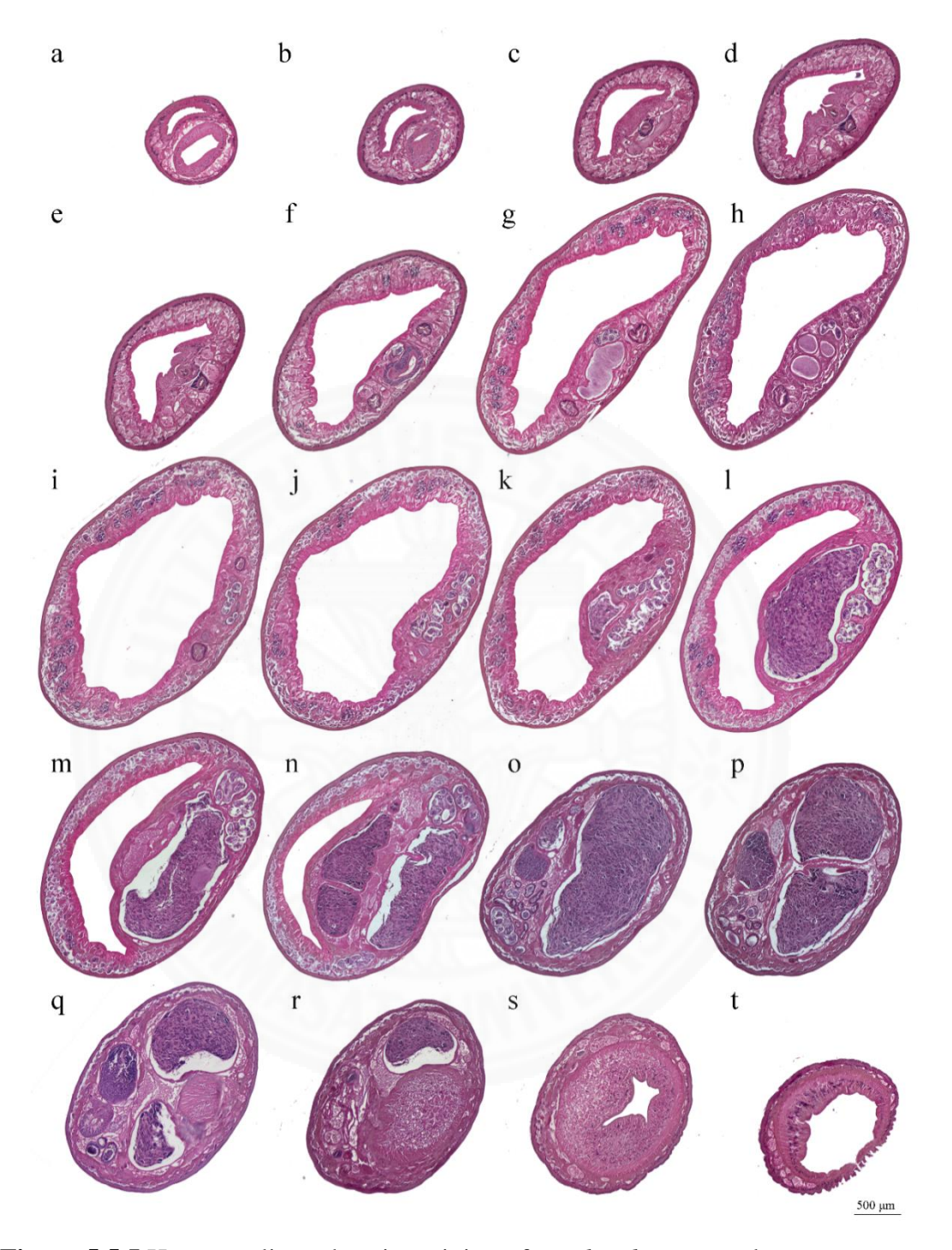


**Figure 5.5-I** Hematoxylin and eosin staining of *Fischoederius* spp. large testes crosssections collected in 2015. (**a–t**) serial cross-sections of the fluke from the anterior to the posterior end.

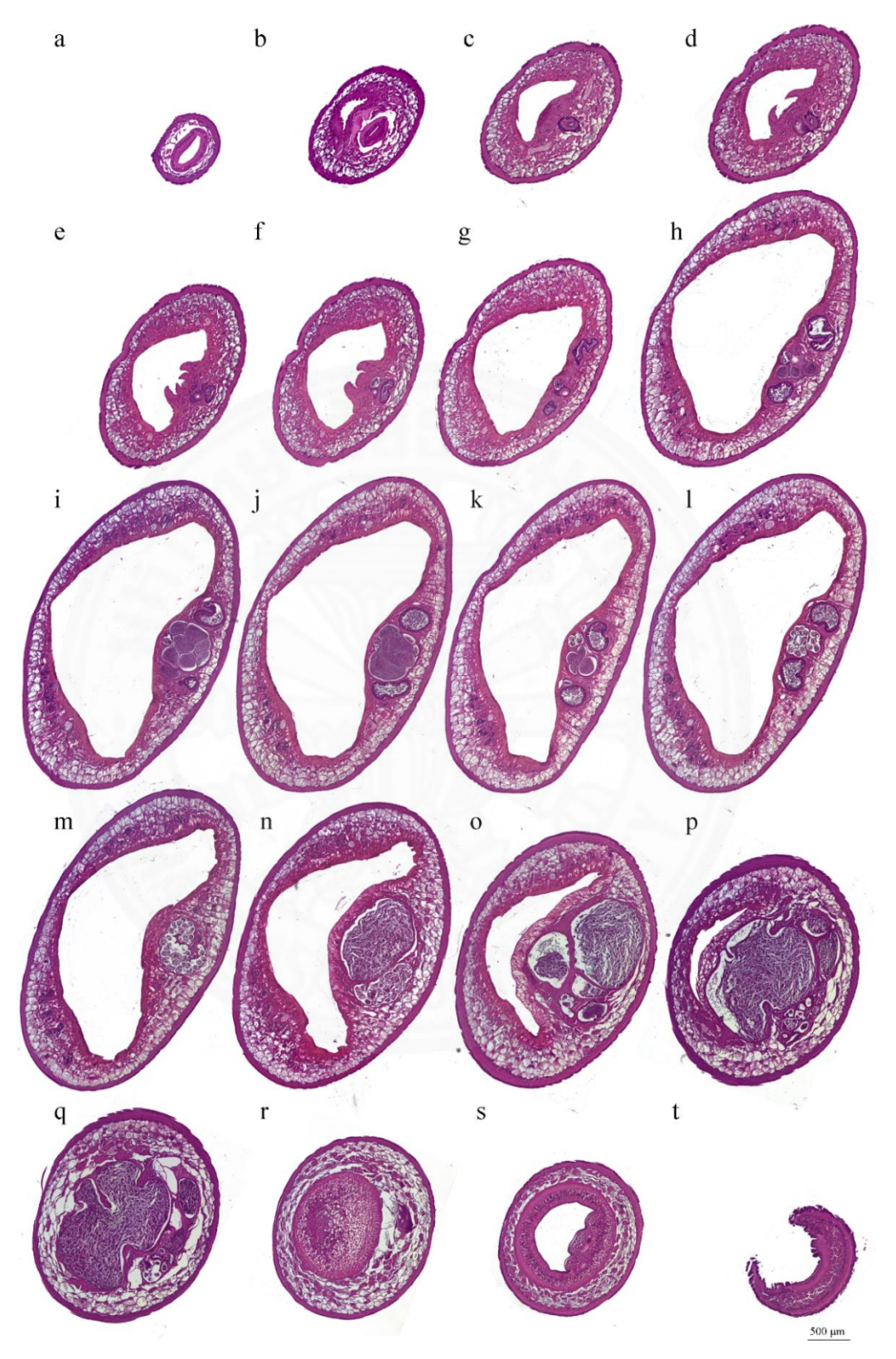


**Figure 5.5-II** Hematoxylin and eosin staining of *Fischoederius* spp. large testes crosssections collected in 2016. (**a–t**) serial cross-sections of the fluke from the anterior to the posterior end.

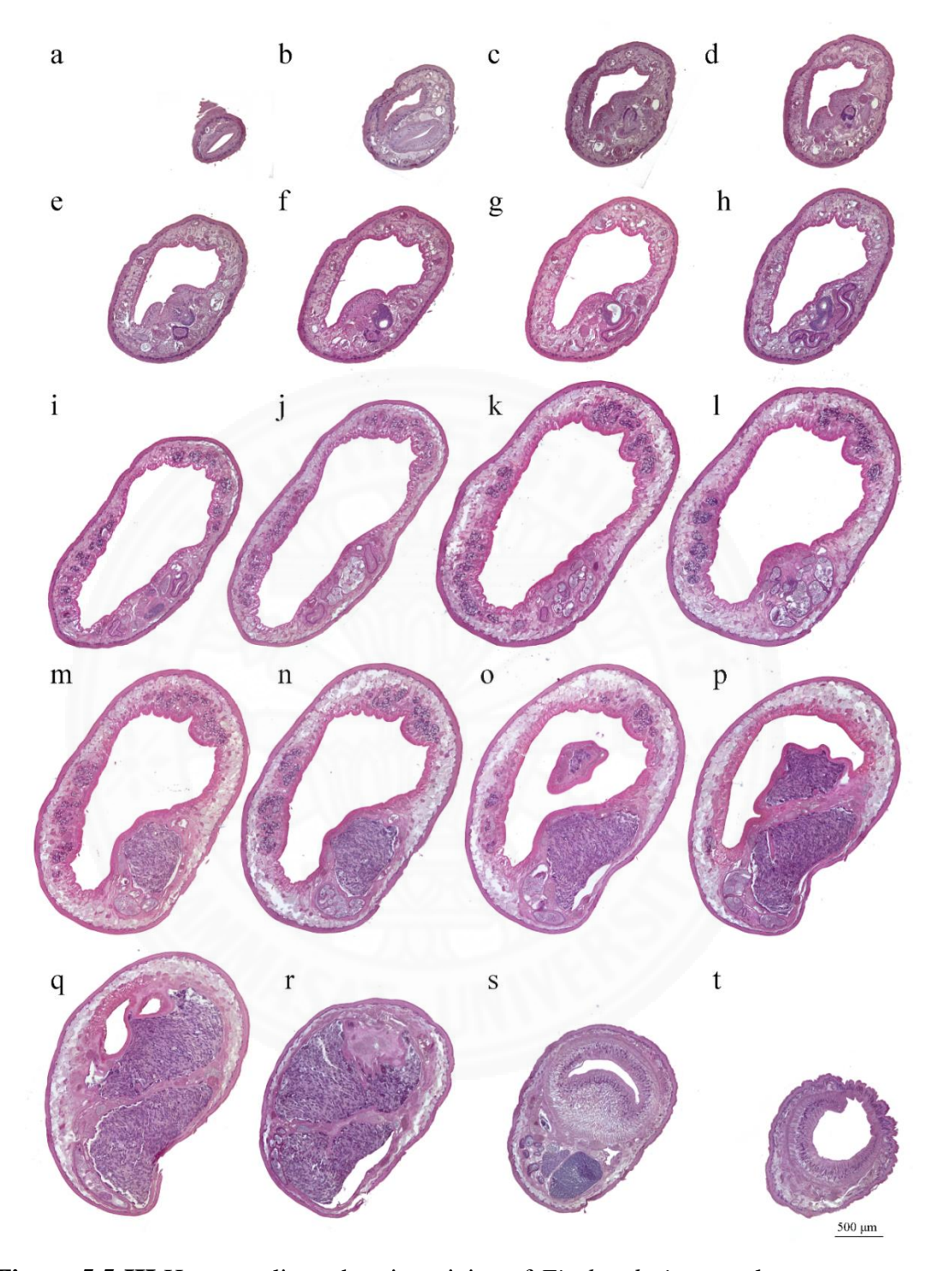


**Figure 5.5-III** Hematoxylin and eosin staining of *Fischoederius* spp. large testes crosssections collected in 2015. (**a–t**) serial cross-sections of the fluke from the anterior to the posterior end.

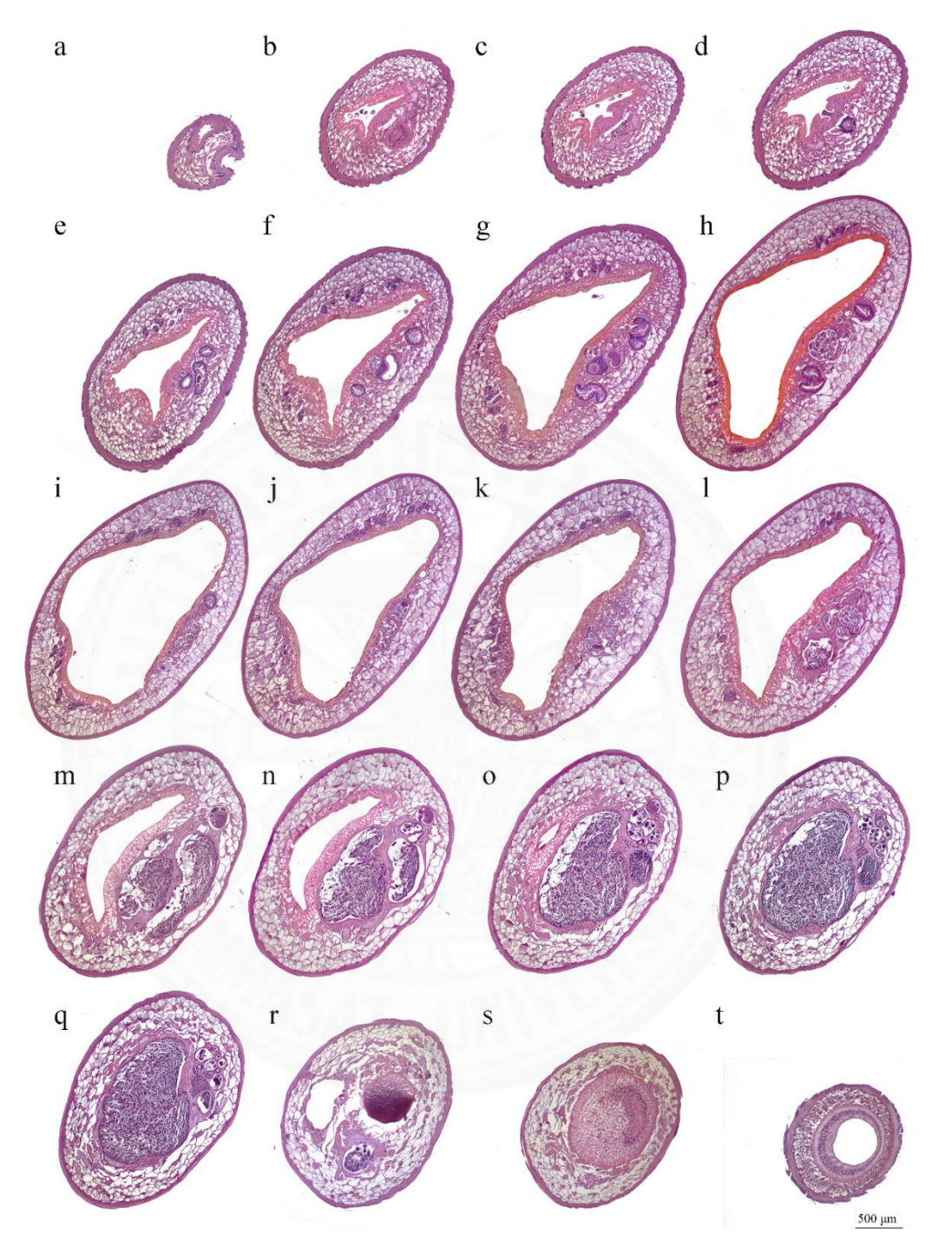
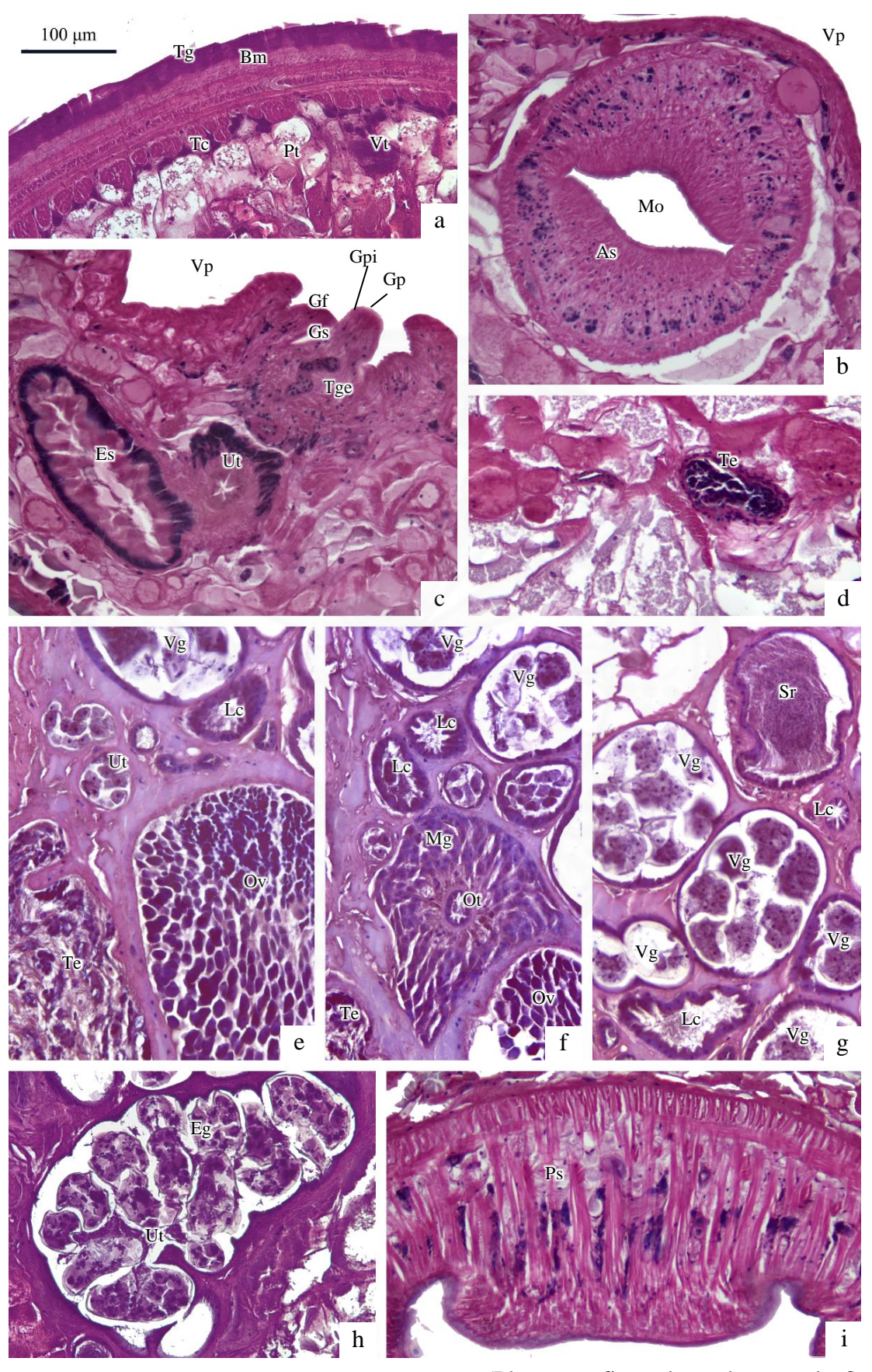


**Figure 5.5-IV** Hematoxylin and eosin staining of *Fischoederius* spp. large testes crosssections collected in 2015. (**a–t**) serial cross-sections of the fluke from the anterior to the posterior end.



(Please see figure legend on overleaf)

**Figure 5.6** Hematoxylin and eosin staining of *Fischoederius* spp. cross-sections collected in the years 2014–2019. (**a–c**) Anterior parts of the fluke, (**d**) Posterior part of the small testes fluke, (**e–i**) Posterior parts of the large testes fluke. Tg: Tegument; Bm: Basement membrane; Tc: Tegumental cells; Pt: Parenchymal tissue; Vt: Vitellaria; Mo: Mouth; As: Anterior sucker; Es: Esophagus; Ut: Uterus; Eg: Eggs; Vp: Ventral pouch; Tge: Terminal genitalium; Gp: Genital pore; Gpi: Genital papilla; Gf: Genital fold; Gs: Genital sphincter; Te: Testis; Sr: Seminal receptacle; Ov: Ovary; Ot: Ootype; Mg: Mehlis' gland; Lc: Laurer's canal; Vg: Vitelline glands; Ps: Posterior sucker.



#### 5.2 Molecular identification of *Fischoederius* spp. ribosomal ITS2 region

Following the study of Ghatani et al., 2011 on ribosomal ITS2 sequences in pouched amphistomes, the universal oligonucleotide primers were used to amplify the ribosomal ITS2 region of *Fischoederius* spp. using the standard RT-PCR protocol for total RNA of the flukes as described in Section 4.2.3. PCR amplicon was separated by its size on a 0.7% [w/v] agarose gel as described in **Section 4.2.4**. The PCR product was resolved at the expected 515 bp size as shown in Figure 5.7. The extracted cDNA fragment was ligated into the pGEM®-T Easy vector and introduced into Escherichia coli XL1-Blue as described in Section 4.2.9. Positive transformants were identified by Colony PCR and NotI restriction analysis to confirm insert size as described in Section **4.2.10**. The inserted DNA of the recombinant plasmid was sequenced by a commercial service using the universal primer SP6. BLASTN searches of the obtained ITS2 sequence against the GenBank nucleotide collection (nr/nt) database showed as top hits 99% identity (E-value: 0.0) to F. elongatus sequences (GenBank: GU133062 and JQ688409). The next hits were with Gastrothylax crumenifer, F. cobboldi and Fischoederius spp. HR-2013 sequences (GenBank: KF564868, JQ688408 and KF564867) as shown in **Table 5.1**.

**Table 5.1** Top 5 hits BLASTN result of 460 bp *Fischoederius* spp. ribosomal ITS2 search against nucleotide collection (nr/nt) database of limited to Platyhelminthes (taxid:6157).

Species	Accession	Query cover	E-value	Identity
F. elongatus	GU133062	99%	0.0	99%
F. elongatus	JQ688409	93%	0.0	99%
G. crumenifer	KF564868	91%	0.0	99%
F. cobboldi	JQ688408	92%	0.0	99%
Fischoederius spp. HR-2013	KF564867	91%	0.0	99%

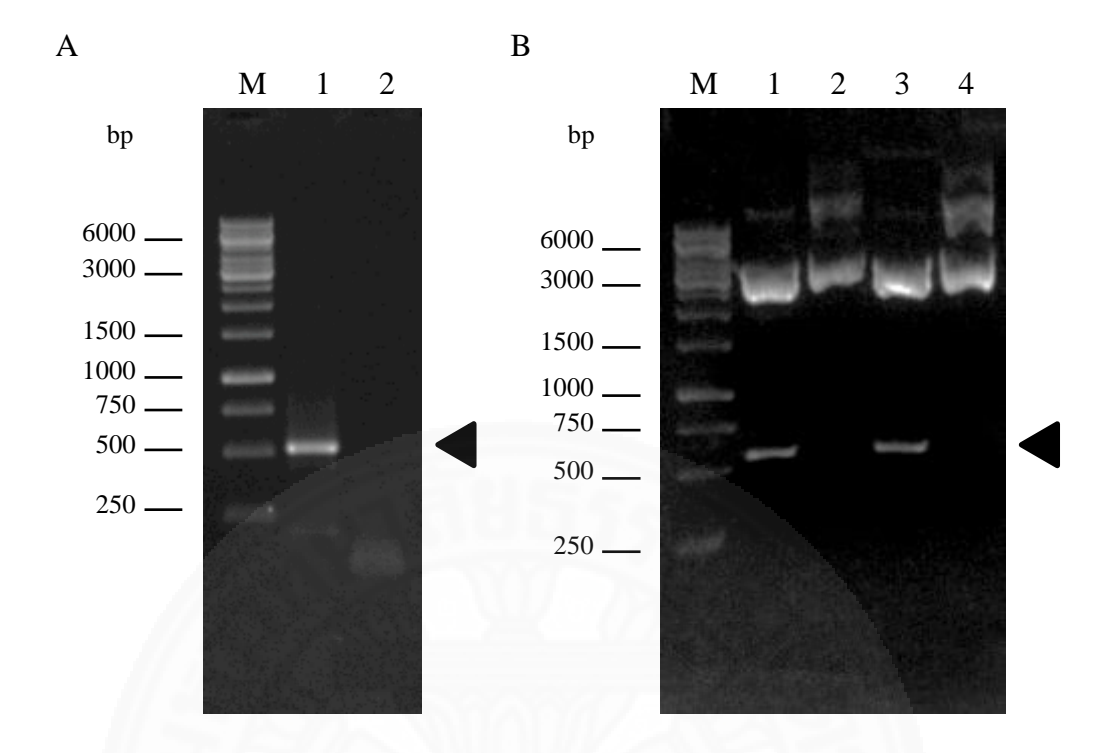


**Figure 5.7** (**A**) Agarose gel electrophoresis of *Fischoederius* spp. ribosomal ITS2; lane 1: RT-PCR amplified 515 bp *Fischoederius* spp. ribosomal ITS2 cDNA fragment (arrowhead); lane 2: Negative control (no template) of RT-PCR; lane M: GeneRuler™ 1 kb DNA ladder (Thermo Fisher Scientific, MA, USA); (**B**) Restriction analysis of pGEM®-T Easy inserted *Fischoederius* spp. ribosomal ITS2 cDNA; lane 1 and 3: *Not*I digestion of recombinant plasmid, *Fischoederius* spp. ribosomal ITS2 cDNA shown by arrowhead: lane 2 and 4: Undigested recombinant plasmid; lane M: GeneRuler™ 1 kb DNA ladder (Thermo Fisher Scientific, MA, USA).

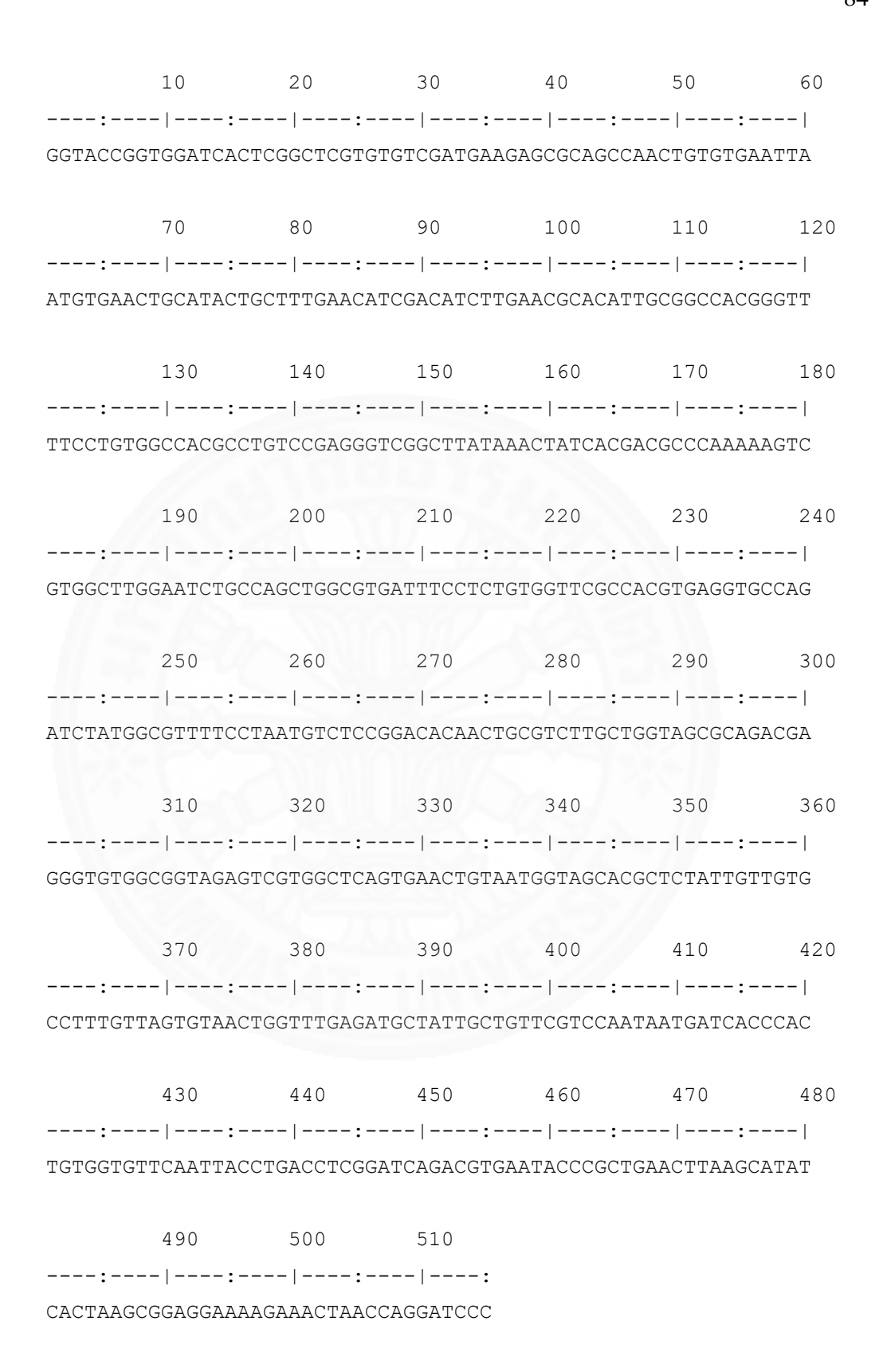


**Figure 5.8** Nucleotide sequences of the isolated *Fischoederius* spp. ribosomal ITS2 cDNA (515 bp) using SHOWSEQ in EMBOSS.

#### 5.3 Restriction analysis of *Fischoederius* spp. mtCOX1

#### 5.3.1 Fischoederius spp. mtCOX1

A 1,536 bp mtCOX1 fragment was amplified by standard PCR from gDNA of each of the 48 specimens shown in **Section 5.3.3**. The PCR primers were designed following the sequence of the previously published *F. elongatus* mitochondrial genome (GenBank: NC\_028001). The PCR product from each specimen was resolved on a 0.7% [w/v] agarose gel (**Figure 5.9**) as described in **Section 4.2.4** and extracted from the gel as described in **Section 4.2.5**. The purified PCR product was used for restriction analysis with *Mse*I as described in **Section 4.4.2**.

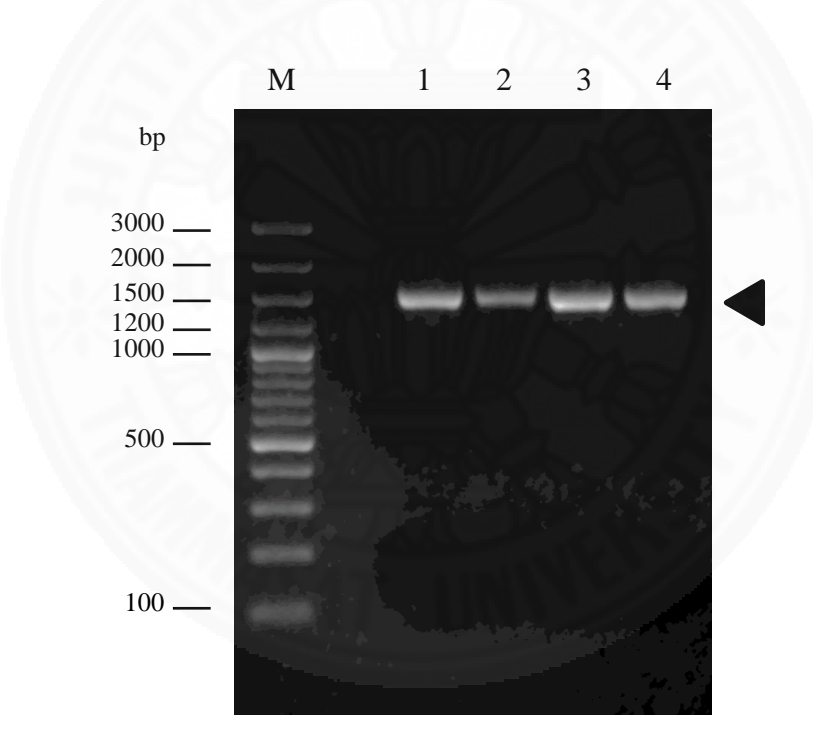


**Figure 5.9** Agarose gel showing the *Fischoederius* spp. 1,536 bp mtCOX1 PCR products (arrowhead) obtained from gDNA of four specimens (lanes 1–4); lane M: GeneRuler<sup>TM</sup> 100 bp Plus DNA ladder (Thermo Fisher Scientific, MA, USA).

## 5.3.2 *Mse*I restriction endonuclease analysis of *Fischoederius* spp. mtCOX1

The purified 1,536 bp mtCOX1 PCR products of the 48 Fischoederius specimens were further characterized by restriction endonuclease

analysis. MseI with the recognition site T^TAA was used for digestion as described in Section 4.4.2. This endonuclease was selected due to the high AT content in F. elongatus mtCOX1 in the previously published mitochondrial genome from China (GenBank: NC\_028001). The MseI-digested PCR products were resolved by 3.0% agarose gel electrophoresis. Ten to twelve fragments with sizes from 20 to 500 bp were observed as shown in Figure 5.11. In the above-mentioned published F. elongatus sequence recognition sites were at positions 100, 118, 211, 277, 293, 343, 349, 433, 472, 577, 775, 947, 973, 1210 and 1259 of the mtCOX1 gene. The 48 Fischoederius specimens in the present analysis did not show this pattern of recognition sites but showed nine different patterns (A-I). Pattern E was most often observed (19/48), followed by pattern D (8/48), C (7/48), H (7/48), A (2/48), F (2/48), B (1/48), G (1/48), and I (1/48). Based on sequence conservation and phylogenetic analysis the nine MseI pattern were assigned to five putative species (Pattern A, [BEG], [CFH], D, and I). Patterns [BEG] and [CFH] with highly conserved sequences are thought to represent polymorphic sequences within their respective species. MseI recognition sites were conserved at positions 100, 433, 947 and 1259 in all patterns. Nine mtCOX1 sequences representing the nine different restriction patterns were cloned into the pGEM®-T Easy and sequenced as described in Sections 4.2.7–4.2.12. Several nucleotide exchanges were observed in the patterns. The 435G>A transition was found in all patterns. The 755T>C transition was only found in pattern B. The 973T>C transition was only found in pattern C. The 345G>A and 351A>G transitions were only found in pattern D. The 483G>A and 1212A>G transitions were only found in pattern I. The T294A transversion was only found in pattern A and D. The 120G>A and 279G>A transitions were only found in pattern I. The 1192T>C transition was only found in pattern D and E.



**Figure 5.10** Virtual *Mse*I restriction map of mtCOX1 sequence *Fischoederius Mse*I pattern A–I created in NEBcutter version 2.0. The blue vertical lines indicate the recognition site T^TAA in each sequence.

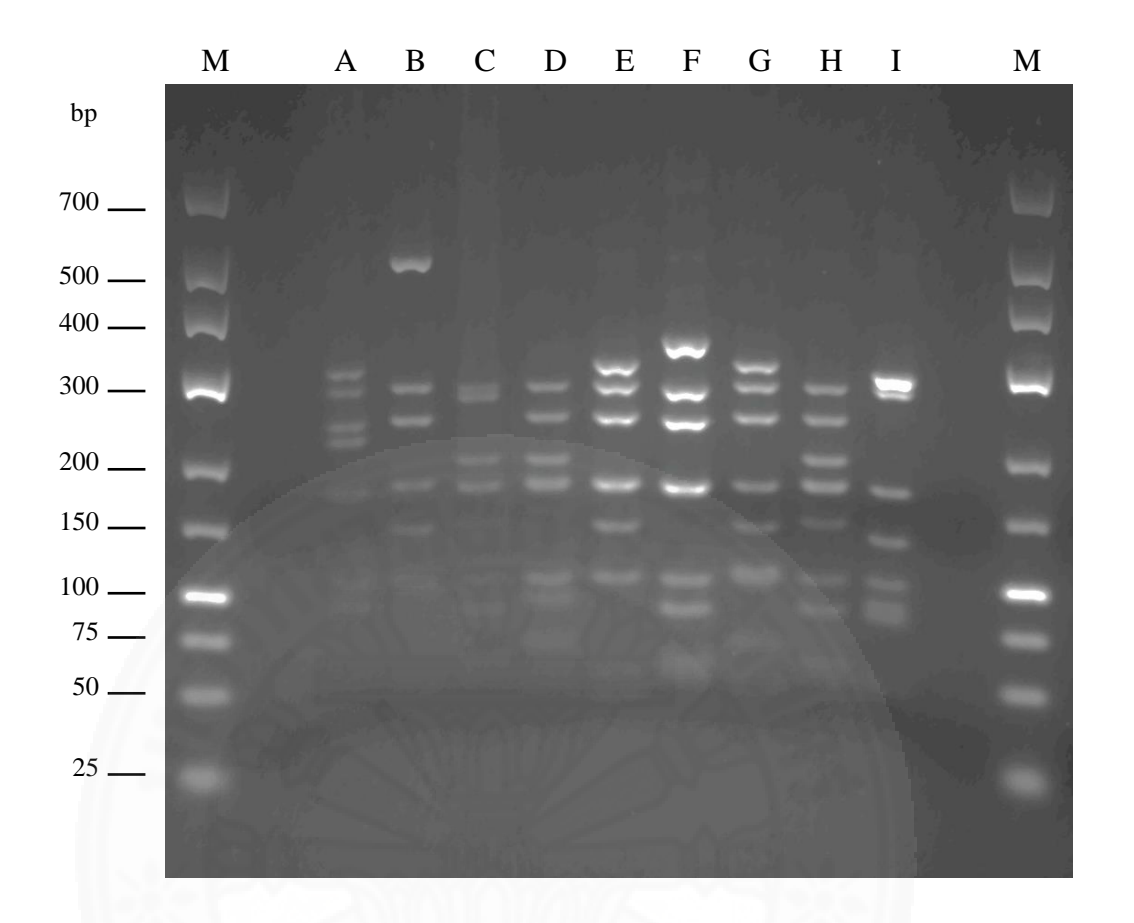


**Figure 5.11** Restriction analysis of *Fischoederius* spp. mtCOX1 with *MseI*; lanes A–I: Nine different restriction patterns of *Fischoederius* spp. mtCOX1 could be discriminated on a 3.0% agarose gel; lane M: GeneRuler<sup>TM</sup> Low Range DNA ladder (Thermo Fisher Scientific, MA, USA).

#### 5.3.3 Images of Fischoederius spp.

Fischoederius specimens were collected from slaughterhouses in the years 2014–2019. Images were taken from forty-eight flukes before extraction of genomic DNA as described in **Section 4.1.2**. The micrographs shown in **Figures 5.12–5.14** were sorted by the *Mse*I restriction pattern of the mtCOX1 gene (**Section 5.3.3**). Specimens A1, B, C1–7, D1–3, E1–9, F1–2, H1–7, I were collected in 2014, specimen A2 in 2016, and specimens D4–8, E10–19, G in 2019. Some flukes were maintained in PBS pH 7.2 at 4°C for six weeks to reduce their body opacity. This allowed to see the internal morphology including ceca, vitellaria, and reproductive system (C1–C4 and H1–H5). Some flukes were damaged because other flukes had attached to them (C3, C6, and H1). All of the flukes showed the morphology as described in **Section 5.1.2**.

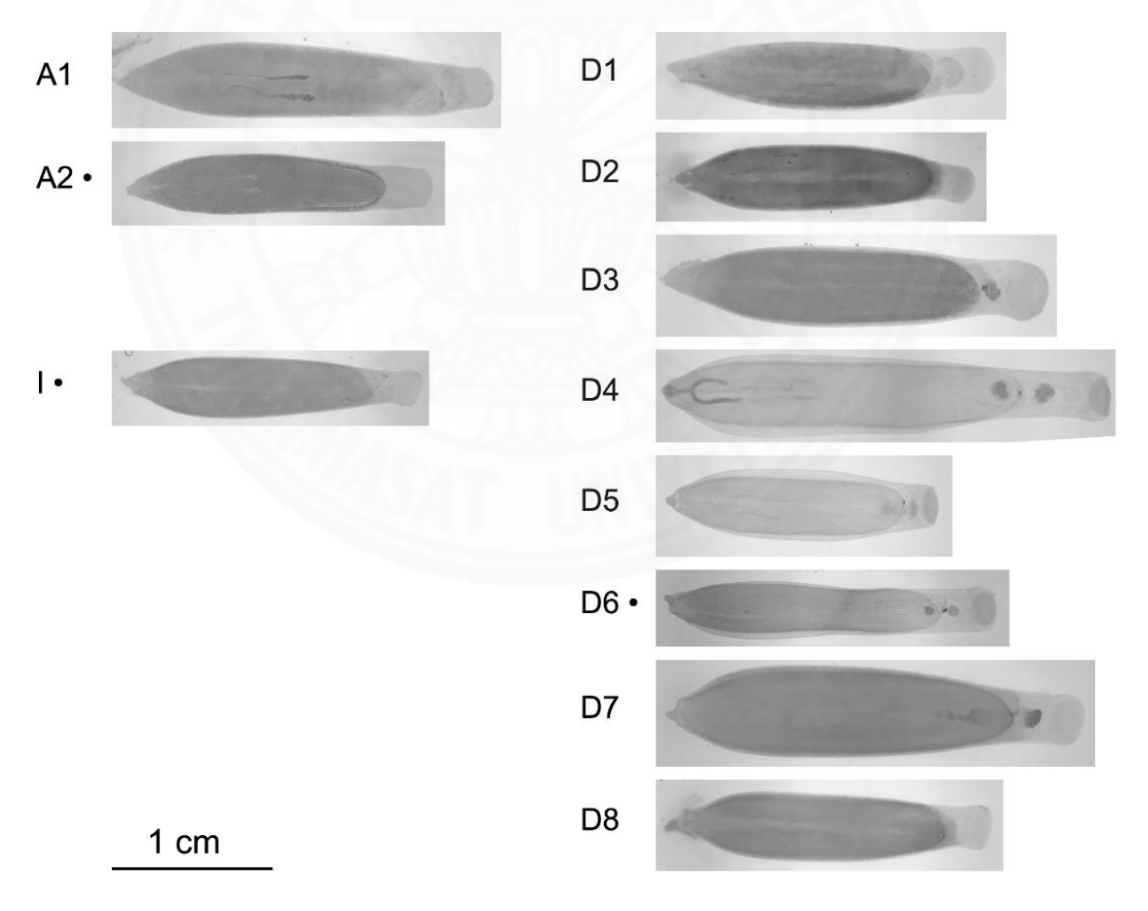


**Figure 5.12** Micrographs of *Fischoederius* spp. mtCOX1 *Mse*I pattern A, D, I. Specimens collected in 2014: A1, D1–3, and I; 2016: A2; 2019: D4–8. Black circles indicate the specimens for which the mtCOX1 restriction patterns are shown in **Figure 5.11** 

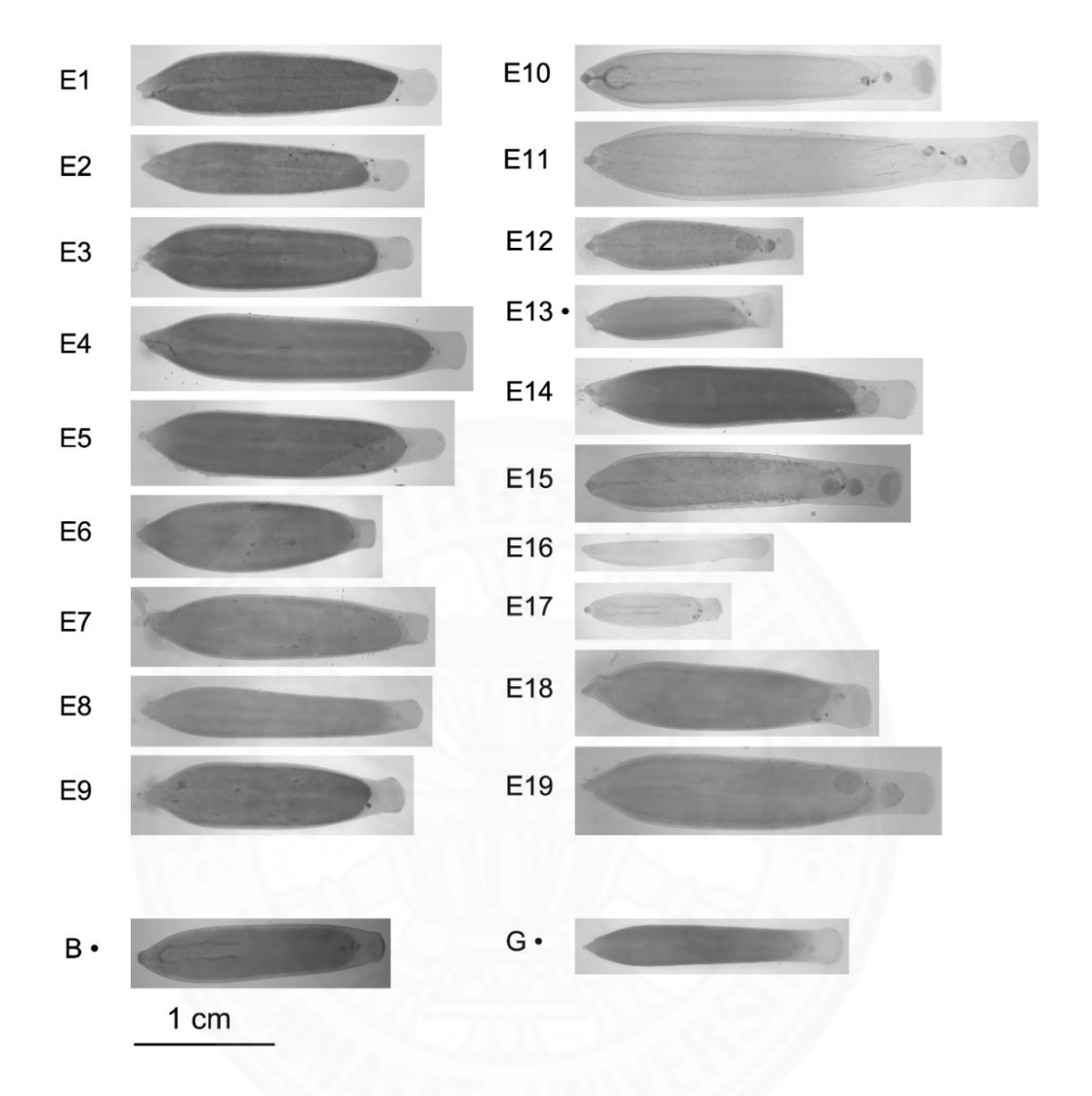


**Figure 5.13** Micrographs of *Fischoederius* spp. mtCOX1 *Mse*I pattern B, E, G. Specimens collected in 2014: B and E1–9; 2019: E10–19, and G. Black circles indicate the specimens for which the mtCOX1 restriction patterns are shown in **Figure 5.11** 

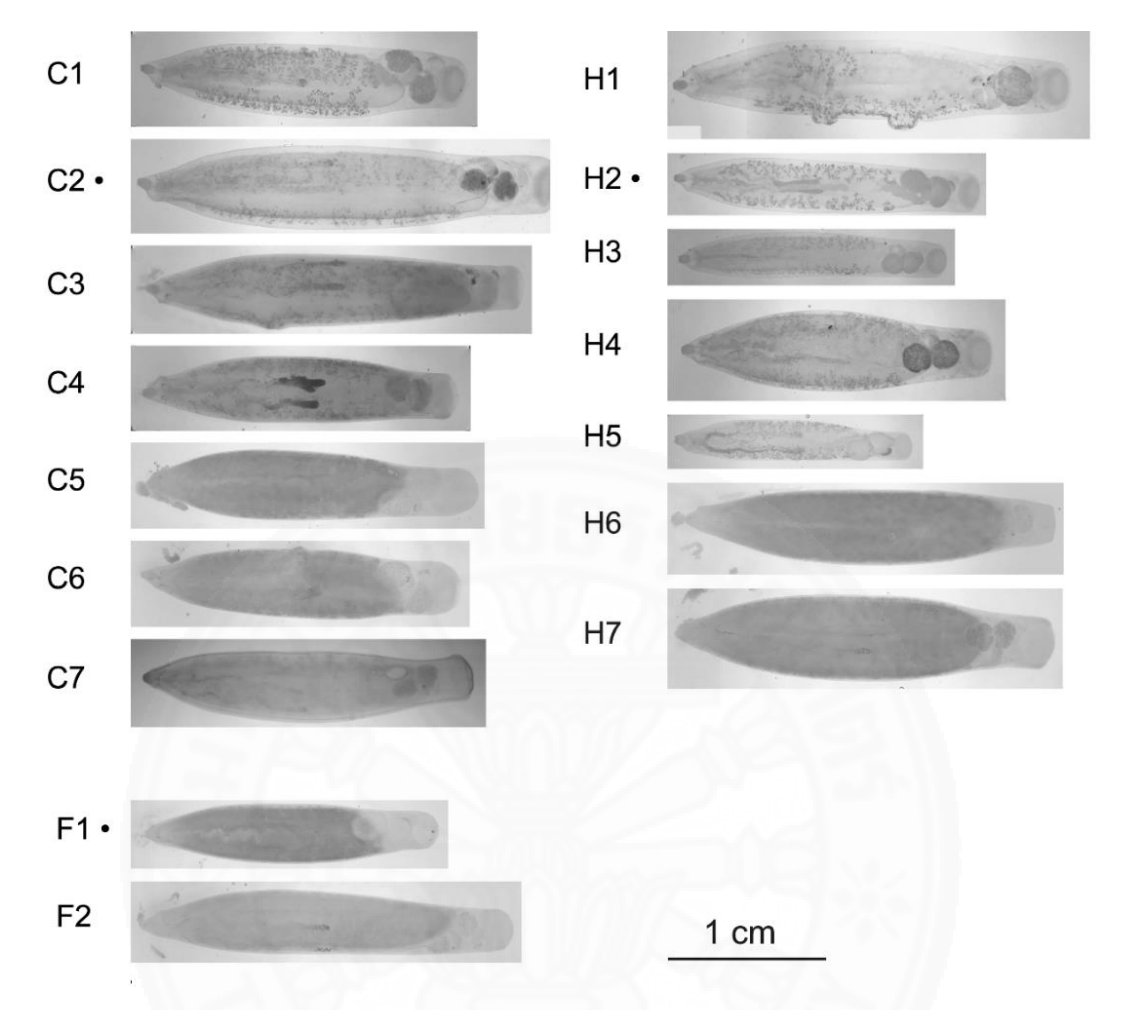


**Figure 5.14** Micrographs of *Fischoederius* spp. mtCOX1 *Mse*I pattern C, F, H. Specimens collected in 2014: C1–7, F1–2, and H1–7. Black circles indicate the specimens for which the mtCOX1 restriction patterns are shown in **Figure 5.11** 

#### 5.3.4 Genetic variation of *Fischoederius* spp. mtCOX1

Sequence identity values between Fischoederius spp. mtCOX1 in this study and previously published sequences of F. elongatus from China (GenBank: NC\_028001, GeneID: 26042463) and other trematodes including F. cobboldi (GenBank: NC\_030529, GeneID: 28255127) and G. crumenifer (GenBank: NC\_027833, GeneID: 25768118) supported that the nine different MseI pattern belonged to five distinct species (Pattern A, [BEG], [CFH], D, and I). Sequence identity values ranged from 88.3–99.3% (Table 5.2). The highest conserved mtCOX1 sequences were Fischoederius spp. pattern C and H (99.3% identity), followed by pattern E and G (99.2%), and pattern F and H (99.2%). The most different sequences from each other were G. crumenifer and Fischoederius spp. pattern I (88.3%), Fischoederius spp. pattern B and C (88.5%), and pattern A, E, F and H (88.6%), respectively. The five suggested species of Fischoederius had 4.2–9.6% sequence difference between each other. Fischoederius spp. pattern [BEG] had intraspecies variation at 0.8–1.3%. Fischoederius spp. pattern [CFH] had intraspecies variation at 0.7–1.0%. The sequence variation between Fischoederius spp. mtCOX1 pattern A–I in this study and F. elongatus from China (GenBank: NC\_028001, GeneID: 26042463) ranged from 5.7–8.3%. Interspecies variations between Fischoederius spp. in this study and F. cobboldi (GenBank: NC\_030529, GeneID: 28255127) and G. crumenifer (GenBank: NC\_027833, GeneID: 25768118) were 6.9-8.9% and 10.8-11.7%, respectively.

Phylogenetic analyses of the available partial sequences of *F. elongatus* mtCOX1 from China, India and other trematodes including *F. cobboldi*, *G. crumenifer*, *E. explanatum*, *C. microbothrioides*, *O. streptocoelium*, *H. Paloniae*, *Ogmocotyle sikae*, *Ogmocotyle* spp. JM-2015, *P. cervi*, and *F. hepatica* were done to evaluate the taxonomic relationship between these trematodes (**Figure 5.15**). Phylogenetic analysis based on the longest mtCOX1 fragment (1536 bp) demonstrated that all *Fischoederius* spp. mtCOX1 sequences obtained in this study were closely related to the sequences of *Fischoederius* spp. from China and India. *Fischoederius* spp. pattern I was the most distant sequence clustered next to *G. crumenifer* which was used as outgroup (**Figure 5.15A**). The phylogenetic tree clearly showed the close relationship of *Fischoederius* spp. pattern [BEG] and [CFH] which formed two highly

supported neighboring clades next to *F. elongatus* (China). *Fischoederius* spp. pattern A and D were clustered together next to *F. cobboldi* (China). Using published data from a study in India by Ghatani *et al.*, 2014 that had analyzed a 364 bp mtCOX1 fragment it was found that *Fischoederius* spp. pattern A was identical to sequences designated *F. elongatus* (India, GeneBank: JX518952, JX518953, JX518954, JQ806365) with pattern D related (**Figure 5.15B**). *F. cobboldi* sequences from India (GeneBank: JX518950, JX518951, and JQ806364) were clustered between *Fischoederius* spp. pattern I and *G. crumenifer* which was used as outgroup. *F. elongatus* (China), *F. cobboldi* (China) were clustered together while *Fischoederius* spp. pattern [BEG] and [CFH] maintained the tree topology shown in **Figure 5.15A**. The third phylogenetic tree based on a 1521 bp mtCOX1 fragment included more distantly related trematode species and clearly showed that mtCOX1 can be used to separate the genus *Fischoederius* from trematodes in other genera (**Figure 5.15C**).

**Table 5.2** Sequence identity values of mtCOX1 region between *Fischoederius* spp. in this study (A–I) and other trematodes including Fe: *F. elongatus* (GenBank: NC\_028001, GeneID: 26042463); Fc: *F. cobboldi* (GenBank: NC\_030529, GeneID: 28255127); Gc: *G. crumenifer* (GenBank: NC\_027833, GeneID: 25768118).

	Gc	Fc	Fe	A	В	C	D	E	F	G	Н
Fc	89.1		4//1	<b>7</b> . Fi							
Fe	88.9	92.5									
A	88.6	93.1	92.8								
В	88.5	91.9	94.3	93.3							
C	88.5	91.3	93.6	92.6	95.4						
D	89.2	92.1	91.7	92.8	91.6	91.1					
E	88.6	91.7	94.1	92.9	98.7	95.0	91.7				
F	88.6	91.7	93.8	93.0	95.8	99.0	91.1	95.4			
G	88.7	91.8	94.2	93.2	99.0	95.1	91.7	99.2	95.6		
H	88.6	91.5	93.6	92.9	95.5	99.3	91.3	95.1	99.2	95.2	
I	88.3	91.1	92.4	90.7	91.5	91.0	90.4	91.5	91.2	91.8	91.4

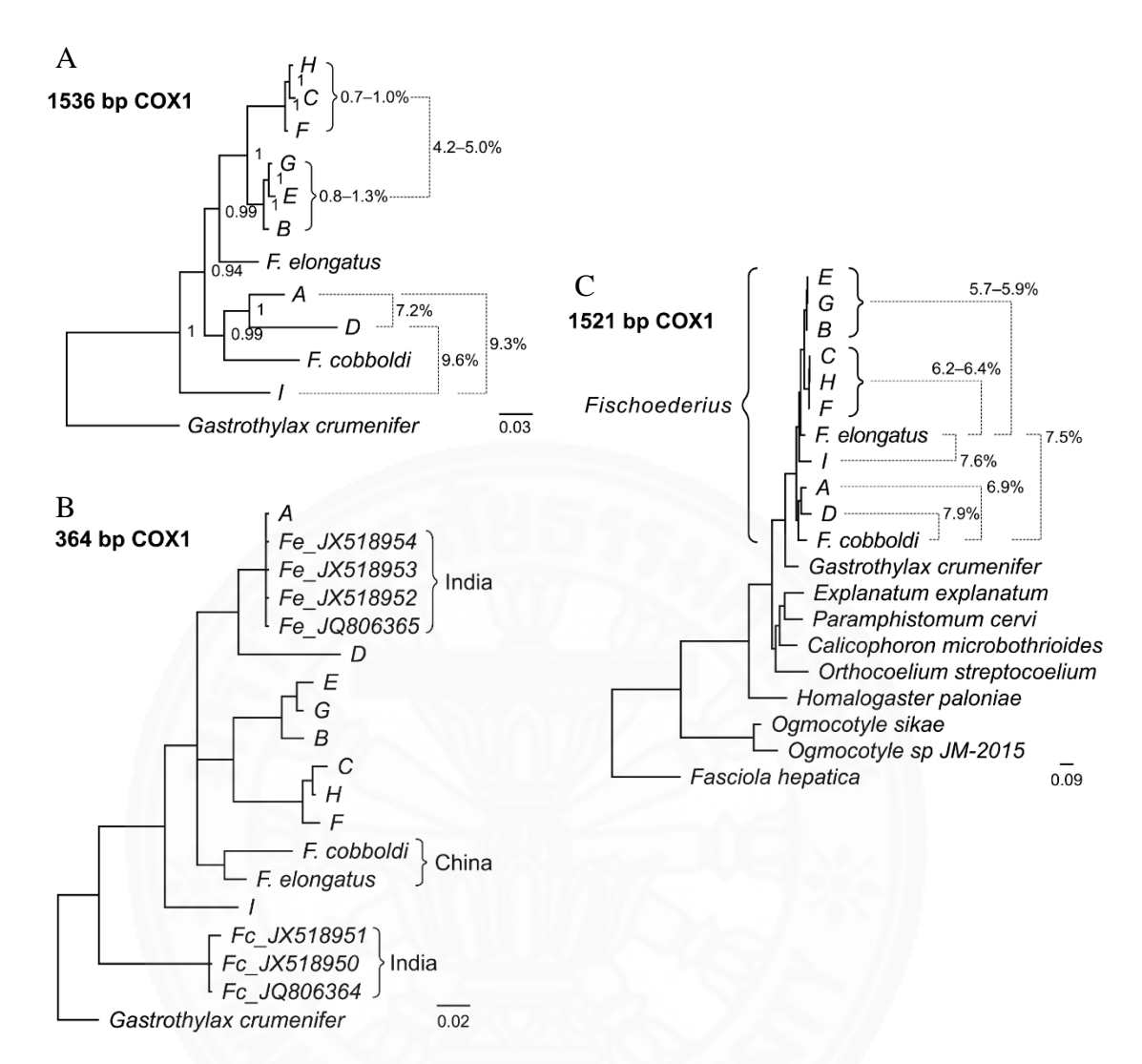


Figure 5.15 Phylogenetic analysis of *Fischoederius* spp. mtCOX1 pattern A–I and other trematodes including *F. elongatus* from China (GenBank: NC\_028001, GeneID: 26042463), *F. elongatus* from India (GeneBank: JX518952, JX518953, JX518954, JQ806365) and, *F. cobboldi* from China (GenBank: NC\_030529, GeneID: 28255127), *F. cobboldi* from India (GeneBank: JX518950, JX518951, and JQ806364), *G. crumenifer* (GenBank: NC\_027833, GeneID: 25768118), *E. explanatum* (GenBank: NC\_027958, GeneID: 26038454), *C. microbothrioides* (GenBank: NC\_027271, GeneID: 24570901), *O. streptocoelium* (GenBank: NC\_028071, GeneID: 26047474), *H. Paloniae* (GenBank: NC\_030530, GeneID: 28255164), *Ogmocotyle sikae* (GenBank: NC\_027112, GeneID: 24286781), *Ogmocotyle* spp. JM-2015 (GenBank: KR006935, Base position: 6897–8441), *P. cervi* (GenBank: NC\_023095, GeneID: 17961305), and *F. hepatica* (GenBank: NC\_002546, GeneID: 800038). A: 1536 bp mtCOX1 fragment, **B**: 364 bp mtCOX1 fragment, **C**: 1,521 bp mtCOX1 fragment.

#### 5.4 Mitochondrial genome of Fischoederius spp.

### 5.4.1 General features of *Fischoederius* spp. mitochondrial genome *Mse*I pattern A

Following *F. elongatus* mitochondrial genome study by Yang *et al.*, 2015 in Tianmen and Han *et al.*, 2020 in Shanghai, China, partial mitochondrial sequences were obtained from *Fischoederius* spp. *MseI* pattern A transcriptome data to assemble the complete mitochondrial genome of the Thailand isolate. Sequences still missing following transcriptome sequencing were obtained by PCR with 16 oligonucleotide primers as described in **Section 4.3.4**. The PCR products had the expected sizes of 1100, 1536, 875, 1508, 989, 1159, 577, 898 bp as shown in **Figure 5.16**. Standard Sanger dideoxy sequencing was performed using commercial services. The mtDNA fragment generated by primers HRG-596/623 was difficult to sequence and sequencing had to be repeated several times at different conditions by the commercial service providers as described in **Section 4.2.12**. The partial sequences of Thai-strain *Fischoederius MseI* pattern A were aligned and manually assembled by comparison with the previously published trematode mitochondrial genome sequences using the program SeaView version 5.0.1 as described in **Section 4.3.6.1**.

The circular mitochondrial genome of *Fischoederius Mse*I pattern A is 14,780 bp in length. Sequence analysis with MITOS and NCBI ORF finder revealed the features of the investigated genome by comparison with nearby trematode including *F. elongatus* China isolated (GenBank: NC\_028001), *F. cobboldi* (GenBank: NC\_030529), *G. crumenifer* (GenBank: NC\_027833), *C. microbothrioides* (GenBank: NC\_027271), *and P. cervi* (GenBank: NC\_023095) as described in **Sections 4.3.6.2–3**. The mitochondrial genome comprises 12 protein-coding genes (*cytb, cox*1–3, *nad*1–6, *nad*4L, and *atp*6), 23 tRNA genes, 2 rRNA genes (rrnS and rrnL), and 2 non-coding regions (SNR and LNR). The protein-coding genes are arranged in the same orientation in the following order; cox3 > cytb > nad4L > nad4 > atp6 > nad2 > nad1 > nad3 > cox1 > cox2 > nad6 > nad5. The mitochondrial genome is lacking *atp*8. The intergenic spacers in the mitochondrial genome range from 1 to 301 bp. The overlapping nucleotides between each feature range from 2 to 39 bp. The features of the mitochondrial genome of *Fischoederius Mse*I pattern A are listed in **Table 5.3**.

The nucleotide composition of the transcribed strand of the *Fischoederius* spp. *Mse*I pattern A mitochondrial genome is 20.0% A, 43.8% T, 26.5% G, and 9.7% C. The A+T content of genes ranges from 63.1–68.8%. The overall A+T content is 63.8% as shown in **Table 5.4**. The overall G-C Skew is 0.463, and A-T Skew is –0.374. The GC content distribution in the full mitochondrial genome is shown in **Figure 5.17**.

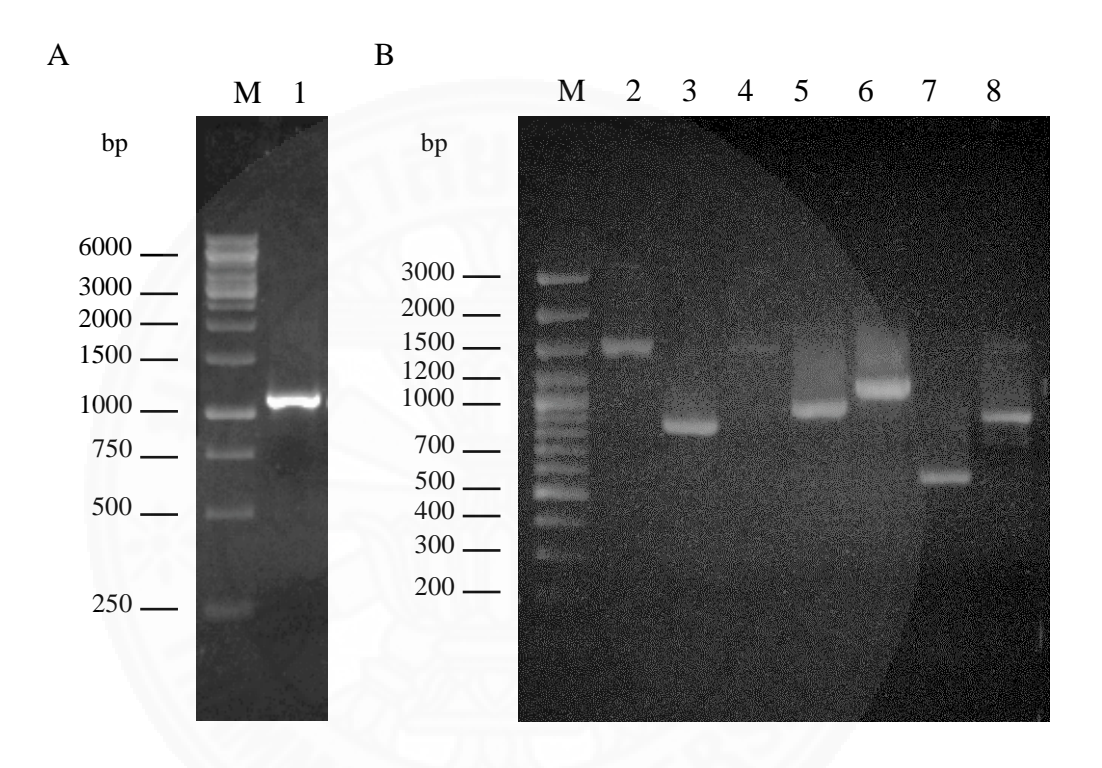


**Figure 5.16** Agarose gel electrophoresis of *Fischoederius Mse*I pattern A mitochondrial genome fragments amplified by PCR; lane 1: 1,100 bp *cytb* fragment; lane 2: 1,536 bp *cox*1 fragment; lane 3: 875 bp *nad4/atp*6 fragment; lane 4: 1,508 bp *nad2/nad*1 fragment; lane 5: 989 bp *nad1/cox*1 fragment; lane 6: 1,159 bp *cox1/trn*C fragment; lane 7: 577 bp *nad6/nad*5 fragment; lane 8: 898 bp nad5/cox3 fragment; lane M: (**A**) GeneRuler<sup>TM</sup> 1 kb DNA ladder; (**B**) GeneRuler<sup>TM</sup> 100 bp Plus DNA ladder (Thermo Fisher Scientific, MA, USA).

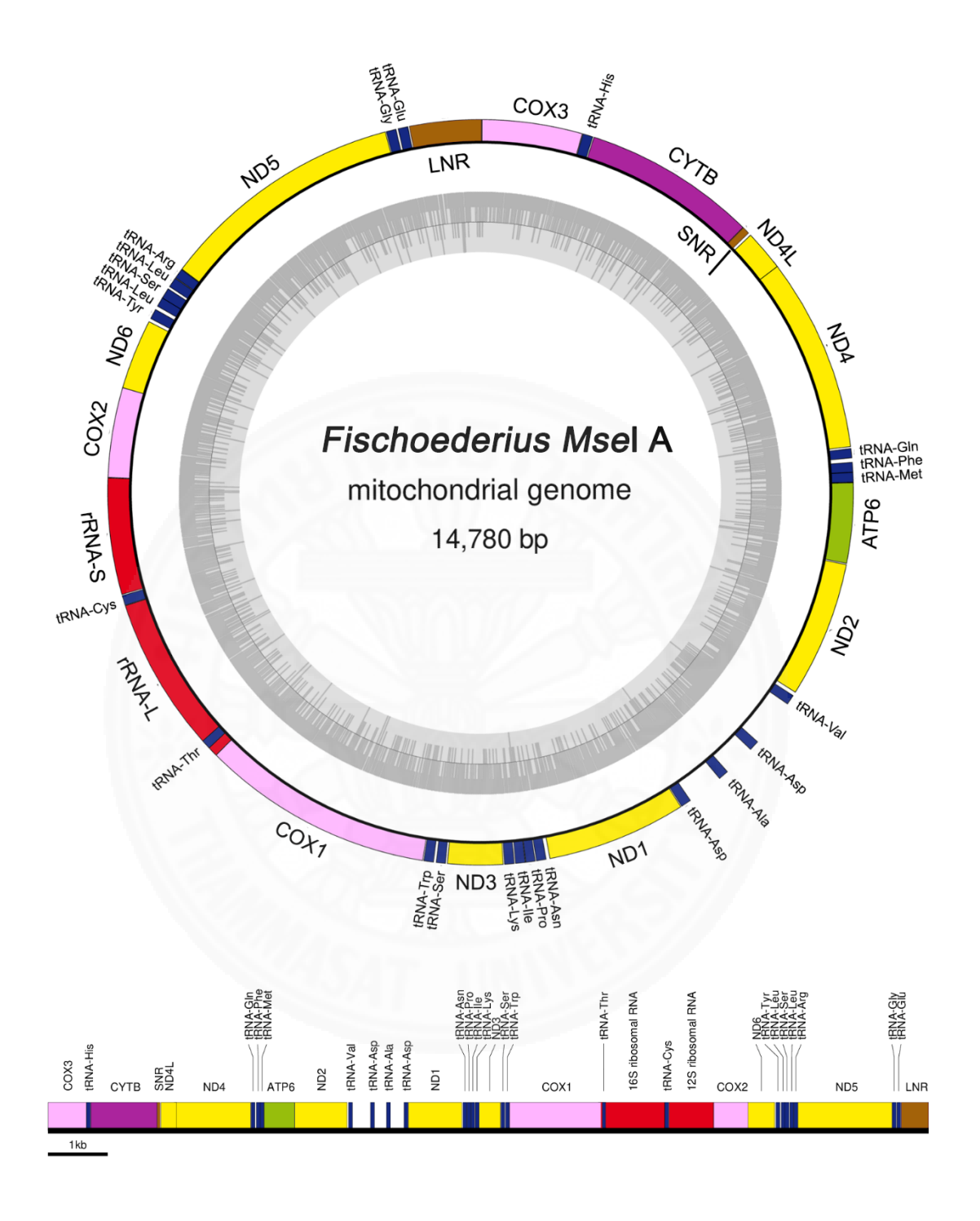


**Figure 5.17** Diagrams of the mitochondrial genome of *Fischoederius* mtCOX1 *Mse*I pattern A using Organellar Genome DRAW (OGDRAW). The mitochondrial genome is 14,780 bp in length containing 12 protein-coding genes, 23 tRNA genes, 2 rRNA genes and 2 non-coding regions, encoded in the same direction. The inner gray circle shows the GC content of the sequence.

 Table 5.3
 Features of the mitochondrial genome of Fischoederius mtCOX1 MseI A

Gene/	Posi		Length	Ini/Ter	Anticodons	No. of	In
Region	Start	Stop	(bp)	Codons		Amino Acids	
cox3	1	645	645	ATG/TAG	am a	215	0
trnH	647	714	68		GTG		+2
cytb	719	1831	1113	ATG/TAA		371	+5
SNR	1832	1880	49				+1
nad4L	1896	2159	264	ATG/TAG		88	+16
nad4	2120	3400	1281	ATG/TAG		427	-39
trnQ	3410	3472	63		TTG		+10
trnF	3497	3563	67		GAA		+25
trnM	3561	3626	66		CAT		-2
atp6	3626	4141	516	ATG/TAG		172	0
nad2	4146	5021	876	GTG/TAG		292	+5
trnV	5044	5111	68		TAC		+23
trnD	5412	5480	69		GTC		+301
trnA	5680	5748	69		TGC		+200
trnD	5976	6044	69		GTC		+228
nad1	6048	6944	897	ATG/TAG		299	+4
trnN	6966	7031	66		GTT		+22
trnP	7036	7098	63		TGG		+5
trnI	7099	7163	65		GAT		+1
trnK	7169	7233	65		CTT		+6
nad3	7238	7594	357	ATG/TAG		119	+5
trnS	7604	7665	62		GCT		+10
trnW	7680	7744	65		TCA		+15
cox1	7748	9289	1542	GTG/TAA		514	+4
trnT	9299	9362	64		TGT		+10
rrnL	9363	10352	990				+1
trnC	10353	10419	67		GCA		+1
rrnS	10424	11170	747				+5
cox2	11171	11752	582	ATG/TAG		194	+1
nad6	11746	12198	453	GTG/TAG		151	-6
trnY	12218	12285	68		GTA		+20
trnL	12307	12370	64		TAG		+22
trnS	12368	12438	71		TGA		-2
trnL	12452	12518	67		TAA		+14
trnR	12520	12586	67		TCG		+2
nad5	12587	14167	1581	GTG/TAA		527	+1
trnG	14171	14236	66		TCC		+4
trnE	14248	14313	66		TTC		+12
LNR	14320	14780	461				+7

**Table 5.4** Nucleotide contents of each protein coding gene within the mitochondrial genome of *Fischoederius* mtCOX1 *Mse*I pattern A

Gene	A (%)	T (%)	G (%)	C (%)	A+T (%)	G+C (%)
cox3	19.8	49.0	23.1	8.1	68.8	31.2
cytb	19.2	45.9	26.0	8.9	65.1	34.9
nad4L	21.6	45.1	25.8	7.6	66.7	33.3
nad4	16.1	47.7	26.2	10.0	63.8	36.2
atp6	17.8	47.7	24.6	9.9	65.5	34.5
nad2	16.2	51.1	25.2	7.4	67.4	32.6
nad1	17.8	46.6	27.4	8.1	64.4	35.6
nad3	16.2	47.3	28.0	8.4	63.6	36.4
cox1	18.5	45.6	24.8	11.1	64.1	35.9
cox2	20.8	42.3	26.6	10.3	63.1	36.9
nad6	17.2	47.7	26.9	8.2	64.9	35.1
nad5	16.4	47.5	28.1	7.9	63.9	36.1

# 5.4.1.1 Protein-coding genes of *Fischoederius* spp. mitochondrial genome *Mse*I pattern A

Based on sequence comparison with other trematodes, *Fischoederius* spp. *Mse*I pattern A mitochondrial genome contains 12 protein-coding genes including *cytb*, *cox*1–3, *nad*1–6, *nad*4L, and *atp*6. A total of 3,363 codons were conceptually translated into amino acid sequences using Echinoderm and flatworm mitochondrial code table 9 (**Figures 5.18–5.41**). The twelve proteins contain 264 to 1581 amino acids. All 64 codons are present in the mitochondrial genome. The most common initiation codon is ATG (8/12) followed by GTG (4/12) and the most common termination codon is TAG (9/13) followed by TAA (3/12). The most frequently used codon is TTT (Phe) 9.49%, followed by TTG (Leu) 8.09%, TTA (Leu) 5.77%, GTT (Val) 5.59%, and TAT (Tyr) 5.03%. The less frequently used codons are CGC (Arg), CTC (Leu), and ACC (Thr) at 0.09%. The third base of the used codons is most often T (51.35%) followed by G (28.20%), A (16.74%), and C (3.71%). The high frequency of T as the third base is also due to the most frequently used TTT (Phe) codon. The

complete codon usage is shown in **Table 5.5**. The five most frequently used amino acids are leucine (16.12%) followed by valine (12.40%), phenylalanine (10.41%), serine (10.20%), and glycine (7.61%), which together make up 56.74% of the total number of amino acids.

**Table 5.5** Codon usage of 12 protein-coding genes of mitochondrial genome of *Fischoederius Mse*I pattern A.

Amino Acid	Codon	Number	Frequency (%)	Amino Acid	Codon	Number	Frequency (%)
Ala	GCG	30	0.89	Asn	AAA	18	0.54
Ala	GCA	15	0.45	Asn	AAT	56	1.67
Ala	GCT	96	2.85	Asn	AAC	4	0.12
Ala	GCC	4	0.12	Pro	CCG	14	0.42
Cys	TGT	107	3.18	Pro	CCA	12	0.36
Cys	TGC	16	0.48	Pro	CCT	52	1.55
Asp	GAT	58	1.72	Pro	CCC	5	0.15
Asp	GAC	4	0.12	Arg	CGG	10	0.30
Glu	GAG	59	1.75	Arg	CGA	7	0.21
Glu	GAA	24	0.71	Arg	CGT	42	1.25
Phe	TTT	319	9.49	Arg	CGC	3	0.09
Phe	TTC	31	0.92	Ser	AGG	38	1.13
Gly	GGG	45	1.34	Ser	AGA	27	0.80
Gly	GGA	27	0.80	Ser	AGT	104	3.09
Gly	GGT	167	4.97	Ser	AGC	4	0.12
Gly	GGC	17	0.51	Ser	TCG	26	0.77
His	CAT	44	1.31	Ser	TCA	23	0.68
His	CAC	4	0.12	Ser	TCT	114	3.39
Ile	ATA	68	2.02	Ser	TCC	7	0.21
Ile	ATT	125	3.72	Thr	ACG	21	0.62
Ile	ATC	4	0.12	Thr	ACA	15	0.45
Lys	AAG	52	1.55	Thr	ACT	52	1.55
Leu	TTG	272	8.09	Thr	ACC	4	0.12
Leu	TTA	194	5.77	Val	GTG	159	4.73
Leu	CTG	23	0.68	Val	GTA	64	1.90
Leu	CTA	13	0.39	Val	GTT	188	5.59
Leu	CTT	37	1.10	Val	GTC	6	0.18
Leu	CTC	3	0.09	Trp	TGG	72	2.14
Met	ATG	106	3.15	Trp	TGA	41	1.22
Gln	CAG	14	0.42	Tyr	TAT	169	5.03
Gln	CAA	13	0.39	Tyr	TAC	9	0.27

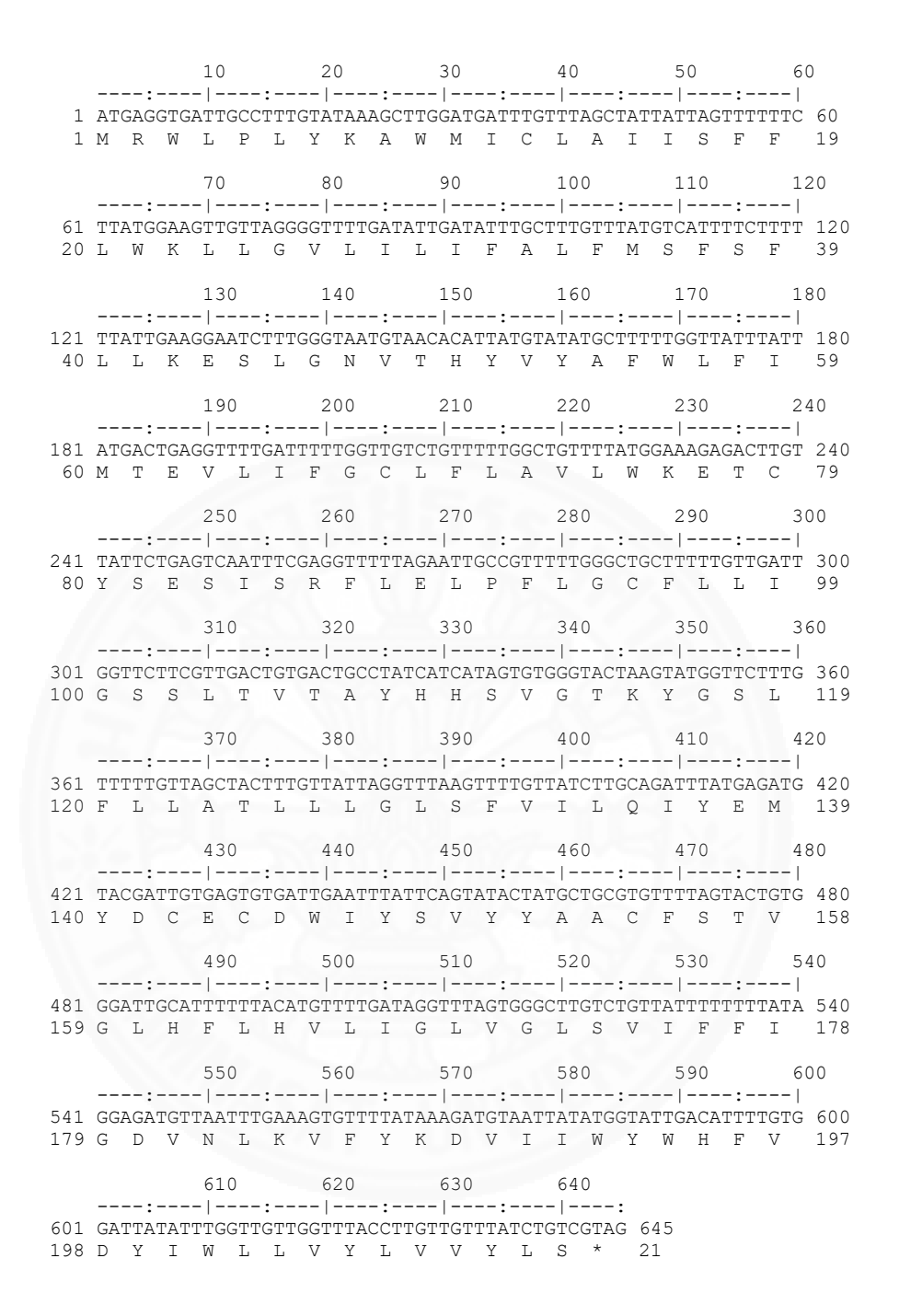


**Figure 5.18** Nucleotide and deduced amino acid sequences of the isolated *Fischoederius* spp. cytochrome c oxidase subunit III (645 bp) using SHOWSEQ in EMBOSS.

F-A Fe Fc Gc Cm	1 1 1 1	MSWLPLYNAWMICLAIISFFLWKLLGVLILIFALFMSFSFLLKESLGNVTHYVYAFWLFI        V	60 60 60 60
Pc	1	IVLV.LVV.LVL.L.YAL	60
F-A Fe Fc Gc Cm Pc	61 61 61 61 61	MTEVLIFGCLFLAVLWNETCYSESISSFLELPFLGCFLLIGSSLTVTAYHHSVGTKYGSL        S	120 120 120 120 120 120
F-A Fe Fc Gc Cm	121 121 121 121 121	FLLATLLIGLSFVILQIYEMYDCECDWIYSVYYAACFSTVGLHFLHVLIGLVGLSVIFFI        F	180 180 180 180
Pc	121	LFFVVF.VVVVV	180

**Figure 5.19** Multiple alignment of cytochrome c oxidase subunit III; F-A: *Fischoederius Mse*I pattern A; Fe: *F. elongatus* isolated from Tianmen, China; Fc: *F. cobboldi*; Gc: *G. crumenifer*; Cm: *C. microbothrioides*, and Pc: *P. cervi*. Black dots indicate conserved positions.

```
10 20 30 40 50 60
  ----:----|----:----|----:----|
 1 ATGGTGTCTCTGGTGCGTTCTAATGTTGTGGATTTGCCTACTAATTTATCTTTGAGGTAT 60
 1\;\mathsf{M}\;\;\mathsf{V}\;\;\mathsf{S}\;\;\mathsf{L}\;\;\mathsf{V}\;\;\mathsf{R}\;\;\mathsf{S}\;\;\mathsf{N}\;\;\mathsf{V}\;\;\mathsf{V}\;\;\mathsf{D}\;\;\mathsf{L}\;\;\mathsf{P}\;\;\mathsf{T}\;\;\mathsf{N}\;\;\mathsf{L}\;\;\mathsf{S}\;\;\mathsf{L}\;\;\mathsf{R}\;\;\mathsf{Y}
  70 80 90 100 110 120
61 TTTTGGTGTGGTGTTTTTATGATTAGTGCTTTTTTAGTGTTGCAAATTGCTTCTGGTGTT 120
21 F W C G G F M I S A F L V L Q I A S G V 40
  130 140 150 160 170 180
41 I L S L L Y V A D S N M R F G C V L A L 60
  190 200 210 220 230 2
181 AAAGATGAAAGTATTTTTATGTGGTTGGTTCGATATATGCATATTTGGGGTGTTACGTTT 240
61\ K D E S I F M W L V R Y M H I W G V T F 80
  250 260 270 280 290 3
241 ATTTTTGTGTTGTTTATAATACATATGGGTCGTGCTTTGTATTATACTAGTTATAGTAAG 300
81 I F V L F I I H M G R A L Y Y T S Y S K 100
              320 330
        310
                             340
                                   350
 ----:---|----:----|----:----|
301 GTGGGTGTATGGAATGTTGGTTTTATTTTGTATTTGGCGATGATGGTTGAAGCTTTTTTG 360
101\ V\ G\ V\ W\ N\ V\ G\ F\ I\ L\ Y\ L\ A\ M\ M\ V\ E\ A\ F\ L\ 120
   370 380 390 400 410
 ----:----|----:----|
361 GGCTATATTTTGCCGTGGCATCAGATGTCTTATTGGGCTGCGACGGTATTAACATCAATT 420
121 G Y I L P W H Q M S Y W A A T V L T S I 140
        430 440 450 460 470
  ----:----|----:----|
141 L N S V P L V G G V L Y K F V V G G F S 160
              500
        490
                      510
                            520
   ----:----|----:----|
481 GTGACAAATGTTACATTAGTTCGTGTGTTTTCCGGCTCATGTGTTTTAGCTTTTGTTATT 540
161 V T N V T L V R V F P A H V C L A F V I 180
   550 560 570 580 590 6
541 CTTGGTTTGAGTGTTCATTTATTTATTTACATCTAAGGGGGTCTAATAATCCATTG 600
181 L G L S V V H L F Y L H L R G S N N P L 200
              620
                      630
        610
                             640
                                    650
   ----:----|----:----|
601 TTCGTTAGGGGGGGTTATAGTGACGTTGTTTTGTTTCATAGTCTTTTTACTAATAAGGAT 660
201 F V R G G Y S D V V L F H S L F T N K D 220
                                    710
        670
               680
                      690
                             700
   ----:----|-----:----|
221 G F V L M C L L W C C C F F L I Y F P D 239
         730
               740
                      750
                             760
  ----:----|----:----|
721 TTTGTTTTAGATGTAGAGAGTTATATACAAGCTGATCCTTTGGTGACTCCGGTGTCTATA 780
240 F V L D V E S Y I Q A D P L V T P V S I 259
                      810
               800
                             820
  ----:----|-----:----|
781\ \mathtt{AAGCCTGAGTGGTATTTTTTGGCGTTTTATGCTATGTTACGTTCAATAGAGTCGAAGATT}\ 840
260 K P E W Y F L A F Y A M L R S I E S K I 279
```

(Please continue on overleaf)

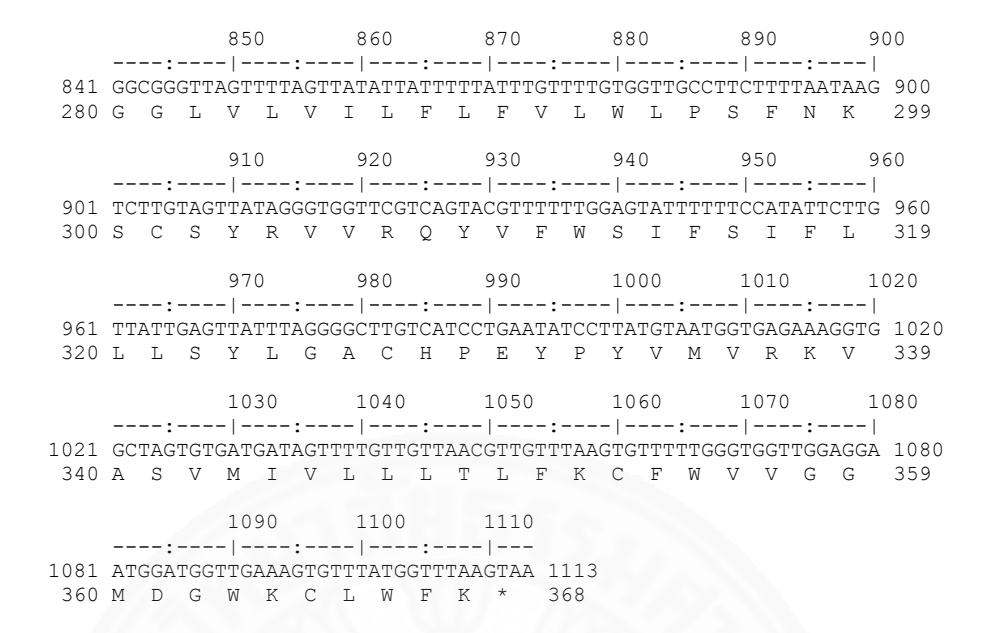


**Figure 5.20** Nucleotide and deduced amino acid sequences of the isolated *Fischoederius* spp. cytochrome b (1,100 bp) using SHOWSEQ in EMBOSS.

F-A	1	MVSLVRSNVVDLPTNLSLSYFWCGGFMISAFLVLQIASGVILSLLYVADSNMSFGCVLAL	60
Fe	1	S	60
Gc	1	.L	60
Fc	1	MSS	60
Cm	1	.LVVG	60
Pc	1	.LVLVGL	60
FC	Τ.	. п	00
F-A	61	NDESIFMWLVRYMHIWGVTFIFVLFIIHMGRALYYTSYSKVGVWNVGFILYLAMMVEAFL	120
Fe	61	V.	120
Gc	61	VVV	120
Fc	61		120
Cm	61	V	120
Pc	61	VLV.D.V	120
F-A	121	GYILPWHOMSYWAATVLTSILNSVPLVGGVLYKFVVGGFSVTNVTLVRVFPAHVCLAFVI	180
Fe	121	I.	180
GC	121	II	180
Fc	121		180
Cm	121	SI.	180
Pc	121	S	180
F-A	181	LGLSVVHLFYLHLSGSNNPLFVSGGYSDVVLFHSLFTNKDGFVLMCLLWCCCFFLIYFPD	240
Fe	181	EGESVVIIEF I ENESGSMAFEF VSGG1SDVVEFNSEF INKDGF VERGEEWCCCFFEITFFD	240
Gc	181		240
Fb	181	I	240
Cm	181	VMS	240
Pc	181	VMLMLS	240
F-A	241	FVLDVESYIOADPLVTPVSIKPEWYFLAFYAMLRSIESKIGGLVLVILFLFVLWLPSFNK	300
		~	
Fe	241		300
Gc	241		300
Fc	241		300
Cm	241	VLVI	300
Pc	241	VLV.A	300
	201		260
F-A	301	SCSYSVVRQYVFWSIFSIFLLLSYLGACHPEYPYVMVSKVASVMIVLLLTLFKCFWVVGG	360
Fr	301	V	360
Gc	301	IVIV	360
Fc	301	V	360
Cm	301	GSLLAFA	360
Pc	301	GLLVFA	360
F-A	361	MDGWKCLWFK 370	
Fe	361	AE 370	
Gc	361	A 370	
Fc	361	VY 370	
Cm	361	VDC. 370	
Pc	361	VNC. 370	
r C	201	viv 570	

**Figure 5.21** Multiple alignment of cytochrome b; F-A: *Fischoederius Mse*I pattern A; Fe: *F. elongatus* isolated from Tianmen, China; Fc: *F. cobboldi*; Gc: *G. crumenifer*; Cm: *C. microbothrioides*, and Pc: *P. cervi*. Black dots indicate conserved positions.

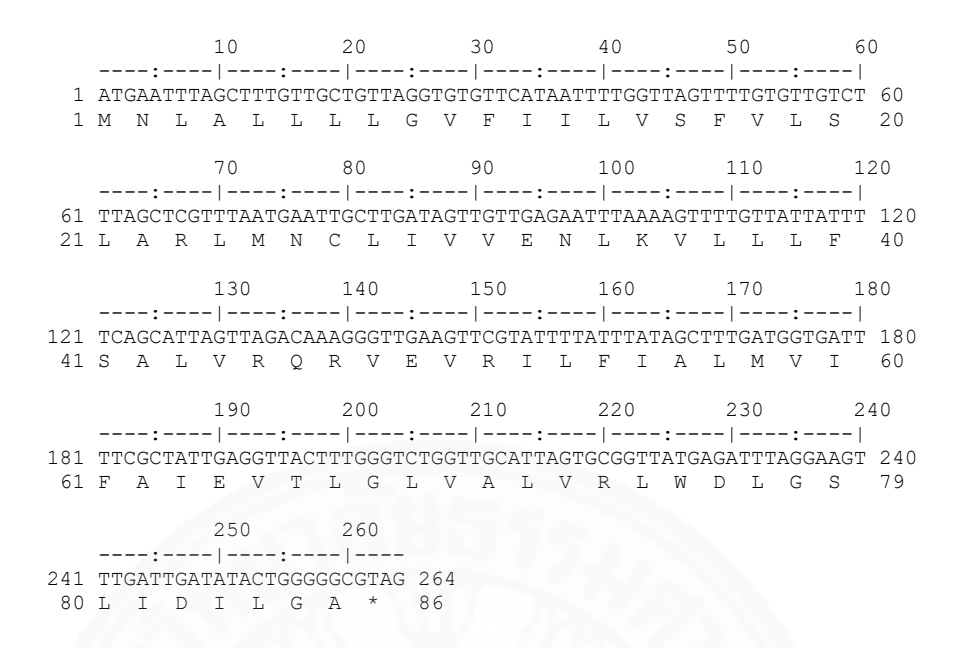


**Figure 5.22** Nucleotide and deduced amino acid sequences of the isolated *Fischoederius* spp. NADH dehydrogenase subunit 4L (264 bp) using SHOWSEQ in EMBOSS.

F-A Fc Gc Fe Cm Pc	1 1 1 1 1	MNLALLLLGVFIILVSFVLSLARLMNCLIVVENLNVLLLFSALVSQSVEVRILFIALMVI	60 60 60 60 60
F-A Fc Gc Fe Cm Pc	61 61 61 61 61	FAIEVTLGLVALVRLWDLGSLIDILG 86	

**Figure 5.23** Multiple alignment of NADH dehydrogenase subunit 4L; F-A: *Fischoederius Mse*I pattern A; Fe: *F. elongatus* isolated from Tianmen, China; Fc: *F. cobboldi*; Gc: *G. crumenifer*; Cm: *C. microbothrioides*, and Pc: *P. cervi*. Black dots indicate conserved positions.

```
10 20 30 40 50 60
   ----:----|----:----|----:----|
 1 ATGAGATTTAGGAAGTTTGATTGATATACTGGGGGCGTAGTTTATGTTTTTAGTCTTTTT 60
 1\;\mathsf{M}\;\mathsf{R}\;\mathsf{F}\;\mathsf{R}\;\mathsf{K}\;\mathsf{F}\;\mathsf{D}\;\mathsf{W}\;\mathsf{Y}\;\mathsf{T}\;\mathsf{G}\;\mathsf{G}\;\mathsf{V}\;\mathsf{V}\;\mathsf{Y}\;\mathsf{V}\;\mathsf{F}\;\mathsf{S}\;\mathsf{L}\;\mathsf{F}
  70 80 90 100 110 120
61 GTGTTATTAGTTTGGGTTGCTGTGAGTGGTTTATGAGATTATTCTTTGATTGGTGGGTTA 120
130 140 150 160 170 180
121 GTGACATCGAGTTATTTCTGTTTTGATAGTGTGAGTTTGTATTTGGTGTTGTTATCTGTG 180
 39 V T S S Y F C F D S V S L Y L V L L S V 58
   190 200 210 220 230 2
181 TTTCTTTGGATGTCTTTGCTATTTTTATTTGGTGTTGTCTTTTGTCCTCTAAGATTTTG 240
 59 F L W M S L L F L F G V V S L S S K I L 78
   250 260 270 280 290 3
241 ATTACTTTAAGGGTTGTGTTCGTTGGTAAGATATTGTTGTTGTTCACTCTTTGGTATTT 300
79 I T L R V V C S L V R Y C C V H S L V F 98
                         330
  310 320 330 340 350 3
                  320
301 TGGGTGTTTTATGAGATGTCTATACTTTCTTTGTTGTTGTTGTTAATATTGGAGTCTCCT 360
99 W V F Y E M S I L S L L L L L L E S P 118
  370 380 390 400 410 42
361 TATTCTGAGCGGTATATAGCTTCTTGGTATTTATTGGGTTATGTTGTATTAACTAGTTTA 420
119 \ Y \ S \ E \ R \ Y \ I \ A \ S \ W \ Y \ L \ L \ G \ Y \ V \ V \ L \ T \ S \ L \ 138
          430 440 450 460 470
   ----:----|----:----|
421 CCAATGTTGTTGTTATATTTTATTTGTCTTTTAATTGGGGGAGGTTCAATTTACGTTTT 480
139 \ \mathsf{P} \ \mathsf{M} \ \mathsf{L} \ \mathsf{L} \ \mathsf{C} \ \mathsf{I} \ \mathsf{F} \ \mathsf{Y} \ \mathsf{L} \ \mathsf{S} \ \mathsf{F} \ \mathsf{N} \ \mathsf{W} \ \mathsf{G} \ \mathsf{R} \ \mathsf{F} \ \mathsf{N} \ \mathsf{L} \ \mathsf{R} \ \mathsf{F} \ 158
   490 500 510 520 530 5
481 TGGTTTGACAGGTATGAGGGTTGTGTTAGATCTGGTGTTTTTGCTGTTTTTGGCTGTGATG 540
159 W F D R Y E G C V R S G V F A V L A V M 178
   550 560 570 580 590 6
179 F I T K V P L P P F H V W L P I V H A E 198
                620
                            630
           610
                                     640
                                             650
   ----:----|----:----|
601 GCTAGAAGTATTGTGTCCGTTTGTTTAAGGGGTTATATTATGAAGTTGGGTATTTTAGGT 660
199 A R S I V S V C L R G Y I M K L G I L G 218
           670
                   680
                            690
                                     700
                                              710
   ----:----|-----:----|
661 GTTTGTCGCTTTTGTTCGCATCTTTTATCTGGGTTGATTTTGTCTAACTTGTACATGGTA 720
219 V C R F C S H L L S G L I L S N L Y M V 238
           730
                   740
                            750
                                     760
   ----:----|-----:----|
721 ATTGCTTTACTTTTAGCGGTTTTGTTCTTTTTTAGGGCCACTCGTGAGTTGGATGGTAAG 780
239\ \mathsf{I}\ \mathsf{A}\ \mathsf{L}\ \mathsf{L}\ \mathsf{L}\ \mathsf{A}\ \mathsf{V}\ \mathsf{L}\ \mathsf{F}\ \mathsf{F}\ \mathsf{F}\ \mathsf{R}\ \mathsf{A}\ \mathsf{T}\ \mathsf{R}\ \mathsf{E}\ \mathsf{L}\ \mathsf{D}\ \mathsf{G}\ \mathsf{K}\ 258
                   800
                            810
                                    820
   ----:----|----:----|----:----|
781 \  \  \, \text{CGCTGGTTGGCGTTTTTGAGGTTATCACATATAATTATAGCTGCGGTGTTTTATGTGCT} \  \  \, 840 \  \  \, \\
259 R W L A F L R L S H I I I A A V C L C A 278
```

(Please continue on overleaf)



**Figure 5.24** Nucleotide and deduced amino acid sequences of the isolated *Fischoederius* spp. NADH dehydrogenase subunit 4 (1,281 bp) using SHOWSEQ in EMBOSS.

F-A	1	MSFSKFDWYTGGVVYVFSLFVLLVWVAVSGLWDYSLIGGLVTSSYFCFDSVSLYLVLLSV	60
Fe	1	SI.AV.GV	60
Gc	1	I	60
Pc	1	S.LFSVI.SSM	60
Fc	1	V	60
Cm	1	.GVG	60
F-A	61	FLWMSLLFLFGVVSLSSKILITLSVVCSLVSYCCVHSLVFWVFYEMSILSLLLLLILESP	120
Fe	61	SII	120
Gc	61	A	120
Pc	61	INL.TLML	120
Fc	61	NIVM	120
Cm	61	NIVMLLV	120
F-A	121	YSERYIASWYLLGYVVLTSLPMLLCIFYLSFNWGSFNLRFWFDSYEGCVSSGVFAVLAVM	180
Fe	121		180
Gc	121	V	180
Pc	121		180
Fc	121	NP	180
Cm	121		180
F-A	181	FITKVPLPPFHVWLPIVHAEASSIVSVCLSGYIMKLGILGVCRFCSHLLSGLILSNLYMV	240
Fe	181	I	240
GC	181	IFF	240
Pc	181	IV.	240
Fc	181	IPF	240
Cm	181	V.IY.NTI	240
OIII	101		210
F-A	241	IALLLAVLFFFSATRELDGKRWLAFLSLSHIIIAAVCLCAVGFEGSSLAFVFSLGHGLSA	300
Fe	241	V	300
Gc	241	V	300
D =			
Pc	241	VSV	300
FC	241	V	300
-			
Fc	241	V	300
Fc Cm	241 241	VV.	300 300
FC Cm F-A	<ul><li>241</li><li>241</li><li>301</li></ul>	VVVVVVVVV	300 300 360
FC Cm F-A Fe	<ul><li>241</li><li>241</li><li>301</li><li>301</li></ul>	VVMV. VIV.  GVTFIFLWLAYEVSGSRNWNILKYCLSSGLFMRCLAASCLCTAASLPPTVQFFSEVFILSV	300 300 360 360
FC Cm F-A Fe GC	241 241 301 301 301	VVMV. VIV.  GVTFIFLWLAYEVSGSRNWNILKYCLSSGLFMRCLAASCLCTAASLPPTVQFFSEVFILSVS.	300 300 360 360 360
FC Cm F-A Fe GC PC	241 241 301 301 301 301	V	300 300 360 360 360 360
FC Cm F-A Fe GC PC FC	241 241 301 301 301 301 301	V.        M.          V.        V.         GVTF1FLWLAYEVSGSRNWN1LKYCLSSGLFMRCLAASCLCTAASLPPTVQFFSEVF1LS            V. <td>300 300 360 360 360 360 360</td>	300 300 360 360 360 360 360
FC Cm F-A Fe GC PC FC Cm	241 241 301 301 301 301 301 301	V.       .M.       V.         V.       .I.       .V.         GVTF1FLWLAYEVSGSRNWN1LKYCLSSGLFMRCLAASCLCTAASLPPTVQFFSEVF1LS       .V.          .S.           .GS.       .V.       .V.          .S.       .V.       .V.          .S.       .V.       .V.          .V.       .S.       .V.       .V.	300 300 360 360 360 360 360 360
FC Cm F-A Fe GC PC FC Cm	241 241 301 301 301 301 301 301 361	V.       .M.       V.         V.       .I.       .V.         GVTFIFLWLAYEVSGSRNWNILKYCLSSGLFMRCLAASCLCTAASLPPTVQFFSEVFILS       .V.          .V.          .S.          .GS.         .V.       .V.          .V.	300 300 360 360 360 360 360 360
FC Cm F-A Fe GC PC FC Cm F-A Fe	241 241 301 301 301 301 301 301 361 361 361	V.        M.       V.         V.        V.         GVTFIFLWLAYEVSGSRNWNILKYCLSSGLFMRCLAASCLCTAASLPPTVQFFSEVFILS           V.       V.	300 300 360 360 360 360 360 360 420 420 420
FC Cm F-A Fe GC PC FC Cm F-A Fe GC	241 241 301 301 301 301 301 301 361 361	V.        M.       V.         V.        V.         GVTFIFLWLAYEVSGSRNWNILKYCLSSGLFMRCLAASCLCTAASLPPTVQFFSEVFILS           V.       V.	300 300 360 360 360 360 360 360 420 420
FC Cm F-A Fe GC PC FC Cm F-A Fe GC	241 241 301 301 301 301 301 301 361 361 361 361	V.	300 300 360 360 360 360 360 360 420 420 420 420
FC Cm F-A Fe GC PC Cm F-A Fe GC PC	241 241 301 301 301 301 301 301 361 361 361 361 361	V.	300 300 360 360 360 360 360 420 420 420 420 415
FC CM F-A Fe GC PC CM F-A Fe CC PC FC CM F-A	241 241 301 301 301 301 301 361 361 361 361 361	V	300 300 360 360 360 360 360 420 420 420 420 415
FC Cm F-A Fe GC PC FC Cm F-A Fe FC Cm F-A Fe FC Cm	241 241 301 301 301 301 301 361 361 361 361 421 421	V	300 300 360 360 360 360 360 420 420 420 420 415
FC Cm  F-A FE GC PC Cm  F-A FE GC PC FC Cm  F-A FC CC FC CC C	241 241 301 301 301 301 301 361 361 361 361 421 421 421	V	300 300 360 360 360 360 360 420 420 420 420 415
FC Cm F-A Fe GC PC FC Cm F-A Fe FC Cm F-A Fe FC Cm	241 241 301 301 301 301 301 361 361 361 361 421 421	V	300 300 360 360 360 360 360 420 420 420 420 415

**Figure 5.25** Multiple alignment of NADH dehydrogenase subunit 4; F-A: *Fischoederius Mse*I pattern A; Fe: *F. elongatus* isolated from Tianmen, China; Fc: *F. cobboldi*; Gc: *G. crumenifer*; Cm: *C. microbothrioides*, and Pc: *P. cervi*. Black dots indicate conserved positions.

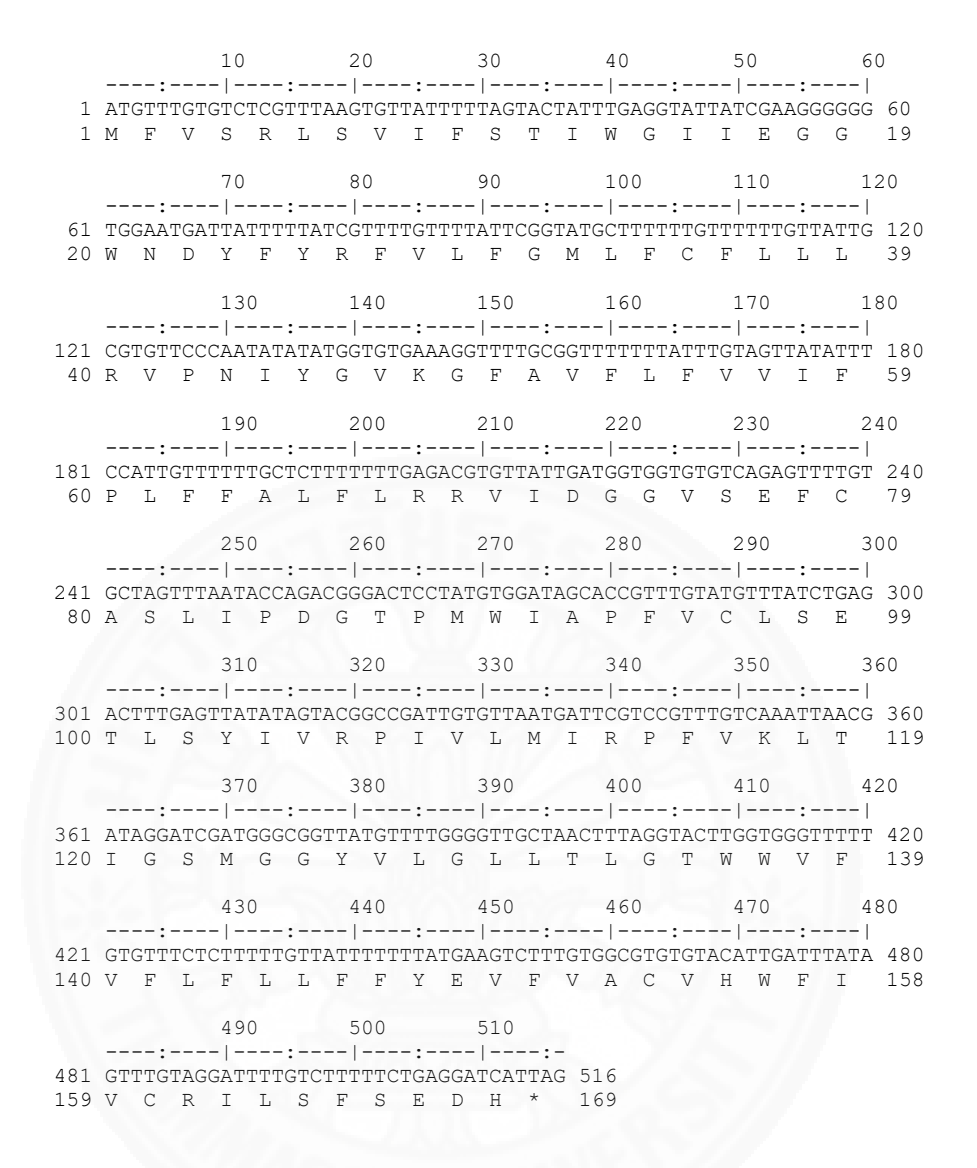


**Figure 5.26** Nucleotide and deduced amino acid sequences of the isolated *Fischoederius* spp. ATP synthase subunit 6 (516 bp) using SHOWSEQ in EMBOSS.

F-A	1	MFVSRLSVIFSTIWGIIEGGWNDYFYRFVLFGMLFCFLLLRVPNIYGVNGFAVFLFVVIF	60
Fe	1	V	60
Fc	1	VII	60
Pc	1	IV	60
Cm	1	INSV	60
Gc	1	GINAVFF	60
F-A	61	PLFFALFLSRVIDGGVSEFCASLIPDGTPMWIAPFVCLSETLSYIVRPIVLMIRPFVNLT	120
Fe	61		120
Fc	61		120
Pc	61	L	120
Cm	61	V	120
Gc	61	L	120
F-A	121	IGSMGGYVLGLLTLGTWWVFVFLFLLFFYEVFVACVHWFIVCSILSFSEDH 171	
Fe	121	171	
Fc	121		
Pc	121	N. 171	
Cm	121		
Gc	121		

**Figure 5.27** Multiple alignment of ATP synthase subunit 6; F-A: *Fischoederius Mse*I pattern A; Fe: *F. elongatus* isolated from Tianmen, China; Fc: *F. cobboldi*; Gc: *G. crumenifer*; Cm: *C. microbothrioides*, and Pc: *P. cervi*. Black dots indicate conserved positions.

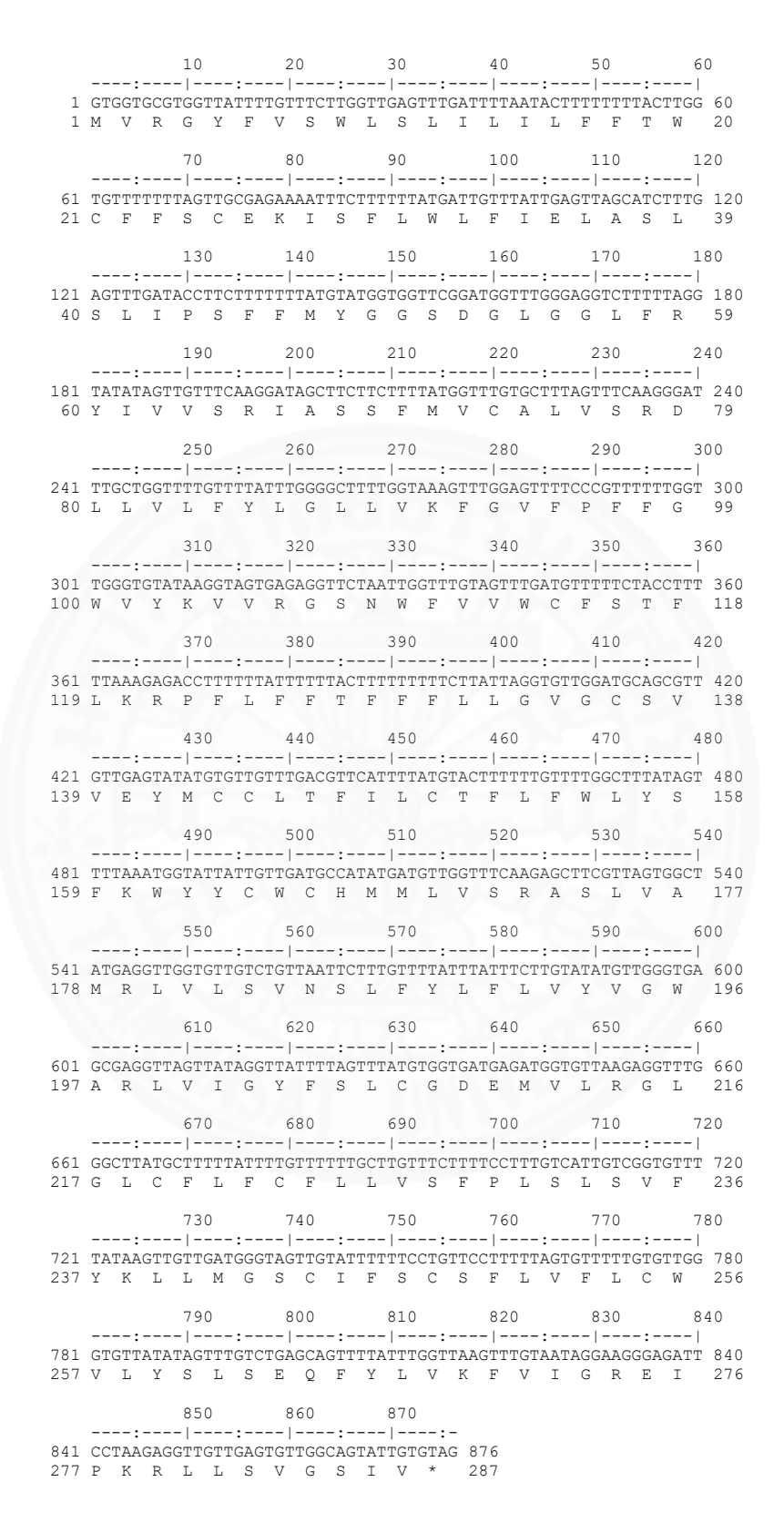


**Figure 5.28** Nucleotide and deduced amino acid sequences of the isolated *Fischoederius* spp. NADH dehydrogenase subunit 2 (876 bp) using SHOWSEQ in EMBOSS.

F-A Fe Cm Fc Pc Gc	1 1 2 1 1	MVRGYFVSWLSLILILFFTWCFFSCENISFLWLFIELASLSLIPSFFMYGGSDGLGGLFS	60 60 59 59 59
F-A	61	YIVVSSIASSFMVCALVSSDLLVLFYLGLLVKFGVFPFFGWVYKVVSGSNWFVVWCFSTF	120
Fe Cm	61 60	VV	120 119
FC	60	vv	119
Fc	60	VI	119
Gc	55	MVSL	114
F-A	121	LKSPFLFFTFFFLLGVGCSVVEYMCCLTFILCTFLFWLYSFNWYYCWCHMMLVSSASLVA	180
Fe	121	IIDGL	180
Cm	120	ASSI.CAFV	179
Fc	120	LIE.DICV	179
Fc	120	F	179
Gc	115	DIS.GCVAF	174
F-A	181	MSLVLSVNSLFYLFLVYVGWASLVIGYFSLCGDEMVLSGLGLCFLFCFLLVSFPLSLSVF	240
Fe	181	DI	240
Cm	180	DIVM.V.FV.SGSFV	239
Fc	180	SFMIM.GDS	239
Fc Gc	180 175	.GD.LFV.S.MFVVA.GV	239 234
GC	175		234
F-A	241	YKLLMGSCIFSCSFLVFLCWVLYSLSEQFYLVKFVIGSEIPKSLLSVGSIV 291	
Fe	241	N.VFGV. 291	
Cm	240	IFIE.VGV. 290	
Fc Fc	240		
F C GC	235	I	
30	200		

**Figure 5.29** Multiple alignment of NADH dehydrogenase subunit 2; F-A: *Fischoederius Mse*I pattern A; Fe: *F. elongatus* isolated from Tianmen, China; Fc: *F. cobboldi*; Gc: *G. crumenifer*; Cm: *C. microbothrioides*, and Pc: *P. cervi*. Black dots indicate conserved positions.

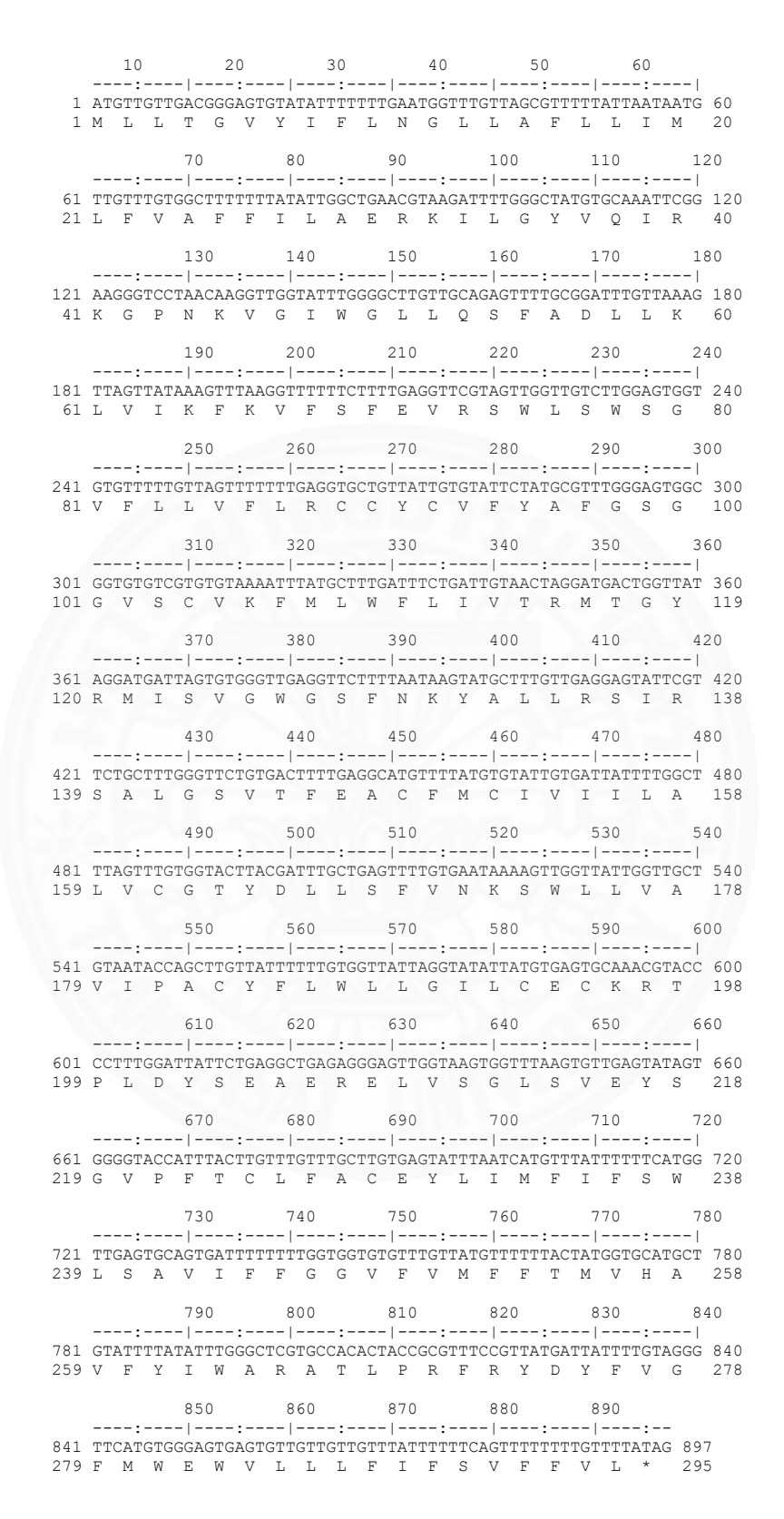


**Figure 5.30** Nucleotide and deduced amino acid sequences of the isolated *Fischoederius* spp. NADH dehydrogenase subunit 1 (897 bp) using SHOWSEQ in EMBOSS.

F-A Fe Fc Gc Pc Cm	1 1 1 3 1	MLLTGVYIFLNGLLAFLLIMLFVAFFILAERKILGYVQIRKGPNKVGIWGLLQSFADLLK	60 60 62 60
F-A Fe Fc Gc Pc Cm	61 61 61 63 61	LVIKFKVFSFEVRSWLSWSGVFLLVFLSCCYCVFYAFGSGGVSCVNFMLWFLIVTSMTGY	120 120 120 122 120 120
F-A Fe Fc Gc Pc Cm	121 121 121 123 121 121	SMISVGWGSFNKYALLSSIRSALGSVTFEACFMCIVIILALVCGTYDLLSFVNNSWLLVA	180 180 182
F-A Fe Fc Gc Pc Cm	181 181 181 183 181 181	VIPACYFLWLLGILCECNRTPLDYSEAESELVSGLSVEYSGVPFTCLFACEYLIMFIFSW	240 240 240 242 240 240
F-A Fe Fc Gc Pc Cm	241 241 241 243 241 241	IL	298 298 298 300 298 298

**Figure 5.31** Multiple alignment of NADH dehydrogenase subunit 1; F-A: *Fischoederius Mse*I pattern A; Fe: *F. elongatus* isolated from Tianmen, China; Fc: *F. cobboldi*; Gc: *G. crumenifer*; Cm: *C. microbothrioides*, and Pc: *P. cervi*. Black dots indicate conserved positions.

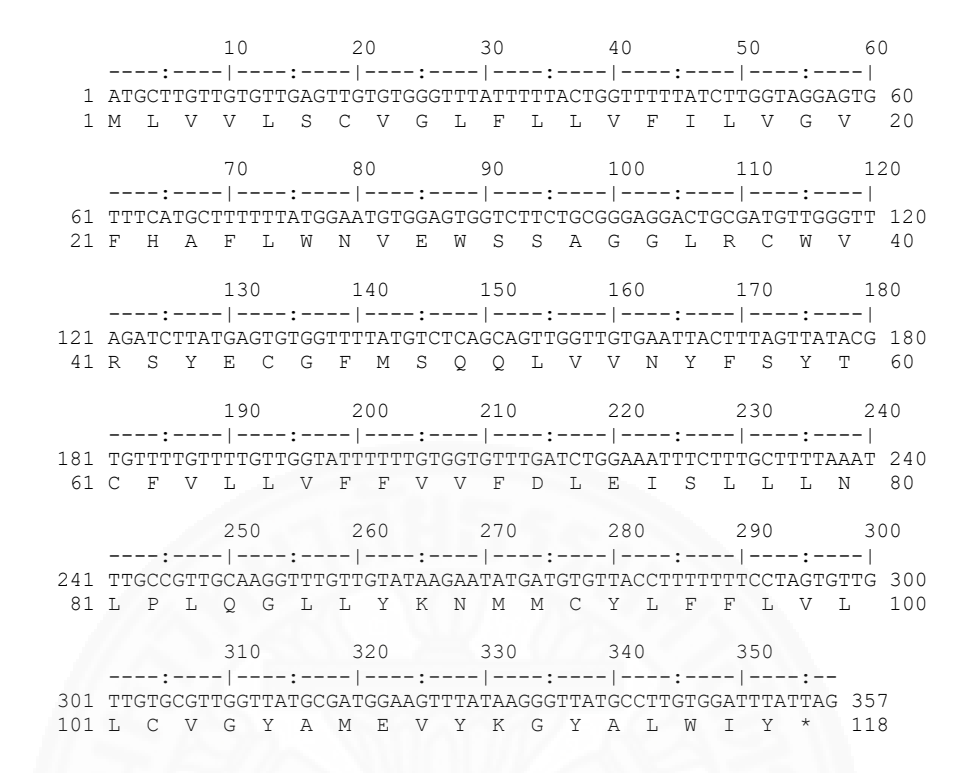


**Figure 5.32** Nucleotide and deduced amino acid sequences of the isolated *Fischoederius* spp. NADH dehydrogenase subunit 3 (357 bp) using SHOWSEQ in EMBOSS.

F-A	1	MLVVLSCVGLFLLVFILVGVFHAFLWNVEWSSAGGLRCWVSSYECGFMSQQLVVNVVE	55
Fe	1		55
Pc	1		55
Fc	1		55
Cm	1		55
Gc	17		62
F-A	56	YFSYTCFVLLVFFVVFDLEISLLINLPLQGLLYKNMMCYLFFLVLLCVGYAMEVYKGYAL	115
Fe	56		115
Pc	56		115
Fc	56		115
Cm	56		115
Gc	63		122
F-A Fe Pc Fc Cm Gc	116 116 116 116 116 123	WIY 118 .V. 118 .V. 118 .V. 118 .V. 118 .X. 125	

**Figure 5.33** Multiple alignment of NADH dehydrogenase subunit 3; F-A: *Fischoederius Mse*I pattern A; Fe: *F. elongatus* isolated from Tianmen, China; Fc: *F. cobboldi*; Gc: *G. crumenifer*; Cm: *C. microbothrioides*, and Pc: *P. cervi*. Black dots indicate conserved positions.

```
10 20 30 40 50 60
  ----:----|----:----|----:----|
 1\ \mathsf{M}\ \mathsf{R}\ \mathsf{K}\ \mathsf{V}\ \mathsf{V}\ \mathsf{W}\ \mathsf{A}\ \mathsf{C}\ \mathsf{T}\ \mathsf{V}\ \mathsf{D}\ \mathsf{H}\ \mathsf{K}\ \mathsf{R}\ \mathsf{V}\ \mathsf{G}\ \mathsf{F}\ \mathsf{I}\ \mathsf{Y}
             80 90
                             100 110 120
        70
  ----:----|----:----|
61 TTGGTTATTGGAATATGAGCTGGGTTTCTGGGTCTTGCGTTAAGAACGCTTATTCGTTTA 120
 21 \; L \; \; V \; \; I \; \; G \; \; I \; \; W \; \; A \; \; G \; \; F \; \; L \; \; G \; \; L \; \; A \; \; L \; \; R \; \; T \; \; L \; \; I \; \; R \; \; L 
  130 140 150 160 170 180
121 AATTTTATGGAGCCTTATTATAATGTTATTTCTCCTGAAGTATATAATTATGTTGTAAGT 180
 40 N F M E P Y Y N V I S P E V Y N Y V V S 59
  190 200 210 220 230 2
181 ATTCATGGTATTGTGATGTTGTTATTCTTTTTAATGCCTATTTTAGTGGGGGGGTTTTGGT 240
60 I H G I V M L L F F L M P I L V G G F G 79
   250 260 270 280 290 3
241 AATTATCTTTTGCCTTTATTGTTAGGGTTGCCTGATTTGATTCTGCCTCGTATAAATGCT 300
80\ N\ Y\ L\ L\ P\ L\ L\ G\ L\ P\ D\ L\ I\ L\ P\ R\ I\ N\ A\quad 99
 310 320 330 340 350 36
301 TTAGGTGCTTGATTATTGTTGCCTTCTACAGTTTGTTTTGTGTTTGAGTTTAGTGAAGGGA 360
100 L G A W L L L P S T V C L C L S L V K G 118
 370 380 390 400 410 42
361 GCTGGTGTTGGACTTTTTATCCTCCGTTAGCTGGTGGAGAGTTTTCTACTGGTCAT 420
119 A G V G W T F Y P P L A G G E F S T G H 138
         430 440 450 460 470
   ----:----|----:----|
421 GGTGTTGATTTTTAATGTTTAGTTTACATTTGTCTGGTGTGTCAAGTATATTAAGTTCG 480
139 G V D F L M F S L H L S G V S S I L S S 158
               500
                                      530
        490
                       510
                               520
   ----:----|----:----|
481 TTGAATTTTATAGCTACTATTTATAGTGCTGTGAATATTTATACATCGTCGCGACAGTCT 540
159 \; L \; N \; F \; I \; A \; T \; I \; Y \; S \; A \; V \; N \; I \; Y \; T \; S \; S \; R \; Q \; S \quad 178
   550 560 570 580 590 6
541 GTTTTAGTGTGGGCTTATTTATTTACATCTATTTTATTGATTTTGTCTTTGCCTGTGTTA 600
179 V L V W A Y L F T S I L L I L S L P V L 198
                620
                        630
                                       650
                               640
         610
   ----:---|----:----|
601 GCTGCTGGTATTACTATGTTACTTTTTGATCGGAATTTTTGGTACATCTTTTTTCGATCCT 660
199 A A G I T M L L F D R N F G T S F F D P 218
         670
                680
                        690
                               700
                                       710
   ----:----|-----:----|-----|-----|-----|
661 TTAGGTGGTGGTGATCCTGTGCTATTTCAACATTTATTTTGATTTTTTGGGCATCCTGAG 720
219 L G G G D P V L F Q H L F W F F G H P E 237
         730
                740
                        750
                               760
   ----:----|----:----|
721 GTTTATGTGCTGATTTTGCCTGGCTTTGGGGCTGTGAGACATATTTGTATGTGTTTAAGT 780
238 V Y V L I L P G F G A V R H I C M C L S 257
                        810
                800
                               820
   ----:----|-----:----|
```

(Please continue on overleaf)

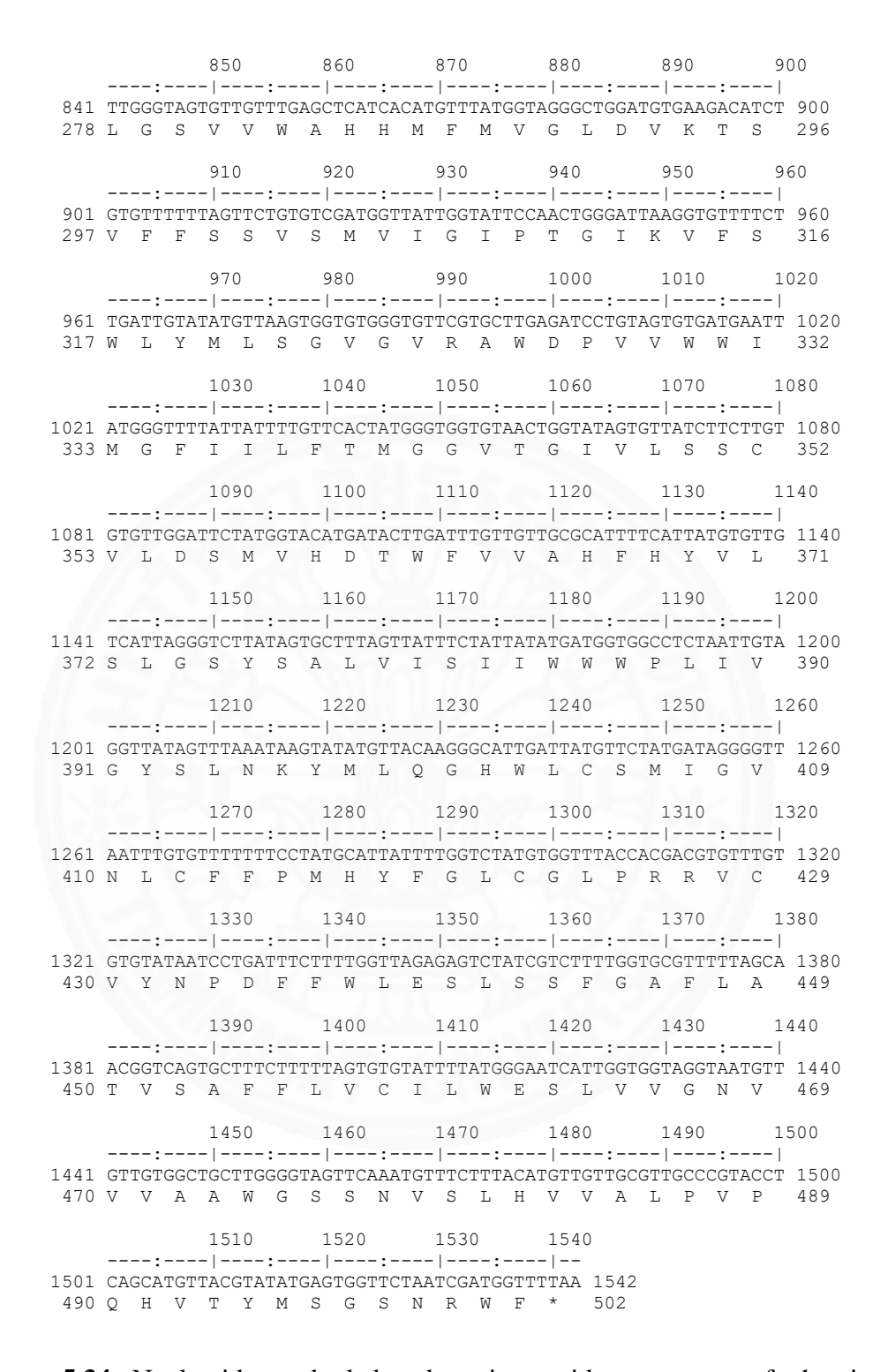


**Figure 5.34** Nucleotide and deduced amino acid sequences of the isolated *Fischoederius* spp. cytochrome c oxidase subunit I (1,542 bp) using SHOWSEQ in EMBOSS.

F-A Fe Fc Cm Gc Pc	1 1 1 1 1 2	MSKVVVWACTVDHKRVGFIYLVIGIWAGFLGLALSTLIRLNFMEPYYNVISPEVYNYVVS	60 60 60 60 60
F-A Fe Fc Cm Gc Pc	61 61 61 61 62	IHGIVMLLFFLMPILVGGFGNYLLPLLLGLPDLILPRINALGAWLLLPSTVCLCLSLVKG  .	120 120 120 120 120 121
F-A	121	AGVGWTFYPPLAGGEFSTGHGVDFLMFSLHLSGVSSILSSLNFIATIYSAVNIYTSSRQS	180
Fe	121		180
Fc	121		180
Cm	121		180
Gc	121		180
Pc	122		181
F-A	181	VLVWAYLFTSILLILSLPVLAAGITMLLFDRNFGTSFFDPLGGGDPVLFQHLFWFFGHPE	240
Fe	181		240
Fc	181		240
Cm	181		240
Gc	181		240
Pc	182		241
F-A	241	VYVLILPGFGAVSHICMCLSNQDSLFGYYGIVFAMASIVCLGSVVWAHHMFMVGLDVKTS  S L S L V S L	300
Fe	241		300
Fc	241		300
Cm	241		300
Gc	241		300
Pc	242		301
F-A	301	VFFSSVSMVIGIPTGIKVFSWLYMLSGVGVRAWDPVVWWIMGFIILFTMGGVTGIVLSSC	360
Fe	301		360
Fc	301		360
Cm	301		360
Gc	301		360
Pc	302		361
F-A	361	VLDSMVHDTWFVVAHFHYVLSLGSYSALVISIIWWWPLIVGYSLNKYMLQGHWLCSMIGV  .	420
Fe	361		420
Fc	361		420
Cm	361		420
Gc	361		420
Pc	362		421
F-A	421	NLCFFPMHYFGLCGLPRRVCVYNPDFFWLESLSSFGAFLATVSAFFLVCILWESLVVGNV         Y         I         L         L         .	480
Fe	421		480
Fc	421		480
Cm	421		480
Gc	421		480
Pc	422		481
F-A Fe Fc Cm Gc Pc	481 481 481 481 481 482	VVAAWGSSNVSLHVVALPVPQHVTYMSGSNRWF       513	

**Figure 5.35** Multiple alignment of cytochrome c oxidase subunit I; F-A: *Fischoederius Mse*I pattern A; Fe: *F. elongatus* isolated from Tianmen, China; Fc: *F. cobboldi*; Gc: *G. crumenifer*; Cm: *C. microbothrioides*, and Pc: *P. cervi*. Black dots indicate conserved positions.

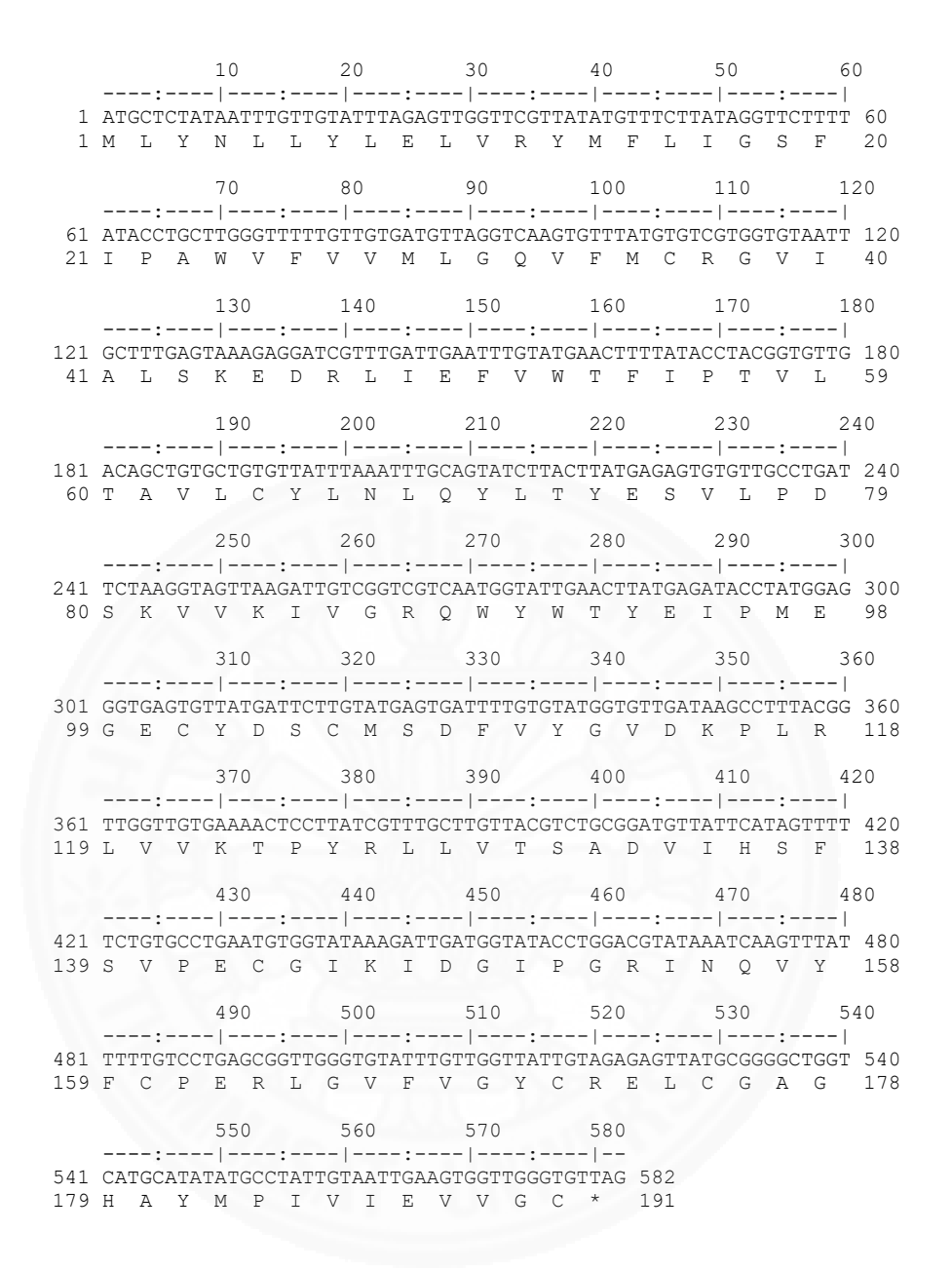


**Figure 5.36** Nucleotide and deduced amino acid sequences of the isolated *Fischoederius* spp. cytochrome c oxidase subunit II (582 bp) using SHOWSEQ in EMBOSS.

F-A Fc Fe Gc Pc Cm	1 1 1 1 1	MLYNLLYLELVRYMFLIGSFIPAWVFVVMLGQVFMCRGVIALSNEDRLIEFVWTFIPTVL              A.          S.       G.       L.          F.C.       V.       I.          K.       VT.       S.       L.	60 60 60 60 60
F-A Fc Fe Gc Pc Cm	61 61 61 61 61	TAVLCYLNLQYLTYESVLPDSKVVKIVGRQWYWTYEIPMEGECYDSCMSDFVYGVDKPLR	120 120 120 120 120 120
F-A	121	LVVNTPYRLLVTSADVIHSFSVPECGIKIDGIPGRINQVYFCPERLGVFVGYCSELCGAG .T	180
Fc	121		180
Fe	121		180
Gc	121		180
Pc	121	.SYSLT	180
Cm	121		180

**Figure 5.37** Multiple alignment of cytochrome c oxidase subunit II; F-A: *Fischoederius Mse*I pattern A; Fe: *F. elongatus* isolated from Tianmen, China; Fc: *F. cobboldi*; Gc: *G. crumenifer*; Cm: *C. microbothrioides*, and Pc: *P. cervi*. Black dots indicate conserved positions.

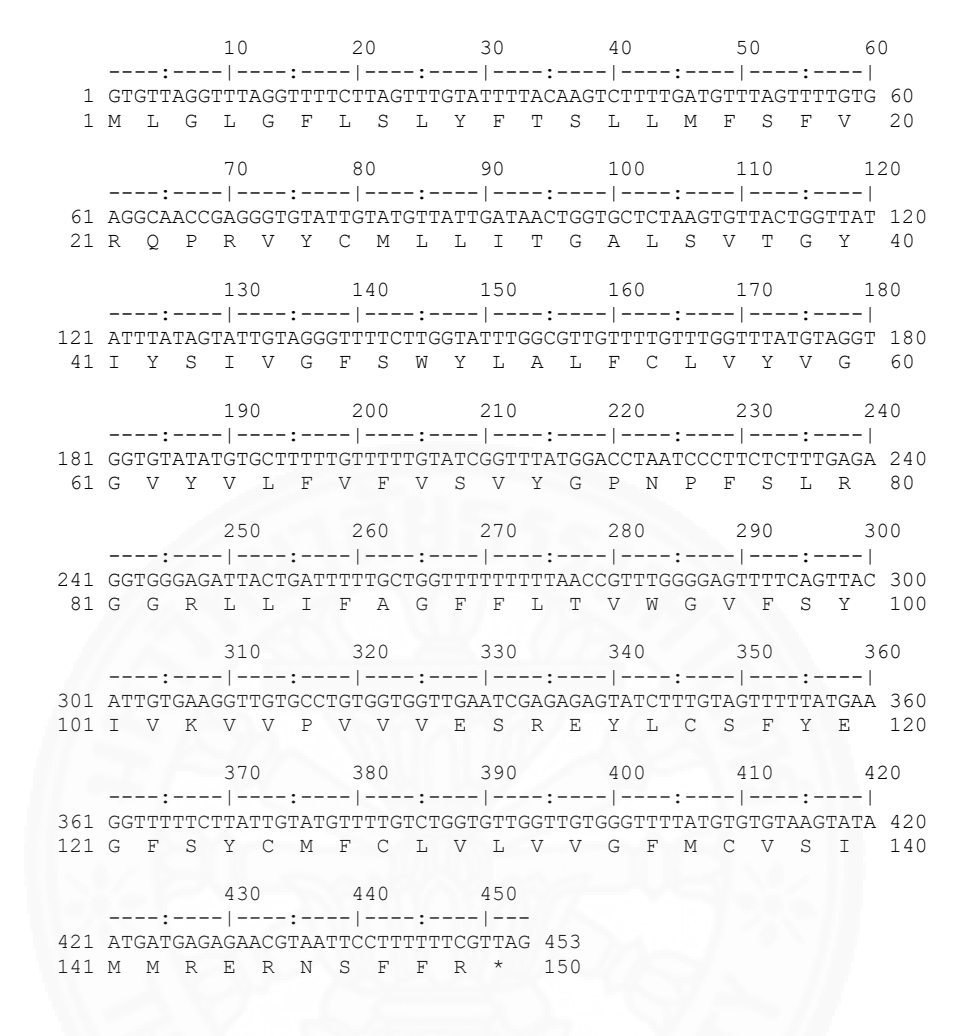


**Figure 5.38** Nucleotide and deduced amino acid sequences of the isolated *Fischoederius* spp. NADH dehydrogenase subunit 6 (452 bp) using SHOWSEQ in EMBOSS.

F-A Fe Fc Cm Gc Pc	1 1 1 1 1	MLGLGFLSLYFTSLLMFSFVSQPSVYCMLLITGALSVTGYIYSI         MWSWSCIHAHCDWGGGM	44 60 44 44 44
F-A Fe Fc Cm Gc Pc	61 61 45 45 45 45	VGFSWYLALFCLVYVGGVYVLFVFVSVYGPNPFSLSGGSLLIFAGFFLTVWGVFSYIVKV         L	104 120 104 104 104 104
F-A Fe Fc Cm Gc Pc	121 121 105 105 105 105	VPVVVESSEYLCSFYEGFSYCMFCLVLVVGFMCVSIMMSERNSFFR       150         L	

**Figure 5.39** Multiple alignment of NADH dehydrogenase subunit 6; F-A: *Fischoederius Mse*I pattern A; Fe: *F. elongatus* isolated from Tianmen, China; Fc: *F. cobboldi*; Gc: *G. crumenifer*; Cm: *C. microbothrioides*, and Pc: *P. cervi*. Black dots indicate conserved positions.

```
10 20 30 40 50 60
   ----:----|-----:----|
  1 GTGTTAGGATTGTCAGTGTTTTTTTTTTTTGGAGTGTTGTGTATATGATGTGTAGGTTTG 60
  1\ \ \text{M}\ \ \text{L}\ \ \text{G}\ \ \text{L}\ \ \text{S}\ \ \text{V}\ \text{L}\ \ \text{F}\ \ \text{F}\ \ \text{G}\ \ \text{V}\ \ \text{L}\ \ \text{C}\ \ \text{I}\ \ \text{W}\ \ \text{C}\ \ \text{V}\ \ \text{G}\ \ \text{L}\ \ \ 19
   70 80 90 100 110 120
 61 GTTGGCTGGTGGGGTTCTTTTACGTTTGTGGGGTATGTGTTAAAGGATTTAATGTTTTGC 120
 20 V G W W G S F T F V G Y V L K D L M F C
   130 140 150 160 170 180
121 TTTTTTATTGATGAGACTAGGTTGGTATGTTTTTTATGTTGTTGTTGTTGTTGTAGAATT 180
 40 F F I D E T R L V C V F M L F C C G R I 59
   190 200 210 220 230 2
181 GCTTTATATTATTGTTATCATTATTTTTAGGGGTAGGACGGAGGGTTGCTATTTCCT 240
 60 A L Y Y C Y H Y F R G S K D G G L L F P 79
   250 260 270 280 290 3
241 TTAATTGTTTTGGTTTTTAGGAGTGATGGGTATTTTGATTTTTACGTCTTCTATGGTTTTT 300
 80 L I V W F L G V M G I L I F T S S M V F 99
                   320 330
  310 320 330 340 350 3
301 TCTTTGGTTTTGTGGGAGTATTTGGGTCTTGTTAGTTTCTTTTTGATTTTATTCT 360
100 S L V L W E Y L G L V S F F L I L F Y S 119
  370 380 390 400 410 42
361 AATATGAGGAGCATGCGTGCTTCTTTAATTACTGTGTTTTGCTTCCCGATTTGGGGATGCA 420
120 N M R S M R A S L I T V F A S R F G D A 139
           430 440 450 460 470
   ----:----|----:----|
421 GCGTTATTCGTATTAATTATGTGGTTTGCGAACTGATTGGAGTTTTCTGGTTTTTTATTT 480
140 \; \text{A} \; \text{L} \; \text{F} \; \text{V} \; \text{L} \; \text{I} \; \text{M} \; \text{W} \; \text{F} \; \text{A} \; \text{N} \; \text{W} \; \text{L} \; \text{E} \; \text{F} \; \text{S} \; \text{G} \; \text{F} \; \text{L} \; \text{F} \; \; 158
                  500
    490 500 510 520 530 5
481 GTTCTTTGTATTTGTTGGTTGTTGTTAAGAAAGAGTGCTGCTTATCCTTTTATTTCTTGG 540
159 \ V \ L \ L \ Y \ L \ L \ V \ V \ L \ R \ K \ S \ A \ A \ Y \ P \ F \ I \ S \ W \ 178
    550 560 570 580 590 6
541 TTGTTAGAAGCTATGCGTGCTCCTACTCCCGTTAGTTCGTTGGTTCATTCTTCGACGTTG 600
179 \; L \; L \; E \; A \; M \; R \; A \; P \; T \; P \; V \; S \; S \; L \; V \; H \; S \; S \; T \; L \quad 198
                   620
                             630
           610
                                       640
                                               650
    ---:---|---:----|
601 GTTGCGGCTGGTGCGTGGTTTGTTTATCGTTATAATTATTTTTTGTACTCCGAGTTTGTTG 660
199 V A A G A W F V Y R Y N Y F C T P S L L 218
           670
                    680
                             690
                                       700
                                                710
    ----:----|-----:----|-----:----|
661 GAGGTTTTATTTTTCTTTAGCTTGGTGTCTGTTATTATAACGGGTTTGTGTGCGGTAGTG 720
219 E V L F F F S L V S V I I T G L C A V V 238
            730
                    740
                             750
                                       760
   ----:----|-----:----|
721 TTTATGGATTTGAAGAAGATTGTTGCTCTGTCAACGTGTAACAATGTAGCTTGATGTTTG 780
239 F M D L K K I V A L S T C N N V A W C L 257
                             810
                    800
                                      820
   ----:----|-----:----|
781 ATTTTTTTTTTTTTTGTTGATGATTTGATGCTGGCTTTGTTGCAGTTGTTGACACATGGTGTG 840
258 \; \text{I} \; \text{F} \; \text{F} \; \text{V} \; \text{C} \; \text{G} \; \text{D} \; \text{L} \; \text{M} \; \text{L} \; \text{A} \; \text{L} \; \text{L} \; \text{Q} \; \text{L} \; \text{L} \; \text{T} \; \text{H} \; \text{G} \; \text{V} \quad 277
```

(Please continue on overleaf)

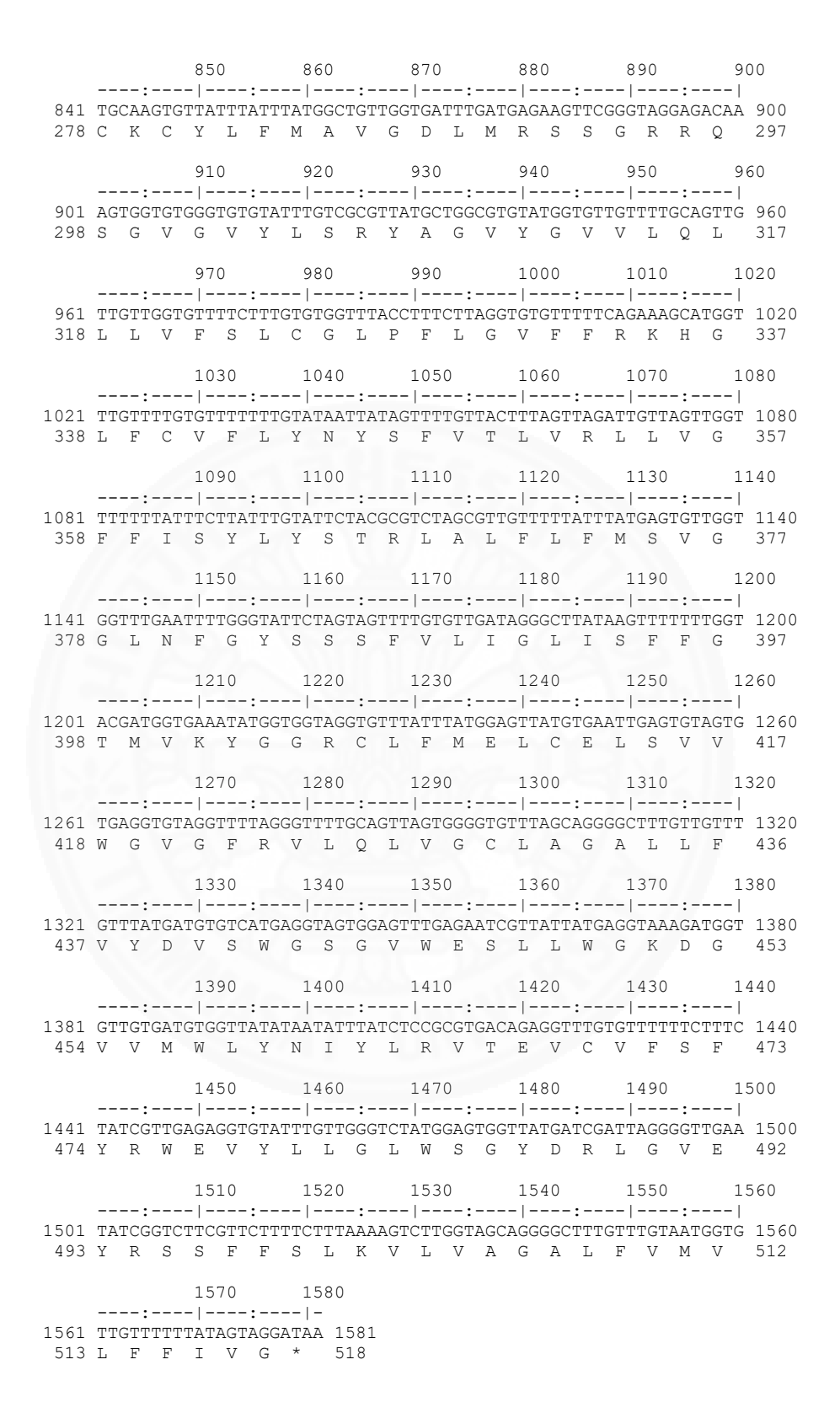


**Figure 5.40** Nucleotide and deduced amino acid sequences of the isolated *Fischoederius* spp. NADH dehydrogenase subunit 5 (1,581 bp) using SHOWSEQ in EMBOSS.

F-A	1	MLGLSVFLFFGVLCIWCVGLVGWWGSFTFVGYVLKDLMFCFFIDETSLVCVFMLFCCGSI	60
Fe	1	VA	60
Fc	1	VMSAA.	60
Cm	14		60
Gc	1	ILVVI.A	60
Pc	14	.V	60
10	11	. v	00
F-A	61	ALYYCYHYFSGSKDGGLLFPLIVWFLGVMGILIFTSSMVFSLVLWEYLGLVSFFLILFYS	120
Fe	61	IE	120
Fc	61	IE	120
Cm	61	L.	120
GC	61	TOE	120
Pc	61	SE	120
I C	01	v	120
F-A	121	NMSSMRASLITVFASRFGDAALFVLIMWFANWLEFSGFLFVLLYLLVVLSKSAAYPFISW	180
Fe	121	DI	180
Fc	121	V	180
Cm	121	.S	180
GC	121		180
Pc	121	.SS	180
FC	121	.3	100
F-A	181	LLEAMRAPTPVSSLVHSSTLVAAGAWFVYRYNYFCTPSLLEVLFFFSLVSVIITGLCAVV	240
Fe	181		240
Fc	181	DV	240
Cm	181	EI	240
GC	181		240
Pc	181		240
FC	101	WA.EA.	240
F-A	241	FMDLKKIVALSTCNNVAWCLIFFVCGDLMLALLOLLTHGVCKCYLFMAVGDLMSSSGSSO	300
Fe	241	NN	300
Fc	241		300
Cm	241	TTG	300
GC	241		300
Pc	241		300
1.0	211		300
F-A	301	SGVGVYLSRYAGVYGVVLQLLLVFSLCGLPFLGVFFSKHGLFCVFLYNYSFVTLVSLLVG	360
Fe	301	A	360
Fc	301	A	360
Cm	301	ALG	360
Gc	301	A	360
Pc	301		360
F-A	361	FFISYLYSTRLALFLFMSVGGLNFGYSSSFVLIGLISFFGTMVNYGGSCLFMELCELSVV	420
Fe	361	IY	420
Fc	361		420
Cm	361	L	420
Gc	361		420
Pc	361	.LLSGI.	420
	401		400
F-A	421	${\tt WGVGFSVLQLVGCLAGALLFVYDVSWGSGVWESLLWGNDGVVMWLYNIYLRVTEVCVFSF}$	480
Fe	421	I	480
Fc	421	AIVN.TAA	480
Cm	421	MCIVM	480
Gc	421	AIW	480
Pc	421	SSD	480
	401	VDWELVVI I CI MOCVDDI CVEVDOGERGI MULUZ CZ I ERZEVI ERTIYO - FOC	
F-A	481	YRWEVYLLGLWSGYDRLGVEYRSSFFSLNVLVAGALFVMVLFFIVG 526	
Fe	481	VMI. 526	
FC	481	GS.NLVM 522	
Cm	481	I	
Gc	481	VVL.L.MI. 526	
Pc	481	IHQSS.GLIL 526	

**Figure 5.41** Multiple alignment of NADH dehydrogenase subunit 5; F-A: *Fischoederius Mse*I pattern A; Fe: *F. elongatus* isolated from Tianmen, China; Fc: *F. cobboldi*; Gc: *G. crumenifer*; Cm: *C. microbothrioides*, and Pc: *P. cervi*. Black dots indicate conserved positions.

### 5.4.1.2 Transfer RNA genes, ribosomal RNA genes and noncoding regions of *Fischoederius* spp. mitochondrial genome *MseI* pattern A

A total of 23 tRNA genes of *Fischoederius* spp. *Mse*I pattern A mitochondrial genome were predicted with a size range from 62 to 71 nucleotides using MITOS, tRNAscan-SE, and ARWEN as described in **Section 4.3.6.2**. Overlapping nucleotides were detected between tRNA-Phe/tRNA-Met and tRNA-Leu/tRNA-Ser. The tRNA-Asp (GTC) was found two times. These tRNAs have a typical cloverleaf secondary structure, except tRNA-Ser (GCT) which lacked the dihydrouridine (DHU) arm. Non-canonical U:U base pairs are present in the arms of tRNA-Asp, tRNA-Ala, tRNA-Asn, tRNA-Pro, tRNA-Trp, tRNA-Cys, and tRNA-Gly. Non-canonical G:A base pairs are present in the arms of tRNA-Trp and tRNA-Leu. The predicted tRNA secondary structures are shown in **Figure 5.42**.

Two ribosomal RNA genes were predicted in this *Fischoederius* mitochondrial genome. L-RNA was found between tRNA-Thr and tRNA-Cys with 990 nucleotides in length. S-RNA was found between tRNA-Cys and *cox*2 with 747 nucleotides in length.

Two non-coding regions were predicted by comparison with the previously published *F. elongatus* mitochondrial genome (China). A short non-coding regions (SNR) was found between *cytb* and *nad*4L with 49 bp in length. A long non-coding region (LNR) was found between tRNA-Glu and *cox*3 with 461 bp in length.

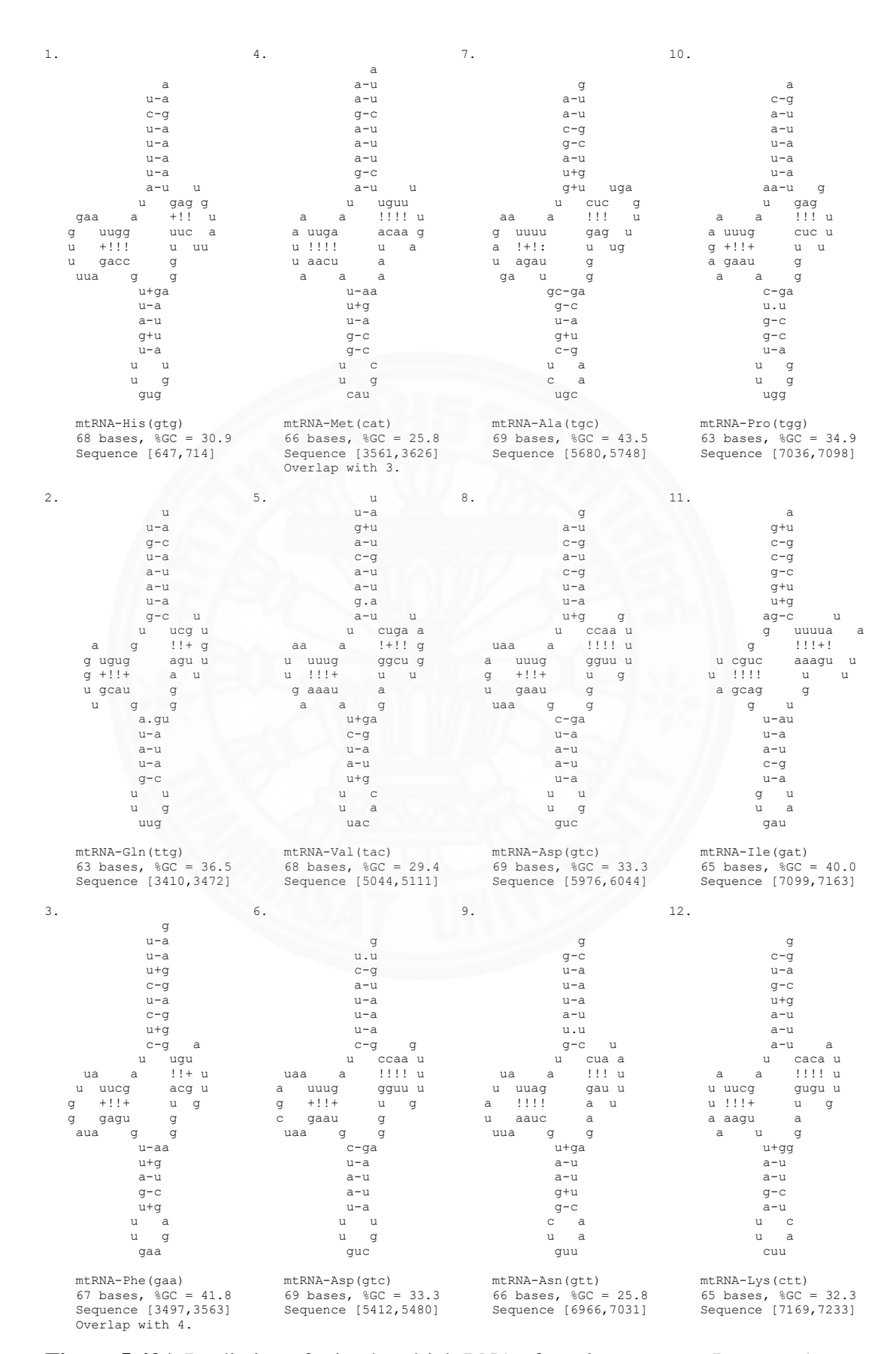


Figure 5.42A Prediction of mitochondrial tRNA of F. elongatus MseI pattern A

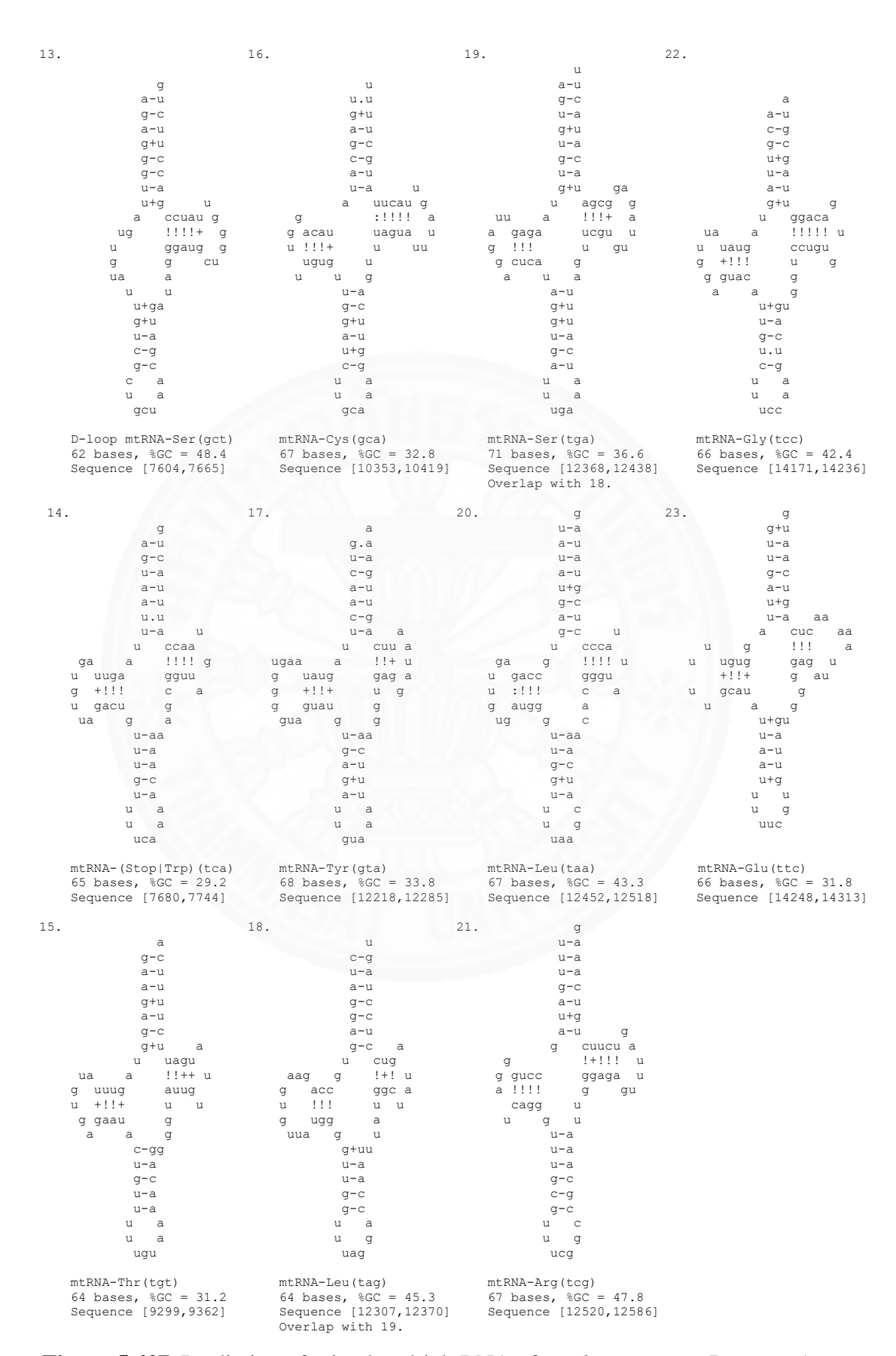


Figure 5.42B Prediction of mitochondrial tRNA of F. elongatus MseI pattern A

## 5.4.2 Genetic variation of 12 protein-coding genes of *Fischoederius* spp. mitochondrial genome *Mse*I pattern A

The mitochondrial genomes of *Fischoederius Mse*I pattern A carries twelve protein-coding genes in the same arrangement as found in *F. elongatus* Tianmen, China, *F. elongatus* Shanghai, China, *F. cobboldi*, and *G. crumenifer*. The overall sequence identity for these genes between *Fischoederius Mse*I pattern A and the abovementioned genomes were 87.2–90.9% nt identity and 92.2–96.6% aa identity as shown in **Table 5.6**. At the nucleotide level, the difference of these sequences between *Fischoederius Mse*I pattern A and the other trematodes ranged from 6.5–12.3% with *F. elongatus* Tianmen, 6.0–14.0% with *F. elongatus* Shanghai, 6.1–13.3% with *F. cobboldi*, and 9.7–16.5% with *G. crumenifer*. At the amino acid level the differences between *Fischoederius Mse*I pattern A and the other trematodes ranged from 1.6–6.9% with *F. elongatus* Tianmen, 1.6–6.9% with *F. elongatus* Shanghai, 2.3–7.9% with *F. cobboldi*, and 3.0–19.2% with *G. crumenifer*. The most conserved genes in the *Fischoederius* spp. mitochondrial genome were *atp*6, *nad*1, and *cox*1 in intraspecies variation and *cytb* in interspecies variation, while the least conserved genes were *nad*2 and *nad*3.

**Table 5.6** Comparsion of sequence identity value between *Fischoederius Mse*I pattern A (FeA) and *F. elongatus* isolated from Tianmen, China (FeT), *F. elongatus* isolated from Shanghai, China (FeS), *F. cobboldi* (Fc), and *G. crumenifer* (Gc)

		nt seq	uence le	ength			nt iden	tity (%)		aa identity (%)					
Gene	FeA	FeT	FeS	Fc	Gc	FeA/ FeT	FeA/ FeS	FeA/ Fc	FeA/ Gc	FeA/ FeT	FeA/ FeS	FeA/ Fc	FeA/ Gc		
cox3	645	645	645	645	645	90.1	90.4	90.1	86.5	96.3	96.3	95.8	92.1		
cytb	1,113	1,113	1,116	1,113	1,113	92.9	92.3	92.1	88.3	98.1	98.1	97.6	97.0		
nad4L	264	264	264	264	264	90.9	91.1	92.7	90.4	96.6	96.6	97.7	95.4		
nad4	1,281	1,281	1,281	1,281	1,281	90.9	90.5	89.2	87.2	96.7	96.2	94.5	93.7		
atp6	516	516	516	516	516	91.9	91.9	90.3	88.2	98.3	98.3	97.7	94.7		
nad2	876	876	876	873	858	89.9	89.3	89.8	85.5	93.1	93.1	92.1	86.3		
nad1	897	897	870	897	903	91.4	90.5	91.1	87.1	98.0	98.7	97.7	93.6		
nad3	357	357	348	357	378	87.7	86.0	88.8	83.5	94.1	93.2	93.2	80.7		
cox1	1,542	1,542	1,542	1,542	1,542	92.9	93.3	93.1	88.7	98.4	98.4	97.3	94.7		
cox2	582	582	582	582	582	93.5	94.0	93.8	88.0	97.9	97.9	97.3	94.3		
nad6	453	501	408	453	453	89.8	90.3	88.1	86.3	97.3	97.3	92.7	91.3		
nad5	1,581	1,581	1,581	1,578	1,581	89.4	89.8	86.7	86.3	94.9	95.3	94.4	92.0		
Overall						90.9	90.8	90.5	87.2	96.6	96.6	95.7	92.2		

# 5.4.3 Genetic relationship of *Fischoederius* mitochondrial genome *Mse*I pattern A to other trematodes

Diagrams of the mitochondria of *Fischoederius Mse*I pattern A and *F. elongatus* from Tianmen and Shanghai, China, *F. cobboldi, G. crumenifer, E. explanatum, P. cervi, C. microbothrioides, O. streptocoelium, H. paloniae, F. hepatica,* and *C. sinensis* are shown in **Figure 5.43**. The mitochondrial genomes ranged from 13,800 to 15,987 bp in length. The diagrams show that all genomes had the same arrangement of protein-coding genes, tRNA, and rRNA except *Fischoederius Mse*I pattern A in which an additional tRNA-Asp was located between tRNA-Val and tRNA-Ala and *F. hepatica* in which tRNA-Gly and tRNA-Glu had switched their positions. The non-coding regions were predicted in all trematode mitochondrial genomes except *C. microbothrioides* and *C. sinensis*.

A phylogenetic analysis of the concatenated amino acid sequences of the twelve protein-coding genes of *Fischoederius* spp. mitochondrial genome *Mse*I pattern A with other trematodes was performed by using neighbor-joining method as described in **Section 4.3.6.4** (**Figure 5.44**). The resulting tree clearly demonstrated the taxonomic relationship between these trematodes. Members of the genus *Fischoederius* are next to *G. crumenifer* that belongs in the same family Gastrothylacidae, next are members of the family Paramphistomidae including *E. explanatum*, *P. cervi*, *C. microbothrioides*, and *O. streptocoelium*.

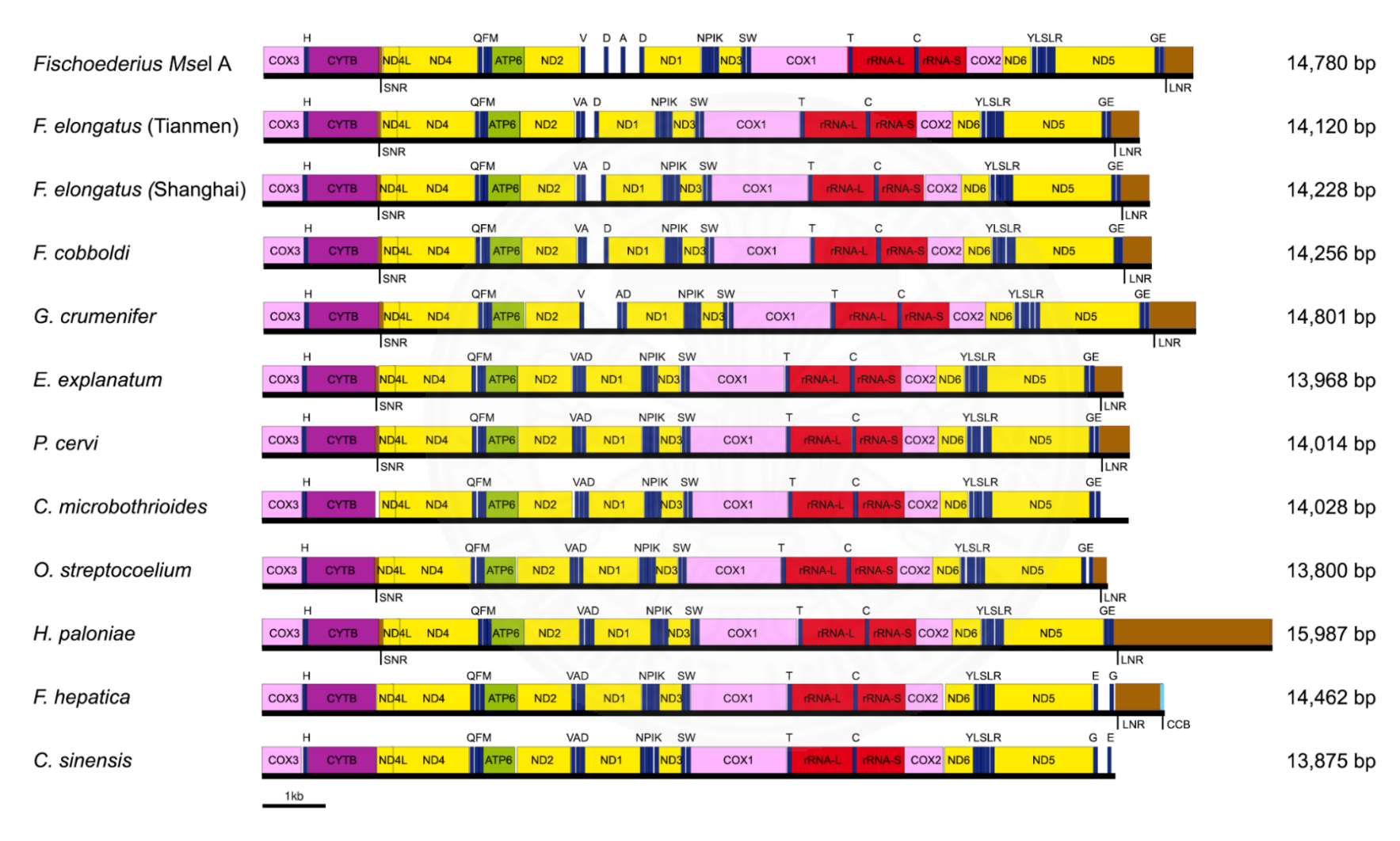
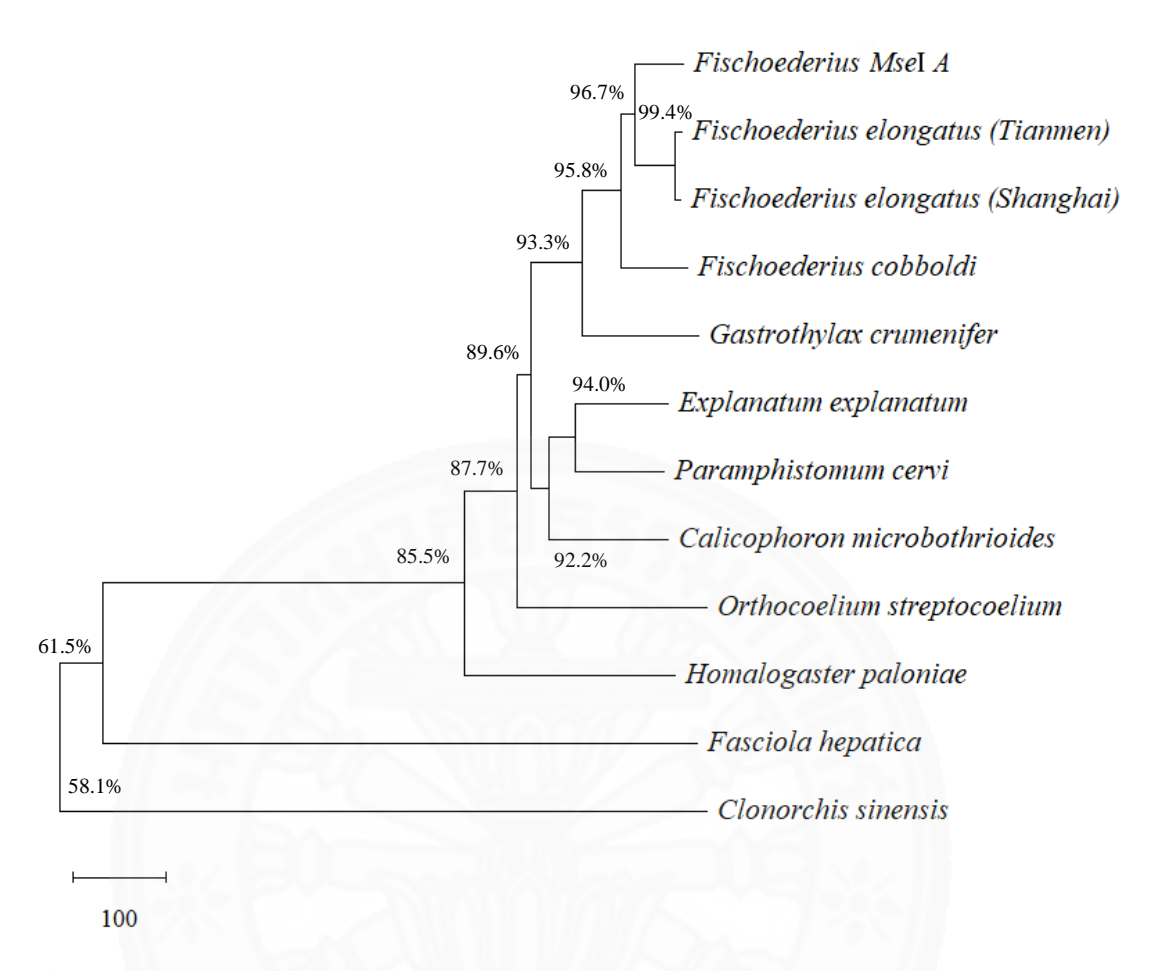


Figure 5.43 Mitochondrial diagrams of Fischoederius spp. mitochondrial genome MseI pattern A and other trematodes using OGDRAW.



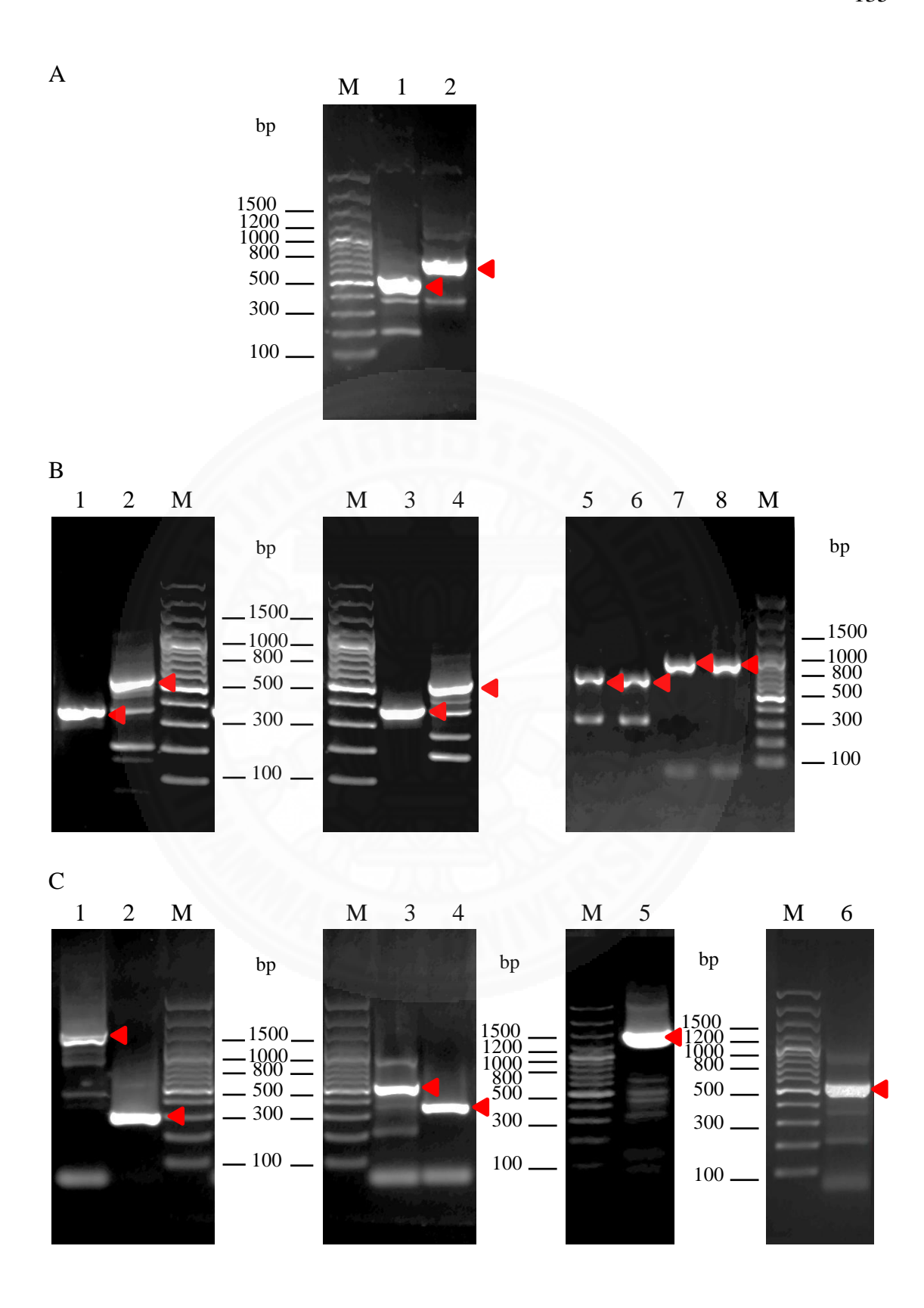
**Figure 5.44** Phylogenetic analysis of concatenated amino acid sequences of twelve protein-coding genes of *Fischoederius* spp. mitochondrial genome *Mse*I pattern A with other trematodes including *F. elongatus*, Tianmen, China (GenBank: NC\_028001), *F. elongatus*, Shanghai, China (GenBank: MN537973), *F. cobboldi* (GenBank: NC\_030529), *G. crumenifer* (GenBank: NC\_027833), *E. explanatum* (GenBank: NC\_027958), *P. cervi* (GenBank: NC\_023095), *C. microbothrioides* (GenBank: NC\_027271), *O. streptocoelium* (GenBank: NC\_028071), *H. paloniae* (GenBank: NC\_030530), *F. hepatica* (GenBank: NC\_002546), and *C. sinensis* (GenBank: NC\_012147) using Neighbor-joining method.

# 5.4.4 Secondary structure in *nad2*–1–3–*cox*1 region of *Fischoederius* spp. mitochondrial genome *Mse*I pattern A, B, C, D and I

At first, standard PCR was used to amplify the *nad2*–1–3–*cox1* region of *Fischoederius* spp. mitochondrial genome *MseI* pattern A to fill in gaps in the NGS transcriptome data. Low-quality Sanger dideoxy sequencing results were observed for the *nad2*–*nad1* region of the *Fischoederius* spp. mitochondrial genome *MseI* pattern A and it was speculated that these were caused by an unusual secondary structure (**Figure 5.46**). New primers were designed to amplify the problematic region between *nad2* and *nad1* for subsequent sequencing as described in **Section 4.3.5**. Interestingly, PCR with these primers showed differently sized PCR products for *Fischoederius* spp. mitochondrial genome *MseI* pattern A, B, C, D, and I (**Figure 5.45**). PCR amplicons were purified, ligated into pGEM®-T Easy and introduced into *E. coli* XL1-Blue as described in **Sections 4.2.7–4.2.11**. Positive clones were selected for sequencing using conditions appropriate for DNA with unusual structure as described in **Section 4.2.12**. Each base in the resulting sequence chromatograms was manually approved. The length of the PCR products and the used primer pairs are shown in **Table 5.7**.

**Table 5.7** Length of PCR amplicons by using the indicated primer sets for the *nad2*–1–3–*cox*1 region of *Fischoederius* spp. mitochondrial genome *Mse*I pattern A, B, C, D, and I.

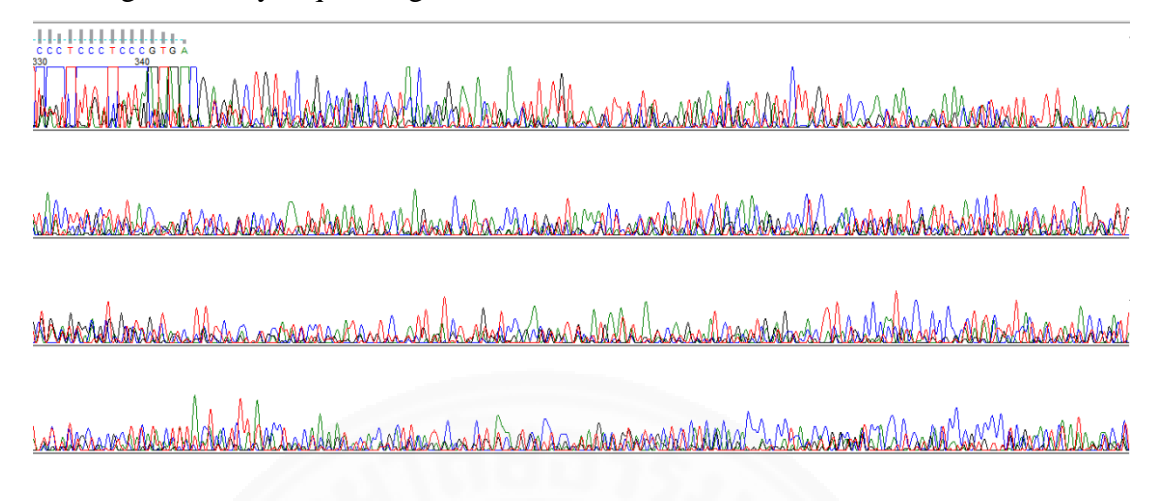
F-spp	pp Length of PCR amplicons (bp)													
Region	n	ad2–nad	<u>'</u> 1	naď	2–IE	IE-	nad1	nad2–IE	nad1	3 cox1				
Primer	HRG-	HRG-	HRG-	HRG-	HRG-	HRG-	HRG-	HRG-	HRG-	HRG-	HRG-			
set	625/623	596/597	596/623	625/670	596/670	669/623	669/597	671/670	672/673	3 598/599	651/568			
A	1,324	_	_	775	_	574	_	_	_	989	1,536			
В	_	881	_	_	394	_	512	1,019	783	979	1,536			
C	_	_	953	_	404	574	574 –		783	978	1,536			
D	_	_	1823	_	350	1,498	_	975	1,388	991	1,536			
I	_	_	978	_	397	606	606 –		783	1,000	1,536			



(Please see figure legend on overleaf)

**Figure 5.45** Images of 0.7% [w/v] agarose gels of resolved PCR products of *nad2*–1–3–*cox*1 region in *Fischoederius* spp. (F-spp) mitochondrial genome. The red arrowheads indicate the relevant fragments in each gel. (**A**) F-spp A; lane 1: HRG-669/623 (574 bp); lane 2: HRG-625/670 (775 bp); (**B**) F-spp B and F-spp C; lane 1: F-spp B with HRG596/670 (394 bp); lane 2: F-spp B with HRG669/597 (512 bp); lane 3: F-spp C with HRG596/670 (404 bp); lane 4: F-spp C with HRG669/623 (574 bp); lane 5: F-spp B with HRG-672/673 (783 bp); lane 6: F-spp C with HRG-672/673 (783 bp); lane 7: F-spp B with HRG-671/670 (1,019 bp); lane 8: F-spp C with HRG-671/670 (1,029 bp); (**C**) F-spp D and F-spp I; lane 1: F-spp D with HRG669/623 (1,498 bp); lane 2: F-spp D with HRG596/670 (350 bp); lane 3: F-spp I with HRG669/623 (606 bp); lane 4: F-spp I with HRG596/670 (397 bp); lane 5: F-spp D with HRG-672/673 (1,388 bp); lane 6: F-spp I with HRG-672/673 (783 bp); lane M: GeneRuler<sup>TM</sup> 100 bp Plus DNA ladder (Thermo Fisher Scientific, MA, USA).

#### A: Sanger dideoxy sequencing with standard condition



#### B: Sanger dideoxy sequencing for difficult template

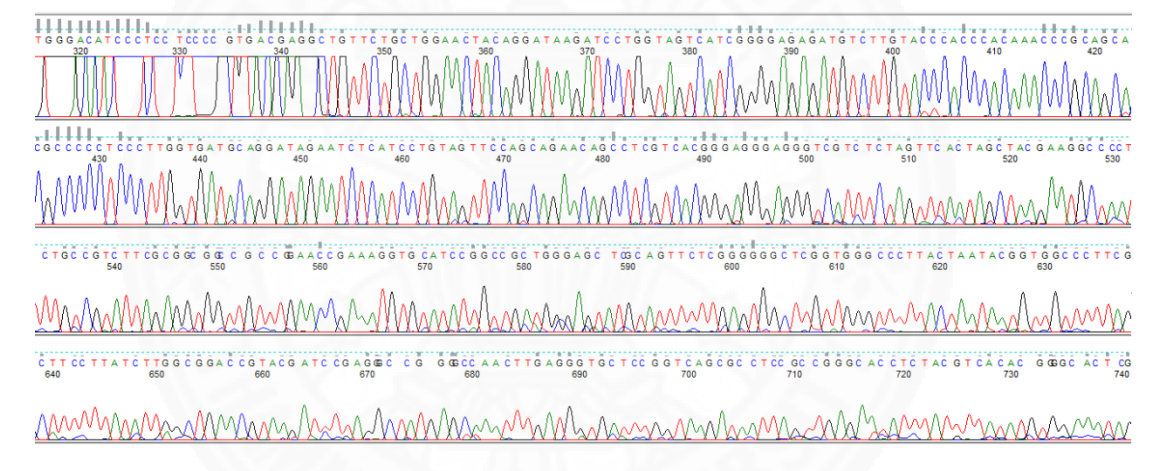


**Figure 5.46** Example of substandard sequencing quality in the *nad2/nad1* problem area that had the secondary structure formation. (**A**) Sanger dideoxy sequencing with standard conditions resulted in overlapping base signals; (**B**) Sanger dideoxy sequencing with conditions for difficult templates provided readable results.

Problems caused by the secondary structure formation of the *nad2*–1 region were confirmed by re-amplification of the *nad2*–1 region. The insert was released from the vector by digestion with *Eco*RI, purified using GeneJET Gel Extraction Kit (Thermo Fisher Scientific, MA, USA) as described in **Section 4.2.5** and used as PCR template as described in **Section 4.3.5**. In addition to the expected fragment of 1,324 bp size several other PCR products were observed (**Figure 5.47**).

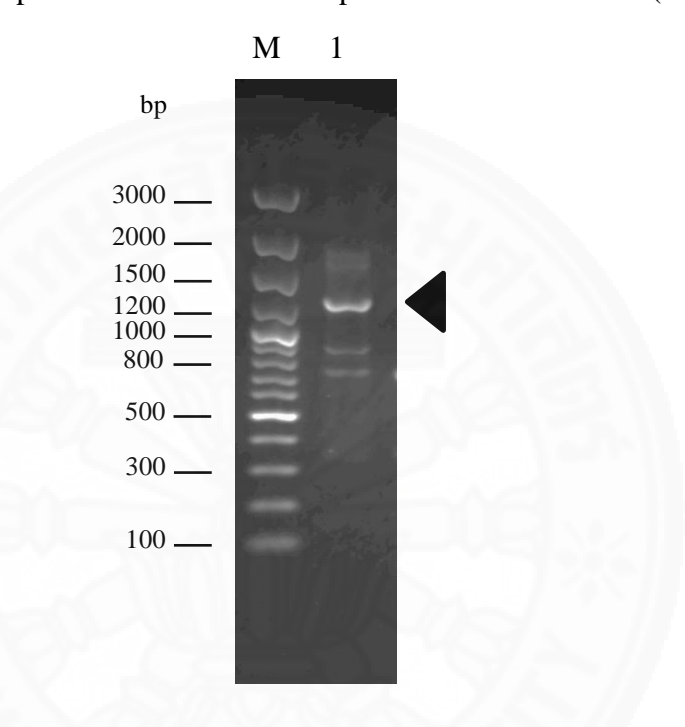


**Figure 5.47** Image of 0.7% [w/v] agarose gel showing the re-amplification products of the *nad2–nad1* fragment with primers HRG-625/623. Size standard: GeneRuler<sup>TM</sup> 100 bp Plus DNA ladder. The arrowhead indicates the expected 1,324 bp fragment.

Sequence analysis of the nad2-1-3-cox1 region included analysis for repeats which are known to cause structural abnormalities. Using EMBOSS EINVERTED revealed large inverted repeat units located in the nad2-nad1 region. Fischoederius MseI pattern A and D had two inverted repeat units. In Fischoederius MseI pattern A, one of inverted repeat units was located between tRNA-Val and the first tRNA-Asp, the other inverted repeat unit was located between the first tRNA-Asp and tRNA-Ala. In Fischoederius MseI pattern D, one of inverted repeat units was located between the first tRNA-Val and tRNA-Tyr, the other inverted repeat unit was located between the second tRNA-Val and the nad1 region. Only one inverted repeat

unit was found in *Fischoederius Mse*I pattern B, C, and I located between tRNA-Ala and tRNA-Asp. Diagrams of the *nad*2–1–3–*cox*1 region of *Fischoederius Mse*I pattern A–I with the positions of the inverted repeats are shown in **Figure 5.48**. All inverted repeats showed high sequence conservation of the repeat sequence on both strands at 93–100% identity suggesting formation of a 100 bp stem loop structure in these regions. The inverted repeat sequences are shown in **Figure 5.49**.

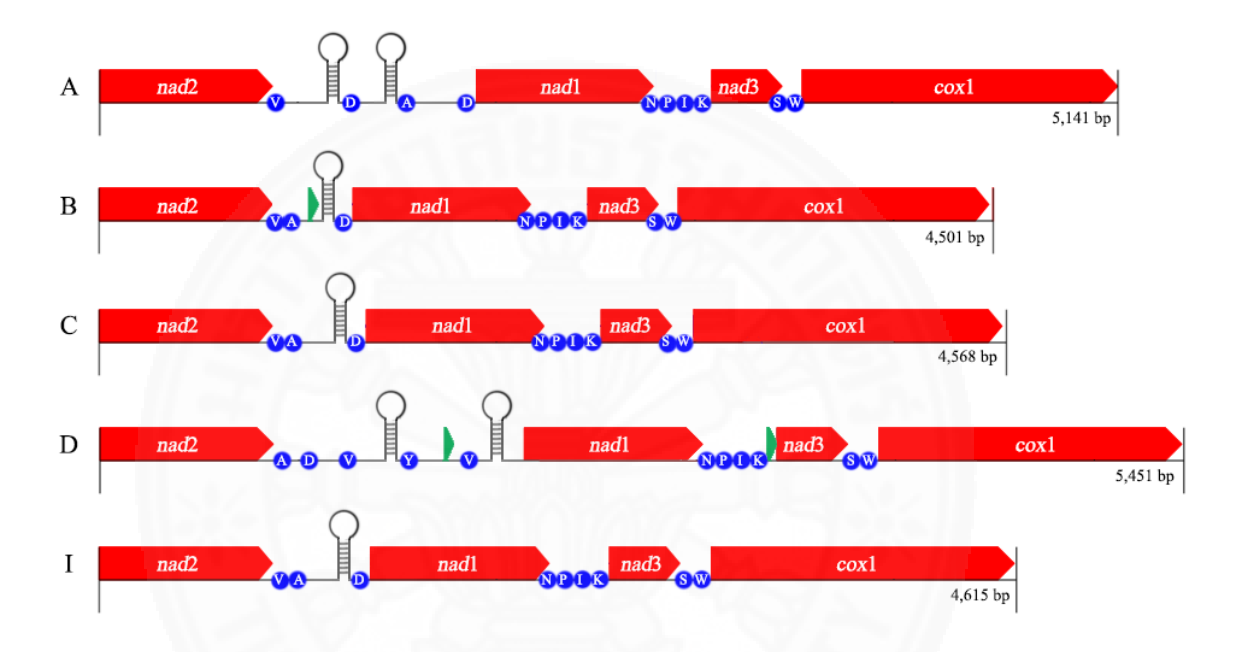


**Figure 5.48** Diagrams of the *nad2*–1–3–*cox*1 region of *Fischoederius Mse*I pattern A, B, C, D and I. The red arrows indicate the protein coding genes (*nad2*–1–3–*cox*1). The green arrows indicate predicted non-coding regions. The blue dots indicate tRNA regions. The stem loops indicate the inverted repeat positions.



**Figure 5.49** Inverted repeat sequences in the *nad*2–1–3–*cox*1 region of the mitochondrial genomes of *Fischoederius Mse*I pattern A, B, C, D and I detected by using EMBOSS EINVERTED.

### 5.4.5 Investigation of trematode genetic relationship based on mitochondrial *nad*1, *nad*2, *nad*3 sequences

Phylogenetic analyses of the deduced amino acid sequences of Fischoederius spp. genes nad1, nad2, nad3 were performed to evaluate the evolutionary relationship between Fischoederius MseI pattern A-I, Thailand, F. elongatus, China and other trematodes including F. cobboldi, G. crumenifer, E. explanatum, C. microbothrioides, O. streptocoelium, H. Paloniae, P. cervi, C. sinensis, and F. hepatica (outgroup) (Figure 5.50) by using neighbor-joining as described in **Section 4.3.6.4**. The three phylogenetic trees show that the *Fischoederius* sequences are clustered in a separate clade from the sequences of other trematodes. These Fischoederius-specific clades for NAD1, NAD2, NAD3 proteins were due to the lower sequence differences within the genus compared to more distant trematodes. The sequence differences in the genus Fischoederius for NAD1, NAD2, NAD3 were between 1.3-6.4%, 4.9-9.9%, and 0.8-6.8%, respectively (**Table 5.8**). The two F. elongatus isolates from Tianmen and Shanghai, China showed high identity in all three sequences with an intraspecies variation of 0.0–0.8%. The five putative species of Fischoederius isolated from Thailand had higher variation to each other. Fischoederius MseI pattern B and C were found closely related in all trees. Fischoederius MseI pattern A and D are closely related to each other while Fischoederius MseI pattern I might be closer related to F. cobboldi (China, remember that F. cobboldi mtCOX1 China was very different from F. cobboldi mtCOX1 India). Among the amphistomes Fischoederius has a closer genetic relationship to other members in the family Gastrothylacidae followed by family Paramphistomidae.

**Table 5.8** Intraspecies and interspecies variation of NAD1, NAD2, NAD3 proteins of *F. elongatus, F. cobboldi,* and *G. crumenifer.* F-A, F-B, F-C, F-D, F-I: *Fischoederius Mse*I pattern A, B, C, D, and I, respectively; FeT: *F. elongatus* isolated from Tianmen, China (GenBank: NC\_028001, ProteinID: YP\_009169428, YP\_009169427, YP\_009169429); FeS: *F. elongatus* isolated from Shanghai, China (GenBank: MN537973, ProteinID: QIJ60107, QIJ60106, QIJ60108); Fc: *F. cobboldi* (GenBank: NC\_030529, ProteinID: YP\_009262375, YP\_009262374, YP\_009262376); Gc: *G. crumenifer* (GenBank: NC\_027833, ProteinID: YP\_009164291, YP\_009164290, YP\_009164292).

	NAD1									NAD2								NAD3							
	A	В	C	D	I	FeT	FeS	Fc	A	В	C	D	I	FeT	FeS	Fc	A	В	C	D	I	FeT	FeS	Fc	
В	3.4								7.1								6.8								
C	3.7	3.4							9.5	2.5							5.9	0.8							
D	4.0	4.7	5.7						4.9	8.1	9.5						5.9	6.8	5.9						
I	5.4	5.0	4.4	6.4					6.7	8.1	9.9	7.4					5.9	5.9	5.9	6.8					
FeT	2.0	4.0	4.4	4.4	6.0				7.1	6.4	7.1	7.1	8.5				5.9	4.2	3.4	5.9	5.9				
FeS	1.3	3.4	3.7	3.7	5.4	0.7			7.1	6.4	7.1	7.1	8.5	0.0			6.8	5.1	4.2	6.8	6.8	0.8			
Fc	2.3	4.7	4.4	4.4	5.7	3.0	2.3		7.8	9.9	11.0	8.1	7.1	9.9	9.9		6.8	5.1	4.2	5.1	6.8	4.2	5.1		
Gc	6.4	6.7	7.4	7.4	7.7	6.4	5.7	6.7	13.8	13.4	14.1	12.7	13.1	12.4	12.4	14.8	22.0	22.0	21.2	24.6	21.2	19.5	20.3	22.9	

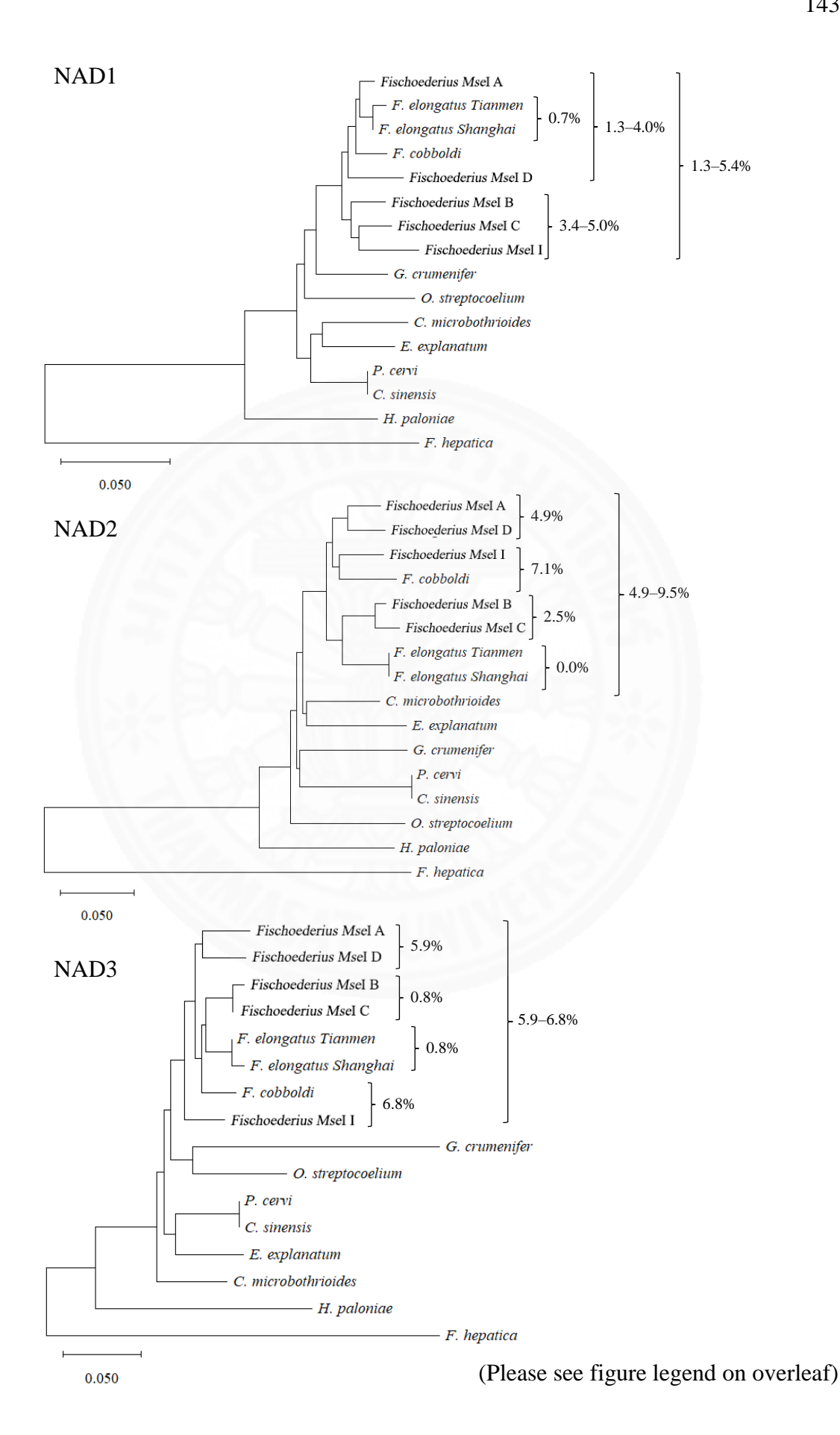
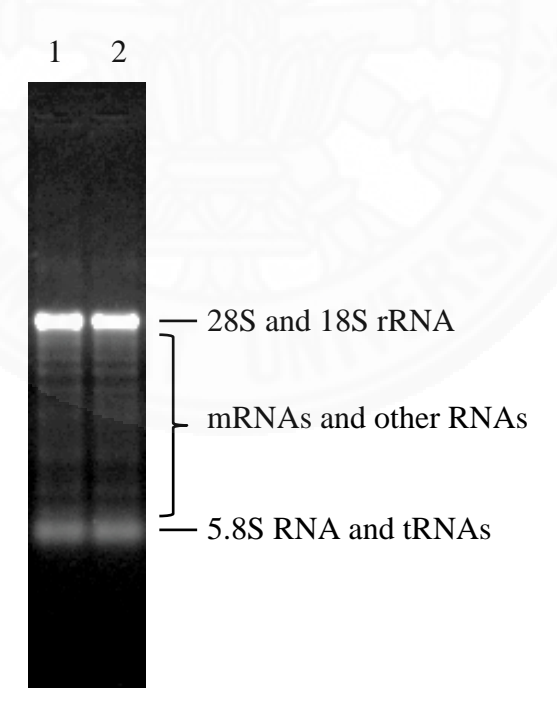


Figure 5.50 Phylogenetic analysis of NAD1, NAD2, NAD3 deduced amino acid sequences of Fischoederius MseI pattern A, B, C, D, I and other trematodes; F. elongatus isolated from Tianmen, China (GenBank: NC\_028001, ProteinID: YP\_009169428, YP\_009169427, YP\_009169429); F. elongatus isolated from Shanghai, China (GenBank: MN537973, ProteinID: QIJ60107, QIJ60106, QIJ60108); F. cobboldi (GenBank: NC\_030529, ProteinID: YP\_009262375, YP\_009262374, YP\_009262376); G. crumenifer (GenBank: NC\_027833, ProteinID: YP\_009164291, YP\_009164290, YP\_009164292); C. microbothrioides (GenBank: NC\_027271, ProteinID: YP\_009144952, YP\_009144951, YP\_009144953); P. cervi (GenBank: ProteinID: YP\_008963801, YP\_008963800, NC 023095, YP\_008963802); E. explanatum, (GenBank: NC\_027958, ProteinID: YP\_009166783, YP\_009166782, YP\_009166784); H. paloniae (GenBank: NC\_030530, ProteinID: YP\_009262387, YP\_009262386, YP\_009262388); O. streptocoelium (GenBank: NC\_028071, ProteinID: YP 009171939, YP 009171938, YP 009171940); C. sinensis (GenBank: YP\_002640629, YP\_002640628, NC\_012147, ProteinID: YP\_002640630); F. hepatica (GenBank: NC\_002546, ProteinID: NP\_066223, NP\_066222, NP\_066224).

## 5.5 Transcriptome analysis of *Fischoederius* spp.

#### 5.5.1 Fischoederius total RNA

Total RNA of immature and mature stage *Fischoederius* spp. was isolated, purified and cleaned from contaminating DNA as described in **Section 4.5.1**. The *Fischoederius* total RNA samples were classified by the PCR-RFLP of mtCOX1 using *Mse*I (Pattern A, [BEG], [CFH], D, and I) as described in **Section 4.2**. The 18S rRNA and 5.8S rRNA were clearly identified following separation by 1.2% [w/v] non-denaturing agarose gel electrophoresis. As has been found in other trematodes there was no 28S RNA. This rRNA contains an internal nick and migrates as two smaller fragments together with 18S rRNA. Several faint distinct bands were observed migrating between 18S rRNA and 5.8S rRNA that might be comprised of abundant mRNAs and other RNAs. RNA quantity was about 3–10 μg per specimen and RNA quality analysis showed the following values, OD260/280 = 1.80–1.99, OD 260/230 = 1.30–1.50, RIN = 7.7–9.4.



**Figure 5.51** Total RNA isolated from *Fischoederius* spp. (lane 1–2).

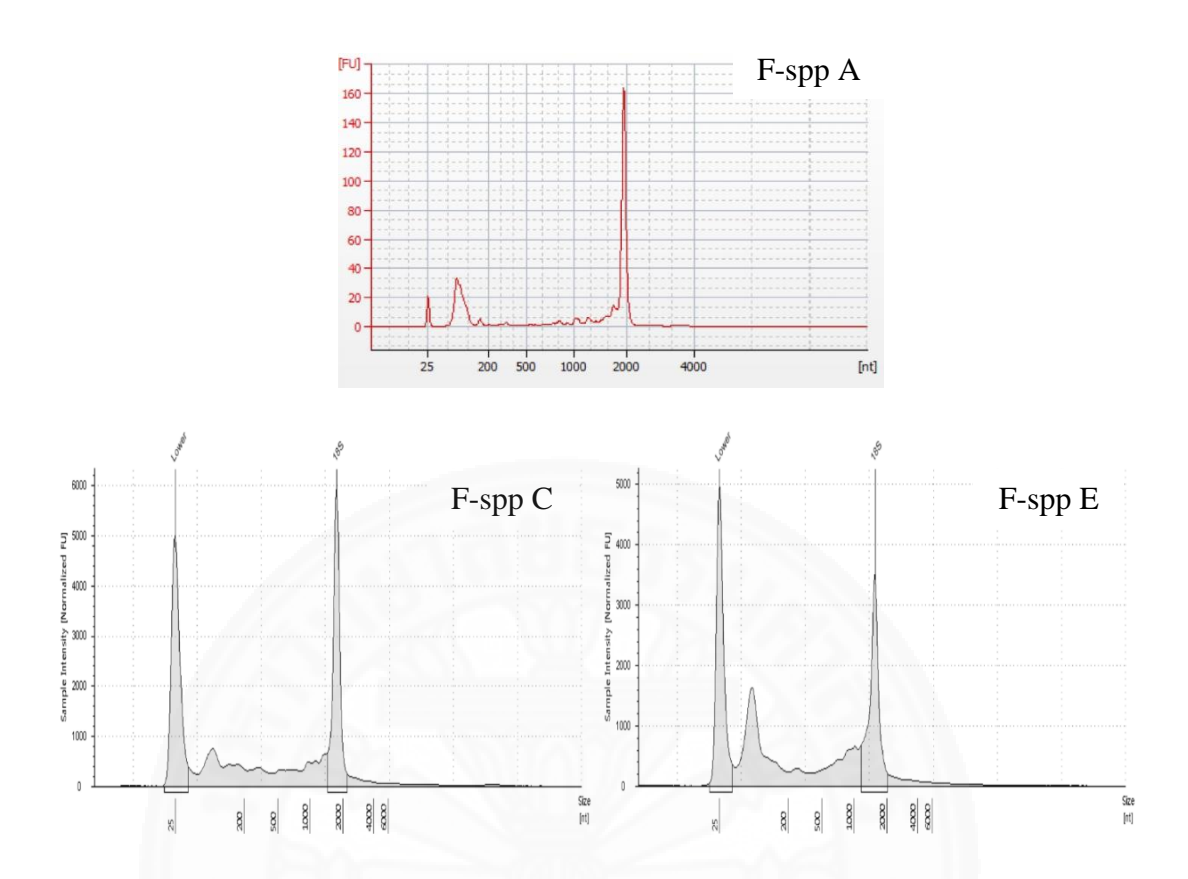


**Figure 5.52** Electropherograms of *Fischoederius* spp. total RNA. (**F-spp A**) *Fischoederius Mse*I pattern A, RIN = 7.7. (**F-spp C**) *Fischoederius Mse*I pattern C, RIN = 9.4. (**F-spp E**) *Fischoederius Mse*I pattern E, RIN = 8.0.

### 5.5.2 Characterization of *Fischoederius* spp. transcriptome

Transcriptome data of *Fischoederius Mse*I pattern A was generated using paired-end Illumina® sequencing as described in **Section 4.5.5**. In a preliminary study at 6 Gb scale, a total of 102,703,888 raw reads were produced with 93.97% at Q30 base quality. The data was assembled into 55,912 unique contigs with an average contig length of 633 bp and 44% GC content. Transcriptome sequencing was repeated at 40 Gb scale and generated 151,216,380 raw reads. The Q30 base quality was at 87.51%. Assembly of the raw reads generated 65,052 contigs with an average length of 870.5 bp and 45.95% GC content. For *Fischoederius Mse*I pattern C and E the sequencing scale was set to 10 Gb and resulted in 78,707,520 raw reads with 95.65% Q30 base quality and 67,164,370 raw reads with 95.46% Q30 base quality, respectively (**Table 5.9**).

**Table 5.9** Summary of *de novo* transcriptome assembly for *Fischoederius Mse*I pattern A, C, and E.

Category	F-spp A		F-spp C	F-spp E
Category	6 Gb 40 Gb		10 Gb	10 Gb
Total raw reads	102,703,888	151,216,380	78,707,520	67,164,370
Total read bases (bp)	9,831,815,713	~45,364,900,000	11,884,835,520	10,141,819,870
Q30 bases	93.97%	87.51%	95.65%	95.46%
GC percentage	44%	45.95%	48.07%	51.27%
Total assembled contigs (bp)	35,404,733	136,883,510	115,224,264	123,298,896
Contigs mapped to raw reads	55,912	65,052	286,223	308,374
Annotation (NCBI NR database)	18,361		27,720	30,462
Annotation (SWISS-Prot database)	10,048	10-	11,711	12,483
Annotation (UniProtKB database)	11	23,897	29,918	32,948
Average contig length (bp)	633	871	403	400

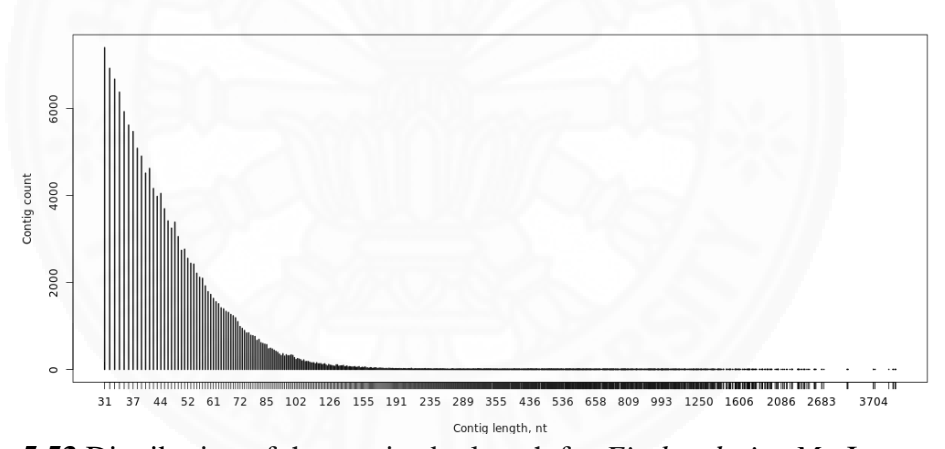
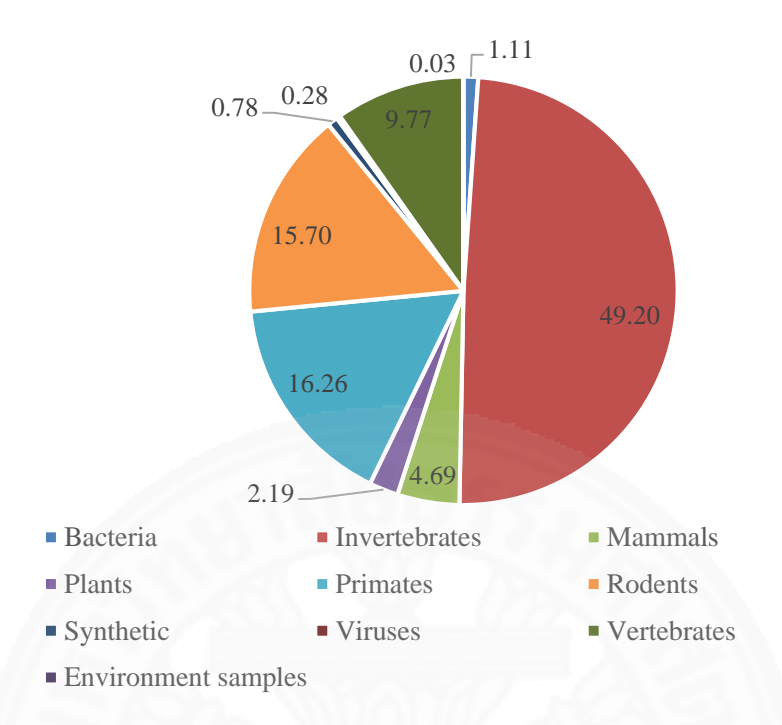


Figure 5.53 Distribution of the contigs by length for Fischoederius MseI pattern A.

### 5.5.3 Annotation of Fischoederius spp. transcriptome

The assembled transcriptome data of *Fischoederius* spp. was annotated by BLASTX searches against the full NCBI non-redundant and UniProtKB databases as described in **Section 4.5.6.1**. About 70% of the unique contigs had no annotation (no hit) in the databases. In the 6 Gb transcriptome data of *Fischoederius Mse*I pattern A, most of the matching unique contigs showed highest sequence conservation with invertebrates (49.20%). The remaining contigs showed highest conservation with sequences from rodents (15.70%), primates (16.26%), mammals (4.69%), plant (2.19%), bacteria (1.11%) and virus (0.28%) as shown in **Figure 5.54**.



**Figure 5.54** Distribution of database hits obtained by BLASTX with *Fischoederius Mse*I pattern A transcriptome data (6 Gb).

Based on the database data from 2017 Fischoederius MseI pattern A (40 Gb) BLASTX showed the following first hit distribution: Opisthorchis viverrini (32.36%), C. sinensis (21.99%), Echinostoma caproni (11.40%), Schistosoma mansoni (5.48%), and S. japonicum (4.20%) as shown in Figure 5.55A. Fischoederius MseI pattern C and E were analyzed using UniProtKB release 2020\_2 (22 April 2020). Therefore, species distribution cannot be compared to Fischoederius MseI pattern A. BLASTX searches with Fischoederius MseI pattern C data showed the following first hit distribution: C. sinensis (15.57%), Paragonimus westermani (13.79%), F. hepatica (9.49%), O. viverrini (8.69%), and Opisthorchis felineus (7.50%) as shown in Figure **5.55B.** In case of *Fischoederius Mse*I pattern E data the distribution was: *C. sinensis* (15.46%), P. westermani (12.70%), F. hepatica (9.54%), O. viverrini (8.34%), and O. felineus (7.16%) as shown in Figure 5.55C. It should be understood that this first hit species distribution depends on the data in the databases, i.e. it will change over time depending on the availability of additional sequence data. Data from amphistomes is very sparse at the present time and thus there are very few first hit matches to amphistomes.

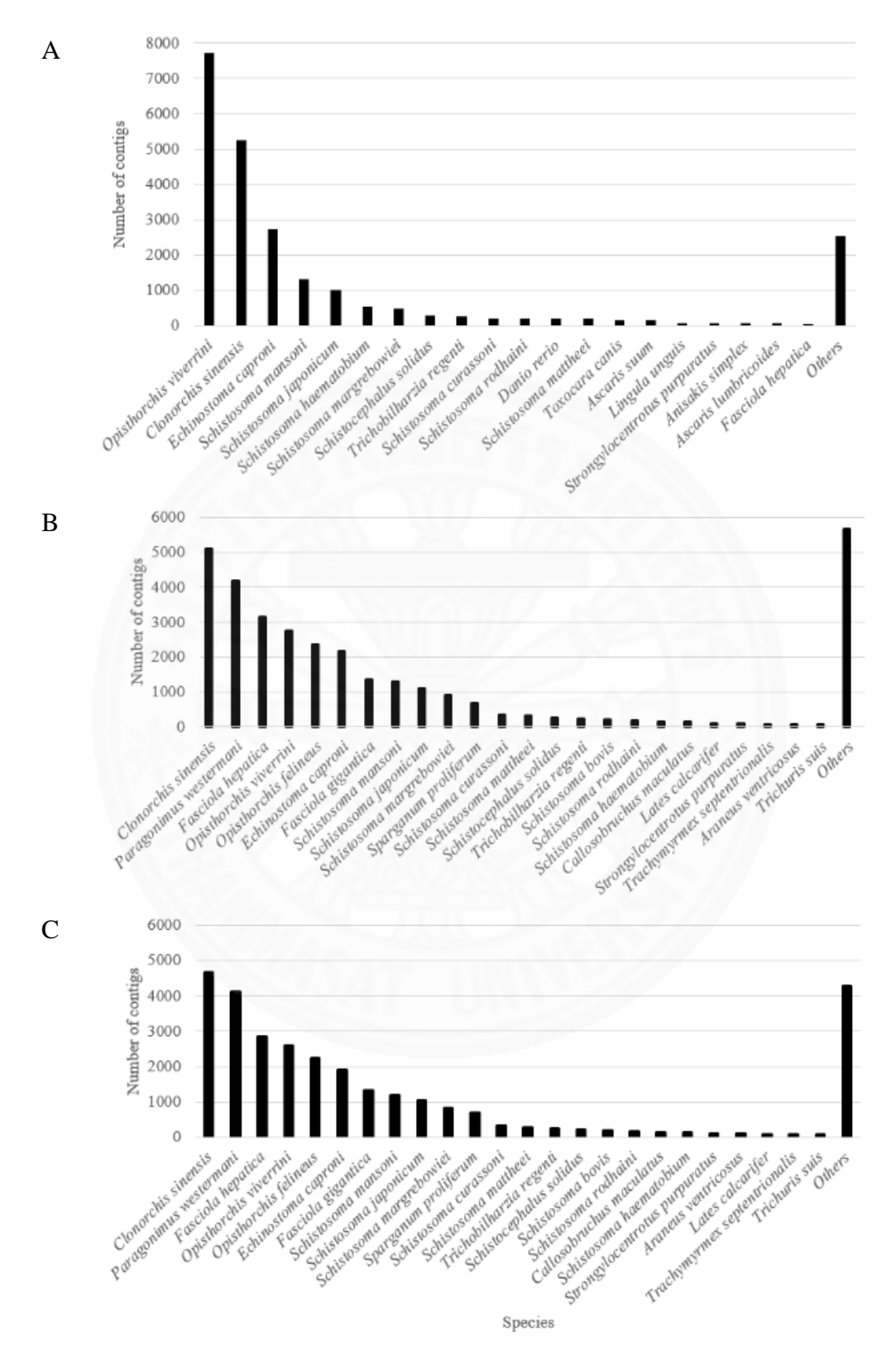


**Figure 5.55** BLASTX first hit species distribution in searches with *Fischoederius Mse*I pattern A, C, and E transcriptome data. (**A**) *Fischoederius Mse*I pattern A (2017); (**B**) *Fischoederius Mse*I pattern C (2020); (**C**) *Fischoederius Mse*I pattern E (2020).

### 5.5.4 Development stage verification of *Fischoederius* spp.

As described in the morphology analysis Fischoederius MseI pattern A specimens collected in 2016 were immature and lacked a developed reproductive system. To investigate the developmental stage at the molecular level, the transcriptome data from immature Fischoederius MseI pattern A and mature Fischoederius MseI pattern C and E were compared with a focus on transcripts involved in reproductive function. Four trematode proteins, vitelline protein, egg protein, major sperm protein, and sperm surface protein Sp17 were selected and used in TBLASTN against the Fischoederius transcriptome data (Table 5.10). The female-specific vitelline B precursor protein (GenBank: AAL23712) was predicted in Fischoederius MseI pattern A, C, and E at about 43–45% identity in the respective first hit transcript. Also, matches to female-specific egg antigen protein (GenBank: AAS19361) were detected in the transcriptome data of three Fischoederius spp. at 51–58% identity. Male reproductive proteins, major sperm protein (GenBank: OON16516) and Sperm surface protein Sp17 (GenBank: THD25339), were identified in the Fischoederius spp. transcriptomes at 63% and 75-83% identity, respectively for the first hit transcripts. However, transcripts encoding these four proteins in Fischoederius MseI pattern A had low abundance supporting that Fischoederius MseI pattern A specimens were immature flukes. Fischoederius MseI pattern C and E showed very high expression of vitelline protein which should be a valuable indicator of an active reproductive system.

**Table 5.10** TBLASTN results of four proteins active in the reproductive system against transcriptome data of *Fischoederius Mse*I pattern A, C, and E

Protein Fischoederius Ms		us MseI	MseI A Fischoederius MseI C				Fischoederius MseI E			
Protein	Transcript	Identity	TPM	Transcript	Identity	<b>TPM</b>	Transcript	Identity	TPM	
Vitelline B precursor protein	comp51464_seq0	44.9	0.0	c181168_g1_i1	42.9	25564.3	c214952_g1_i1	42.9	3045.9	
[Opisthorchis viverrini] GenBank: AAL23712	comp6613_seq0	41.0	1.6	c218068_g1_i1	42.5	2.1	c44433_g1_i1	42.4	0.5	
	comp18663_seq0	38.8	0.0	c182213_g1_i1	38.9	6964.0	c223997_g1_i1	40.0	554.8	
Egg antigen	comp491_seq0	51.3	0.0	c180268_g1_i2	57.6	1.1	c225934_g3_i2	51.2	95.3	
[Paragonimus westermani] GenBank: AAS19361	comp1319_seq0	44.3	30.6	c186713_g1_i2	44.6	26.1	c281472_g1_i1	48.1	3.9	
	comp1370_seq0	43.5	30.7	c189932_g1_i1	43.5	68.5	c225583_g1_i2	43.9	16.3	
MSP domain protein	comp1301_seq0	63.0	31.0	c184983_g1_i1	63.0	115.8	c226293_g1_i1	63.0	34.6	
[Opisthorchis viverrini] GenBank: OON16516	comp40441_seq0	38.1	0.4	c20023_g1_i2	42.9	0.6	c276444_g1_i1	43.5	1.4	
	comp8493_seq0	35.6	2.3	c183712_g2_i2	41.3	0.5	c195184_g1_i1	38.5	4.0	
Sperm surface protein Sp17	comp8254_seq0	75.0	0.9	c191008_g2_i3	82.9	38.1	c231615_g1_i1	82.9	11.7	
[Fasciola hepatica] GenBank: THD25339	comp36942_seq0	56.5	1.6	c136425_g1_i1	52.2	0.0	c215200_g1_i1	48.6	0.5	
	comp45374_seq0	54.1	0.0	c92486_g1_i1	48.3	1.2	c224644_g1_i2	48.3	46.7	

### 5.5.5 Gene ontology of *Fischoederius* spp. transcriptome

Following annotation, the transcripts were classified by their gene ontology (GO) category using Blast2GO as described in **Section 4.5.6.6**. The term categories of GO assignment were identified related to biological process, molecular function, and cellular components. 26,405 GO terms, most of them in the molecular process category, were assigned to transcripts in the *Fischoederius Mse*I pattern A transcriptome. The majority of GO terms under biological process category (7,433: 28.15%) represented biosynthesis processes involved in protein translation, DNA integration, DNA transcription and its regulation and were followed by biological pathways and metabolic processes (**Figure 5.56A**). For GO terms under molecular function category (11,282: 42.73%), the found sub-majority categories included binding function, structural constituent of ribosome, GTPase activity, protein kinase activity and catalytic activity (**Figure 5.56B**). For GO terms of cellular components (7,609: 28.82%) most sub-majority categories were associated with membrane component, nucleus, cytoplasm, intracellular, and ribosome (**Figure 5.56C**).

71,299 GO terms were assigned to transcripts in the *Fischoederius Mse*I pattern C transcriptome. The majority of GO terms were in the biological process category (28,783: 40.37%) with sub-majority categories including cellular process, metabolic process, biological regulation, biogenesis, and localization (**Figure 5.57A**). GO terms under molecular function category (14,901: 20.90%) included terms catalytic activity, binding function, transporter activity, and molecular function regulator (**Figure 5.57B**). GO terms in the cellular component category (27,615: 38.73%) were associated with cell, membrane, and organelle component (**Figure 5.57C**).

MseI pattern E transcriptome. Again, the majority of GO terms were in the biological process category (31,324: 40.23%) with sub-majority categories including cellular process, metabolic process, biological regulation, biogenesis, and localization (**Figure 5.58A**). GO terms under molecular function category (16,343: 21.00%) included catalytic activity, binding function, transporter activity, and molecular function regulator (**Figure 5.58B**). GO terms in the cellular component category (30,188: 38.77%) were associated with cell, membrane, and organelle component (**Figure 5.58C**).

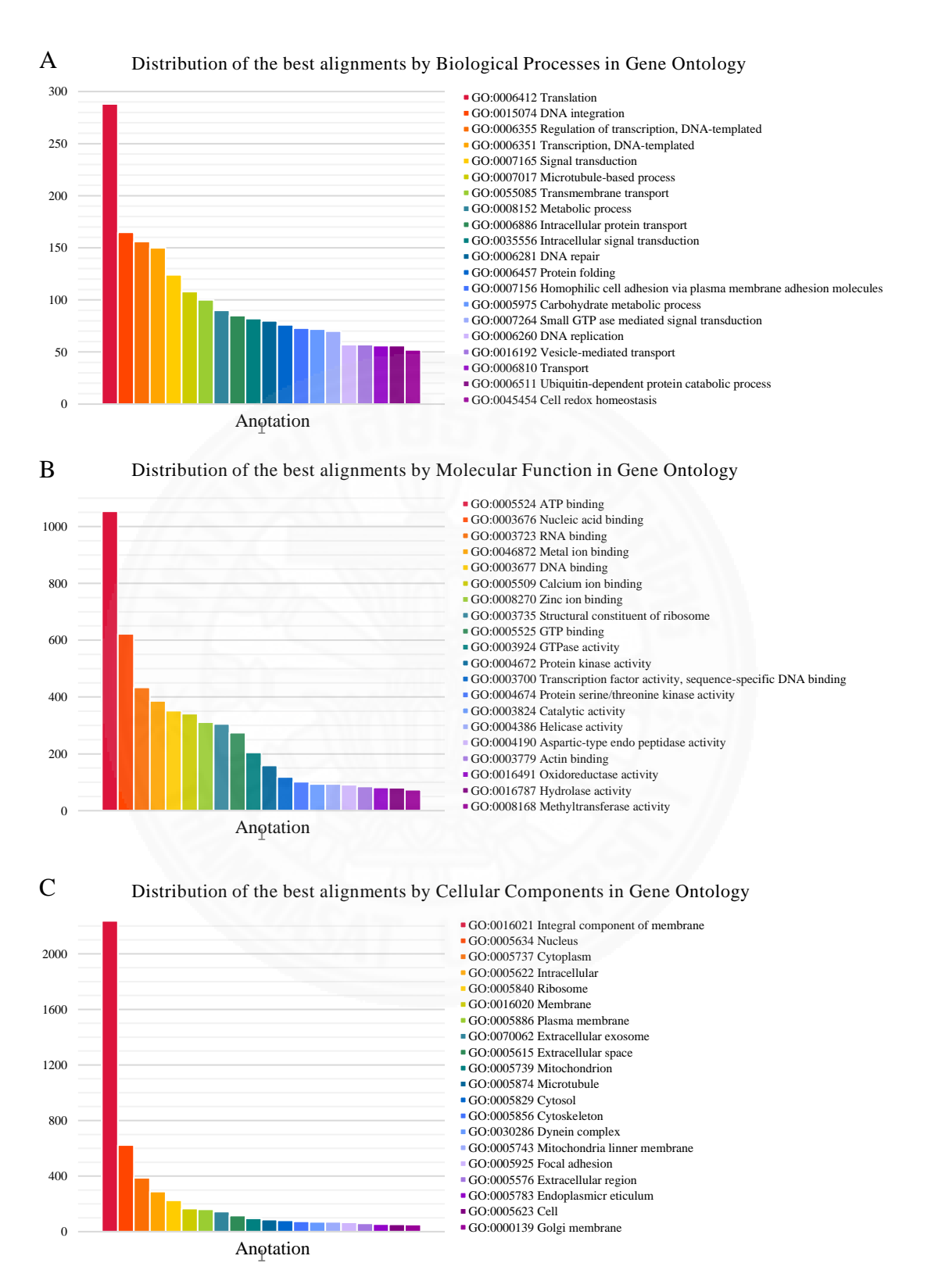


**Figure 5.56** Top 20 of gene ontology of *Fischoederius Mse*I pattern A transcriptome in each major category (2017); (**A**) Biological process; (**B**) Molecular function; (**C**) Cellular component.

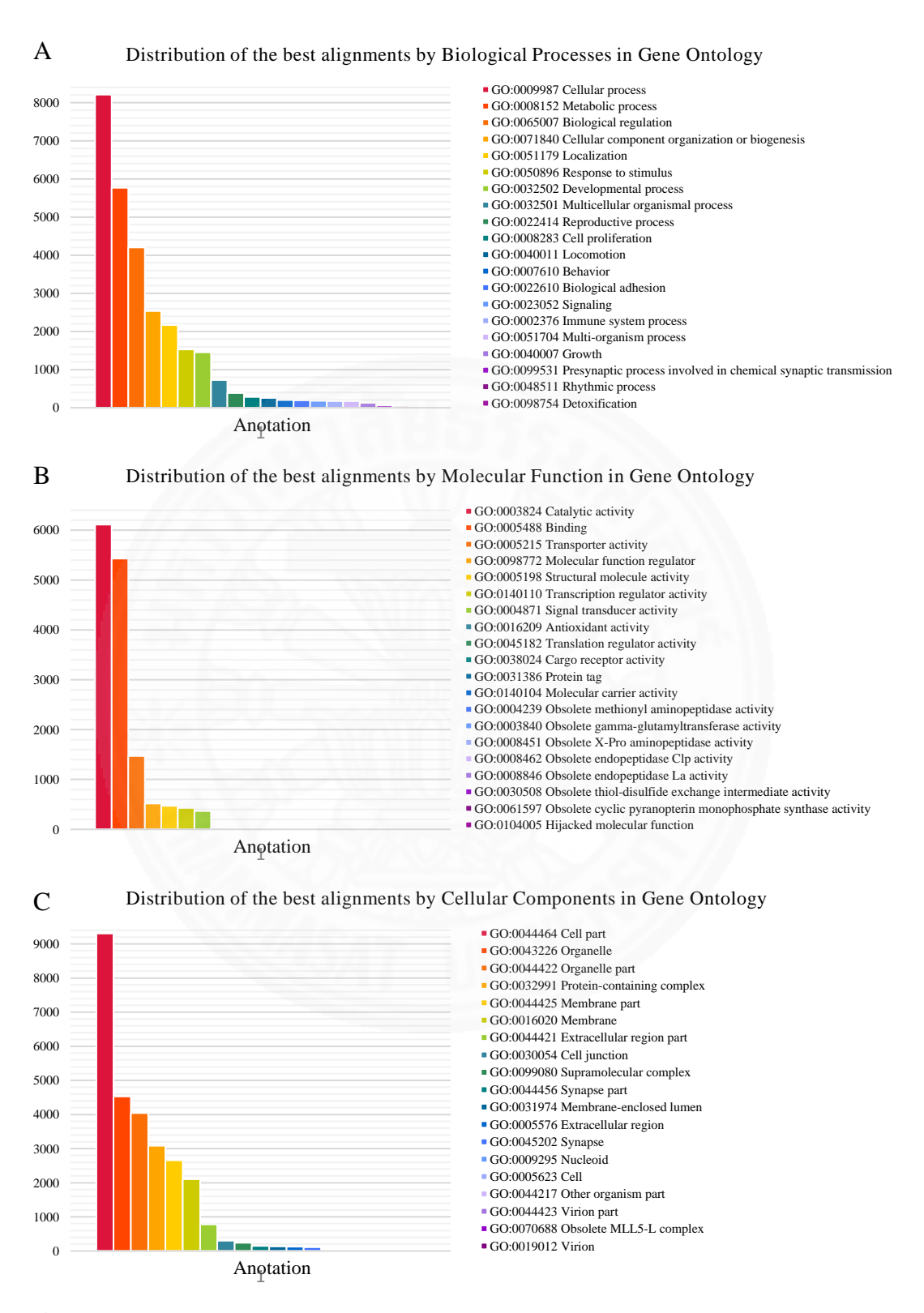


**Figure 5.57** Top 20 of gene ontology of *Fischoederius Mse*I pattern C transcriptome in each major category (2020); (**A**) Biological process; (**B**) Molecular function; (**C**) Cellular component.

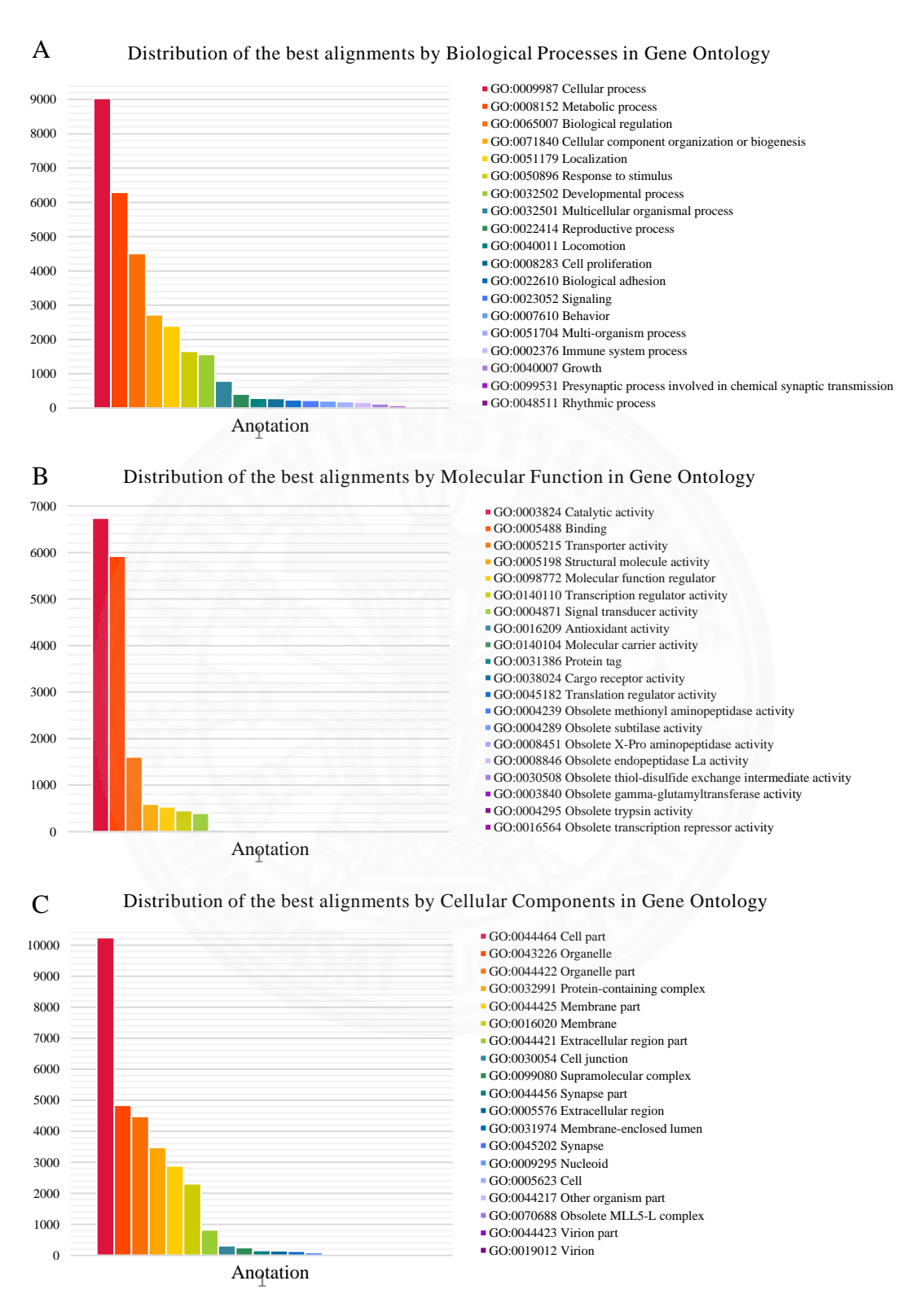


**Figure 5.58** Top 20 of gene ontology of *Fischoederius Mse*I pattern E transcriptome in each major category (2020); (**A**) Biological process; (**B**) Molecular function; (**C**) Cellular component.

# 5.5.6 Transcript abundance in the *Fischoederius Mse*I A, C, and E transcriptome

The transcription levels of *Fischoederius* spp. were estimated using the TPM (transcripts per million) values. The top 100 abundant transcripts revealed that 25–35% of them encoded uncharacterized proteins in the databases. The top 50 abundant known transcripts in the transcriptomes of *Fischoederius Mse*I pattern A, C, and E are listed in **Figures 5.59–5.61**. Concluding the transcript abundancy in the transcriptome data of the three *Fischoederius* spp. transcriptomes they showed high expression of genes including (1) mitochondrial gene for chemical energy production *e.g.* cytochrome b, cytochrome c oxidase, and NADH dehydrogenase with their function in the electron transport chain, (2) genes associated with transport of cations and anions, *e.g.* myoglobin, globin-3, and calcium-binding protein, (3) gene associated cellular process, *e.g.* ubiquitin and poly-ubiquitin, (4) genes associated with oxidative phosphorylation, *e.g.* thioredoxin peroxidase, (5) nutrient transport genes, *e.g.* fatty-acid binding protein, (6) catalytic enzyme genes, *e.g.* glutathione S-transferase, and cathepsin B. *Fischoederius Mse*I pattern C and E transcriptomes, the adult stage, showed high expression of genes associated with embryonic development, *i.e.* ferritin.

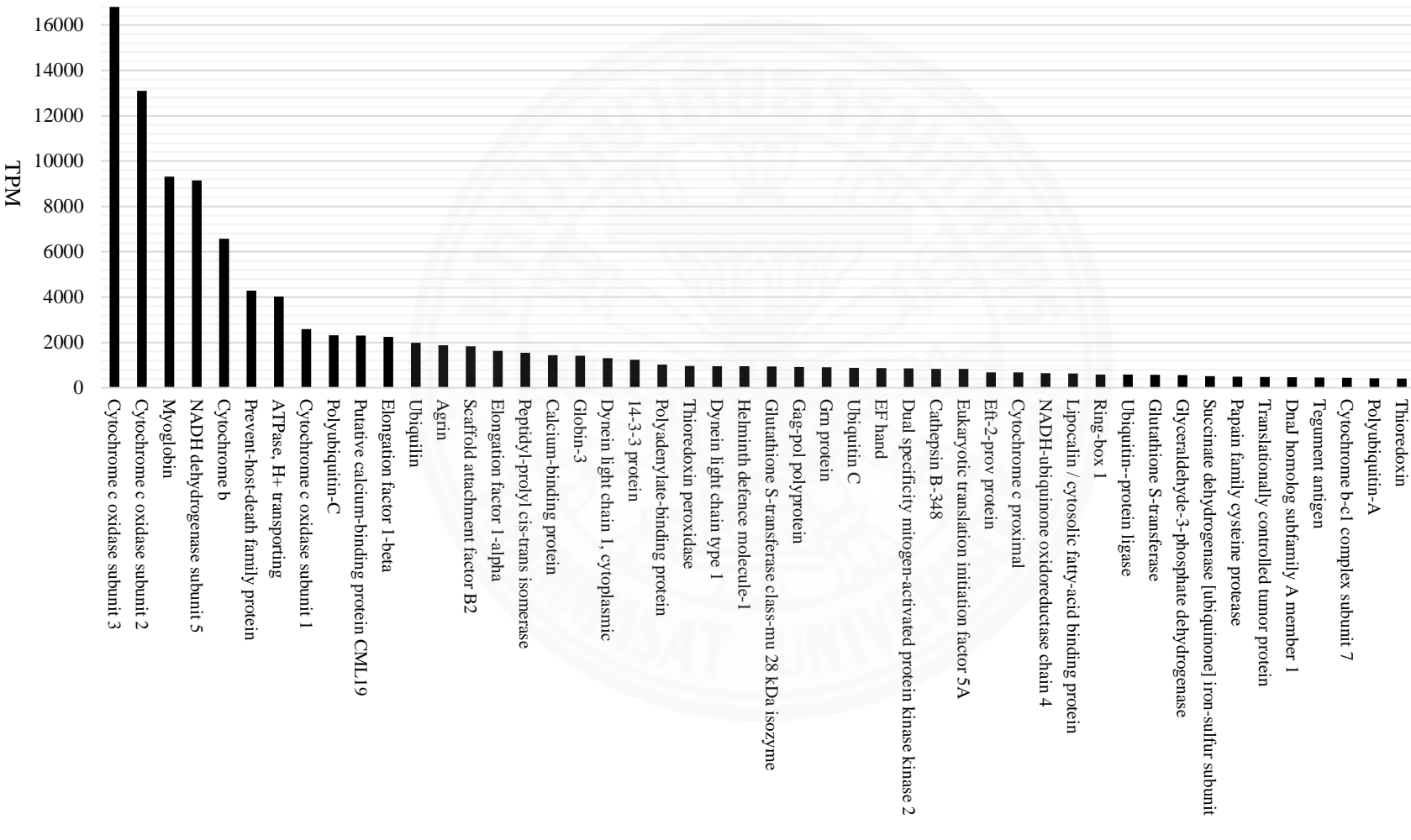


Figure 5.59 Top 50 abundant known transcripts of Fischoederius MseI A transcriptome.

18000

157

CHCH domain protein

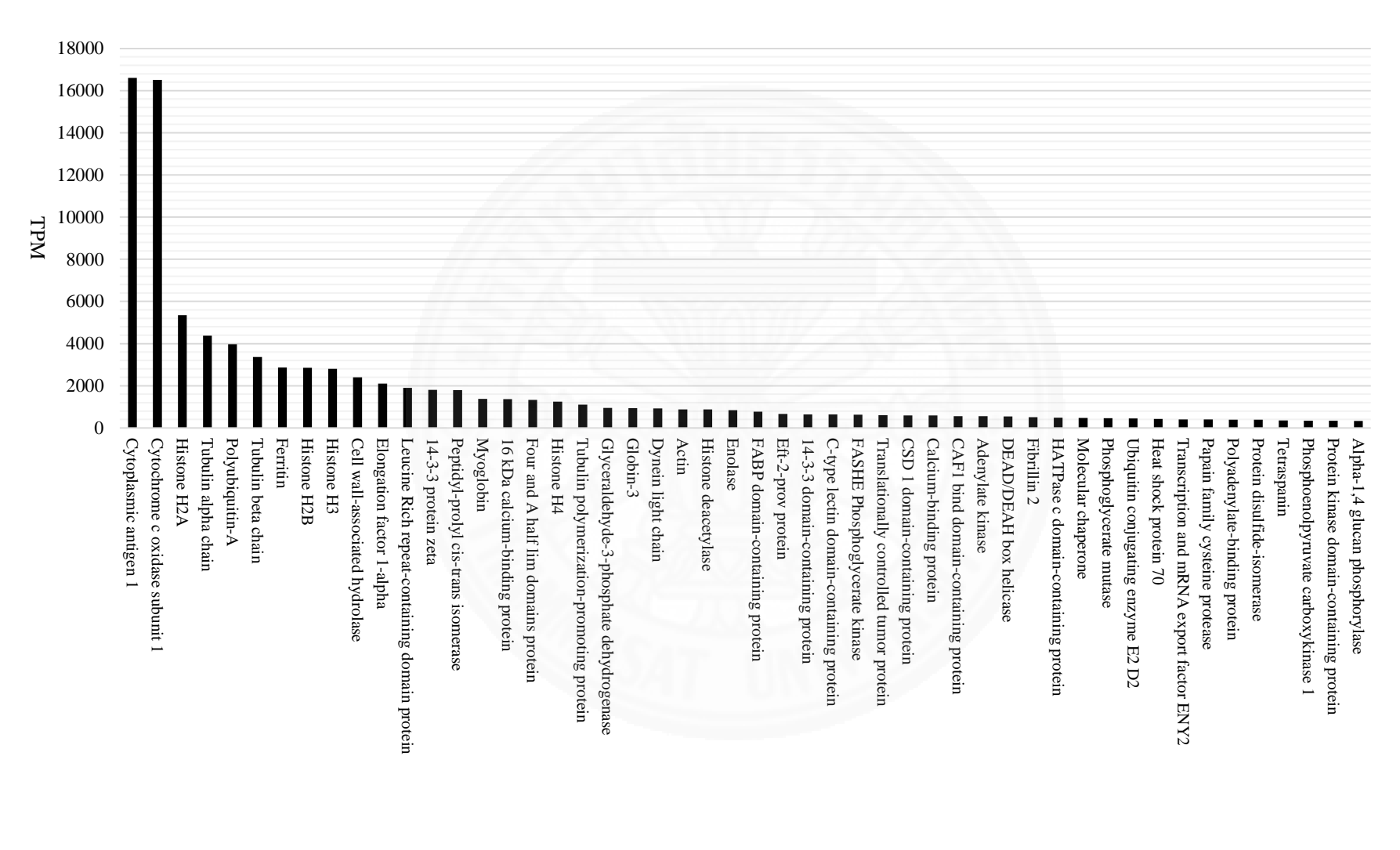


Figure 5.60 Top 50 abundant known transcripts of Fischoederius MseI C transcriptome.

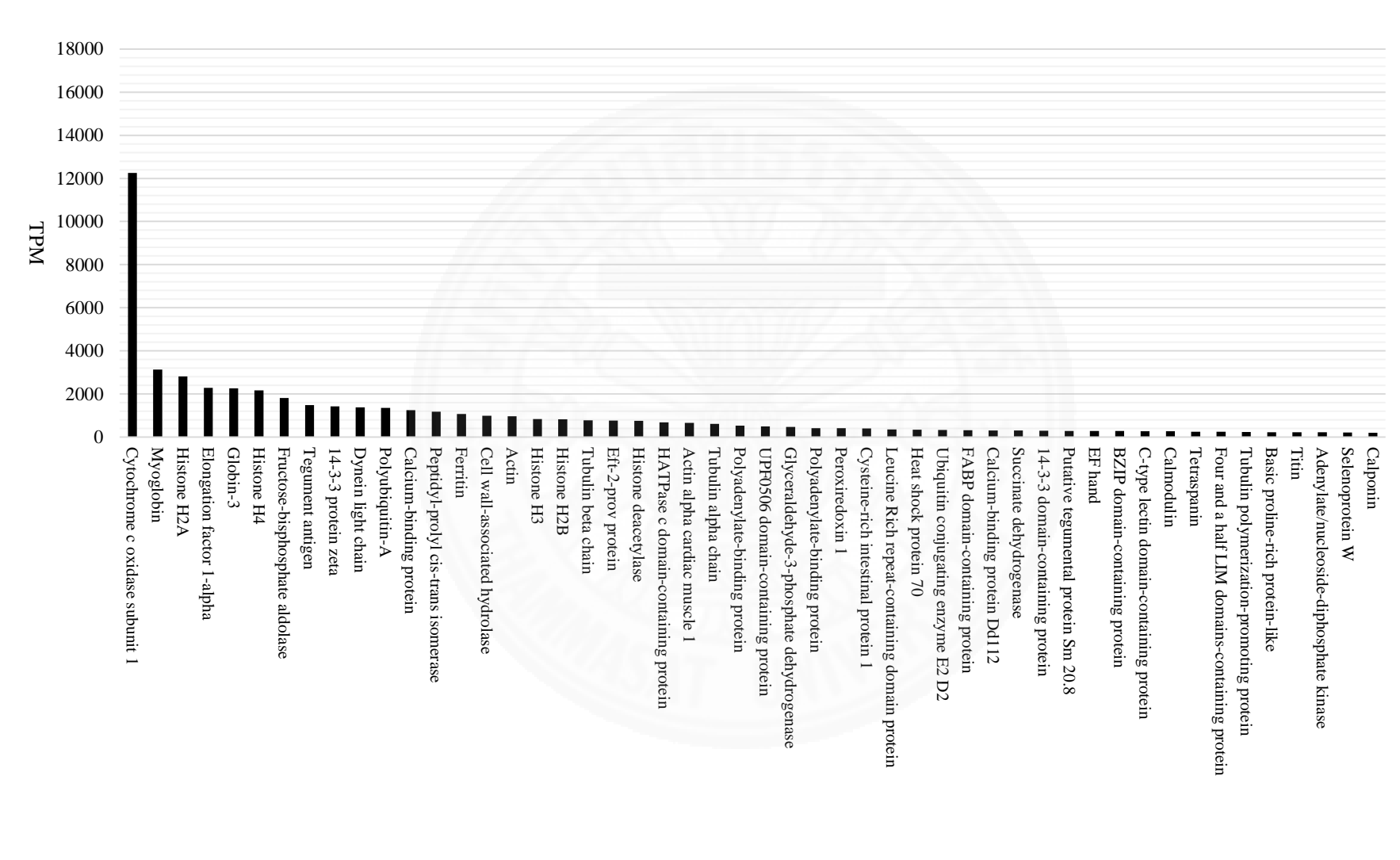


Figure 5.61 Top 50 abundant known transcripts of Fischoederius MseI E transcriptome.

# 5.5.7 Highly abundant transcripts with complete coding sequence and potential for application in the transcriptome data of *Fischoederius Mse*I A

Transcripts with a complete coding sequence were selected from the list of highly abundant transcripts with known function of the encoded proteins (Section 5.5.6). EMBOSS-PATMATMOTIFS (prosite database) was used to detect conserved motifs in the conceptually translated sequences. Putative N-terminal signal peptides were predicted using SignalP and internal transmembrane regions were predicted using TMHMM as described in Section 4.5.6.4. NCBI-BLASTP was used to find homologous proteins in the NCBI nonredundant (nr) protein database. Among the proteins with a complete sequence were cathepsin B-like cysteine proteinase, cathepsin L-like cysteine proteinase, cathepsin C-like cysteine proteinase, fatty acid-binding protein, thioredoxin, and calcium-binding protein.

### 5.5.7.1 Cathepsin B-like cysteine proteinase

The transcriptome sequence no. TBIU011911 was annotated as cathepsin B-like cysteine proteinase at base positions 163–1176 with the ORF in R1 (**Figure 5.62**). The encoded protein of 377 amino acids size has a calculated molecular weight of 38.05 kDa, an isoelectric point of 5.2, a signal peptide of 21 amino acids size and no transmembrane region (**Figures 5.62–5.64**). The deduced amino acid sequence was predicted to contain several motifs, an amidation site (LGKK) at residues 43–46, eukaryotic thiol (cysteine) proteases cysteine active site (QSACGSCWAVAA) at residues 109–120, and eukaryotic thiol (cysteine) proteases histidine active site (GGHAVRILGWG) at residues 281–291. Related proteins in the database were found with identity values of 48.36%, 47.16%, 49.25%, 49.25%, and 47.55% for *Fasciola gigantica* cathepsin B (GenBank: TPP60838), *F. gigantica* Sarcophaga pro-cathepsin B (GenBank: TPP63328), *S. haematobium* cathepsin B-like cysteine proteinase (GenBank: XP\_012801037 and KAF1337776), *Trichobilharzia szidati* cathepsin B1 (GenBank: ACG50796), respectively (**Table 5.11**).

Furthermore, a second cathepsin B-like cysteine proteinase was predicted from the reverse sequence of transcriptome sequence no. Comp1676\_seq3 at base positions 162–1151 with an ORF in R1. The encoded protein of 329 amino acids size has a calculated molecular weight of 37.30 kDa and an

isoelectric point of 7.1 (**Figure 5.65**). A signal peptide of 19 amino acids length was predicted at the N-terminus (**Figure 5.66**). No internal transmembrane region was predicted (**Figure 5.67**). An amidation motif was predicted at amino acid residues 43–46 (SGKK). Several motifs were found, eukaryotic thiol (cysteine) proteases cysteine and histidine active site, were indicated at residues 106–117 (QSNCGSCWAFGA) and residues 273–283 (GGHAVRMIGWG), respectively. NCBI-BLASTP showed the following related proteins, *F. gigantica* Sarcophaga pro-cathepsin B (GenBank: TPP63328), *F. buski* Cathepsin B endopeptidase (GenBank: KAA0187027), and *T. regenti* cathepsin B1 isotype 1–3 precursor (GenBank: AAV65881, AAV65882, AAV65883) at 51.67%, 51.49%, and 49.71% identity, respectively (**Table 5.12**).

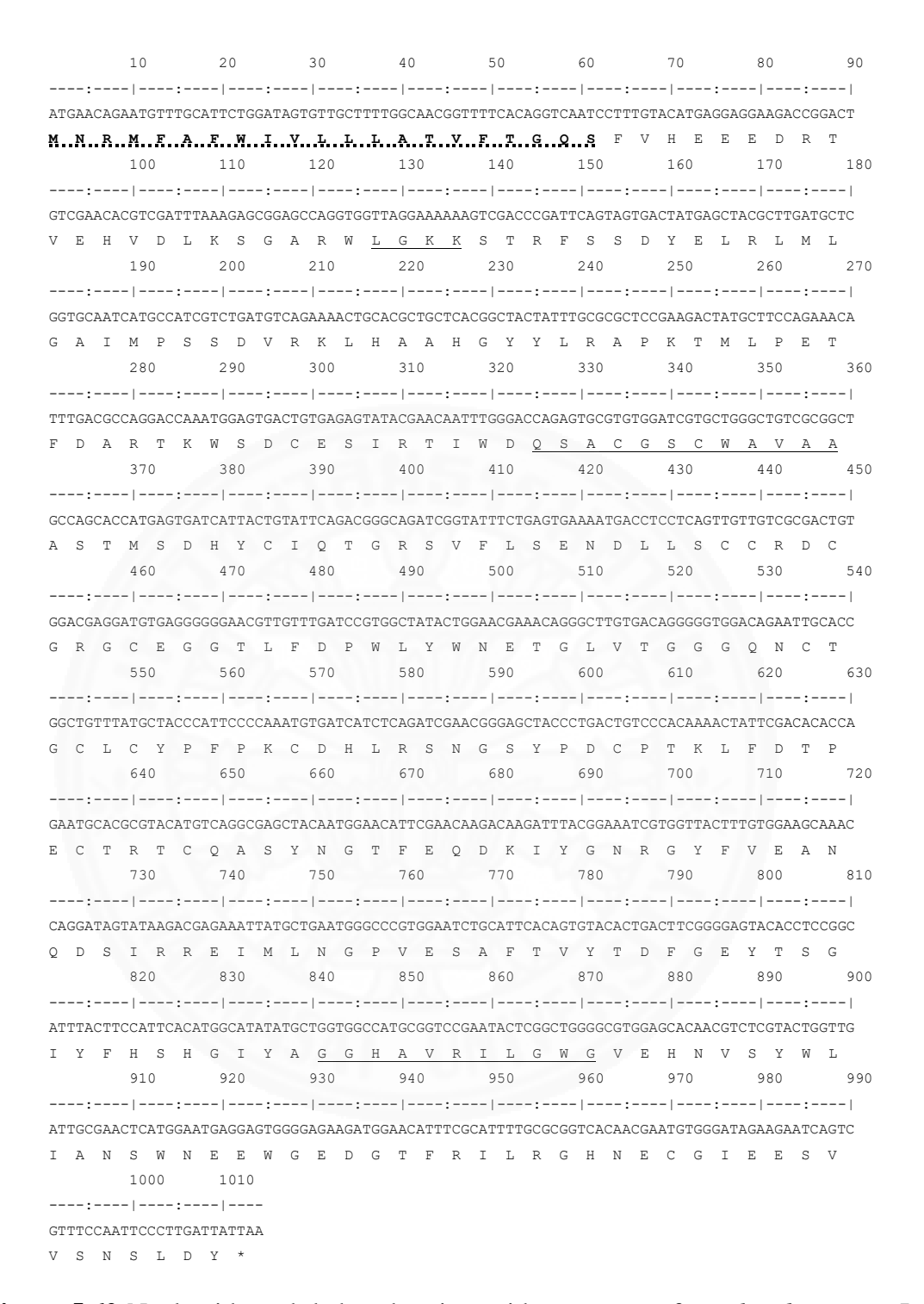
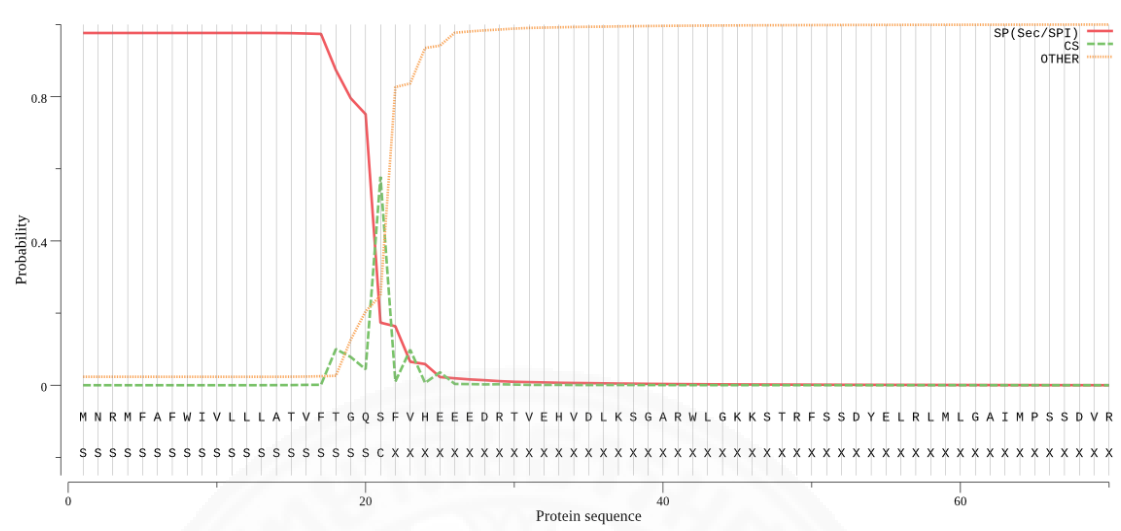


**Figure 5.62** Nucleotide and deduced amino acid sequences of *Fischoederius Mse*I A cathepsin B-like cysteine proteinase (TBIU011911) using SHOWSEQ in EMBOSS. The signal peptide is indicated by the dot-underlined bold sequence. Motifs are indicated by an underlined sequence, *i.e.* amidation site (LGKK), eukaryotic thiol (cysteine) proteases cysteine active site (QSACGSCWAVAA), and eukaryotic thiol (cysteine) proteases histidine active site (GGHAVRILGWG).





Cleavage site between positions: 21 and 22 (GQS-FV)

Probability: 0.5779 Protein type: Likelihood

Signal Peptide (Sec/SPI): 0.976 Other: 0.024

**Figure 5.63** Signal peptide prediction of *Fischoederius Mse*I A cathepsin B-like cysteine proteinase (TBIU011911) using SignalP.

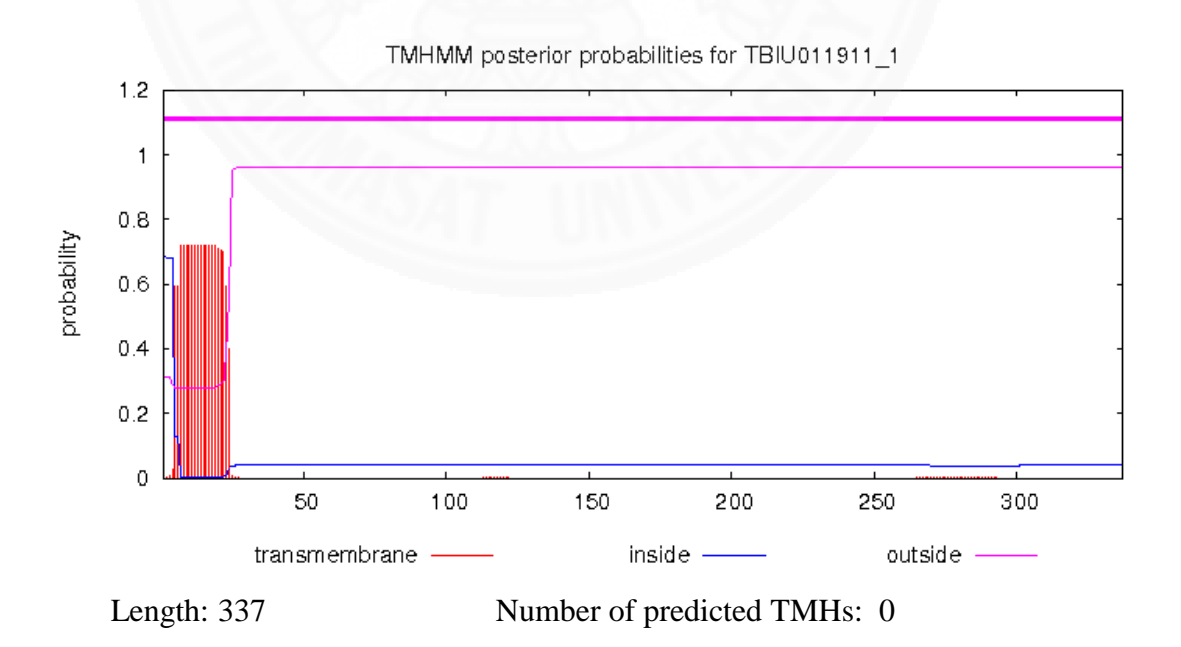


**Figure 5.64** Transmembrane region prediction of *Fischoederius Mse*I A cathepsin B-like cysteine proteinase (TBIU011911) using TMHMM.

**Table 5.11** Sequence identity values of *Fischoederius Mse*I A cathepsin B-like cysteine proteinase (TBIU011911) with other trematode cathepsin B sequences.

	Identity	Positive	E-value
98%	10.000		
	48.36%	61.49%	5e-103
98%	47.16%	60.60%	1e-102
12801037 98%	49.25%	61.79%	2e-102
337776 98%	49.25%	61.79%	9e-102
0796 95%	47.55%	61.96%	4e-101
	3328 98% 12801037 98% 337776 98%	3328 98% 47.16% 12801037 98% 49.25% 337776 98% 49.25%	3328 98% 47.16% 60.60% 12801037 98% 49.25% 61.79% 337776 98% 49.25% 61.79%

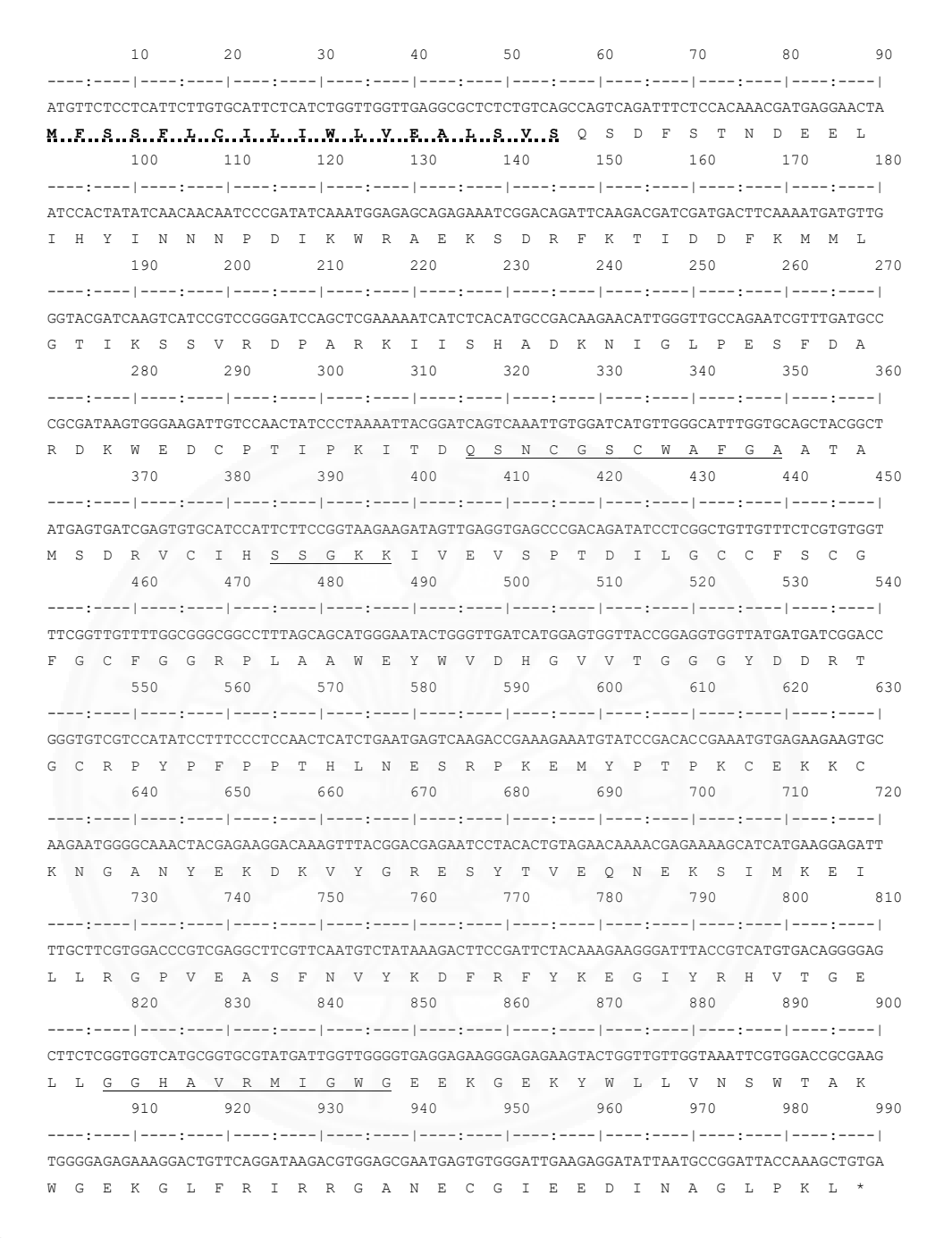
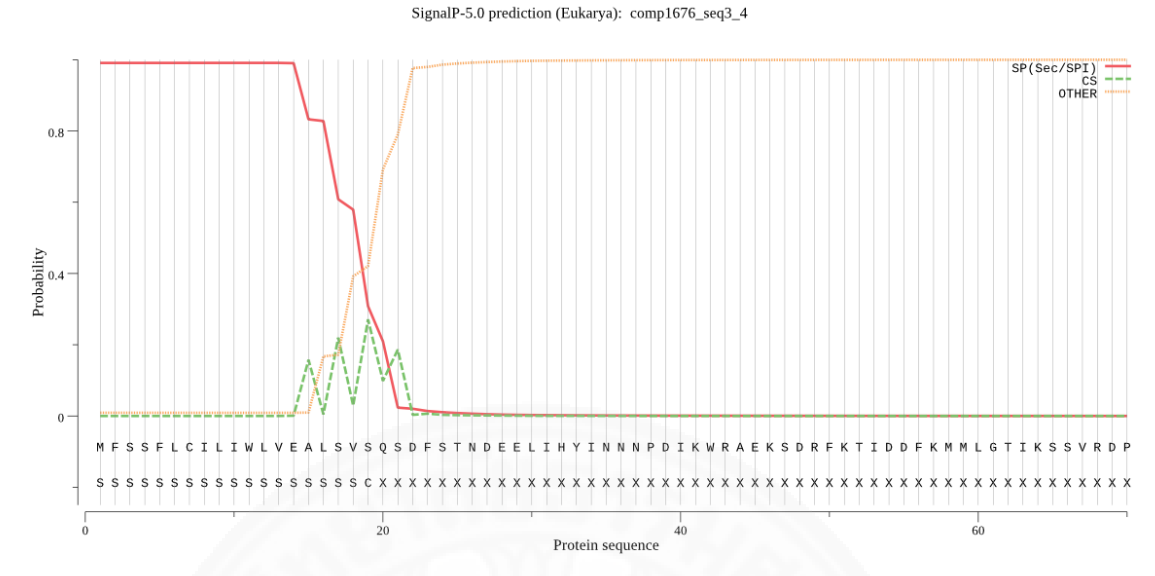


**Figure 5.65** Nucleotide and deduced amino acid sequences of *Fischoederius Mse*I A cathepsin B-like cysteine proteinase (Comp1676\_seq3) using SHOWSEQ in EMBOSS. The signal peptide is indicated by the dot-underlined bold sequence. Motifs are indicated by an underlined sequence, *i.e.* amidation site (SGKK), eukaryotic thiol (cysteine) proteases cysteine active site (QSNCGSCWAFGA), and eukaryotic thiol (cysteine) proteases histidine active site (GGHAVRMIGWG).



Cleavage site between positions: 19 and 20 (SVS-QS)

Probability: 0.9029 Protein type: Likelihood

Signal Peptide (Sec/SPI): 0.9899 Other: 0.0101

**Figure 5.66** Signal peptide prediction of *Fischoederius Mse*I A cathepsin B-like cysteine proteinase (Comp1676\_seq3) using SignalP.

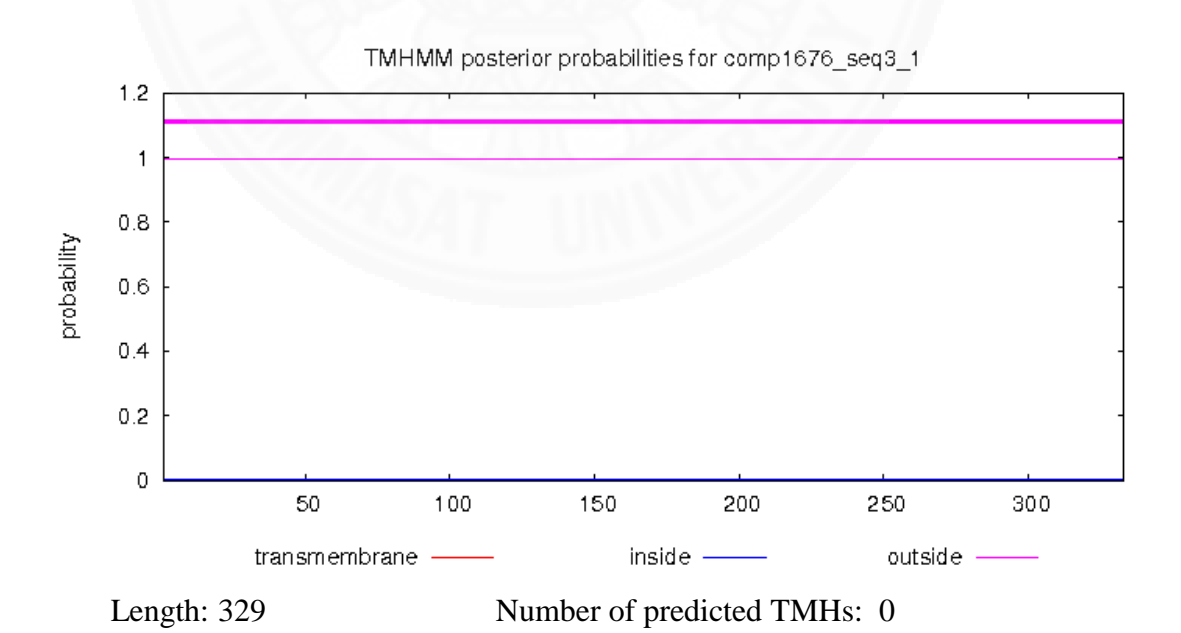


**Figure 5.67** Transmembrane region prediction of *Fischoederius Mse*I A cathepsin B-like cysteine proteinase (Comp1676\_seq3) using TMHMM.

**Table 5.12** Sequence identity values of *Fischoederius Mse*I A cathepsin B-like cysteine proteinase (Comp1676\_seq3) with other trematode cathepsin B sequences.

Description	A	Query	%	%	E malma
Description	Accession	Cover	Identity	Positive	E-value
Sarcophaga pro-cathepsin B	TPP63328	95%	51.67%	66.87%	3e-121
[Fasciola gigantica]					
Cathepsin B endopeptidase	KAA0187027	97%	51.49%	66.96%	1e-119
[Fasciolopsis buski]					
Cathepsin B1 isotype 1 precursor	AAV65881	97%	49.71%	65.29%	5e-117
[Trichobilharzia regenti]					
Cathepsin B1 isotype 2 precursor	AAV65882	98%	49.71%	64.91%	4e-117
[Trichobilharzia regenti]					
Cathepsin B1 isotype 3 precursor	AAV65883	97%	47.71%	65.59%	6e-117
[Trichobilharzia regenti]					

### 5.5.7.2 Cathepsin L-like cysteine proteinase

Transcriptome sequence no. Comp422\_seq1 was identified as encoding a cathepsin L-like cysteine proteinase at base positions 236–1375 with the ORF in R1 (**Figure 5.68**). This protein contained 379 amino acids, had a molecular weight of 42.64 kDa and a theoretical isoelectric point of 6.7. SignalP predicted a signal peptide of 21 amino acids length (**Figure 5.69**). Transmembrane regions were not predicted (**Figure 5.70**). EMBOSS-PATMATMOTIFS detected following motifs, eukaryotic thiol (cysteine) proteases cysteine active site at residues 174–185 (QGACGSCWAFSS), eukaryotic thiol (cysteine) proteases histidine active site at residues 324–334 (LDHGVLLVGYG), and eukaryotic thiol (cysteine) proteases asparagine active site at residues 341–360 (YWLIKNSWGTAWGENGYVRI). NCBIBLASTP resulted in best hits to *C. sinensis* cathepsin L-like proteinase precursor (GenBank: ABK91809) at 53.23% identity, *P. westermani* cathepsin L (GenBank: KAA3679270) at 55.82%, *O. viverrini* cathepsin L (GenBank: OON14246) at 51.72%, and *C. sinensis* cathepsin L (GenBank: GAA57175 and RJW67986) at 51.30% and 50.92% identity (**Table 5.13**).

**Table 5.13** Sequence identity values of *Fischoederius Mse*I A cathepsin L-like cysteine proteinase (Comp422\_seq1) with other trematode cathepsin L sequences.

Description	Accession	Query	Query %		E volue
Description	Accession	Cover	Identity		E-value
Cathepsin L-like proteinase precursor	ABK91809	97%	53.23%	68.28%	5e-134
[Clonorchis sinensis]					
Cathepsin L	KAA3679270	98%	55.82%	69.31%	3e-132
[Paragonimus westermani]					
Papain family cysteine protease	OON14246	99%	51.72%	67.28%	4e-131
[Opisthorchis viverrini]					
Cathepsin L	GAA57175	97%	51.30%	66.15%	6e-130
[Clonorchis sinensis]					
Cathepsin L	RJW67986	96%	50.92%	66.23%	7e-128
[Clonorchis sinensis]					

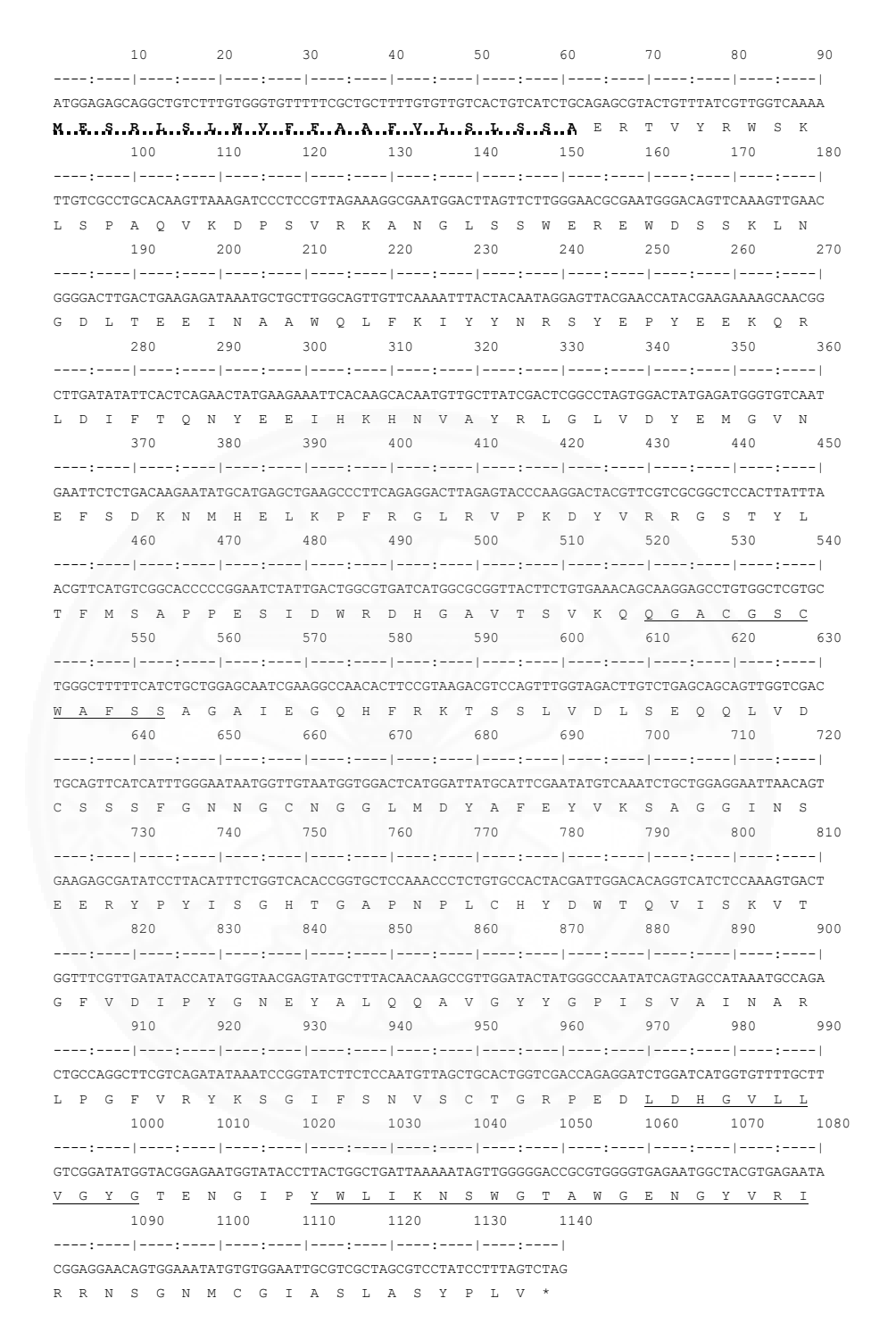
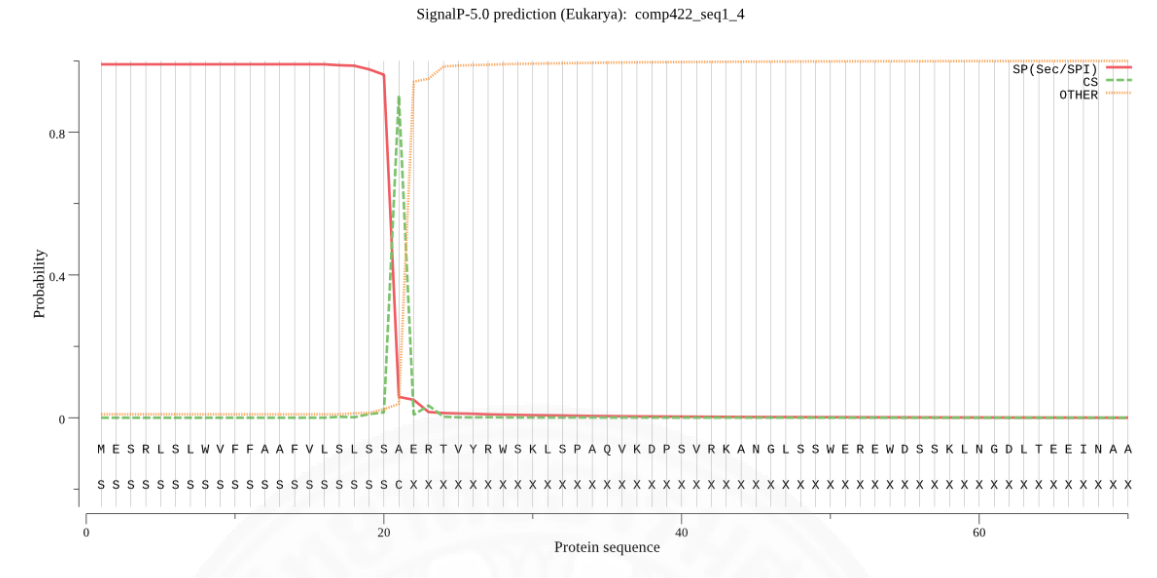


**Figure 5.68** Nucleotide and deduced amino acid sequences of *Fischoederius Mse*I A cathepsin L-like cysteine proteinase (Comp422\_seq1) using SHOWSEQ in EMBOSS. The signal peptide is indicated by the dot-underlined sequence. Motifs are indicated by underlined sequences; eukaryotic thiol (cysteine) proteases cysteine active site (QGACGSCWAFSS), eukaryotic thiol (cysteine) proteases asparagine active site (LDHGVLLVGYG), and eukaryotic thiol (cysteine) proteases histidine active site (YWLIKNSWGTAWGENGYVRI).



Cleavage site between positions: 21 and 22 (SSA-ER)

Probability: 0.9029 Protein type: Likelihood

Signal Peptide (Sec/SPI): 0.9899 Other: 0.0101

**Figure 5.69** Signal peptide prediction of *Fischoederius Mse*I A cathepsin L-like cysteine proteinase (Comp422\_seq1) using SignalP.

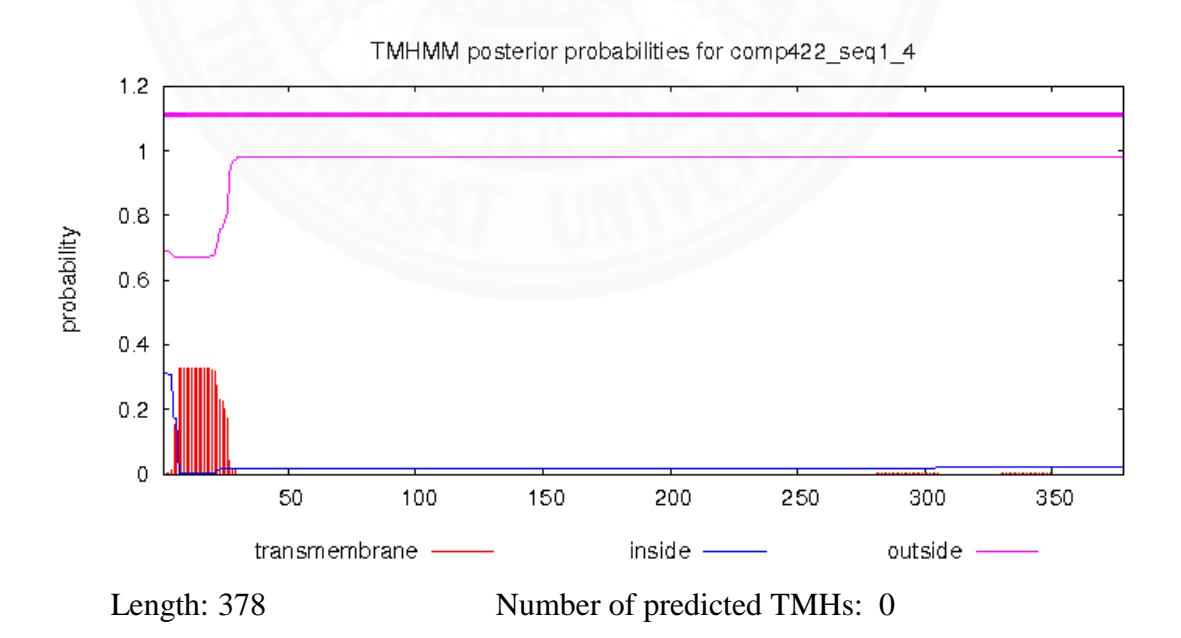


**Figure 5.70** Transmembrane region prediction of *Fischoederius Mse*I A cathepsin L-like cysteine proteinase (Comp422\_seq1) using TMHMM.

### 5.5.7.3 Cathepsin C-like cysteine proteinase

A cathepsin C-like cysteine proteinase was predicted in transcriptome sequence no. TBIU021593 at base positions 294–1679 with the ORF in R1 and transcriptome sequence no. Comp1034\_seq0 at base positions 334–1719 with the ORF in R1 (**Figure 5.71**). The deduced sequence of 461 amino acids had a calculated molecular weight of 52.50 kDa and an isoelectric point of 8.1. The first 22 amino acids at the N-terminus were predicted to form a signal peptide and putative transmembrane regions were not detected (**Figures 5.72–5.73**). Two protease active site motifs were found in the sequence, eukaryotic thiol (cysteine) proteases cysteine active site at residues 248–259 (QGHCGSCYAFAS) and eukaryotic thiol (cysteine) proteases histidine active site at residues 403–413 (VNHGVVIVGYG). Related proteins in the NCBI nonredundant protein database were *S. japonicum* cathepsin C isoform 2–4 (GenBank: TNN09560, TNN09561, TNN09558), *Schistosoma bovis* cathepsin C (GenBank: RTG87036), and *S. haematobium* cathepsin C (GenBank: XP\_012799794) at 58.67%, 56.25%, and 56.03% sequence identity, respectively (**Table 5.14**).

**Table 5.14** Sequence identity values of *Fischoederius Mse*I A cathepsin C-like cysteine proteinase (TBIU021593) with other trematode cathepsin C sequences.

Description	A	Query	%	%	E-value
Description	Accession	Cover	Identity	Positive	
Cathepsin C isoform 2	TNN09560	99%	58.67%	70.02%	0.0
[Schistosoma japonicum]					
Cathepsin C isoform 3	TNN09561	99%	58.67%	70.02%	0.0
[Schistosoma japonicum]					
Cathepsin C isoform 4	TNN09558	99%	58.67%	70.02%	0.0
[Schistosoma japonicum]					
Cathepsin C	RTG87036	99%	56.25%	69.83%	0.0
[Schistosoma bovis]					
Cathepsin C	XP_012799794	99%	56.03%	69.40 %	4e-180
[Schistosoma haematobium]					

```
10 20 30 40 50 60 70 80
 ----:
\tt ATGATTTCTTGGCTGGTTTACCAGTTAGTGTTTTGTGGTCTTATCATACCGTTATCGTTCGCGGATACTCCGGCCAATTGTACATAT
100 110 120 130 140 150
                                                                                                                                                                 160 170
 ----:----|----:|----|----:|----|----:|----|----:|----|----:|----|----:|----|----
 \texttt{E} \quad \texttt{D} \quad \texttt{A} \quad \texttt{R} \quad \texttt{G} \quad \texttt{R} \quad \texttt{W} \quad \texttt{M} \quad \texttt{F} \quad \texttt{S} \quad \texttt{Y} \quad \texttt{C} \quad \texttt{D} \quad \texttt{K} \quad \texttt{K} \quad \texttt{D} \quad \texttt{C} \quad \texttt{K} \quad \texttt{E} \quad \texttt{K} \quad \texttt{E} \quad \texttt{K} \quad \texttt{N} \quad \texttt{I} \quad \texttt{T} \quad \texttt{F} \quad \texttt{S} \quad \texttt{L} \quad
                                       200 210 220 230 240 250 260 270
 ----:----|----:|-----|----:|----|----:|----|----:|----|----:|----|----:|----|----
 \begin{smallmatrix} Y \end{smallmatrix} \hspace{0.1cm} P \hspace{0.1cm} N \hspace{0.1cm} L \hspace{0.1cm} A \hspace{0.1cm} V \hspace{0.1cm} D \hspace{0.1cm} E \hspace{0.1cm} Y \hspace{0.1cm} G \hspace{0.1cm} R \hspace{0.1cm} G \hspace{0.1cm} T \hspace{0.1cm} W \hspace{0.1cm} T \hspace{0.1cm} M \hspace{0.1cm} I \hspace{0.1cm} Y \hspace{0.1cm} N \hspace{0.1cm} Q \hspace{0.1cm} G \hspace{0.1cm} F \hspace{0.1cm} E \hspace{0.1cm} I \hspace{0.1cm} T \hspace{0.1cm} V \hspace{0.1cm} Q \hspace{0.1cm} N \hspace{0.1cm} R \hspace{0.1cm} A \hspace{0.1cm} R \hspace{0.1cm} A \hspace{
                   280 290 300 310 320 330 340 350 360
 ----:----|----:----|----:----|----:----|----:----|----:----|----:----|----:----|----:
K W L V M F A F N D G G K F F C D R G M P G W T H D T L L R
                   370 380 390 400 410 420 430 440
 ----:----|----:----|----:----|----:----|----:----|----:----|----:----|----:----|
 \begin{smallmatrix} Q & W & K & W & F & T & S & V & K & L & N & P & R & K & A & V & S & S & T & Q & G & T & L & S & K & K & L & I & S \\ \end{smallmatrix} 
                460 470 480 490 500 510 520 530 540
 ----:----|----:----|----:----|----:----|----:----|----:----|----:----|----:----|
E A T L N R A V Q S N P D F V N R I N S V Q N S W L A T D Y
                 550 560 570 580 590 600 610 620 630
 P E L R Q F T L G D L R R R A G G A K S V F S R P Q L P L I
                                                               660 670
                                                                                                                680
                                                                                                                                          690
                                                                                                                                                                   700
                                           650
 ----:----|----:----|----:----|----:----|-----|----:----|----:|----:|----:|----:|-----|-----|
Q S T I S T E L L Q A A A N L P E D F D W R F P K D G R P S
                                   740 750 760 770 780 790 800 810
  \begin{smallmatrix} P & V & T & P & V & R & D & Q & G & H & C & G & S & C & Y & A & F & A & S & L & A & A & L & E & A & R & I & R & L & R \\ \end{smallmatrix} 

  820
  830
  840
  850
  860
  870
  880

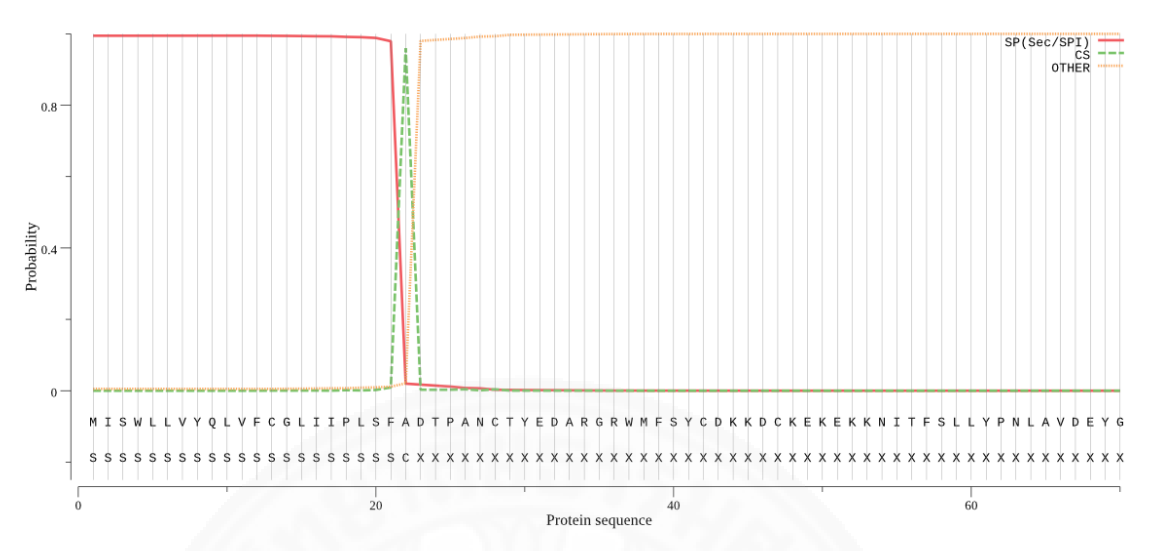
    ---:----|----:|-----|----:|-----|----:|----|----:|----|----:|----|----:|----|----
 \verb|S| N F T H Q P I L S P Q D V V D C G N Y S E G C E G G F P Y \\
                   910 920 930 940 950 960 970 980
 L V G G K Y A E D Y G I P L E S C N N Y T G K E S G I C K T
               1000 1010 1020 1030 1040 1050 1060 1070 1080
 ----:----|----:|----:|----:|----:|----:|----:|----:|----:|----:|----:|----:|----:|----:|----:|----:|----:|----
 \texttt{K} \ \ \texttt{P} \ \ \texttt{N} \ \ \texttt{C} \ \ \texttt{T} \ \ \texttt{R} \ \ \texttt{Y} \ \ \texttt{Y} \ \ \texttt{A} \ \ \texttt{T} \ \ \texttt{N} \ \ \texttt{E} \ \ \texttt{L} \ \ \texttt{L} \ \ \texttt{M} \ \ \texttt{R} \ \ \texttt{L} \ \ \texttt{E} 
                                                                 1110 1120 1130 1140 1150
 ----:----|----:----|----:----|----:----|----:----|----:----|----:----|----:----|----:
1190 1200 1210 1220 1230 1240 1250 1260
        K D E V N R F D P F E L V N H G V V I V G Y G F D K K S N L
                    1270 1280 1290 1300 1310 1320 1330 1340 1350
 ----:----|----:|-----|----:|----|----:|----|----:|----|----:|----|----:|----|----
\tt CCGTACTGGGCTGTCAAGAATAGTTGGGGCCCCACGTGGGGTGAATCAGGATACTTCCGAATTCTGCGCGGAAAGGATGAATGTGCTATTGCGCAGGATGAATGTGCTATTGGGCGGAAAGGATGAATGTGCTATTGGGCGGGAAAGGATGAATGTGCTATTGTGCTATTGTGCTATTGTGCTATTGTGCTATTGTGCTATTGTGCTATTGTGCTATTGTGCTATTGTGCTATTGTGCTATTGTGCTATTGTGCTATTGTGCTATTGTGCTATTGTGCTATTGTGCTATTGTGCTATTGTGCTATTGTGCTATTGTGCTATTGTGCTATTGTGCTATTGTGCTATTGTGCTATTGTGCTATTGTGCTATTGTGCTATTGTGCTATTGTGCTATTGTGCTATTGTGCTATTGTGCTATTGTGCTATTGTGCTATTGTGCTATTGTGCTATTGTGCTATTGTGCTATTGTGCTATTGTGCTATTGTGCTATTGTGCTATTGTGCTATTGTGCTATTGTGCTATTGTGCTATTGTGCTATTGTGCTATTGTGCTATTGTGCTATTGTGCTATTGTGCTATTGTGCTATTGTGCTATTGTGCTATTGTGCTATTGTGCTATTGTGCTATTGTGCTATTGTGCTATTGTGCTATTGTGCTATTGTGCTATTGTGCTATTGTGCTATTGTGCTATTGTGCTATTGTGCTATTGTGCTATTGTGCTATTGTGCTATTGTGCTATTGTGCTATTGTGCTATTGTGTATTGTGTATTGTGTATTGTGTATTGTGTGTATTGTGTGTATTGTGTATTGTGTATTGTGTATTGTGTATTGTGTATTGTGTATTGTGTATTGTGTATTGTGTATTGTGTATTGTGTATTGTGTATTGTGTATTGTGTATTGTGTATTGTGTATTGTGTATTGTGTATTGTGTATTGTGTATTGTGTATTGTGTATTGTGTATTGTGTATTGTGTATTGTGTATTGTGTATTGTGTATTGTGTATTGTGTATTGTGTATTGTGTATTGTGTATTGTGTATTGTGTATTGTGTATTGTGTATTGTGTATTGTGTATTGTGTATTGTGTATTGTGTATTGTGTATTGTGTATTGTGTATTGTGTATTGTGTATTGTGTATTGTGTATTGTGTATTGTGTATTGTGTATTGTGTATTGTGTATTGTGTATTGTGTATTGTGTATTGTGTATTGTGTATTGTGTATTGTGTATTGTGTATTGTGTATTGTGTATTGTGTATTGTGTATTGTGTATTGTGTATTGTGTATTGTGTATTGTGTATTGTGTATTGTGTATTGTGTATTGTGTATTGTGTATTGTGTATTGTGTATTGTGTATTGTGTATTGTGTATTGTGTATTGTGTATTGTGTATTGTGTATTGTGTATTGTGTATTGTGTATTGTGTATTGTGTATTGTGTATTGTGTATTGTGTATTGTGTATTGTGTATTGTGTATTGTGTATTGTGTATTGTGTATTGTGTATTGTGTATTGTGTATTGTGTATTGTGTATTGTGTATTGTGTATTGTGTATTGTGTATTGTGTATTGTGTATTGTGTATTGTGTATTGTGTATTGTGTATTGTGTATTGTGTATTGTGTATTGTGTATTGTGTATTGTGTATTGTGTATTGTGTATTGTGTATTGTGTATTGTGTATTGTGTATTGTGTATTGTGTATTGTGTATTGTGTATTGTGTATTGTGTATTGTGTATTGTGTATTGTGTATTGTGTATTGTGTATTGTGTATTGTGTATTGTGTATTGTGTATTGTGTATTGTGTATTGTGTATTGTGTATTGTGTATTGTGTATTGTGTATTGTGTATTGTGTATTGTGTATTGTGTATTGTGTATTGTGTATTGTGTATTGTGTATTGTGTATTGTGTATTGTGTATTGTGTATTGTGTATTGTGTATTGTGTATTGTGTATTGTGTATTGTGTATTGTGTATTGTGTATTGTGTATTGTGTATTGTATTGTGTATTGTGTATTGTGTATTGTGTATTGTGTATTGTGTATTGTGTA
 PYWAVKNSWGPTWGESGYFRILRGKDECAI
                                                                 1380
                    1360
                                          1370
 ----:----|----:----|----:
GAAAGCTTGGCAACTTCCATGGATCCAGTTCTCTAA
E S L A T S M D P V L *
```

(Please see figure legend on overleaf)

**Figure 5.71** Nucleotide and deduced amino acid sequences of *Fischoederius Mse*I A cathepsin C-like cysteine proteinase (TBIU021593) using SHOWSEQ in EMBOSS. The predicted signal peptide is indicated by the dot-underlined sequence. Conserved motifs are indicated by underlined sequences; eukaryotic thiol (cysteine) proteases cysteine active site (QGHCGSCYAFAS), eukaryotic thiol (cysteine) proteases histidine active site (VNHGVVIVGYG).







Cleavage site between positions: 22 and 23 (SFA-DT)

Probability: 0.9595 Protein type: Likelihood

Signal Peptide (Sec/SPI): 0.9947 Other: 0.0053

**Figure 5.72** Signal peptide prediction of *Fischoederius Mse*I A cathepsin C-like cysteine proteinase (TBIU021593) using SignalP.

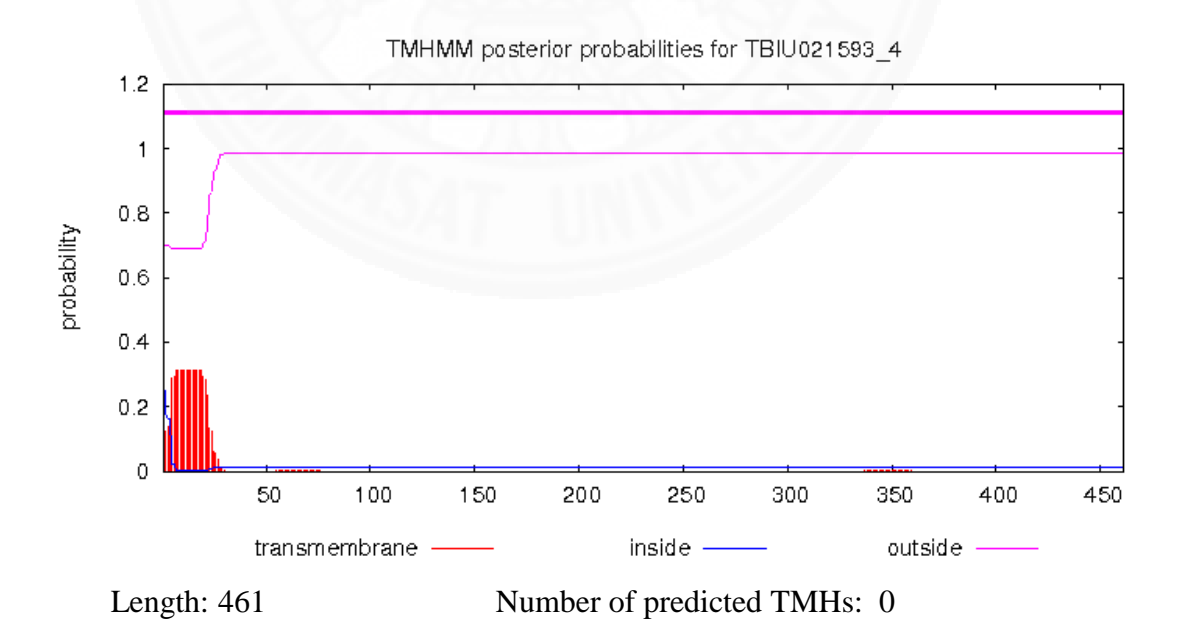


**Figure 5.73** Transmembrane region prediction of *Fischoederius Mse*I A cathepsin C-like cysteine proteinase (TBIU021593) using TMHMM.

### 5.5.7.4 Fatty acid-binding protein

Gene annotation analysis of transcriptome sequence no. TBIU012177 revealed that this sequence encoded a fatty acid-binding protein. The deduced sequence of 133 amino acids was found encoded in an ORF in F1 at base positions 66–467 (**Figure 5.74**). An amination motif was predicted at residues 77–80 (DGKK). No signal peptide and transmembrane regions were predicted. The protein had a molecular weight of 14.96 kDa and an isoelectric point of 7.5. NCBI-BLASTP detected related sequences at low identity values compared to the above described proteases. *C. sinensis* fatty acid-binding protein (GenBank: Q8MUC1) with 28.80% identity, a predicted fatty acid-binding protein from *Poecilia reticulate* (GenBank: XP\_008409747) with 35.11% identity, and *Poecilia formosa* (GenBank: XP\_007551827) with 34.35% identity (**Table 5.15**).

### 5.5.7.5 Thioredoxin

Transcriptome no. Comp175\_seq0 was annotated as thioredoxin at base positions 53–367 with the ORF in F1 (**Figure 5.75**). Signal peptide and transmembrane regions were not predicted. The protein contained 104 amino acids, had a molecular weight of 12.15 kDa, and an isoelectric point of 6.7. Detected motifs included an amidation site at residues 81–84 (DGKR) and a thioredoxin family active site at residues 23–41 (VLDFYAQWCPPCRMLAPKF). NCBI-BLASTP detected related proteins in other trematodes, *Paragonimus westermani* thioredoxin (GenBank: KAA3675358), *F. gigantica* thioredoxin (GenBank: AKU75588), *F. hepatica* thioredoxin and Chain A thioredoxin (GenBank: AAF14217 and 2VIM\_A), and *C. sinensis* thioredoxin-2 (GenBank: RJW73364) with 43.00, 43.27, 43.27, 43.27, and 42.31% identity, respectively (**Table 5.16**).

### **5.5.7.6** Calcium-binding protein

Transcriptome sequence no. TBIU007768 encoded a tegumental calcium-binding protein at base positions 130–669. The deduced sequence of 189 amino acids (**Figure 5.76**) had a molecular weight of 22.00 kDa and an isoelectric point of 5.4. Signal peptide and transmembrane regions were not predicted. An EF-hand calcium-binding domain was detected at residues 54–66 (DTDKDGKVSLTEF). NCBI-BLASTP detected several highly conserved sequences in other trematodes with identity values of 66.67, 66.49, 66.14, 66.14, and 65.95% for

*F. buski* tegumental calcium-binding EF-hand protein 4 (GenBank: KAA0189126), *F. gigantica* tegumental calcium-binding EF-hand protein 3–4 (GenBank: TPP63277, TPP63278), *F. hepatica* tegumental calcium-binding EF-hand protein 4 (GenBank: THD25974), and *F. hepatica* CaBP1 (GenBank: AML33332), respectively (**Table 5.17**).



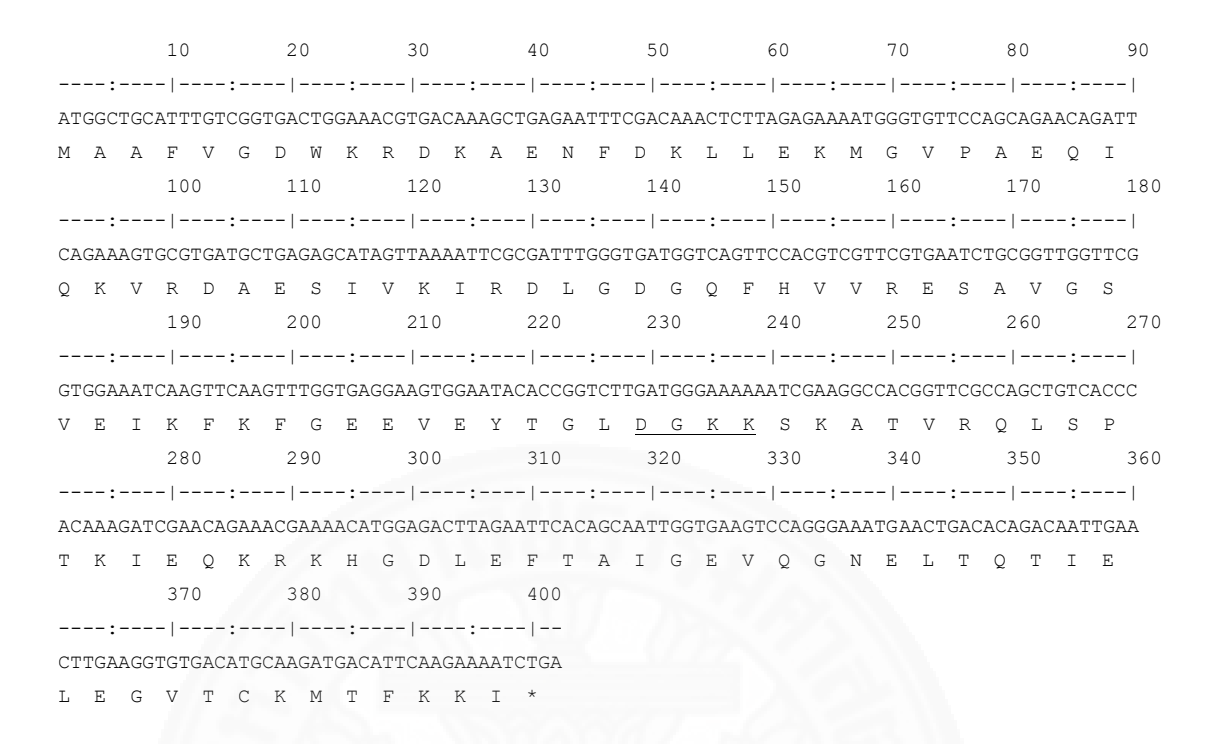


**Figure 5.74** Nucleotide and deduced amino acid sequences of *Fischoederius Mse*I A fatty acid-binding protein (TBIU012177) using SHOWSEQ in EMBOSS. A putative amination motif (DGKK) is indicated by the underlined sequence.

**Table 5.15** Sequence identity values of *Fischoederius Mse*I A fatty acid-binding protein (TBIU012177) with other fatty acid-binding protein sequences.

Description	A	Query	%	%	El
Description	Accession	Cover	Identity	Positive	E-value
Fatty acid-binding protein	Q8MUC1	93%	28.80%	55.20%	8e-13
[Clonorchis sinensis]					
PREDICTED: Fatty acid-binding protein,	XP_008409747	97%	35.11%	49.61%	2e-12
intestinal [Poecilia reticulata]					
Cellular retinoic acid-binding protein 1	XP_004069529	97%	37.50%	54.41%	4e-12
[Oryzias latipes]					
PREDICTED: Fatty acid-binding protein,	XP_007551827	97%	34.35%	48.09 %	5e-12
intestinal [Poecilia formosa]					
Fatty acid-binding protein, intestinal	XP_012705247	97%	34.35%	51.15 %	5e-12
[Fundulus heteroclitus]					

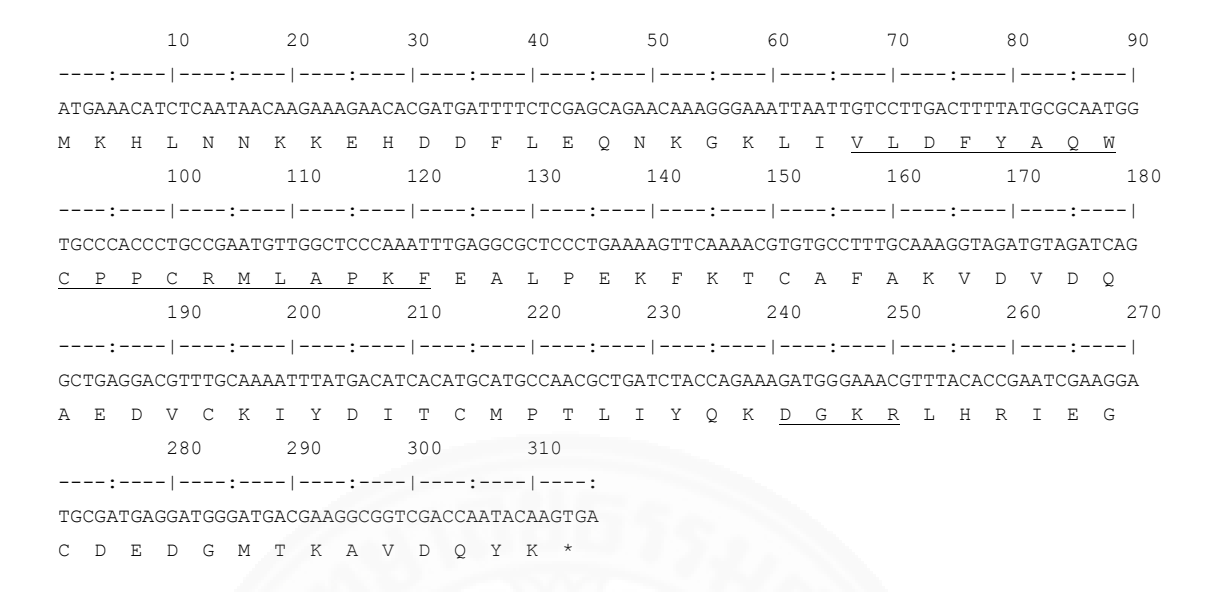


**Figure 5.75** Nucleotide and deduced amino acid sequences of *Fischoederius Mse*I A thioredoxin (Comp175\_seq0) using SHOWSEQ in EMBOSS. Amidation motif (DGKR) and thioredoxin family active site (VLDFYAQWCPPCRMLAPKF) are indicated by underlined sequences.

**Table 5.16** Sequence identity values of *Fischoederius Mse*I A thioredoxin (Comp175\_seq0) with other thioredoxin sequences.

D	A	Query	%	%	E1	
Description	Accession	Cover	Identity	Positive	E-value	
Thioredoxin 1 [Paragonimus westermani]	KAA3675358	95%	43.00%	69.00%	6e-28	
Thioredoxin [Fasciola gigantica]	AKU75588	99%	43.27%	65.38%	3e-27	
Thioredoxin [Fasciola hepatica]	AAF14217	99%	43.27%	64.42%	3e-27	
Chain A, Thioredoxin [Fasciola hepatica]	2VIM_A	99%	43.27%	64.42%	5e-27	
Thioredoxin-2 [Clonorchis sinensis]	RJW73364	99%	42.31%	64.42 %	2e-26	

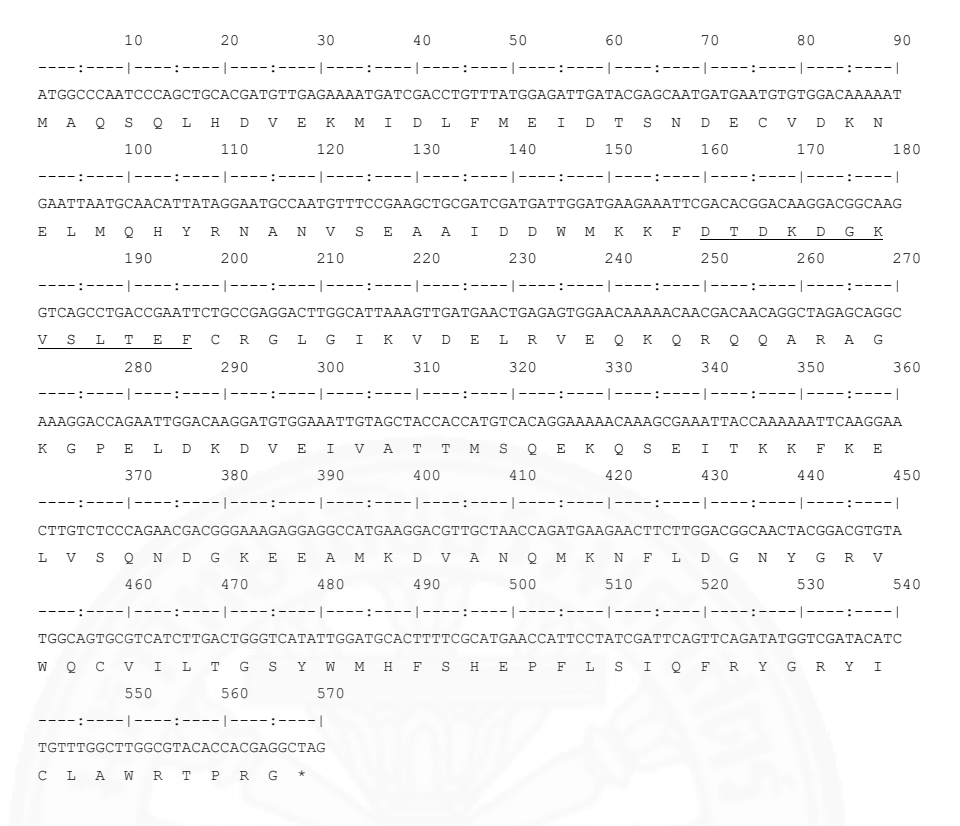


**Figure 5.76** Nucleotide and deduced amino acid sequences of *Fischoederius Mse*I A tegumental calcium-binding protein (TBIU007768) by SHOWSEQ in EMBOSS. The EFhand calcium-binding domain (DTDKDGKVSLTEF) is indicated by the underlined sequence.

**Table 5.17** Sequence identity values of *Fischoederius Mse*I A tegumental calciumbinding protein (TBIU007768) with other calciumbinding protein sequences.

Description	A	Query	%	%	E volvo	
Description	Accession	Cover	Identity	Positive	E-value	
Tegumental calcium-binding EF-hand	KAA0189126	99%	66.67%	82.54%	4e-95	
protein 4 [Fasciolopsis buski]						
Tegumental calcium-binding EF-hand	TPP63277	97%	66.49%	83.78%	7e-94	
protein 3 [Fasciola gigantica]						
Tegumental calcium-binding EF-hand	THD25974	99%	66.14%	82.01%	8e-94	
protein 4 [Fasciola hepatica]						
Tegumental calcium-binding EF-hand	TPP63278	99%	66.14%	82.01%	2e-93	
protein 4 [Fasciola gigantica]						
CaBP1 [Fasciola hepatica]	AML33332	97%	65.95%	83.24 %	3e-93	

# 5.6 Efficacy of polyclonal mouse *Fischoederius* spp. anti-ES antibody

### 5.6.1 Fischoederius spp. excretion/secretion (ES) products

Fischoederius spp. excretion/secretion products were collected at 37°C, 4 hours with 10 mM PBS pH 7.2 buffers. The protein concentrations of each conditions were measured with Bradford assay as described in **Section 4.6.1.2**. The concentration of ES products was 2.79 μg/μL. The protein pattern results showed various size of protein bands range from 6 to 200 kDa with no degradation. The predominated protein band were observed at molecular weight approximately 6, 15, 17, 18, 21, 26, 28, 31, 35, 45, 54 kDa. The 6 and 15 kDa had highly expression in *Fischoederius* spp. ES products. The gel image of these ES products had shown in **Figure 5.74**.

## 5.6.2 Fischoederius spp. crude worm (CW) extracts

Fischoederius spp. crude worm extracts were prepared and then revealed by a 12.5% SDS-PAGE as described in **Section 4.6.1.1**. The protein pattern results showed various size of protein bands range from 6 to 200 kDa with no degradation. The predominated protein band were observed at molecular weight approximately 6, 15, 17, 18, 26, 28, 38, 45, 54, 66, 110, 200 kDa. The gel image of these ES products had shown in **Figure 5.76**.

# 5.6.3 Production of polyclonal mouse *Fischoederius* spp. anti-ES antibody

Antibody against *Fischoederius* spp. excretion/secretion (ES) product was produced in 6–8 weeks-old female BALB/c mice. Pre-immune sera were collected from the two mice before immunization, and then the priming, first-boost and second boost sera were collected after immunization in a 3-weeks interval as described in **Section 4.6.2.1**. The curve of anti-ES title and their specificity were determined with indirect ELISA were established described in **Section 4.6.2.2**. The results showed the immunized sera were found to be sensibly increased in both mice with a correlational response as shown in **Figure 5.73**. The first-boost and second boost sera had slightly similar level in Mouse no. 1. Meanwhile, the second boost serum had been gradually increased in Mouse no. 2. These polyclonal mouse anti-ES sera were used in Western blot analysis. Animal Ethics was performed under Thammasat University Animal Care and Use Committee with the protocol Number: 012/2560.

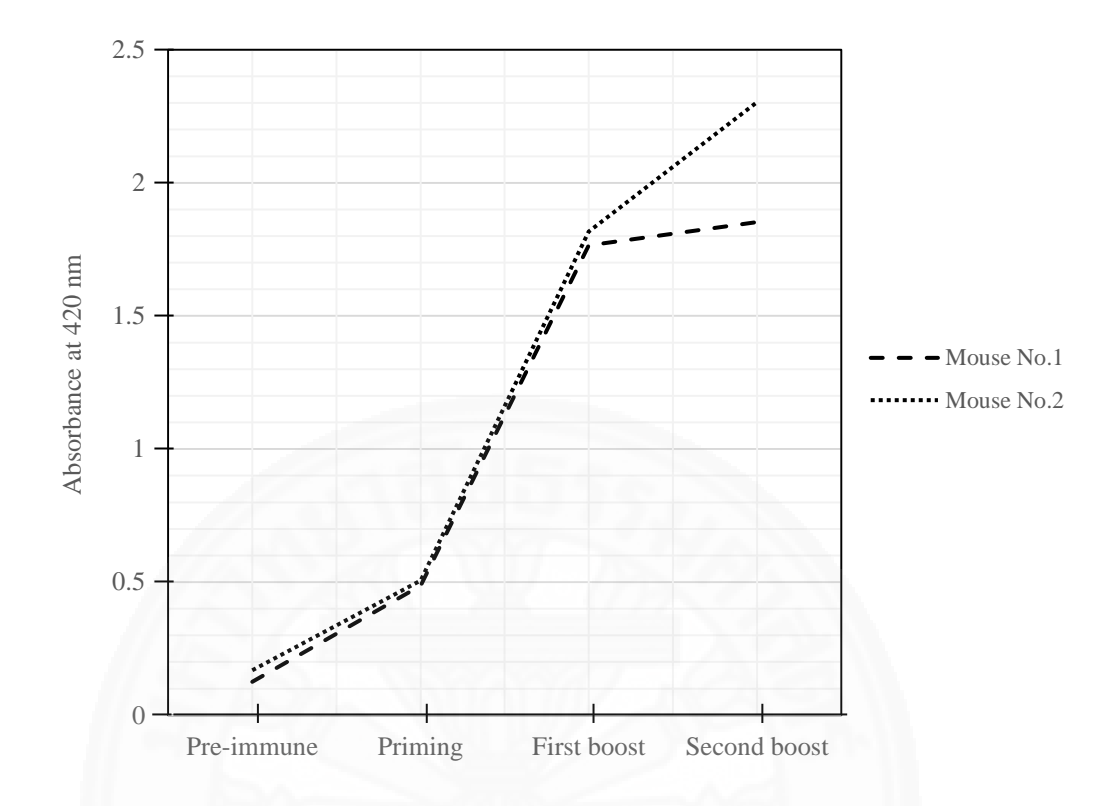


**Figure 5.77** Line graph of polyclonal antibody level of *Fischoederius* spp. excretion/secretion (ES) product immunized Balb/c mice determined by indirect ELISA (Dilution 1:25,600).

# 5.6.4 Western blot analysis of polyclonal mouse *Fischoederius* spp. anti-ES antibody against ES product

Fischoederius spp. excretion/secretion (ES) products were prepared and resolved by 12.5% SDS-PAGE as described in **Section 4.6.1.5**. Then, the proteins were semi-dry transferred onto a nitrocellulose membrane for immunoblot analysis. Mouse anti-ES sera (the second boost) and pre-immunized sera were used to detect the effective antigens in 10 μg of *Fischoederius* spp. and *F. gigantica* ES products at dilution 1:3000 as described in **Section 4.6.2.3**. The antibodies reacted with proteins in the *Fischoederius* spp. ES product ranging from 6 to 200 kDa molecular weight (**Figure 5.75**). Antigenic proteins with molecular weights of approximately 15, 18, 26, 31, 35, 54, 97, and 120 kDa were strongly detected by both mice sera. There were some differences in the reactivity of the two mouse antisera as can be seen in **Figure 5.75**. The mouse *Fischoederius* spp. anti-ES antisera showed almost no cross reactivity with *F. gigantica* ES product. Only an antigen of approximately 17 kDa molecular weight was detected. No reactivity was observed with pre-immunized sera.

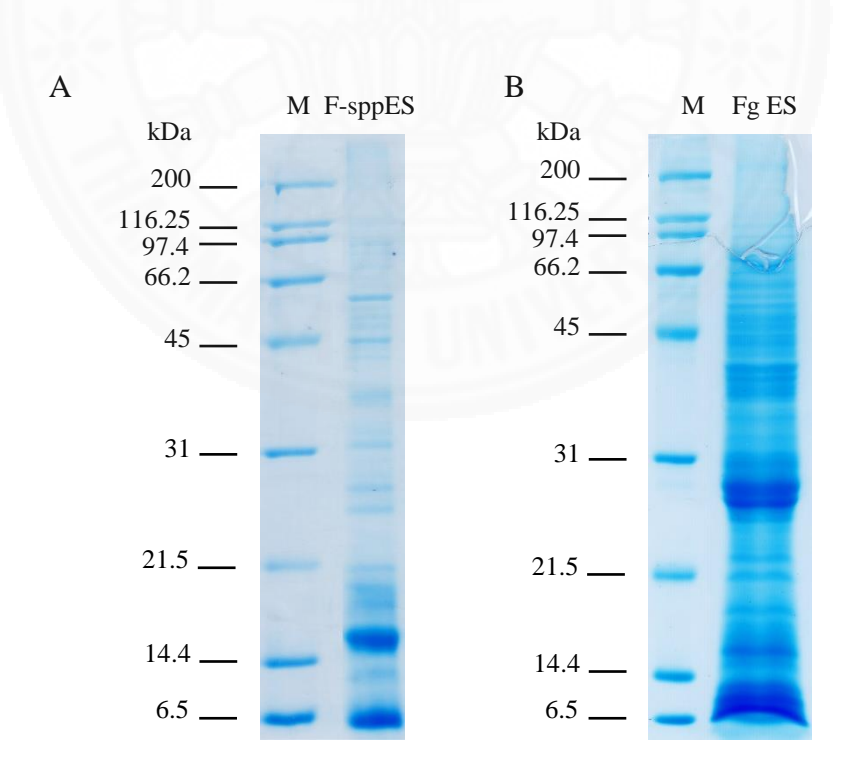


**Figure 5.78** SDS-PAGE (12.5% acrylamide gel) of parasite excretion/secretion (ES) products. (**A**) *Fischoederius* spp. ES products; (**B**) *F. gigantica* ES products; lane M: Broad Range Molecular Weight Standards (Bio-Rad, Hercules, CA, USA).

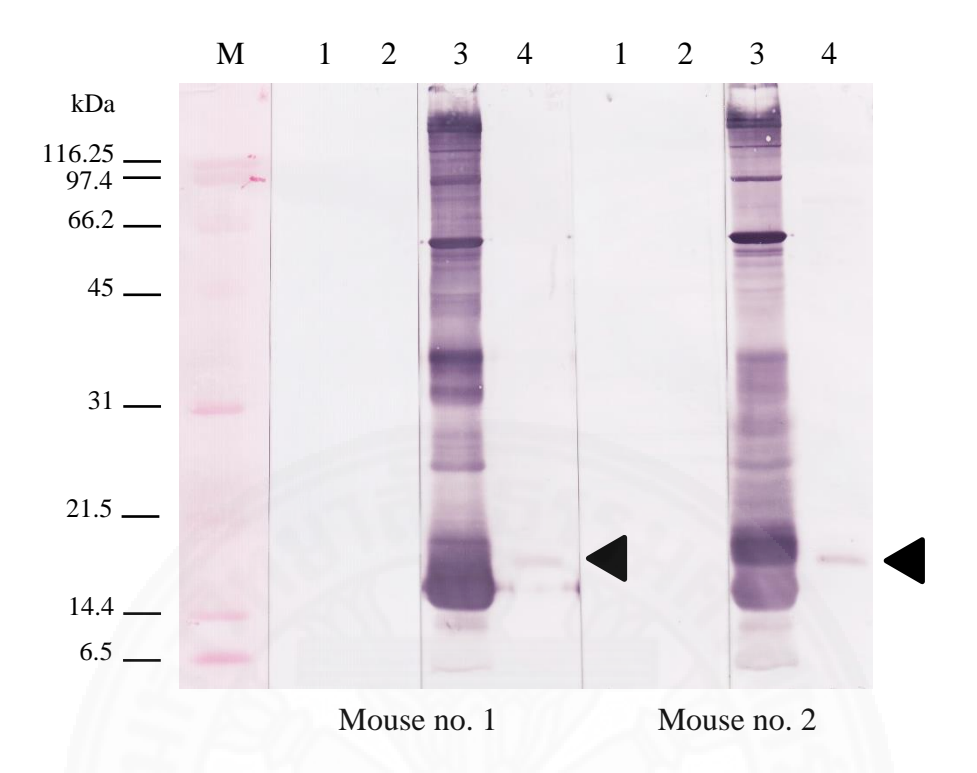


**Figure 5.79** Western blot analysis of *Fischoederius* spp. anti-ES and ES product. Parasite antigens (10 μg each) were transferred onto membrane, and then probed with *Fischoederius* spp. anti-ES at antibody dilution 1:3,000; lane 1: *Fischoederius* spp. ES products probed with pre-immune serum; lane 2: *F. gigantica* ES products probed with immunized serum; lane 3: *Fischoederius* spp. ES products probed with immunized serum; lane 4: *F. gigantica* ES products probed with immunized serum; lane M: Broad Range Molecular Weight Standards (Bio-Rad, Hercules, CA, USA). The cross-reaction between *Fischoederius* spp. anti-ES antiserum and a 17 kDa *F. gigantica* ES antigen is indicated by an arrowhead.

# 5.6.5 Cross reactivity of polyclonal mouse *Fischoederius* spp. anti-ES antibody against crude worm extracts of other trematodes

The mouse *Fischoederius* spp. anti-ES antiserum was analyzed for cross-reactivity with crude worm (CW) extracts of other trematodes including *Paramphistomum* spp. and *F. gigantica*. The crude worm extracts of *Fischoederius* spp. were prepared as described in **Section 4.6.1.1**, and then used as positive control. Western blot analysis of the mouse anti-ES antiserum was performed at 1:3,000 dilution detecting 10 µg of each parasite antigens as described in **Section 4.6.2.3**. In support of taxonomic classification, the antiserum showed higher cross-reactivity to the crude worm extract of *Paramphistomum* spp. than to *F. gigantica* crude worm extract. Detected antigens in the crude worm extract of *Paramphistomum* spp. had molecular weights of approximately 26, 30, 31, 40, 52, 54, 97, and 120 kDa. A single 17 kDa *F. gigantica* antigen was detected. No cross-reactivity was observed with pre-immunized sera. The results are shown in **Figure 5.77**.

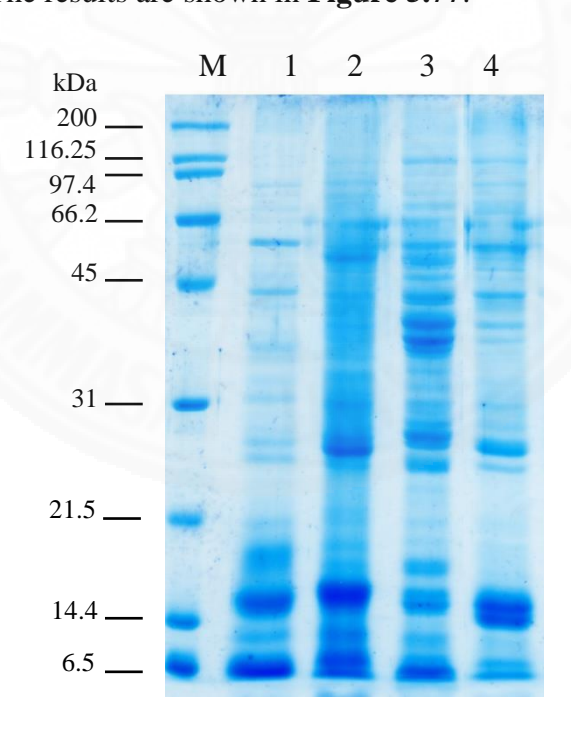


**Figure 5.80** SDS-PAGE (12.5% acrylamide gel) of parasite antigens (10 μg each); lane 1 *Fischoederius* spp. ES products; lane 2: *Paramphistomum* spp. CW extracts; lane 3: *F. gigantica* CW extracts; lane 4: *Fischoederius* spp. CW extracts; lane M: Broad Range Molecular Weight Standards (Bio-Rad, Hercules, CA, USA).

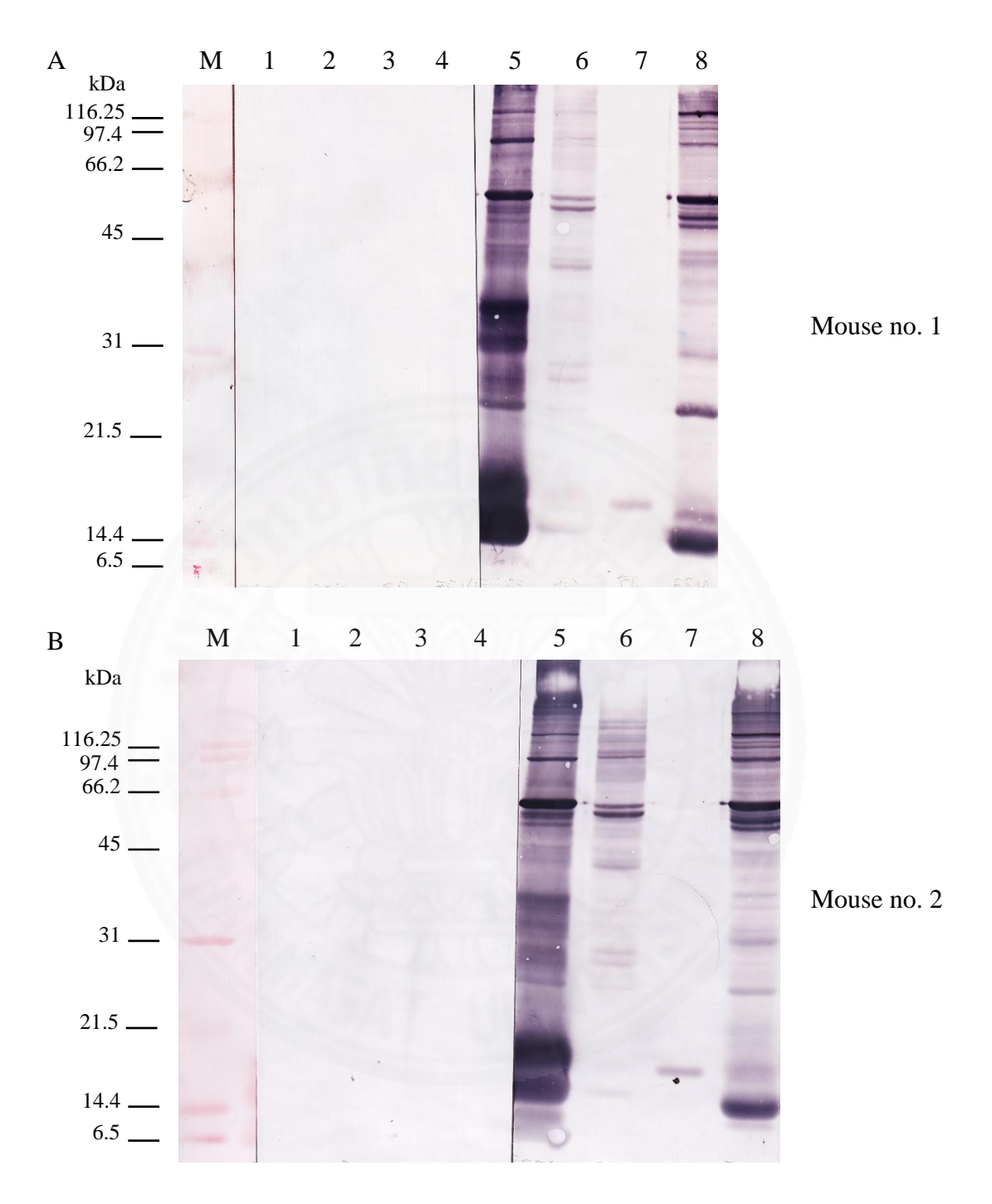


**Figure 5.81** Cross-reactivity analysis of *Fischoederius* spp. anti-ES antiserum against parasite antigens (10 μg each) at dilution 1:3,000 from (**A**) Mouse no. 1 and (**B**) Mouse no. 2; lane 1 and 5: *Fischoederius* spp. ES products; lane 2 and 6: *Paramphistomum* spp. CW extracts lane 3 and 7: *F. gigantica* CW extracts; lane 4 and 8: *Fischoederius* spp. CW extracts; lane 1–4: Probed with mouse pre-immune sera; lane 5–6: Probed with mouse immunized sera; lane M: Broad Range Molecular Weight Standards (Bio-Rad, Hercules, CA, USA).

# CHAPTER 6 DISCUSSION

## 6.1 Morphology and histology of Fischoederius spp.

Fischoederius spp. were characterized in the present study. Specimens were collected from rumen of slaughtered cattle at slaughterhouses in Pathumthani Province, Thailand during the years 2014–2019. Due to data sharing restrictions of the slaughterhouses, the origin of the infected cattle originated in Thailand was not specified. Gross fluke morphology was observed from unstained specimens and Semichon's carmine-stained whole mounts under a stereo microscope. Morphological details were observed from hematoxylin and eosin-stained serial tissue cross-sections. The flukes had a reddish colored body with a sword-like shape, were sometimes extremely elongated and could reach a body length of more than 2 cm (Figure 5.2). Images of unstained flukes showed often few morphological details due to strong pigmentation within the area of the ventral poach (Figures 5.9–5.11). Carmine-stained whole mounts of *Fischoederius* spp. showed the ventral poach opening anteriorly ventral to the pharynx and the poach extending posteriorly to the region of ovary and testes. The collected flukes were classified as F. elongatus by morphology using the key characteristics that distinguishes this species from other gastrointestinal flukes including, (1) cecal bifurcation posterior to esophagus with the branches extending to the middle length of the body in the dorsal field, and (2) overlapped lobed testes with median and vertical orientation. The morphology of the collected Fischoederius spp, Thailand was found following the literature description.<sup>6-8</sup>

However, the molecular sequence data obtained from *Fischoederius* spp. in this study suggested that the specimens represent a complex of morphologically indistinguishable (cryptic) species. Cryptic species were also reported in other trematodes including *Diplodus sargus*, *D. vulgaris* and *D. annularis*, <sup>111</sup> *Hurleytrematoides loi* and *H. sasali*, <sup>112</sup> and *Stellantchasmus falcatus*. <sup>113</sup> Stiles and Goldberger (1910) described three new species of *Fischoederius* including *F. fischoederi*, *F. siamensis*, and *F. ceylonensis*<sup>114</sup> which were later synonymized under

*F. elongatus* by Maplestone (1923).<sup>115</sup> *F. fischoederi* was described as the fluke with 6.4 mm body length containing ceca slightly longer than *F. elongatus* and end in the fourth zone of body and ovary and shell gland lay between the two testes. *F. ceylonensis* and *F. siamensis* were separately classified by the absence of prominent bulging around the genital pore. *F. siamensis* was described as a fluke with 6.6–15.5 mm body length with overlapping testes and ventral pouch ending before the posterior testes. *F. ceylonensis* was described as a fluke of 6–7 mm body length with overlapping testes and the end of the ventral pouch overlapping with the posterior testis.<sup>114</sup> Maplestone (1923) concluded upon reexamination that their morphological differences were not significant and that only a limited number of sample specimens was available.<sup>115</sup> The present study supports that (1) the length of ceca, (2) the length of ventral pouch, and (3) the position of the testes are important in morphological classification of the genus *Fischoederius*. However, based on the collected molecular sequence data morphological data was found to be insufficient to clarify the species of the fluke. This suggests that taxonomic classification in this genus requires molecular data.

Images of whole Fischoederius spp. showed two different testis sizes among the samples, either a pair of large or small testes (Figure 5.3). The histological analysis suggested that flukes with small testes were immature (Figure 5.4) and carried not fully developed reproductive organs. The terminal genitalium, the outlet for eggs located in the anterior ventral poach close to the cecal bifurcation, showed genital pore, genital papilla, and genital fold. On the other hand, the reproductive organs in the posterior field of the flukes were hard to identify in the sections. The immature testes and ovary were represented by groups of strong basophilic cells. Accordingly, eggs were not observed in the uterus of small testes flukes, neither in whole mounts nor in tissue sections. Only sparse putative vitelline cell clusters were present. However, flukes with small testes could also have a body length >2 cm. Tandon (1973) studied crowding effects in F. elongatus and Gastrothylax crumenifer under natural conditions in the host rumen. High parasite load in the host resulted in decreased size and poor development of reproductive organs. A fluke might be of large size with poorly developed reproductive organs. On the other hand, a fluke might be of small size with fully developed reproductive organs. Two morphology appearances of Fischoederius spp. were listed in this report. The immature flukes had a large body size (37.0×5.8 mm) in less intensive condition (about 40 flukes per host) whereas mature stage flukes of smaller size  $(13.0-16.0\times3.4-4.0 \text{ mm})$  were observed in highly intensive condition (about 2,500 flukes per host). The crowding effect might be a consequence of limited living space and nutrients. The high intensity infection caused a high competition that encouraged the development of the reproductive organs. The immature flukes also fully developed if they were kept in good conditions for some time.  $^{116}$ 

Serial tissue cross-sections from the anterior to posterior end of the fluke were used for histological characterization of Fischoederius spp. in the present study (Figures 5.4–5.5). Fischoederius spp. showed a thick acidophilic tegument with nonciliated papilla. The thick tegument should support fluke survival in the extreme conditions of the host rumen. Spines were absent on the tegument, thus the fluke must be able to move without them. The highly developed anterior sucker and pharynx were similar to other trematodes such as Fasciola hepatica<sup>117</sup> and Fasciola gigantica.<sup>118</sup> The cecal bifurcation ending in the middle part of the body was found in nearby species including F. compressus and F. skrjabibi. The large ventral pouch contained a strong reddish-brown pigmentation of hemoglobin. 119, 120 The function of the ventral pouch has not been investigated. It might act as a liquid reservoir that allows undisturbed digestion and filtration of nutrients. The genital pore is opening inside the pouch towards its anterior end and sometimes trapped eggs were observed in the pouch. The reproductive organs were found located near the posterior sucker in the posterior field similar to other rumen flukes. The posterior sucker was distinctively larger than the anterior sucker. The posterior sucker contained thick and strong muscle fibers and enables the fluke to attach itself to the villi of the host rumen comparable to other amphistomes such as F. cobboldi, 121 Paramphistomum epiclitum, 32 and P. gracile. 122

### 6.2 Molecular identification of *Fischoederius* spp. ribosomal ITS2 region

Due to the limited set of sequences of *Fischoederius* spp. in the GenBank database, the available ribosomal ITS2 sequence was selected for molecular identification of the fluke according to the study of Ghatani *et al.*, 2011.<sup>43</sup> In the present study, *Fischoederius* spp. ITS2 amplicon was found to be identical with the previously reported ITS2 sequence and thus supported classification of the collected rumen fluke

specimen as *F. elongatus*. However, the ITS2 sequence alone might not be sufficient for classification as it is highly conserved and BLAST analysis revealed 99% identity to the closely related species *G. crumenifer*. Ribosomal RNA genes are often applied as molecular marker in molecular diagnosis due to high conservation. ITS2 is located between 5.8S rRNA and 28S rRNA genes and has a function in rRNA subunit formation. ITS2 region has fewer repeat elements than ITS1 region. ITS4 However, the length of the repeat sequence is highly variable within each family and it is highly conserved within species. This sequence had only 2.8% sequence variation in the genus *Fasciola*, while it had 13.2% sequence variation between the genera *Fasciola* and *Fascioloides*. ITS2 sequence analysis of Gastrothylacid species including *F. elongatus*, *F. cobboldi*, *G. crumenifer*, *Carmyerius spatiosus* and *Velasquezotrema tripurensis* showed 1.4 to 4.9% interspecies variations. The variation data showed that this sequence is effective for phylogenetic analysis above the genus taxon. Italiana in the sufficient to the sufficien

# 6.3 Molecular characterization of Fischoederius spp. mtCOX1

Due to the high intragenic conservation of the ribosomal ITS2 sequence the mtCOX1 gene was selected as additional molecular marker in the present study. The mtCOX1 gene had shown higher interspecies variation than the ITS2 region and low intraspecies variation. 45, 127, 128 The present study amplified a 1,536 bp fragment of mtCOX1 lacking the two 3'-terminal codons due to low sequence conservation. PCR-RFLP was performed to discriminate the mtCOX1 sequences among the collected specimens by restriction patterns. *MseI* with the recognition site T^TAA was selected due to the high A+T content of published *F. elongatus* mtCOX1, 61 suggesting a sufficiently high number of *MseI* sites in this sequence. The 1,536 bp *Fischoederius* spp. mtCOX1 PCR products amplified from DNA of 48 specimens collected in the years 2014–2019 showed nine different restriction patterns (A–I). Pattern E was the most frequent and pattern I the least frequent pattern.

Based on sequence conservation, the nine different restriction patterns could be clustered into five distinct groups, *i.e.* pattern A, [BEG], [CFH], D, and I. *Fischoederius* spp. pattern [BEG] had intraspecies variation of 0.8–1.3%. *Fischoederius* spp. pattern [CFH] had intraspecies variation of 0.7–1.0%. The

interspecies variation between each group was 4.2–9.6%, and 5.7–8.3% among published *Fischoederius* sequences. The intergenus variation among Gastrothylacid species was 6.9–11.7%. The intraspecies and interspecies/ intergenus variation in this study was similar to the previous study by Ghatani *et al.*, 2014 at 0.6–9.7% and 5.6–11.9%, respectively. This intraspecies variation of mtCOX1 was still close to the value from the report in *C. sinensis* at 0–1.58%. In a study of sequence divergence among mtCOX1 and ITS1 by Vilas *et al.*, 2005 it was reported that the mtCOX1 gene had a higher rate of nucleotide substitutions than the ITS1 region in Platyhelminthes. This will cause the observed high value of intraspecies and interspecies variation of mtCOX1. Thus, the high mutation rate of mtCOX1 is advantageous in taxonomic phylogenies and biological relevance studies.

Phylogenetic analysis of *Fischoederius* mtCOX1 fragments with sequence lengths of 364, 1,521, and 1,536 bp (**Figure 5.15**) revealed that the mtCOX1 sequences obtained in this study were closely related to the sequences of published F. elongatus and F. cobboldi mtCOX1 from China and India. The Fischoederius mtCOX1 sequences from China and India were reported without morphological data to support classification. Recently, Anucherngchaia et al., 2020 reported phylogenetic trees based on trematode mtCOX1 sequences that revealed clearly separated clades among Fischoederius spp. from Thailand and F. elongatus, F. cobboldi from China. 19 Interestingly, this report supported that mtCOX1 might be a useful molecular marker for discriminating Paramphistomoidea and Fasciolidae. However, the present study demonstrated that Fischoederius mtCOX1 sequences cannot be used to identify the exact species because there is at present no confirmed link between molecular data and morphological data. Furthermore, mtCOX1 data and morphological data collected in the present study strongly suggested that there are several species in the genus Fischoederius resembling the morphology of F. elongatus as described in classical literature.6,8

### 6.4 Mitochondrial genome of Fischoederius spp.

Following the mtCOX1 gene analysis, the complete mitochondrial genome of *Fischoederius Mse*I pattern A from Thailand was investigated in this study. An

incomplete mitochondrial genome sequence was obtained in a whole transcriptome sequencing project. Sequence information in the region between the *nad2* and *nad1* genes was missing. DNA of the missing region was amplified by PCR with primers designed from the known sequence and used to complete the mitochondrial genome. The mitochondrial genome contains 37 genes (12 protein-encoding genes, 23 tRNAs, 2 rRNAs) and two non-coding regions and has a size of 14,780 bp (**Figure 5.17**). This mtDNA is larger than the previously published sequences in database including *F. elongatus* Tianmen isolate (14,120 bp)<sup>61</sup> and *F. elongatus* Shanghai isolate (14,228 bp)<sup>62</sup> due to an additional region between *nad2* and *nad1*. This mtDNA is also larger than other amphistome mtDNA such as from *F. cobboldi* (14,256 bp), *Explanatum explanatum* (13,968 bp), *Paramphistomum cervi* (14,014 bp),<sup>130</sup> *Calicophoron microbothrioides* (14,028 bp), and *Orthocoelium streptocoelium* (13,800 bp), but smaller than *G. crumenifer* (14,801 bp).<sup>131</sup> The overall A+T content of *Fischoederius Mse*I pattern A mtDNA was found to be 63.8% which is similar to the previously published sequences.<sup>61,62</sup>

All 37 genes of this mtDNA are transcribed from the same strand similar to other trematodes. The order of genes is the same as in other flatworm mtDNA that contains 36 genes and lacks *atp*8<sup>132-134</sup> with the exception of an additional tRNA-Asp located between tRNA-Val and tRNA-Ala. A duplicated tRNA was reported in the mtDNA of *Reduvius tenebrosus*, an assassin bug. It contained an additional tRNA-Ile which was explained by the tandem duplication/random loss (TDRL) model that seems to be common in insects. <sup>135</sup> In the present case the duplication of tRNA-Asp is likely due to recombination events caused by nearby located inverted repeats (see next section). The two tRNA-Asp are predicted to form a secondary structure with conserved stem loops and GUC anticodon sequence which suggests that both tRNAs are functional. Aspartate promotes stability of protein structure and has been found involved in protein active or binding sites. <sup>136</sup>

In respect to conservation of the twelve protein-encoding genes among Gastrothylacid species, the highest conserved genes were *atp*6, *nad*1, and *cox*1 in intraspecies divergences and *cytb* in interspecies divergences, while the least conserved genes were *nad*2 and *nad*3. The rRNA genes and tRNA genes were the most conserved with other species.<sup>137</sup> The two non-coding regions which are commonly found in

trematode mtDNA are A+T rich similar to other amphistomes such as *F. cobboldi*, *G. crumenifer*, <sup>131</sup> and *P. cervi*. <sup>130</sup> These regions are composed of polymorphic minisatellite and homopolymer sequences with still unclear function. <sup>132, 138</sup>

Phylogenetic analysis of the concatenated conceptually translated amino acid sequences of the twelve protein-coding genes of *Fischoederius* spp. mitochondrial genome *MseI* pattern A among the trematoda revealed the closest genetic relationship to *Fischoederius* spp. followed by members in the families Gastrothylacidae and Paramphistomidae and then families Fasciolidae and Opisthorchiidae (**Figure 5.44**). The mitochondrial genome has been shown to be highly suitable for phylogenetic analysis due to its high rate of evolution compared with the nuclear genome. Many mtDNA features were used for molecular systematics in Platyhelminthes. Moreover, the mitochondrial genome provides potential molecular markers in genetic diversity and taxonomic zoology. <sup>127, 128, 132, 139</sup>

# 6.5 Inverted repeat elements in Fischoederius spp. mitochondrial genome

Fischoederius spp. mitochondrial genome MseI pattern A is about 550–660 bp larger than the previously published Fischoederius mitochondrial genomes due to the presence of an extra region between nad2 and nad1. Upon further investigation, additional sequences in this region were also found in the mitochondrial genomes of Fischoederius MseI pattern B, C, D, E. Sequencing difficulties in this region suggested structural abnormalities. After several attempts to overcome this problem by using modified sequencing conditions and the use of an additional sequencing service provider inverted repeats in this region were found to be the cause for the problem. In Fischoederius spp. mitochondrial genome MseI pattern A, the two detected inverted repeat units possibly form ~50 bp hairpin-like structures that block progress of DNA synthesis in the sequencing reactions and lead to premature stop of synthesis. Two hairpin-like elements were found in Fischoederius MseI pattern A and D while only one inverted repeat unit was found in Fischoederius MseI pattern I. In Fischoederius MseI pattern [BE], C the full sequence could not be obtained but incomplete data suggests the presence of more than one inverted repeat unit. Further experiments are needed to obtain the complete sequence in these cases if possible, at all. Interestingly,

the additional tRNA-Asp in *Fischoederius Mse*I pattern A was located between the two inverted repeat elements (**Figures 5.48–5.49**) suggesting that recombination involving the repeat elements led to duplication of this tRNA. Analysis of the published mitochondrial genomes of *F. elongatus* and *F. cobboldi* from China showed that both carried a single repeat unit in this region. This is not indicated in the feature list of the GenBank entries (GenBank: KM\_397348 and MN537973) of these genomes and also not mentioned in the publication. <sup>61, 62</sup> Inverted repeat elements were frequently found in insect mitochondrial genomes. <sup>140</sup> Direct and inverted repeats in the A+T rich regions were reported in mitochondrial genomes of *Caenorhabditis elegans* and *Ascaris suum.* <sup>141</sup> Moreover, a large tandem repeat region was also found in the *Echinococcus granulosus* mitochondrial genome. <sup>142</sup> In this study, the inverted repeat elements might have originated from transposable elements and possibly affect DNA recombination, replication and transcription. <sup>143, 144</sup>

# 6.6 Fischoederius spp. transcriptome

Paired-end Illumina® sequencing was used to obtain transcriptome data of the collected Fischoederius specimens. Total RNA was extracted from single worms and examined for its mtCOX1 MseI pattern. RNA of three to five worms with the same MseI pattern was pooled for transcriptome analysis. Quality control of the extracted total RNA showed absence of the 28S rRNA as separate band in gel electrophoresis because like in other trematodes it is split into two fragments that migrate together with the 18S rRNA. 145, 146 Sequencing results showed >80% of Q30 base quality that indicated 99.9% base call accuracy. 147, 148 In the present study, more than 50,000 unique contigs were identified for the transcriptome of Fischoederius MseI pattern A, C and E. In BLAST searches about 70% of the unique contigs had matches to sequences without known function in the database (UniProtKB). It must be considered that many transcripts are incomplete due to short read length in Illumina® sequencing. 149 Possibly, this limitation could be solved by (1) bioinformatics to enhance assembly and annotation quality, and (2) more recent sequencing platforms such as Oxford Nanopore to increase read length. 150 Other limitations are that at the present time GenBank and UniProtKB contain only very few sequences of Fischoederius (mitochondrial genome

and partial sequences of 5.8S rRNA, 18S rRNA, 28S rRNA and ribosomal ITS2) and the general fact that most genes in trematodes have not been analyzed yet for their function.

Fischoederius spp. transcriptome annotation revealed that about 50% of the unique sequences matched to homologous sequences in invertebrates. Most of these matches were found to trematodes, especially Opisthorchis viverrini, Clonorchis sinensis, F. hepatica, Paragonimus westermani. The transcriptome data showed also matches to sequences of unrelated animals, plants, bacteria and viruses. These will be due to contamination of the specimens because the flukes were naturally living in the rumen of the bovine host which is obviously not a sterile site. Flukes were washed several times in 10 mM PBS pH 7.2 and then cultured in RPMI-1640 to allow regurgitation of cecal contents. However, these biological contaminations might be absorbed/attached on cecal epithelium and tegument surface, especially the tegument inside of the large ventral poach of the flukes. Only sequences that resulted in first hits (matches) to trematodes were considered to be valid transcriptome data originating from Fischoederius. It is possible that transcripts generating some low scoring first hits to other Platyhelminthes, e.g. cestodes are in fact Fischoederius sequences and that some low scoring first hits to trematodes are originating from cestodes. Only genome data of Fischoederius could help to make final decisions on such edge cases.

Based on morphology *Fischoederius Mse*I pattern A specimens were not mature. In support of morphology data, the transcriptome data was searched for transcripts encoding proteins active in the reproductive system. A prominent example was vitelline protein. Transcripts encoding this protein were absent in *Fischoederius Mse*I pattern A but highly abundant in mature *Fischoederius Mse*I pattern C and E. Ferrintin is another example which was present in *Fischoederius Mse*I pattern C and E but absent in pattern A. Ferrintin is important for iron storage which is an essential element for egg yolk. <sup>151, 152</sup>

Gene ontology assignment showed that *Fischoederius* spp. transcriptome data mapped to essential pathways such as transcription, translation, regulation and metabolic processes that supported the fluke growth and development. Some biological processes were linked to protein biosynthesis, protein secretory pathway, and catalytic pathway. GO terms of *Fischoederius Mse*I pattern A in the molecular function category

represented ATP binding, GTP binding, and GTPase activity with proteins involved in energy metabolism, membrane transporter, and cellular signaling that are also found in *Fasciola gigantica*<sup>79</sup> and *Fasciolopsis buskt*<sup>90</sup> transcriptomes. These proteins act as glucose transporters to uptake the nutrient across the tegument in helminths. Also, they are involved in epidermal growth factor signaling in helminth development. <sup>153, 154</sup> In *Fischoederius Mse*I pattern C, and E the major GO term in the biological process category was cellular and metabolism process and might point to proteins active in the mature helminth. The KEGG pathway map should be the database resource for clear understanding in molecular biological system of proteins in these GO terms. <sup>155</sup> Furthermore, a major GO term in *Fischoederius Mse*I pattern A, C, and E was catalytic activity that might include parasite proteins in the ES product that affect host rumen immunity and that are important in nutrient supply. <sup>91, 156, 157</sup>

Many of the highly abundant transcripts in the *Fischoederius* spp. transcriptome encoded proteins found and described in other trematodes. These proteins included cysteine proteases, fatty acid-binding proteins, antioxidants, and calcium-binding proteins. <sup>78, 79, 83-90, 158-160</sup> Paramphistomiasis is usually caused by the immature rumen flukes migrating through the intestinal tract. The immature stage releases virulence factors in defense against the host immune system during this pathogenic phase. <sup>33, 34, 161</sup> Therefore, the transcriptome of immature *Fischoederius Mse*I pattern A, was analyzed for highly abundant transcripts with complete coding sequence to detect proteins with potential in drug and vaccine development.

Transcripts of several different cysteine proteases were abundant. Based on bioinformatics analysis, complete sequences were obtained for cathepsin B-like, cathepsin L-like, and cathepsin C-like proteases. While sequence conservation was not especially high the characteristic motifs of cysteine proteases were identified in all these predicted proteins. Cysteine proteases have been found as the predominant proteases in several trematode species including *S. mansoni*, *S. japonicum*, *F. hepatica*, and *F. gigantica*. This protease family plays important roles in parasite feeding, host tissue invasion, and immune evasion. <sup>162-166</sup> Transcripts encoding cathepsin B-like cysteine proteases were the most abundant molecules in the transcriptome data. Analysis of morphology showed that *Fischoederius Mse*I pattern A collected in 2016 were immature, lacking a developed reproductive system. In *Fasciola* cathepsin B is more

abundant in juveniles than adult worms.<sup>167</sup> Furthermore, cathepsin B was also found to be the most abundant transcript in transcriptome analyses of *F. gigantica*<sup>79</sup> and *P. cervi.*<sup>88</sup> Care has be taken in *de novo* assembly and transcript abundance analysis that highly conserved isoforms and paralogous transcripts affect the abundance accuracy.<sup>168</sup> Transcript abundancy should be verified by qRT-PCR.

Fatty acid binding protein was also well represented in the *Fischoederius* spp. transcriptome similar to other intestinal flukes such as *P. cervi*<sup>88</sup> and *F. buski*. On this protein has critical roles involved in lipid acquiring and storage. Due to a low glucose enrichment in the anaerobic condition of the host rumen, fatty acids might be energy sources for parasite metabolism that can be taken up from the host rumen. Lipid biosynthesis of the fluke and lipid uptake in the host rumen should be studied for further conclusions.

Thioredoxin was another molecule found transcribed at high levels in the present transcriptome data. It was also abundant in several other trematodes, *e.g. S. mansoni*, <sup>170</sup> *F. hepatica*, <sup>86</sup> and *F. gigantica*. <sup>79</sup> The role of this antioxidant protein is for example in immune modulation. It also protects the parasite from host reactive oxygen species. <sup>171, 172</sup>

Transcripts encoding calcium-binding protein were abundant too in the *Fischoederius* spp. transcriptome. Calcium-binding protein was also reported in several other trematodes including *S. mansoni*, <sup>173</sup> *S. japonicum*, <sup>174</sup> *F. gigantica*, <sup>175</sup> and *O. viverrini*. <sup>176</sup> This protein might be located at the tegument and act as parasite antigen. The EF-hand calcium-binding domain was predicted in this calcium-binding protein and might play a role in the uptakes of calcium from the host environment. <sup>177, 178</sup>

The analyzed *Fischoederius* spp. transcriptome data provides significant biological data that can be used to study fluke development and evolution, to reveal parasite-host interactions and pathogenesis, and to find candidate proteins for diagnosis and vaccine development.

### 6.7 Polyclonal mouse *Fischoederius* spp. anti-ES antibody

Fischoederius spp. excretory/secretory (ES) product was collected and resolved on a 12.5% acrylamide gel. The observed protein pattern was somewhat

similar to the result in a previous study by Arunkumar and Hrupakaran (2016) in which the authors investigated the ES product of *F. elongatus* isolated from India.<sup>48</sup> In their study predominant bands were observed at about 15 kDa. Strong protein bands at about 66 kDa were observed in ES of *Fischoederius* spp. collected in different regions. In addition, several bands between 25–45 kDa were detected. The present study observed a smaller number of bands because it did not use silver staining as applied in the study from India.

The Fischoederius spp. ES product was used for immunization of female BALB/c mice to produce antisera. The sensitivity of the mouse Fischoederius spp. anti-ES antisera was evaluated against Fischoederius spp. ES antigens and showed a high titer antibody at 25,600. The anti-ES reacted with Fischoederius spp. ES antigens at a molecular weight range from 15 to 120 kDa (Figure 5.75). The predominantly detected bands were at 35 and 54 kDa molecular weight which is similar in size to the highly expressed proteins in transcriptome data, cathepsin B and C, respectively. The bands might represent the secreted forms of those proteases. Cathepsin B plays role as a virulence factor of parasite infection in several trematodes. <sup>179</sup> Cathepsin C was shown to support parasite feeding by hemoglobin degradation. <sup>166</sup> Furthermore, the antisera did not cross-react with F. gigantica ES product and crude worm (CW) extracts. Only few bands at 17 kDa were observed. However, the antisera showed cross-reaction with Paramphistomum spp. CW extract with several bands at high molecular weight including a 54 kDa protein that might be cathepsin C. Interestingly, the 35 kDa protein mentioned above was not detected. These specific proteins and cross-reacted proteins should be identified by molecular biology techniques, e.g. MALDI-TOF MS. The protein migrating at 35 kDa molecular weight will serve as a specific target in future research in Fischoederius.

### **6.8** Further research and application

This investigation provides basic knowledge of the rumen fluke *Fischoederius* spp.. Transcriptome analysis allows faster identification of species-specific and cross-reacting antigens. The gene annotated transcripts will be compared among the species in genus *Fischoederius* to reveal their taxonomic relationship. The

obtained data will be compared with the already published transcriptomes of the rumen flukes *Paramphistomum* and *Calicophoron*, the liver flukes *Fasciola* and *Opisthorchis*, and the blood fluke *Schistosoma* to find species-specific proteins that can be applied as diagnosis antigens and/or drug targets. Furthermore, the achieved data might lead to insight in the adaptations of rumen flukes to the extreme conditions in the host digestive tract. In silico identified proteins must be further evaluated by immunological and functional analyses. Only then will it be possible to decide whether these proteins can be of any use in in the fight against rumen fluke infection.



# CHAPTER 7 CONCLUSIONS

The findings in this dissertation include morphology data, molecular phylogenetic data, transcriptome data, and immunologic data of *Fischoederius* spp. specimens that resembled *Fischoederius elongatus*. These specimens were collected from naturally infected cattle in Thailand in the years 2014–2019. The conclusions of the major findings are as follows;

- 1. The body of the collected *Fischoederius* spp. had a reddish color and could exceed a length of 2 cm. The flukes had an anterior opening of the digestive tract at the pharynx and a posterior located large sucker (acetabulum). The cecal bifurcation was closely posterior to the esophagus and the two ceca ended at the middle of the body. Vitellaria were present in the lateral field of the body. The lobed testes were found in a median and ventral position in the posterior region. The ovary was located beside the testes. A large ventral pouch was present.
- 2. Fischoederius spp. had a thick acidophilic tegument. The anterior end containing the pharynx was surrounded by strong muscle layers. The esophagus extended from the pharynx without muscular bulb. The cecal bifurcation was located next to the esophagus and the ceca had a tubular structure covered with two layers of muscles. The terminal genitalium did not contain a cirrus sac, it opened to the ventral pouch and consisted of genital pore, genital papilla with papillae, enormously developed genital fold, poorly developed genital sphincter, and radial muscle fibers. The testes were tandem lobed with globular bodies. The ovary had ovoid shape and was located between the anterior and posterior testis. The seminal receptacle with spermatozoa had an ovoid shape and was located in a lateral position to testes and ovary. The ovoid ootype was found in the center of the Mehlis' gland as a basophilic layer duct. Laurer's canal was connected to the ootype and located in the dorsal field. The vitellaria were in the lateral field and contained basophilic granules. Eggs had ovoid shape with a thin shell. The large acetabulum had an ovoid shape with arranged layers of strong muscle fibers.
  - 3. Fischoederius specimens collected in the present study had either large

or small testes. Specimens with large testes were mature and contained often intrauterine eggs. Specimens with small testes were immature and also had an undeveloped ovary and only a small number of vitellaria.

- 4. A PCR-amplified 515 bp DNA fragment of ribosomal ITS2 of a *Fischoederius* specimen collected in this study showed significant identity (99%, E-value: 0.0) to *F. elongatus* sequences in GenBank (accession no. GU133062 and JQ688409).
- 5. A 1,536 bp DNA fragment of *Fischoederius* spp. mtCOX1 was successfully amplified from gDNA extracts from single worms.
- 6. Nine restriction patterns of *Mse*I-digested mtCOX1 (Pattern A–I) were observed in a total of 48 analyzed *Fischoederius* specimens. Phylogenetic analysis of the mtCOX1 sequences representing pattern A–I clustered them in five branches, *i.e.* A, [BEG], [CFH], D, and I that most likely represent five distinct species.
- 7. *Mse*I pattern E was the most frequent pattern among the 48 samples while *Mse*I pattern I was the least frequent pattern.
- 8. The five mtCOX1 phylogenetic branches of the collected *Fischoederius* specimens had 4.2–9.6% sequence difference between the branches. *Fischoederius* pattern [BEG] had 'intraspecies' variation of 0.8–1.3%. *Fischoederius* pattern [CFH] had 'intraspecies' variation of 0.7–1.0%. The interspecies variation to the published *F. elongatus* (China) and *F. cobboldi* (China) sequences was 5.7–8.3%. The interspecies variation to Gastrothylacid species was 6.9–11.7%.
- 9. Further phylogenetic analysis demonstrated that *Fischoederius* pattern A–I mtCOX1 in this study were closely related to *Fischoederius* species from China and India (with *F. elongatus* India identical to *Fischoederius* pattern A) followed by the members in family Gastrothylacidae, Paramphistomidae, and Fasciolidae, respectively.
- 10. The complete mitochondrial genome of *Fischoederius Mse*I Pattern A is 14,780 bp in length. It carries 12 protein-coding genes (*cytb*, cox1–3, nad1–6, nad4L, and atp6), 23 tRNA genes, 2 rRNA genes (rrnS and rrnL), and 2 non-coding regions (SNR and LNR). The protein-coding genes are arranged on the same DNA strand in the following order; cox3 > cytb > nad4L > nad4 > atp6 > nad2 > nad1 > nad3 > cox1 > cox2 > nad6 > nad5. The overall A+T content is 63.8%.

- 11. The most conserved genes in the *Fischoederius* spp. mitochondrial genome were *atp*6, *nad*1, and *cox*1 in intraspecies variation and *cytb* in interspecies variation, while the least conserved genes were *nad*2 and *nad*3.
- 12. Phylogenetic analysis of concatenated amino acid sequence of the 12 protein-coding genes of *Fischoederius* mitochondrial genome *Mse*I pattern A showed its close relationship to previously published *Fischoederius* species and members in families Gastrothylacidae and Paramphistomidae, followed by families Fasciolidae and Opisthorchiidae.
- 13. Transcriptome analysis of *Fischoederius* spp. was performed by paired-end Illumina<sup>®</sup> sequencing, resulting in data with >80% of Q30 sequence quality.
- 14. Gene annotation of transcriptome data showed that about 70% of the unique contigs had no annotation in the databases.
- 15. Species distribution of transcriptome data showed significant similarity to invertebrates including *Opisthorchis viverrini*, *O. felineus*, *Clonorchis sinensis*, *Paragonimus westermani*, *Echinostoma caproni*, *Fasciola hepatica*, *Schistosoma mansoni*, and *S. japonicum*.
- 16. Fischoederius MseI pattern A specimens were immature flukes that did not express genes encoding vitelline protein while Fischoederius MseI pattern C and E showed high expression of these genes in support of their fully developed reproductive system.
- 17. Transcriptome data of *Fischoederius Mse*I pattern A was assembled into 55,912 unique contigs with an average contig length of 633 bp and 44% GC content. A total of 26,405 GO terms were found for 16,942 annotated contigs (analysis from 2018); GO terms under biological process category (7,433: 28.15%); GO terms under molecular function category (11,282: 42.73%); GO terms of cellular components (7,609: 28.82%).
- 18. BLASTX of the assembled transcriptome data of *Fischoederius Mse*I pattern C against the UniProtKB database resulted in 29,918 annotated contigs with an average contig length of 403 bp and 48% GC content. Gene ontology analysis resulted in 71,299 GO terms; GO terms under biological process category (28,783: 40.37%); GO terms under molecular function category (14,901: 20.90%); GO terms of cellular components (27,615: 38.73%).

- 19. The transcriptome data of *Fischoederius Mse*I pattern E had 51% GC content. BLASTX of the assembled transcriptome data of *Fischoederius Mse*I pattern E against the UniProtKB database resulted in 32,948 annotated transcripts. Gene ontology analysis resulted in 77,855 GO terms; GO terms under biological process category (31,324: 40.23%); GO terms under molecular function category (31,324: 40.23%); GO terms of cellular components (30,188: 38.77%).
- 20. Fischoederius MseI pattern A, C, and E showed similar gene expression profiles, except for genes that have role in reproduction. The transcriptome data revealed highly expressed genes including (1) mitochondrial genes, genes associated with (2) transport, (3) cellular process, (4) oxidative phosphorylation, (5) nutrient transport, (6) catalytic enzyme.
- 21. Highly abundant genes with complete sequence and known function included cathepsin-like cysteine protease (B, C, L), fatty acid-binding protein, thioredoxin, and tegumental calcium-binding protein.
- 22. Highly sensitive polyclonal mouse *Fischoederius* anti-ES reacted with antigens in the *Fischoederius* ES product in the molecular weight range from 15 to 120 kDa.
- 23. Cross-reactivity of *Fischoederius* anti-ES antiserum was limited to a 17 kDa antigen in *F. gigantica* ES product and to several high molecular weight proteins of *Paramphistomum* spp. CW extract.
- 24. By its molecular weight and in accordance with the transcriptome data, the predominant 35 kDa antigen detected by *Fischoederius* anti-ES antiserum might be *Fischoederius* cathepsin B.

## REFERENCES

- 1. Rudolphi KA. Entozoorum, sive vermium intestinalium : historia naturalis. Amstelaedami: Sumtibus Tabernae Librariae et Artium; 1809. p. 340–52.
- 2. Nitzsch CL. Artikel Amphistoma in Ersch und Gruber's Allgemeine encyclopaedie der Wissenschaften und Kunste: Leipzig; 1819. p. 1–398.
- 3. Tandon V, Roy B, Shylla JA, Ghatani S. Amphistomes. In: Toledo R, Fried B, editors. Digenetic Trematodes. New York, NY: Springer New York; 2014. p. 365–92.
- 4. Nasmark KE. A revision of the trematode family Paramphistomidae. Zoologiska Bidrag fran Uppsala. 1937;16(1):301–565.
- 5. Horak IG. Paramphistomiasis of domestic ruminants. Advances in parasitology. 1971;9(1):33–72.
- 6. Jones A, Bray RA, Gibson DI. Keys to the Trematoda: Volume 2. Family Gastrothylacidae. Wallingford: CABI Publishing; 2005. p. 337–41.
- 7. Sey O. Keys to the Identification of the Taxa of the Amphistomes (Trematoda, Amphistomida): Regional Centre of the Hungarian Acad. of Sciences; 2005. p. 6–91.
- 8. Sey O. Handbook of the Zoology of Amphistome. Fischoederius Stiles et Goldberger, 1910. USA: CRC Press, Inc.; 1991. p. 301–6.
- 9. Eduardo SL, Javellana CRH. *Fischoederius skrjabini* Kadenatsii, 1963 (Gastrothylacidae) from Philippine ruminants with notes on related species. Philippine Journal of Veterinary Medicine. 1990;27(2):17–20.
- 10. Zhang FS, Yang JZ. A new species of *Fischoederius* from sheep in Zhejiang Province. Acta Zootaxonomica Sinica. 1986;113(3):250–2.
- 11. Eduardo SL, Javellana CRH. *Fischoederius philippinensis*, a new species of gastrothylacid parasite from ruminants in the Philippines. Transactions of the National Academy of Science and Technology. 1989;10(4):177–86.
- 12. Eduardo S, Javellana CRH. *Fischoederius upiensis* new species from ruminants in the Philippines with remarks on other species of the genus Fischoederius Stiles & Goldberger, 1910 (Trematoda: Paramphistomoidea: Gastrothylacidae). Philippine Journal of Veterinary Medicine. 2008;45(1):22–9.

- 13. Eduardo S. *Fischoederius emiljavieri*, a New Species of Pouched Amphistome from Ruminants in the Philippines and Indonesia and Redescription of *Fischoederius cobboldi* (Poirier, 1883) Stiles & Goldberger, 1910 (Trematoda: Gastrothylacidae). Philippine Journal of Veterinary Medicine. 2009;46(5):44–52.
- 14. Eduardo SL. *Fischoederius brevisaccus*, a new species of pouched amphistome (Gastrothylacidae) from ruminants in the Philippines. Systematic Parasitology. 1981;3(1):01–6.
- 15. Eduardo SL, Javellana CRH. A new genus, *Velasquezotrema*, for *Fischoederius brevisaccus* Eduardo, 1981. Philippine Journal of Veterinary Medicine. 1987;24(1):29–34.
- 16. Sey O, Prasitirat P, Romratanapun S, Mohkaew K, editors. Morphological study and identification of rumen flukes of cattle in Thailand. 34th Kasetsart University annual conference; 1996; Bangkok, Thailand: Kasetsart University. 1996.
- 17. Mukherjee RP. Studies on the life history of *Fischoederius elongatus* (Poirier, 1883) Stiles and Goldberger, 1910, an amphistome parasite of cow and buffalo in India. Indian Journal of Helminthology. 1966;18(1):5–14.
- 18. Mukherjee RP. The Fauna of India: Larval Trematodes (Amphistome Cercariae). India: Zoological Survey of India; 1986. p. 1–89.
- 19. Anucherngchai S, Chontananarth T, Tejangkura T, Wongsawad C. Molecular classification of rumen fluke eggs in fecal specimens from Suphanburi Province, Thailand, based on cytochrome C oxidase subunit 1. Veterinary Parasitology: Regional Studies and Reports. 2020:100382.
- 20. Swell RBS. Cercariae Indicae. Indian Journal of Medical Research. 1922;10(Special Supplement)(1):1–370.
- 21. Rao MA, Ayyar LSP. Cercaria of *Fischoederius elongatus*. Indian Journal of Veterinary Science and Animal Husbandry. 1932;2:402–5.
- 22. Waal Td. Paramphistomum—a brief review. Irish Veterinary Journal. 2010;63(5):313–5.
- 23. Kishore B, Shoeb M. The Encystment and an Early Development of Cercaria of *Fischoederius elongatus* in Experimental Animals. Indian Journal of Research. 2017;6(7):2.

- 24. Sripalwit P. Genetic Diversity of Rumen Cow Flukes in Amphoe Muang Chiang Mai and Lamphum Province. Chiang Mai: Chiang Mai University; 2001.
- 25. Hafeez M, Rao BV. Check-list of Amphistomes from cattle and buffaloes in Andhra Pradesh. The Veterinarian. 1980;4:5.
- 26. Yu SH, Mott KE, Unit WHOSC. Epidemiology and morbidity of food-borne intestinal trematode infections. Geneva: World Health Organization; 1994. p. 1–26.
- 27. Boray JC. Studies on Intestinal Amphistomosis in Cattle. Australian Veterinary Journal. 1959;35(6):282–7.
- 28. Chai JY, Shin EH, Lee SH, Rim HJ. Foodborne Intestinal Flukes in Southeast Asia. The Korean Journal of Parasitology. 2009;47(Suppl):S69–S102.
- 29. Chai JY, Jung BK. Foodborne intestinal flukes: A brief review of epidemiology and geographical distribution. Acta tropica. 2020;201(1):105210.
- 30. Sathaporn J, Arkom S, Burin N, Tawin I, Chamnonjit P, Nongnuch P, *et al.* Prevalence of Gastro-Intestinal Parasites of Dairy Cows in Thailand. Agriculture and Natural Resources—formerly Kasetsart Journal (Natural Science). 2011;045(1):40–5.
- 31. Sripalwit P, Wongsawad C, Anantalabhochai S, editors. Biodiversity Research and Training Program (BRT) Abstracts Research and Thesis 2001: Genetic Diversity of Cow Rumen Flukes in Muang District of Chiangmai and Lamphun Provinces. 5th BRT Annual Conference; 2001; Udonthani, Thailand. Jirawat Express Co., Ltd., Bangkok: Biodiversity Research and Training Program; 2001.
- 32. Balachandran C, Raman A, Pazhanivel N. An outbreak of Amphistomosis in an organized sheep farm. Indian Journal of Veterinary and Animal Sciences Research. 2010;6(6):3.
- 33. Huson KM, Oliver NAM, Robinson MW. Paramphistomosis of Ruminants: An Emerging Parasitic Disease in Europe. Trends in parasitology. 2017;33(11):836–44.
- 34. Pfukenyi DM, Mukaratirwa S. Amphistome infections in domestic and wild ruminants in East and Southern Africa: A review. Onderstepoort J Vet Res. 2018;85(1):e1–e13.
- 35. Toledo R, Esteban JG, Fried B. Immunology and Pathology of Intestinal Trematodes in Their Definitive Hosts. Advances in parasitology. 2006;63(1):285–365.
- 36. Kumar V. Trematode Infections and Diseases of Man and Animals. Dordrecht Springer; 1999.

- 37. Li D. A case of *Fischoederius elongatus* infection in China. Annual Bulletin of the Society of Parasitology. 1991;12(11–13):155–6.
- 38. Lynsdale CL, Santos DJFd, Hayward AD, Mar KU, Htut W, Aung HH, *et al.* A standardised faecal collection protocol for intestinal helminth egg counts in Asian elephants, Elephas maximus. International Journal for Parasitology: Parasites and Wildlife. 2015;4(3):307–15.
- 39. Maria Ornela B, Eleonor T, Alberto Enrique P, Norma Haydee S. First paleoparasitological record of digenean eggs from a native deer from Patagonia Argentina (Cueva Parque Diana archaeological site). Veterinary parasitology. 2017;235(1):83–5.
- 40. Sindicic M, Martinkovic F, Striskovic T, Spehar M, Stimac I, Bujanic M, *et al.* Molecular identification of the rumen flukes *Paramphistomum leydeni* and Paramphistomum cervi in a concurrent infection of the red deer Cervus elaphus. Journal of helminthology. 2017;91(5):637–41.
- 41. Wongsawad C, Wongsawad P, Chai JY, Paratasilpin T, Anuntalabhochai S. Dna quantities and qualities from various stages of some trematodes using optical and HAT-RAPD methods. The Southeast Asian journal of tropical medicine and public health. 2006;37(Suppl 3):62–8.
- 42. Sripalwit P, Wongsawad C, Wongsawad P, Anuntalabhochai S. High annealing temperature-random amplified polymorphic DNA (HAT-RAPD) analysis of three paramphistome flukes from Thailand. Experimental parasitology. 2007;115(1): 98–102.
- 43. Ghatani S, Shylla JA, Tandon V, Chatterjee A, Roy B. Molecular characterization of pouched amphistome parasites (Trematoda: Gastrothylacidae) using ribosomal ITS2 sequence and secondary structures. Journal of helminthology. 2012;86(1):117–24.
- 44. Schultz J, Wolf M. ITS2 sequence–structure analysis in phylogenetics: A how to manual for molecular systematics. Molecular Phylogenetics and Evolution. 2009;52(2):520–3.
- 45. Ghatani S, Shylla JA, Roy B, Tandon V. Multilocus sequence evaluation for differentiating species of the trematode Family Gastrothylacidae, with a note on the utility of mitochondrial COI motifs in species identification. Gene. 2014;548(2):277–84.

- 46. Hassan SS, Juyal PD. Diagnosis of paramphistomosis in domestic ruminants in Punjab, India: International Symposia on Veterinary Epidemiology and Economics; 2006. p. 843–48.
- 47. Salib F, Halium M, Mousa W, Massieh E. Evaluation of Indirect ELISA and Western blotting for the diagnosis of Amphistomes infection in Cattle and Buffaloes. International Journal of Livestock Research. 2015;5(3):71–81.
- 48. Arunkumar S, Krupakaran RP. Analysis of Polypeptide Profile of Excretory/Secretory Antigens of *Fischoederius elongatus* from Cattle Origin using Silver Staining. Life Sciences International Research Journal. 2016;3(1):3.
- 49. GIDEON Informatics I, Berger S. Infectious Diseases of China: 2017 edition: GIDEON Informatics, Incorporated; 2017.
- 50. Sey O. A review of chemotherapy of paramphistomosis of domesticated ruminants in Europe. Parasitologia Hungarica. 1989;22(1):51–5.
- 51. Rolfe PF, Boray JC. Chemotherapy of paramphistomosis in cattle. Aust Vet J. 1987;64(11):328–32.
- 52. Horak IG. Host-parasite relationships of Paramphistomum microbothrium Fischoeder, 1901, in experimentally infested ruminants, with particular reference to sheep. Onderstepoort Journal of Veterinary Research. 1967;34(2):451–540.
- 53. Petkov A, Bankov D, Rusev I, Tomov P. Bithionol sulfoxide against mixed infections in ruminants. Veterinarna Sbirka. 1986;84(5):28–30.
- 54. Sanabria R, Moreno L, Alvarez L, Lanusse C, Romero J. Efficacy of oxyclozanide against adult *Paramphistomum leydeni* in naturally infected sheep. Veterinary parasitology. 2014;206(3–4):277–81.
- 55. Jeyathilakan N, G.Radha, Sankaralingam G, K.Senthilvel, John L. Reduced efficacy of oxyclozanide against amphistomes in naturally infected sheep. Indian Journal of Small Ruminants. 2005;11(1):96–7.
- 56. Vanden Bossche H, Arundel JH, Thienpont D, Boersema JH, Janssens PG, Bruyning CFA, *et al.* Chemotherapy of Gastrointestinal Helminths: Springer Berlin Heidelberg; 2012.

- 57. Prasitirat P, Nithiuthai S, Ruengsuk K, Kitwan P, Bunmatid C, Roopan S, *et al.*, editors. Efficacy of bithionol sulfoxide, niclosamide and fenbendazole against natural rumen fluke infections in cattle. 34th Kasetsart University annual conference; 1996; Bangkok, Thailand: Kasetsart University. 1996.
- 58. Prasitirat P, Nithiuthai S, Chompoochan T, Anutarapong J, Roopan S, Chinone S, editors. Anthelmintic effects of bithionol sulfoxide against natural rumen fluke infections in dairy cattle. 34th Kasetsart University annual conference; 1996; Bangkok, Thailand: Kasetsart University. 1996.
- 59. COWS. Control of liver and rumen fluke in cattle. Liver and rumen fluke; 2013. [updated 2013; cited January 2020]. 12 p. Available from: https://www.cattleparasites.org.uk/app/uploads/2018/04/Control-liver-and-rumen-fluke-in-cattle.pdf.
- 60. Nzalawahe J, Hannah R, Kassuku AA, Stothard JR, Coles G, Eisler MC. Evaluating the effectiveness of trematocides against *Fasciola gigantica* and amphistomes infections in cattle, using faecal egg count reduction tests in Iringa Rural and Arumeru Districts, Tanzania. Parasit Vectors. 2018;11(1):384.
- 61. Yang X, Zhao Y, Wang L, Feng H, Tan L, Lei W, *et al.* Analysis of the complete *Fischoederius elongatus* (Paramphistomidae, Trematoda) mitochondrial genome. Parasites & Vectors. 2015;8(1):279.
- 62. Han Z, Li K, Luo H, Shahzad M, Mehmood K. Characterization of the Complete Mitochondrial Genome of *Fischoederius elongatus* Derived from Cows in Shanghai, China. BioMed research international. 2020;2020(1):7975948.
- 63. Adams JU. Transcriptome: Connecting the Genome to Gene Function. Nature Education. 2008;1(1):195.
- 64. Perkel JM. Transcriptome Analysis: Microarrays, qPCR and RNA-Seq: Biocompare; 2013 [updated 21 May 2013; cited January 2020]. Available from: http://www.biocompare.com/Editorial-Articles/137520-Transcriptome-Analysis-Microarrays-qPCR-and-RNA-Seq.
- 65. Srivastava A, George J, Karuturi RKM. Transcriptome Analysis. In: Ranganathan S, Gribskov M, Nakai K, Schönbach C, editors. Encyclopedia of Bioinformatics and Computational Biology. Oxford: Academic Press; 2019. p. 792–805.

- 66. Rangan P, Furtado A, Henry R, Gaikwad A. Development of Transcriptome Analysis Methods. Reference Module in Food Science: Elsevier; 2019.
- 67. Arya M, Shergill IS, Williamson M, Gommersall L, Arya N, Patel HR. Basic principles of real-time quantitative PCR. Expert review of molecular diagnostics. 2005;5(2):209–19.
- 68. Wong ML, Medrano JF. Real-time PCR for mRNA quantitation. BioTechniques. 2005;39(1):75–85.
- 69. Overbergh L, Giulietti AP, Valckx D, Mathieu C. Chapter 7—Real-Time Polymerase Chain Reaction. In: Patrinos GP, Ansorge WJ, editors. Molecular Diagnostics (Second Edition). San Diego: Academic Press; 2010. p. 87–105.
- 70. Gibthai. Technical Note: Real-time PCR technology Bangkok: Thailand: Gibthai: A 3N Holding Company; 2015. [updated 2015; cited January 2020]. Available from: http://www.gibthai.com/service/note\_detail/12.
- 71. Schuster SC. Next-generation sequencing transforms today's biology. Nature methods. 2008;5(1):16–8.
- 72. Wilantho A, Praditsup O, Charoenchim W, Kulawonganunchai S, Assawamakin A, Tongsima S. Next generation sequencing (NGS) technologies and their applications in omics-research. Genomics and Genetics. 2012;5(2):104–29.
- 73. Bentley DR, Balasubramanian S, Swerdlow HP, Smith GP, Milton J, Brown CG, *et al.* Accurate whole human genome sequencing using reversible terminator chemistry. Nature. 2008;456(7218):53–9.
- 74. Illminar. Technology spotlight: Illumina Sequencing California: Illumina, Inc.; 2010 [updated 2010; cited January 2020]. Available from: https://www.illumina.com/documents/products/techspotlights/techspotlight\_sequencing.pdf.
- 75. Rajesh T, Jaya M. Chapter 7—Next-Generation Sequencing Methods. In: Gunasekaran P, Noronha S, Pandey A, editors. Current Developments in Biotechnology and Bioengineering: Elsevier; 2017. p. 143–58.
- 76. Buermans HPJ, den Dunnen JT. Next generation sequencing technology: Advances and applications. Biochimica et Biophysica Acta (BBA)—Molecular Basis of Disease. 2014;1842(10):1932–41.

- 77. Zhang FK, Zhang XX, Elsheikha HM, He JJ, Sheng ZA, Zheng WB, *et al.* Transcriptomic responses of water buffalo liver to infection with the digenetic fluke *Fasciola gigantica*. Parasit Vectors. 2017;10(1):56.
- 78. Liu GH, Xu MJ, Chang QC, Gao JF, Wang CR, Zhu XQ. *De novo* transcriptomic analysis of the female and male adults of the blood fluke *Schistosoma turkestanicum*. Parasites & Vectors. 2016;9(1):143.
- 79. Young ND, Jex AR, Cantacessi C, Hall RS, Campbell BE, Spithill TW, *et al.* A portrait of the transcriptome of the neglected trematode, *Fasciola gigantica*—biological and biotechnological implications. PLoS neglected tropical diseases. 2011;5(2):e1004.
- 80. Grabherr MG, Haas BJ, Yassour M, Levin JZ, Thompson DA, Amit I, *et al.* Full-length transcriptome assembly from RNA-Seq data without a reference genome. Nat Biotech. 2011;29(7):644–52.
- 81. Miller JR, Koren S, Sutton G. Assembly algorithms for next-generation sequencing data. Genomics. 2010;95(6):315–27.
- 82. Babarinde IA, Li Y, Hutchins AP. Computational Methods for Mapping, Assembly and Quantification for Coding and Non-coding Transcripts. Computational and Structural Biotechnology Journal. 2019;17(1):628–37.
- 83. Oliveira G. The *Schistosoma mansoni* transcriptome: an update. Experimental parasitology. 2007;117(3):229–35.
- 84. Verjovski-Almeida S, DeMarco R, Martins EA, Guimaraes PE, Ojopi EP, Paquola AC, *et al.* Transcriptome analysis of the acoelomate human parasite *Schistosoma mansoni*. Nature genetics. 2003;35(2):148–57.
- 85. Robinson MW, Menon R, Donnelly SM, Dalton JP, Ranganathan S. An Integrated Transcriptomics and Proteomics Analysis of the Secretome of the Helminth Pathogen *Fasciola hepatica*: Proteins Associated with Invasion and Infection of the Mammalian host. Molecular & cellular proteomics: MCP. 2009;8(8):1891–907.
- 86. Young ND, Hall RS, Jex AR, Cantacessi C, Gasser RB. Elucidating the transcriptome of *Fasciola hepatica*—a key to fundamental and biotechnological discoveries for a neglected parasite. Biotechnology advances. 2010;28(2):222–31.

- 87. Young ND, Campbell BE, Hall RS, Jex AR, Cantacessi C, Laha T, *et al.* Unlocking the Transcriptomes of Two Carcinogenic Parasites, *Clonorchis sinensis* and *Opisthorchis viverrini*. PLoS neglected tropical diseases. 2010;4(6):e719.
- 88. Choudhary V, Garg S, Chourasia R, Hasnani JJ, Patel PV, Shah TM, *et al.* Transcriptome analysis of the adult rumen fluke *Paramphistomum cervi* following next generation sequencing. Gene. 2015;570(1):64–70.
- 89. Huson KM, Morphew RM, Allen NR, Hegarty MJ, Worgan HJ, Girdwood SE, *et al.* Polyomic tools for an emerging livestock parasite, the rumen fluke *Calicophoron daubneyi*; identifying shifts in rumen functionality. Parasit Vectors. 2018;11(1):617.
- 90. Biswal DK, Roychowdhury T, Pandey P, Tandon V. *De novo* genome and transcriptome analyses provide insights into the biology of the trematode human parasite *Fasciolopsis buski*. PloS one. 2018;13(10):e0205570.
- 91. Hewitson JP, Grainger JR, Maizels RM. Helminth immunoregulation: The role of parasite secreted proteins in modulating host immunity. Molecular and biochemical parasitology. 2009;167(1–9):1–11.
- 92. López-Otín C, Bond JS. Proteases: Multifunctional Enzymes in Life and Disease. The Journal of Biological Chemistry. 2008;283(45):30433–7.
- 93. McKerrow JH, Caffrey C, Kelly B, Loke P, Sajid M. Proteases in parasitic diseases. Annual review of pathology. 2006;1(1):497–536.
- 94. Rice P, Longden I, Bleasby A. EMBOSS: the European Molecular Biology Open Software Suite. Trends in genetics: TIG. 2000;16(6):276–7.
- 95. Altschul SF, Gish W, Miller W, Myers EW, Lipman DJ. Basic local alignment search tool. Journal of molecular biology. 1990;215(3):403–10.
- 96. Larkin MA, Blackshields G, Brown NP, Chenna R, McGettigan PA, McWilliam H, *et al.* Clustal W and Clustal X version 2.0. Bioinformatics. 2007;23(21):2947–8.
- 97. Gouy M, Guindon S, Gascuel O. SeaView version 4: A multiplatform graphical user interface for sequence alignment and phylogenetic tree building. Mol Biol Evol. 2010;27(2):221–4.

- 98. Bernt M, Donath A, Jühling F, Externbrink F, Florentz C, Fritzsch G, *et al.* MITOS: Improved *de novo* metazoan mitochondrial genome annotation. Molecular Phylogenetics and Evolution. 2013;69(2):313–9.
- 99. Rombel IT, Sykes KF, Rayner S, Johnston SA. ORF-FINDER: a vector for high-throughput gene identification. Gene. 2002;282(1):33–41.
- 100. Stothard P. The sequence manipulation suite: JavaScript programs for analyzing and formatting protein and DNA sequences. BioTechniques. 2000;28(6): 1102–4.
- 101. Chan PP, Lowe TM. tRNAscan-SE: Searching for tRNA Genes in Genomic Sequences. Methods in molecular biology (Clifton, NJ). 2019;1962(1):1–14.
- 102. Laslett D, Canback B. ARWEN: a program to detect tRNA genes in metazoan mitochondrial nucleotide sequences. Bioinformatics. 2008;24(2):172–5.
- 103. Greiner S, Lehwark P, Bock R. OrganellarGenomeDRAW (OGDRAW) version 1.3.1: expanded toolkit for the graphical visualization of organellar genomes. Nucleic acids research. 2019;47(W1):W59–w64.
- 104. Kumar S, Stecher G, Li M, Knyaz C, Tamura K. MEGA X: Molecular Evolutionary Genetics Analysis across Computing Platforms. Molecular Biology and Evolution. 2018;35(6):1547–9.
- Jones P, Binns D, Chang HY, Fraser M, Li W, McAnulla C, *et al.* InterProScan 5: genome-scale protein function classification. Bioinformatics (Oxford, England). 2014;30(9):1236–40.
- 106. Wingett SW, Andrews S. FastQ Screen: A tool for multi-genome mapping and quality control. F1000 Research. 2018;7(1):1338.
- 107. Chang Z, Li G, Liu J, Zhang Y, Ashby C, Liu D, *et al.* Bridger: a new framework for d*e novo* transcriptome assembly using RNA-seq data. Genome biology. 2015;16(1):30.
- 108. Simão F, Waterhouse R, Ioannidis P, Zdobnov E. BUSCO: Assessing genome assembly and annotation completeness with single-copy orthologs. Bioinformatics (Oxford, England). 2015;31(19):3210–2.
- 109. Almagro Armenteros JJ, Tsirigos KD, Sonderby CK, Petersen TN, Winther O, Brunak S, *et al.* SignalP 5.0 improves signal peptide predictions using deep neural networks. Nature biotechnology. 2019;37(4):420–3.

- 110. Moller S, Croning MD, Apweiler R. Evaluation of methods for the prediction of membrane spanning regions. Bioinformatics. 2001;17(7):646–53.
- 111. Jousson, Bartoli, Pawlowski. Cryptic speciation among intestinal parasites (Trematoda: Digenea) infecting sympatric host fishes (Sparidae). Journal of Evolutionary Biology. 2000;13(5):778–85.
- 112. McNamara MK, Miller TL, Cribb TH. Evidence for extensive cryptic speciation in trematodes of butterflyfishes (Chaetodontidae) of the tropical Indo-West Pacific. International journal for parasitology. 2014;44(1):37–48.
- 113. Wongsawad C, Nantarat N, Wongsawad P. Phylogenetic analysis reveals cryptic species diversity within minute intestinal fluke, *Stellantchasmus falcatus* Onji and Nishio, 1916 (Trematoda, Heterophyidae). Asian Pacific Journal of Tropical Medicine. 2017;10(2):165–70.
- Goldberger J, Stiles CW, Royal College of Physicians of E. A study of the anatomy of Watsonius (n.g.) watsoni of man, and of nineteen allied species of mammalian trematode worms of the superfamily Paramphistomoidea. 1910.
- 115. Maplestone PA. A Revision of the Amphistomata of Mammals. Annals of Tropical Medicine & Parasitology. 1923;17(2):113–213.
- 116. Tandon RS. Studies on 'crowding effect' on *Gastrothylax crumenifer* and *Fischoederius elongatus*, the common amphistome parasites of ruminants, observed under natural conditions. Research Bulletin of the Meguro Parasitological Museum. 1973;7(1):3.
- 117. Dawes B. A histological study of the caecal epithelium of *Fasciola hepatica* L. Parasitology. 2009;52(3–4):483–93.
- 118. Meemon K, Khawsuk W, Sriburee S, Meepool A, Sethadavit M, Sansri V, *et al. Fasciola gigantica*: histology of the digestive tract and the expression of cathepsin L. Experimental parasitology. 2010;125(4):371–9.
- 119. Lal MB. Occurrence of a pigment layer in *Gastrothylax crumenifer* (Creplin, 1847). Experientia. 1959;15(5):176–8.
- Dunn TS, Hanna REB, Nizami WA. Ultrastructural and cytochemical studies on the ventral pouch of *Gastrothylax crumenifer* (Digenea: Paramphistomidae). International journal for parasitology. 1987;17(6):1163–73.

- 121. Anuracpreeda P, Panyarachun B, Ngamniyom A, Tinikul Y, Chotwiwatthanakun C, Poljaroen J, *et al. Fischoederius cobboldi*: A scanning electron microscopy investigation of surface morphology of adult rumen fluke. Experimental parasitology. 2012;130(4):400–7.
- 122. Panyarachun B, Ngamniyom A, Sobhon P, Anuracpreeda P. Morphology and histology of the adult *Paramphistomum gracile* Fischoeder, 1901. Journal of Veterinary Science. 2013;14(4):425–32.
- 123. Schlotterer C, Hauser MT, von Haeseler A, Tautz D. Comparative evolutionary analysis of rDNA ITS regions in Drosophila. Mol Biol Evol. 1994;11(3):513–22.
- 124. Kane RA, Rollinson D. Repetitive sequences in the ribosomal DNA internal transcribed spacer of *Schistosoma haematobium*, *Schistosoma intercalatum* and *Schistosoma mattheei*. Molecular and biochemical parasitology. 1994;63(1):153–6.
- 125. Adlard RD, Barker SC, Blair D, Cribb TH. Comparison of the second internal transcribed spacer (ribosomal DNA) from populations and species of Fasciolidae (Digenea). International journal for parasitology. 1993;23(3):423–5.
- Nolan MJ, Cribb TH. The use and implications of ribosomal DNA sequencing for the discrimination of digenean species. Advances in parasitology. 2005;60(1):101–63.
- 127. Vilas R, Criscione CD, Blouin MS. A comparison between mitochondrial DNA and the ribosomal internal transcribed regions in prospecting for cryptic species of platyhelminth parasites. Parasitology. 2005;131(Pt 6):839–46.
- 128. Waikagul J, Thaenkham U. Chapter 5—Molecular Systematics of Fish-Borne Trematodes. In: Waikagul J, Thaenkham U, editors. Approaches to Research on the Systematics of Fish-Borne Trematodes. Amsterdam: Academic Press; 2014. p. 61–76.
- 129. Tatonova YV, Chelomina GN, Besprozvannykh VV. Genetic diversity of *Clonorchis sinensis* (Trematoda: Opisthorchiidae) in the Russian southern Far East based on mtDNA cox1 sequence variation. Folia parasitologica. 2013;60(2):155–62.
- 130. Yan HB, Wang XY, Lou ZZ, Li L, Blair D, Yin H, *et al.* The mitochondrial genome of *Paramphistomum cervi* (Digenea), the first representative for the family Paramphistomidae. PloS one. 2013;8(8):e71300.

- 131. Yang X, Wang L, Chen H, Feng H, Shen B, Hu M, *et al.* The complete mitochondrial genome of *Gastrothylax crumenifer* (Gastrothylacidae, Trematoda) and comparative analyses with selected trematodes. Parasitology research. 2016;115(6):2489–97.
- 132. Le TH, Blair D, McManus DP. Mitochondrial genomes of human helminths and their use as markers in population genetics and phylogeny. Acta tropica. 2000;77(3):243–56.
- 133. Taanman JW. The mitochondrial genome: structure, transcription, translation and replication. Biochimica et Biophysica Acta (BBA)—Bioenergetics. 1999;1410(2):103–23.
- 134. Thanh Hoa L, Blair D, McManus D. Mitochondrial genomes of parasitic flatworms. Trends in parasitology. 2002;18(5):206–13.
- 135. Jiang P, Li H, Song F, Cai Y, Wang J, Liu J, *et al.* Duplication and Remolding of tRNA Genes in the Mitochondrial Genome of Reduvius tenebrosus (Hemiptera: Reduviidae). Int J Mol Sci. 2016;17(6):951.
- 136. Betts MJ, Russell RB. Amino Acid Properties and Consequences of Substitutions. Bioinformatics for Geneticists 2003. p. 289–316.
- 137. Garner KJ, Ryder OA. Mitochondrial DNA diversity in gorillas. Mol Phylogenet Evol. 1996;6(1):39–48.
- 138. Pena HB, de Souza CP, Simpson AJ, Pena SD. Intracellular promiscuity in *Schistosoma mansoni*: nuclear transcribed DNA sequences are part of a mitochondrial minisatellite region. Proc Natl Acad Sci U S A. 1995;92(3):915–9.
- 139. Le TH, Blair D, Agatsuma T, Humair PF, Campbell NJH, Iwagami M, *et al.* Phylogenies Inferred from Mitochondrial Gene Orders—A Cautionary Tale from the Parasitic Flatworms. Molecular Biology and Evolution. 2000;17(7):1123–5.
- 140. Cechova J, Lysek J, Bartas M, Brazda V. Complex analyses of inverted repeats in mitochondrial genomes revealed their importance and variability. Bioinformatics. 2018;34(7):1081–5.
- 141. Okimoto R, Macfarlane JL, Clary DO, Wolstenholme DR. The mitochondrial genomes of two nematodes, *Caenorhabditis elegans* and *Ascaris suum*. Genetics. 1992;130(3):471–98.

- 142. Kinkar L, Korhonen PK, Cai H, Gauci CG, Lightowlers MW, Saarma U, *et al.* Long-read sequencing reveals a 4.4 kb tandem repeat region in the mitogenome of *Echinococcus granulosus* (sensu stricto) genotype G1. Parasit Vectors. 2019;12(1):238.
- 143. Fattash I, Rooke R, Wong A, Hui C, Luu T, Bhardwaj P, *et al.* Miniature inverted-repeat transposable elements: Discovery, distribution, and activity 1. Genome/National Research Council Canada = Génome/Conseil national de recherches Canada. 2013;56(9):475–86.
- 144. Bikard D, Loot C, Baharoglu Z, Mazel D. Folded DNA in action: hairpin formation and biological functions in prokaryotes. Microbiol Mol Biol Rev. 2010;74(4):570–88.
- 145. Barrett J. Biochemical Constituents. Biochemistry of Parasitic Helminths. London: Macmillan Education UK; 1981. p. 12–71.
- 146. Hacariz O, Sayers G. Fasciola hepatica—where is 28S ribosomal RNA? Experimental parasitology. 2013;135(2):426–9.
- 147. Ewing B, Hillier L, Wendl MC, Green P. Base-calling of automated sequencer traces using phred. I. Accuracy assessment. Genome research. 1998;8(3): 175–85.
- 148. Ewing B, Green P. Base-calling of automated sequencer traces using phred. II. Error probabilities. Genome research. 1998;8(3):186–94.
- 149. Cardinali G, Corte L, Robert V. Next Generation Sequencing: problems and opportunities for next generation studies of microbial communities in food and food industry. Current Opinion in Food Science. 2017;17(1):62–7.
- 150. Jain M, Olsen HE, Paten B, Akeson M. The Oxford Nanopore MinION: delivery of nanopore sequencing to the genomics community. Genome biology. 2016;17(1):239.
- Dunaief D, Cwanger A, Dunaief JL. Chapter 63—Iron-Induced Retinal Damage. In: Preedy VR, editor. Handbook of Nutrition, Diet and the Eye. San Diego: Academic Press; 2014. p. 619–26.
- Jones MK, McManus DP, Sivadorai P, Glanfield A, Moertel L, Belli SI, *et al.* Tracking the fate of iron in early development of human blood flukes. Int J Biochem Cell Biol. 2007;39(9):1646–58.

- Dissous C, Khayath N, Vicogne J, Capron M. Growth factor receptors in helminth parasites: Signalling and host–parasite relationships. FEBS Letters. 2006;580(12):2968–75.
- 154. Spiliotis M, Brehm K. *Echinococcus multilocularis*: identification and molecular characterization of a Ral-like small GTP-binding protein. Experimental parasitology. 2004;107(3):163–72.
- 155. Kanehisa M, Goto S. KEGG: kyoto encyclopedia of genes and genomes. Nucleic acids research. 2000;28(1):27–30.
- 156. Lightowlers MW, Rickard MD. Excretory-secretory products of helminth parasites: effects on host immune responses. Parasitology. 1988;96(Suppl):S123–66.
- 157. Harnett W. Secretory products of helminth parasites as immunomodulators. Molecular and biochemical parasitology. 2014;195(2):130–6.
- 158. Almeida GT, Amaral MS, Beckedorff FC, Kitajima JP, DeMarco R, Verjovski-Almeida S. Exploring the *Schistosoma mansoni* adult male transcriptome using RNA-seq. Experimental parasitology. 2012;132(1):22–31.
- 159. Garg G, Bernal D, Trelis M, Forment J, Ortiz J, Valero ML, *et al.* The transcriptome of *Echinostoma caproni* adults: further characterization of the secretome and identification of new potential drug targets. Journal of proteomics. 2013;89(1): 202–14.
- 160. Sun J, Wang SW, Li C, Hu W, Ren YJ, Wang JQ. Transcriptome profilings of female *Schistosoma japonicum* reveal significant differential expression of genes after pairing. Parasitology research. 2014;113(3):881–92.
- 161. Mason C, Stevenson H, Cox A, Dick I, Rodger C. Disease associated with immature paramphistome infection in sheep. The Veterinary record. 2012;170(13):343–4.
- 162. Sajid M, McKerrow JH. Cysteine proteases of parasitic organisms. Molecular and biochemical parasitology. 2002;120(1):1–21.
- Robinson MW, Dalton JP, Donnelly S. Helminth pathogen cathepsin proteases: it's a family affair. Trends in biochemical sciences. 2008;33(12):601–8.
- 164. Kasny M, Mikes L, Hampl V, Dvorak J, Caffrey CR, Dalton JP, *et al.* Chapter 4. Peptidases of trematodes. Advances in parasitology. 2009;69(1):205–97.
- Dixit AK, Dixit P, Sharma R. Cysteine Proteases of Parasitic Helminths. 2017. p. 657–71.

- 166. Caffrey CR, Goupil L, Rebello KM, Dalton JP, Smith D. Cysteine proteases as digestive enzymes in parasitic helminths. PLoS neglected tropical diseases. 2018;12(8):e0005840.
- Meemon K, Grams R, Vichasri-Grams S, Hofmann A, Korge G, Viyanant V, *et al.* Molecular cloning and analysis of stage and tissue-specific expression of cathepsin B encoding genes from *Fasciola gigantica*. Molecular and biochemical parasitology. 2004;136(1):1–10.
- 168. Liu Y. Bioinformatics: The Impact of Accurate Quantification on Proteomic and Genetic Analysis and Research: Apple Academic Press; 2014.
- Huang Y, Chen W, Wang X, Liu H, Chen Y, Guo L, *et al.* The carcinogenic liver fluke, *Clonorchis sinensis*: new assembly, reannotation and analysis of the genome and characterization of tissue transcriptomes. PloS one. 2013;8(1):e54732.
- 170. Kuntz AN, Davioud-Charvet E, Sayed AA, Califf LL, Dessolin J, Arner ES, *et al.* Thioredoxin glutathione reductase from *Schistosoma mansoni*: an essential parasite enzyme and a key drug target. PLoS medicine. 2007;4(6):e206.
- 171. Ross F, Hernandez P, Porcal W, Lopez GV, Cerecetto H, Gonzalez M, *et al.* Identification of thioredoxin glutathione reductase inhibitors that kill cestode and trematode parasites. PloS one. 2012;7(4):e35033.
- 172. Otero L, Bonilla M, Protasio AV, Fernández C, Gladyshev VN, Salinas G. Thioredoxin and glutathione systems differ in parasitic and free-living platyhelminths. BMC genomics. 2010;11(1):237.
- 173. Carson J, Thomas CM, McGinty A, Takata G, Timson DJ. The tegumental allergen-like proteins of *Schistosoma mansoni*: A biochemical study of SmTAL4-TAL13. Molecular and biochemical parasitology. 2018;221(1):14–22.
- Thang Z, Xu H, Gan W, Zeng S, Hu X. *Schistosoma japonicum* calciumbinding tegumental protein SjTP22.4 immunization confers praziquantel schistosomulumicide and antifecundity effect in mice. Vaccine. 2012;30(34):5141–50.
- 175. Vichasri-Grams S, Subpipattana P, Sobhon P, Viyanant V, Grams R. An analysis of the calcium-binding protein 1 of *Fasciola gigantica* with a comparison to its homologs in the phylum Platyhelminthes. Molecular and biochemical parasitology. 2006;146(1):10–23.

- 176. Emmanoch P, Kosa N, Vichasri-Grams S, Tesana S, Grams R, Geadkaew-Krenc A. Comparative Characterization of Four Calcium-Binding EF Hand Proteins from *Opisthorchis viverrini*. Korean J Parasitol. 2018;56(1):81–6.
- 177. Thomas CM, Timson DJ. A mysterious family of calcium-binding proteins from parasitic worms. Biochemical Society transactions. 2016;44(4):1005–10.
- 178. Thomas CM, Timson DJ. Characterization of Calcium-Binding Proteins from Parasitic Worms. Methods in molecular biology (Clifton, NJ). 2019;1929(1): 615–41.
- 179. Smooker PM, Jayaraj R, Pike RN, Spithill TW. Cathepsin B proteases of flukes: the key to facilitating parasite control? Trends in parasitology. 2010;26(10): 506–14.



#### **APPENDIX A**

#### REAGENT PREPARATIONS

#### 1. General reagents

#### 1.1 10 mM Phosphate Buffered Saline (PBS), pH 7.2

Na <sub>2</sub> HPO <sub>4</sub>	1.44	g
KH <sub>2</sub> PO <sub>4</sub>	0.24	g
NaCl	8.00	g
KCl	0.20	g
Distilled water	to 1	L

All components were dissolved in the indicated volume of water, the pH was adjusted to 7.2, the buffer was autoclaved and stored at room temperature.

#### 1.2 0.85% [w/v] NaCl

NaCl	8.5	g
Distilled water	to 1	L

The NaCl was dissolved in the indicated volume of water. The solution was autoclaved and stored at room temperature.

#### 1.3 5.0 M NaCl stock solution

NaCl	29.2	g
Distilled water	to 100	mL

The NaCl was dissolved in the indicated volume of water. The solution was autoclaved and stored at room temperature.

#### 1.4 3.0 N NaOH

NaOH	12.0	g
Distilled water	to 100	mL

The NaOH was dissolved in the indicated volume of water. The solution was autoclaved and stored at room temperature.

#### 1.5 Diethylpyrocarbonate (DEPC) treated water

1 ml of DEPC solution was mixed with 1 L of distilled water by shaking for 2–3 minutes. The uncapped bottle was placed in a fume hood for overnight. The solution was autoclaved and stored at room temperature.

#### 1.6 60% [v/v] Glycerol

Glycerol 60 mL Distilled water to 100 mL

The mixed solution was autoclaved and stored at room temperature.

#### 1.7 3.0 M NaOAc, pH 5.5

 $C_2H_3NaO_2$  24.6 g DEPC-treated water to 100 mL

The  $C_2H_3NaO_2$  was dissolved in the indicated volume of DEPC-treated water and the pH was adjusted to 5.5 by adding glacial acetic acid. The solution was sterile by 0.22  $\mu$ m filter filtration and stored at room temperature.

#### 1.8 5.0 M KOAc

Potassium acetate 49.1 g

Distilled water to 100 mL

The solution was stored at room temperature.

#### 1.9 2.0 M Tris-HCl stock solution

Tris-HCl 24.23 g
Distilled water to 100 mL

Tris-HCl was dissolved in the indicated volume of distilled water and adjusted to pH 6.8, 7.2, 8.0 and 9.5 by using HCl according to be prepared reagents. The solution was autoclaved and stored at room temperature.

#### 1.10 0.5 M EDTA, pH 8.0 stock solution

EDTA·Na<sub>2</sub>· H<sub>2</sub>O 18.6 g Distilled water to 100 mL

EDTA was dissolved in in the indicated volume of distilled water and the pH was adjusted to 8.0 by using NaOH. The solution was autoclaved and stored at room temperature.

#### 1.11 1.0 M MgCl<sub>2</sub> stock solution

MgCl<sub>2</sub> (anhydrous) 9.5 g

Distilled water to 100 mL

The solution was sterile by filtration through a 0.22  $\mu m$  filter and stored at room temperature.

#### 1.12 1.0 M CaCl<sub>2</sub> stock solution

CaCl<sub>2</sub> (anhydrous) 11.0 g

Distilled water to 100 mL

The solution was sterile by filtration through a 0.22  $\mu m$  filter and stored at room temperature.

#### 2. Antibiotics stock solutions

#### 2.1 Ampicillin stock solution (100 mg/ml)

An amount of 1.0 g of ampicillin was dissolved in 10 mL of distilled water. The solution was sterile by 0.22  $\mu m$  filter filtration. The stock solution was aliquoted into 1 mL per microcentrifuge tube and stored at  $-20^{\circ}C$ .

#### 2.2 Tetracycline stock solution (12.5 mg/ml)

An amount of 125.0 mg of tetracycline hydrochloride was dissolved in 10 ml distilled water. The solution was sterile by 0.22  $\mu$ m filter filtration. The stock solution was aliquoted into 1 mL per microcentrifuge tube and stored at  $-20^{\circ}$ C.

#### 3. Morphology and histology staining reagents

#### 3.1 Alcohol-formalin acetic acid (AFA) fixative

Formalin 60 mL 95% Ethanol 500 mL Glacial acetic acid 40 mL Distilled water 400 mL

The components were mixed and stored at room temperature.

#### 3.2 Semichon's carmine staining

Semichon's carmine powder	1.5	mg
Glacial acetic acid	100	mL
Distilled water	100	mL

The components were mixed and heated in a boiling water bath for 15 minutes. The cooled down stock solution was filtered by filter paper and stored at room temperature. The working staining solution was prepared by mixing with an equal volume of 70% [v/v] ethanol.

#### 3.3 Serial-ethanol solution

Absolute ethanol 70, 80, 90, 95 mL was mixed with distilled water to a final volume of 100 mL to obtain 70%, 80%, 90%, 95% [v/v] serial-ethanol solutions.

#### 3.4 Gelatin coating solution

Gelatin	1.50	g
Chromium potassium sulfate	0.25	g
Distilled water	to 500	mL

The components were added to the indicated volume of distilled water and then completely dissolved by heating at 60°C. The solution was stored at room temperature.

#### 4. Genomic DNA extraction reagents

## 4.1 Homogenization buffer (30 mM Tris-HCl, pH 8.0, 0.1 mM NaCl, 10 mM EDTA and 0.5% Triton X-100)

2.0 M Tris-HCl pH 8.0	1.5	mL
5.0 M NaCl	2.0	mL
0.5 M EDTA pH 8.0	2.0	mL
Distilled water	to 100	mL

The components were dissolved in the indicated volume of distilled water. An amount of 0.5 ml of Triton X-100 was added, the solution was carefully mixed and stored at room temperature.

### 4.2 Extraction buffer (0.1 M Tris-HCl, pH 8.0, 0.1 mM NaCl, 20 mM EDTA)

 2.0 M Tris-HCl pH 8.0
 5
 mL

 5.0 M NaCl
 2
 mL

 0.5 M EDTA, pH 8.0
 4
 mL

 Distilled water
 to 100
 mL

All components were dissolved in the indicated volume of distilled water and the solution was stored at room temperature.

#### 5. Mitochondrial DNA extracts reagents

#### 5.1 Mitochondria isolation medium

250 mM Sucrose

10 mM Tris-HCl. pH 7.4

2 mM EDTA

0.5% BSA

All components were mixed in sterile distilled water. The mixed solution was sterile by 0.22  $\mu m$  filter filtration and stored at 4°C.

#### 5.2 Mitochondrial lysis buffer

150 mM NaCl

10 mM Tris-HCl, pH 8.0

50 mM EDTA

All components were mixed in sterile distilled water. The mixed solution was autoclaved and stored at  $4^{\circ}$ C.

#### 5.3 KOAc/acetic acid (5 M acetate, 3 M potassium)

5.0 M KOAc 240 mL Glacial acetic acid 46 mL Distilled water 114 mL

All components were mixed in sterile distilled water. The mixed solution was sterile by 0.22  $\mu m$  filter filtration and stored at  $4^{\circ}C.$ 

#### 6. Crude worm extraction reagents

## 6.1 Lysis buffer (10 mM Tris-HCl, pH 7.2, 150 mM NaCl, 0.5% [v/v] Triton X-100, 1 mM PMSF, and 1 mM EDTA)

2.0 M Tris-HCl, pH 7.2	0.5	mL
Triton-X 100	1.0	mL
5.0 M NaCl	3.0	mL
0.5 M EDTA	0.1	mL
PMSF	0.17	mg
Distilled water	to 100	mL

All components were dissolved in the indicated volume of distilled water. The solution was stored at room temperature.

#### 6.2 0.1 M Sodium acetate

Sodium acetate 0.82 g

Distilled water to 100 mL

The pH of the solution was adjusted to 5.0 by using glacial acetic acid. The solution was autoclaved and stored at room temperature.

#### 6.3 Soluble crude worm extraction buffer

10 mM PBS pH 7.2

150 mM NaCl

1 mM EDTA

1 mM PMSF

0.5% [v/v] Triton X-100

The first three components were mixed in sterile distilled water. PMSF and Triton X-100 were added before use.

#### 7. Media for *E. coli* bacterial culture

#### 7.1 Luria Bertani (LB) Broth

Bacto peptone	10	g
Bacto yeast extract	5	g
NaCl	5	g
Distilled water	to 1000	mL

All components were dissolved in the indicated volume of distilled water. The solution was autoclaved and stored at room temperature.

#### 7.2 Luria Bertani (LB) agar plates

Bacto peptone	10	g
Bacto yeast extract	5	g
NaCl	5	g
Agar	15	g
Distilled water	to 1000	mL

All components were dissolved in the indicated volume of distilled water. The solution was autoclaved, the medium was allowed to cool down to  $60^{\circ}$ C and then poured into petri dishes. The hardened agar plates were stored at  $4^{\circ}$ C.

#### 7.3 LB/Tetracycline agar plates

Bacto peptone	10	g
Bacto yeast extract	5	g
NaCl	5	g
Agar	15	g
Distilled water	to 100	00 mL

All components were dissolved in the indicated volume of distilled water. The solution was autoclaved and the medium was allowed to cool down to  $60^{\circ}$ C before tetracycline stock solution was added to a final concentration of 12.5  $\mu$ g/mL. The medium was poured into petri dishes. The hardened agar plates were stored protected from light at  $4^{\circ}$ C.

#### 7.4 LB/Ampicillin agar plates

Bacto peptone	10	g
Bacto yeast extract	5	g
NaCl	5	g
Agar	15	g
Distilled water	to 100	00 mL

All components were dissolved in the indicated volume of distilled water. The solution was autoclaved and the medium was allowed to cool down to  $60^{\circ}$ C before ampicillin stock solution was added to a final concentration of  $100 \, \mu g/mL$ . The medium was poured into petri dishes. The hardened agar plates were stored at  $4^{\circ}$ C.

#### 8. Competent cell preparation and transformation reagents

#### 8.1 0.1 M MgCl<sub>2</sub>

 $\begin{array}{cccc} 1.0 \text{ M MgCl}_2 & 10 & \text{mL} \\ \text{Distilled water} & \text{to } 100 & \text{mL} \end{array}$ 

The freshly prepared solution was kept on ice.

#### 8.2 0.1 M CaCl<sub>2</sub>

 $\begin{array}{cccc} 1.0 \text{ M CaCl}_2 & & 10 & \text{mL} \\ \text{Distilled water} & & \text{to } 100 & \text{mL} \end{array}$ 

The freshly prepared solution was kept on ice.

#### **8.3** 100% Glycerol

Glycerol 100 mL

The solution was autoclaved and stored at room temperature.

#### 9. Agarose gel electrophoresis reagents

#### 9.1 10× DNA/RNA agarose gel loading buffer

50% [v/v] Glycerol

0.25% [w/v] Bromophenol blue

0.25% [w/v] Xylene cyanol FF

All components were mixed in sterile distilled water (DEPC-treated water in case of RNA loading buffer), aliquoted into 1.5 mL microcentrifuge tubes and stored at 4°C.

#### 9.2 5× Tris-Boric EDTA (TBE) stock buffer

Distilled water	to 1000	mL
EDTA·Na <sub>2</sub> · H <sub>2</sub> O	4.56	g
Boric acid	27.5	g
Tris-base	52.0	g

The pH of the solution was adjusted to 8.0 by using HCl and the solution was stored at room temperature.

#### 9.3 0.5× Tris-Boric EDTA (TBE) running buffer

 $5\times$  TBE stock buffer was 1:10 diluted with distilled water and stored at room temperature.

### 10. Sodium Dodecyl Sulfate Polyacrylamide Gel Electrophoresis (SDS-PAGE) reagents

#### 10.1 10% [w/v] Ammonium persulfate

 $10\,\mathrm{g}$  of ammonium persulfate was dissolved in a total volume of  $100\,\mathrm{mL}$  sterile ultrapure water, aliquoted into  $1.5\,\mathrm{ml}$  microcentrifuge tubes and stored at  $-20\,\mathrm{^{\circ}C}$ .

#### 10.2 20% [w/v] SDS

 $20~{\rm g}$  of SDS was dissolved in a total volume of  $100~{\rm mL}$  sterile ultrapure water and stored at room temperature.

#### 10.3 Preparation of acrylamide gel

	Separating gel		Stacking gel	
	12.5%	16%	4%	
30% Acrylamide stock	3.13	4.00	0.33	mL
1.5 M Tris-HCl, pH 8.8	1.88	1.88	-	mL
0.5 M Tris-HCl, pH 6.8	-	-	0.63	mL
Ultrapure water	2.38	1.51	1.50	mL
10% SDS	0.08	0.08	0.03	mL
10% Ammonium persulfate	37.50	37.50	12.50	μL
TEMED	2.50	2.50	1.25	μL

## 10.4 2× Sample buffer (125 mM Tris-HCl, pH 6.8, 4% SDS, 20% [v/v] glycerol, 0.2 M DTT and 0.02% bromophenol blue)

 1.0 M Tris-HCl, pH 6.8
 1.25
 mL

 20% SDS
 2.00
 mL

 Glycerol
 2.00
 mL

 DTT
 0.30
 g

 1% Bromophenol blue
 0.20
 mL

All components were mixed in a final volume of 10 mL sterile ultrapure water, aliquoted into 1.5 mL microcentrifuge tubes and stored at -20°C.

## 10.5 Electrophoresis buffer (0.1 M Tris, 0.1 M Tricine, and 0.1% [w/v] SDS)

Tris-base	3.03	g
Glycine	15.20	g
SDS	1.00	g
Ultrapure water	to 1000	mL

The solution was stored at 4°C.

#### 10.6 0.008% Coomassie Blue G-250

Coomassie Blue G-250 0.08 g 1 M HCl 70 mL Distilled water to 1 L

Coomassie Blue G-250 was mixed with water until homogeneous and filtered through Whatman filter paper. Then the HCl was added.

#### 11. Enzyme linked-immunosorbent assay (ELISA) reagents

#### 11.1 Antibody diluents (0.25% [w/v] BSA in 10 mM PBS pH 7.2)

25~mg of BSA was dissolved in 10 mL of 10 mM PBS pH 7.2 and stored at  $4^{\circ}\text{C}.$ 

#### 11.2 Blocking solution (0.25% [w/v] BSA in coating buffer, pH 9.6)

50~mg of BSA was dissolved in 20 mL of carbonate coating buffer and stored at  $4^{\circ}\text{C}.$ 

#### 11.3 Carbonate coating buffer

30 mM Na<sub>2</sub>CO<sub>3</sub>

75 mM NaHCO<sub>3</sub>

All components were dissolved in ultrapure water and adjusted to pH 9.6. The solution was autoclaved and stored at 4°C.

#### 11.4 Washing buffer

10 mM PBS pH 7.2 999.5 mL

Tween<sup>®</sup> 20 0.5 mL

The solution was freshly prepared.

#### 12. Western blot analysis reagents

#### 12.1 Antibody diluent (1% skim milk in TBS)

 $100~\rm mg$  of skim milk was dissolved in 10 ml TBS, pH 7.5. The solution was stirred until homogenous and stored at  $4^{\circ}C.$ 

#### 12.2 Blocking solution (5% skim milk in TBS)

500 mg of skim milk was dissolved in 10 ml TBS, pH 7.5. The solution was stirred until homogenous and stored at 4°C.

#### 12.3 Detection buffer, pH 9.5

0.1 M Tris-HCl

0.1 M NaCl

50 mM MgCl<sub>2</sub>

All components were dissolved in sterile ultrapure water, the pH was adjusted to 9.5 by using NaOH and the solution was stored at room temperature.

#### 12.4 Ponceau S dye solution

0.1% [w/v] Ponceau S dye

5% [v/v] Acetic acid

Ponceau S dye was dissolved in sterile distilled water. Then glacial acetic acid was added and the solution was stored at room temperature.

#### 12.5 Semi-dry transfer buffer

50 mM Tris-base

40 mM Glycine

0.04% [w/v] SDS

20% [v/v] Methanol

The first three components were dissolved in sterile ultrapure water.

Then methanol was added and the buffer was stored at 4°C in a tight container.

#### 12.6 Washing buffer

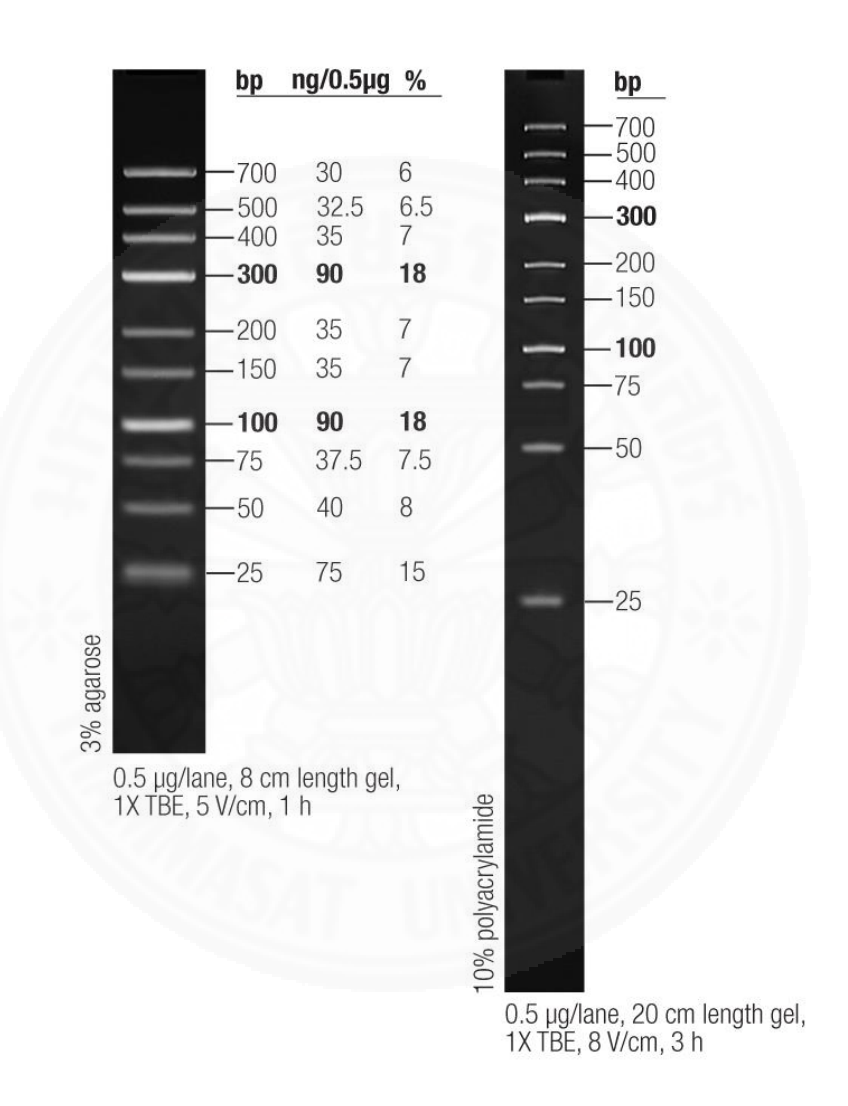
10 mM PBS pH 7.2 999.5 mL

Tween® 20 0.5 mL

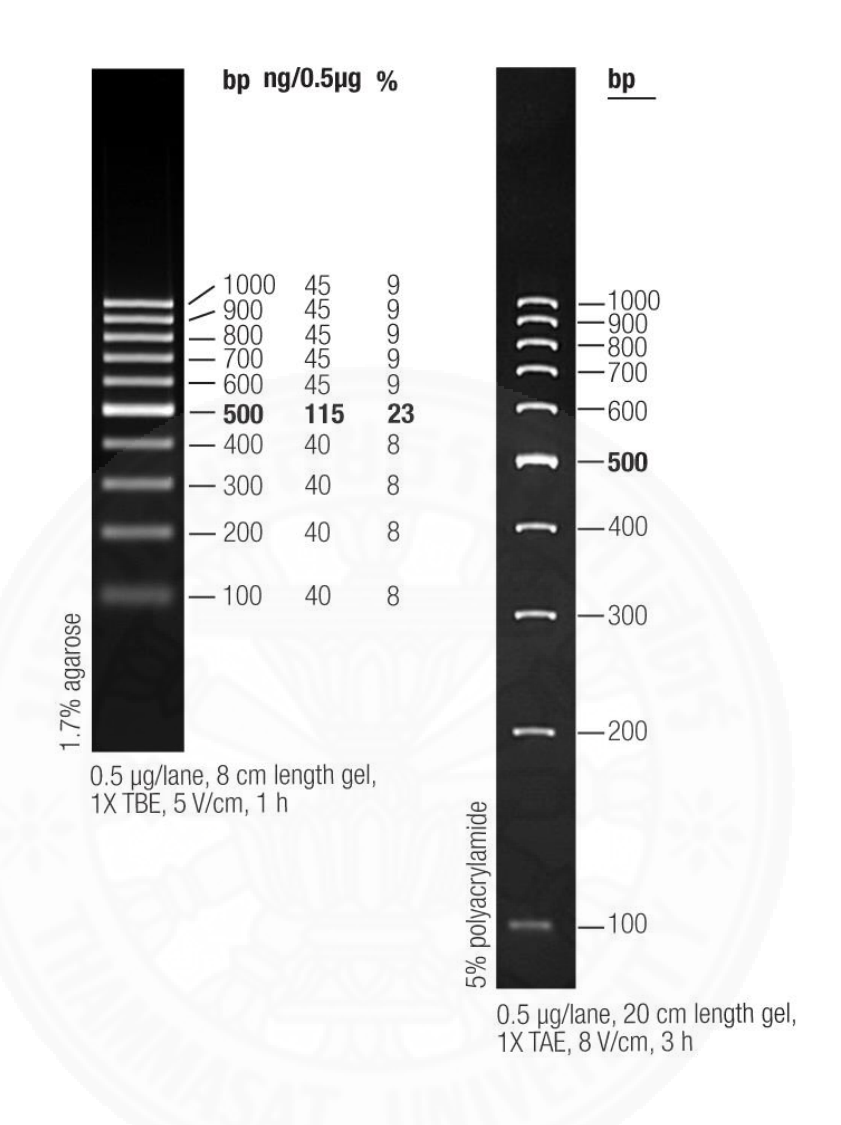
The buffer was freshly prepared.

# APPENDIX B DNA AND PROTEIN STANDARD

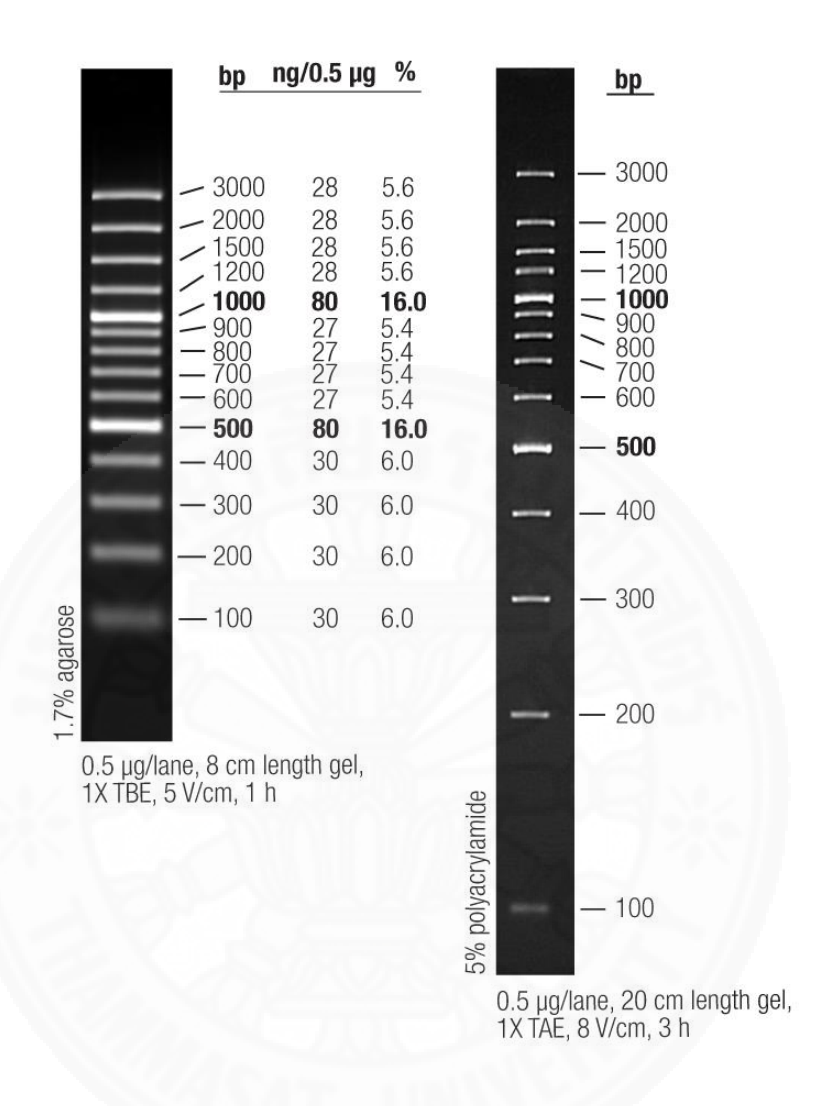
1. GeneRuler<sup>TM</sup> Low Range DNA ladder (Thermo Fisher Scientific, MA, USA)



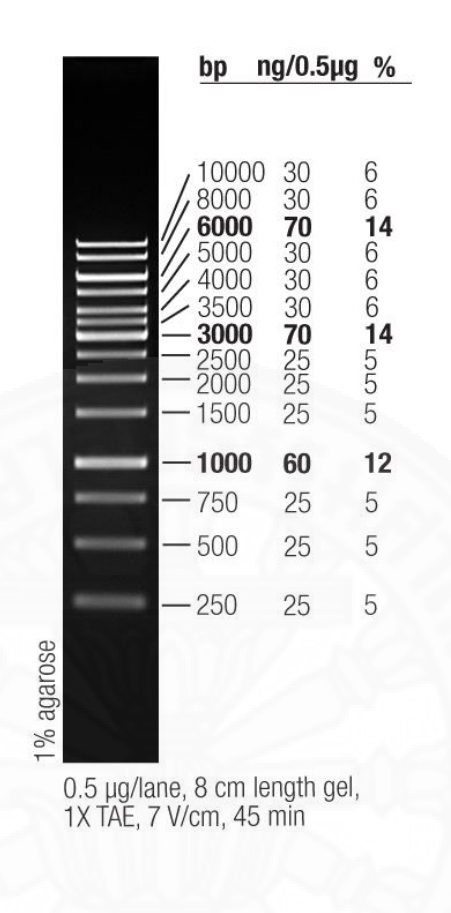
#### 2. GeneRuler<sup>TM</sup> 100 bp DNA ladder (Thermo Fisher Scientific, MA, USA)



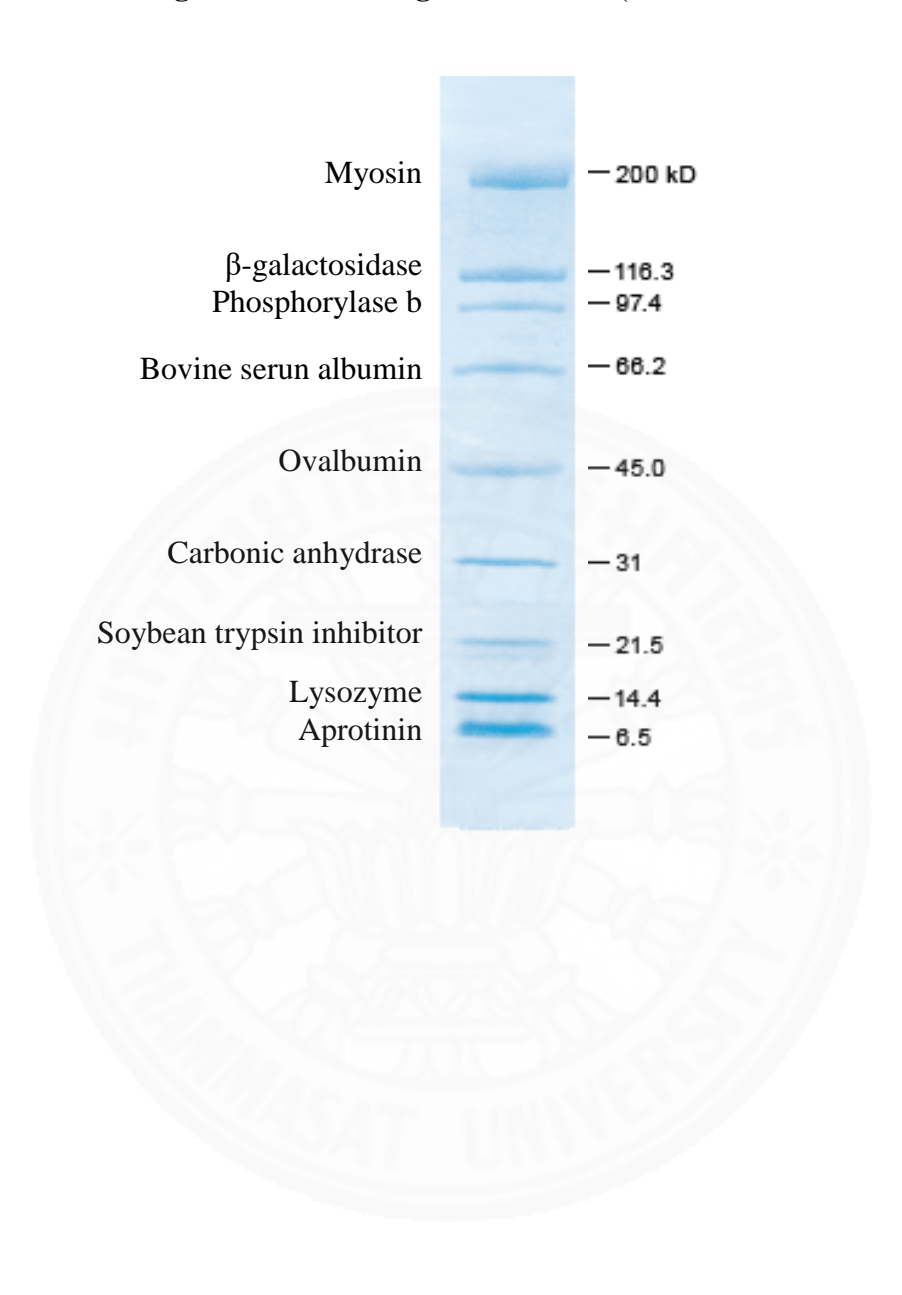
#### 3. GeneRuler<sup>TM</sup> 100 bp Plus DNA ladder (Thermo Fisher Scientific, MA, USA)



### **4. GeneRuler™ 1 kb DNA ladder** (Thermo Fisher Scientific, MA, USA)

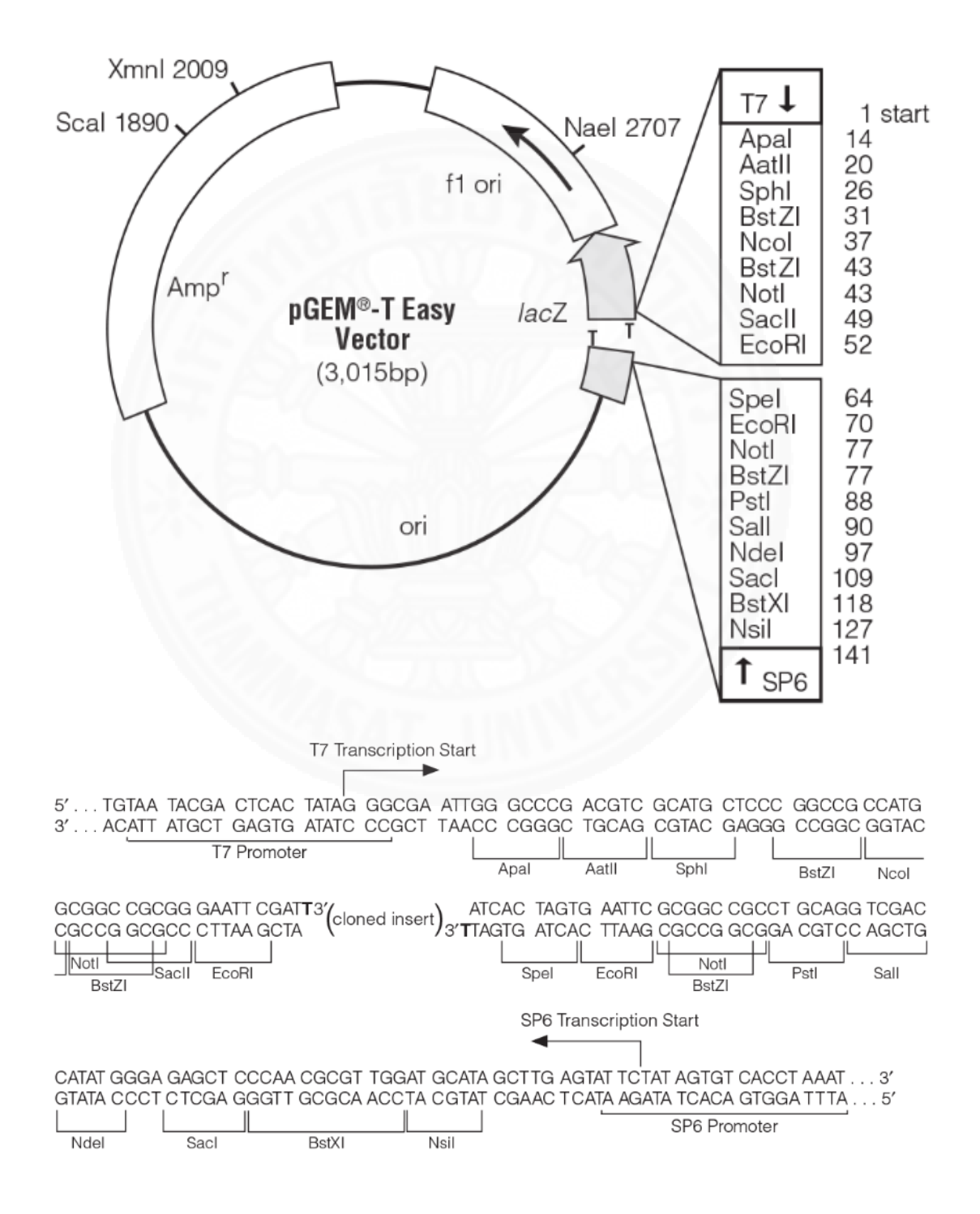


#### 5. Broad Range Molecular Weight Standards (Bio-Rad, Hercules, CA, USA)



### APPENDIX C VECTOR MAP

#### 1. pGEM®-T Easy vector (Promega<sup>TM</sup>, WI, USA)



#### pGEM®-T Easy Vector sequence reference points:

T7 RNA polymerase transcription initiation site 1

Multiple cloning region 10–128

SP6 RNA polymerase promoter (-17 to +3) 139–158

SP6 RNA polymerase transcription initiation site 141

pUC/M13 Reverse Sequencing Primer binding site 176–197

lacZ start codon 180

lac operator 200–216

β-lactamase coding region 1337–2197

Phage f1 region 2380–2835

*lac* operon sequences 2836–2996, 166–395

pUC/M13 Forward Sequencing Primer binding site 2949–2972

T7 RNA polymerase promoter (-17 to +3) 2999-3

# APPENDIX D ANIMAL ETHICAL PERMISSION



#### ANIMAL USE PROTOCOL APPROVAL

Protocol Number 012/2560	
THOUSEN MATTER SEELENAM.	
Animal Protocol Title	
(Thai) การศึกษาทรานสคริปโตมและวิเคราะห์	คุณลักษณะของแอนติเจนในพยาธีใบไม้ใน
กระเพาะอาหารฟิสโชอิเคเรียส อีลองก	าตุส
(English) Transcriptome Profiling and Circu	lating Antigen Characterization of the
Rumen Fluke Fischoederius elon	gatus
Main Project/Proposal Title (If available)	
(Thai) การศึกษาทรานสคริปโตมของพยาธิในไม่	มีในระบบทางเดินอาหารฟิสโชอิเคเรียส อีลองกาตุส
	of the Rumen Fluke Fischoederius elongatus
Dringinal Investigator	
Principal Investigator	(a. ( 4 . (
Name-Surname (Thai) รองศาสตราจา	
Name-Surname (English) Associate Pro	ofessor Dr. Hans Rudi Grams
Location of Animal Housing Laboratory A	nimal Center, Thammasat University
Location of Animal Experiments <u>Laboratory A</u>	nimal Center, Thammasat University
Start Date 9 October 2017 Expi	iration Date 9 October 2018
This Animal Protocol Established under	Ethical Principles and Guidelines for the Use
of Animals, National Research Council of Thail	and and Approved by Animal Care and Use
Committee of Thammasat University.	
5-8	Pramuga Capolum
(Thunyatorn Yimsoo, DVM)	(Prof.Dr. Pramuan Tapchaisri)
Chair of Animal Ethical and Post Approval	Vice Rector for Research
Monitoring Subcommittee	Chair of Animal Care and Use Committee

Thammasat University

Thammasat University

#### **BIOGRAPHY**

Name Miss Pichanee Watthanasiri

**Date of Birth** 29<sup>th</sup> September 1990

Place of Birth Nakornsrithammarat, Thailand

**Educational Attainment** 

2013–Present: Ph.D. candidate in Doctor of Philosophy

(Biomedical Sciences),

Graduate Program in Biomedical Sciences,

Faculty of Allied Health Sciences,

Thammasat University, Thailand

2009–2012: Bachelor of Science (Medical Technology)

with 2<sup>nd</sup> class honor,

Department of Medical Technology,

Faculty of Allied Health Sciences,

Thammasat University, Thailand

**Scholarships** 

2013–Present: The Thailand Research Fund through a Royal Golden Jubilee

Ph.D. Scholarship (PHD/0061/2556)

2019 Teaching Assistant Scholarship (1/2019)

from Thammasat University

Official address Molecular Biology and Parasitology Unit,

Graduate Program in Biomedical Sciences,

Faculty of Allied Health Sciences,

Thammasat University,

99 Moo 18 Paholyothin Road, KlongNueng Klong Luang,

Pathumthani 12120, Thailand

E-mail address pichanee.w@outlook.com

#### Licenses

- 1. License on Medical Technologist from The Medical Technology Council of Thailand (2013–present)
- License on Scientific Use of Animals License from Institute for Animals for Scientific Purpose Development, National Research Council of Thailand (2016– present)

#### **Training attended**

- 1. Student Trainee (Medical Technology) in Medical Technology Laboratory at Thammasat Hospital, Pathumthani, Thailand (December 2012)
- Student Intern (Medical Technology) in Department of Pathology and Laboratory medicine at Rajavithi Hospital, Bangkok, Thailand (January–March 2013)
- 3. Animal Ethics Training, 9<sup>th</sup> June, 2014, Faculty of Allied Health Sciences, Laboratory Animal Center, Thammasat University, Rangsit Campus, Pathumthani, Thailand
- 4. Animal Ethics Training in Ethical Principles and Guidelines for the Use of Animals for Scientific Purposes, 20<sup>th</sup> January 2015, Laboratory Animal Center, Thammasat University, Rangsit Campus, Pathumthani, Thailand
- 5. Animal Ethics Training in Basic Knowledge of Experimental Animals for Scientific Purposes and Management, 9<sup>th</sup> April 2015, Laboratory Animal Center, Thammasat University, Rangsit Campus, Pathumthani, Thailand
- 6. Human Ethics Training, 6<sup>th</sup> July 2015, Faculty of Allied Health Sciences, Thammasat University, Rangsit Campus, Pathumthani, Thailand
- 7. Biosafety Training in Guidelines for Biological Safety (Basic course), 15<sup>th</sup> July 2015, Thammasat University, Rangsit Campus, Pathumthani, Thailand
- Animal Ethics Training in Proposal Writing for the Use of Animals for Scientific Purposes, 20<sup>th</sup> July 2015, Laboratory Animal Center, Thammasat University, Rangsit Campus, Pathumthani, Thailand
- 9. Human Ethics Training in Human Ethics Research Certification, 10<sup>th</sup> November 2015, Thammasat University, Pathumthani, Thailand

#### **Training attended (Cont.)**

- Animal Ethics Training in Criteria for Consideration for the Use of Animals for Scientific Purposes, 30<sup>th</sup> March 2016, Laboratory Animal Center, Thammasat University, Rangsit Campus, Pathumthani, Thailand
- Animal Ethics Training in The Association for Assessment and Accreditation of Laboratory Animal Care International: AAALAC, 27<sup>th</sup>–28<sup>th</sup> April 2016, Laboratory Animal Center, Thammasat University, Rangsit Campus, Pathumthani, Thailand
- 12. Animal Ethics Training for the 15th Scientific Use of Animals License Training, Institute of Animals for Scientific Purpose Development (IAD), 11<sup>th</sup>–12<sup>th</sup> May 2016, Miracle Grand Convention Hotel, Bangkok, Thailand
- 13. Human Ethics Training in Good Clinical Practice: GCP, 28<sup>th</sup>–29<sup>th</sup> July 2016, Faculty of Allied Health Sciences, Thammasat University, Rangsit Campus, Pathumthani, Thailand
- 14. Biosafety Training in Improvment of the Biosecurity Guidelines for Modern Biological Technology, 2<sup>nd</sup> May 2017, Thammasat University, Rangsit Campus, Pathumthani, Thailand
- Training in Real Time PCR for Molecular Research, 14<sup>th</sup> June 2017, Office of Advanced Science and Technology, Thammasat University, Rangsit Campus, Pathumthani, Thailand
- 16. Biosafety Training in Biosafety guidelines for the implementation of Modern Biotechnology (General practice course), 12<sup>th</sup> September 2017, Thammasat University, Rangsit Campus, Pathumthani, Thailand
- 17. Bioinformatics Training in Asian Institute in Statistical Genetics and Genomics (1<sup>st</sup> Asian Workshop), 18<sup>th</sup>–19<sup>th</sup> December 2017, Faculty of Allied Health Sciences, Thammasat University, Rangsit Campus, Pathumthani, Thailand
- Research Student in research entitled Investigation of the transcriptome of the rumen fluke Fischoederius elongatus and related species at School of Science, RMIT University, Bundoora West Campus, Bundoora, Victoria, Australia (October 2019–May 2020)

#### Conferences

- The 1<sup>st</sup> International Allied Health Sciences Conference "Medical Innovation for Health", 4<sup>th</sup>–6<sup>th</sup> November 2014, Rama Gardens Hotel, Bangkok, Thailand
- The 2<sup>nd</sup> Joint Symposium of BK21-PLUS of CUK and Thammasat University, 21<sup>st</sup>–23<sup>rd</sup> January 2015, Thammasat University, Rangsit Campus, Pathumthani, Thailand
- 3. Genomics, Bioinformatics, and System Biology Conference; GBSBC2015. Thailand Lab 2015. 10<sup>th</sup>–11<sup>th</sup> September 2015, Bangkok International Trade & Exhibition Centre, Bangkok, Thailand
- Asian Institute in Statistical Genetics and Genomics Conference (AISGG 2017), 18<sup>th</sup>–19<sup>th</sup> December 2017, Faculty of Allied Health Sciences, Thammasat University, Rangsit Campus, Pathumthani, Thailand
- 5. Innovation Challenges toward Thailand 4.0: Research Inspiration, Connectivity and Transformation (RGJ-Ph.D. Congress 19), 7<sup>th</sup>–9<sup>th</sup> June 2018, Jomtien Palm Beach Hotel & Resort, Pattaya, Thailand
- 6. The 5<sup>th</sup> Joint Symposium of Thammasat University, BK21 PLUS of CUK and National Defense Medical Center "Biomedical Sciences and Biomechanics for Health", 9<sup>th</sup>–10<sup>th</sup> November 2018, Thammasat University, Rangsit Campus, Pathumthani, Thailand
- 7. RMIT University Bioinformatics Symposium, 21<sup>st</sup>–23<sup>rd</sup> October 2019, RMIT University, Melbourne, Victoria, Australia

#### **Publications**

Acharawadee Tanon, Supitcha Pannengpetch, <u>Pichanee Watthanasiri</u>, Kitipong Chuanboon, Pongsakorn Kanokkantrakorn, Jinjuta Pinthong, and Patcharee Isarankura-Na-Ayudhya. Proteomics Technologies as Potential Tools for Investigation of Differentially-expressed Proteins in Standard and Environmental Isolates of *Pseudomonas aeruginosa*. Original Article in Journal of the Medical Technologist Association of Thailand, Vol. 44, No. 3 (2016): 5801–5823.

#### **Oral Presentations**

- 1. <u>Pichanee Watthanasiri</u>. Morphology and Molecular Characterization of Adult *Fischoederius elongatus* (Poirier, 1883). The 7<sup>th</sup> Graduate Research Conference, 12<sup>th</sup> December 2015, Faculty of Allied Health Sciences, Thammasat University, Rangsit Campus, Pathum Thani, Thailand
- 2. <u>Pichanee Watthanasiri</u>. Morphology and Molecular Characterization of Adult *Fischoederius elongatus* (Poirier, 1883). The 9<sup>th</sup> Graduate Research Conference, 17<sup>th</sup>–18<sup>th</sup> December 2016, Faculty of Allied Health Sciences, Thammasat University, Rangsit Campus, Pathum Thani, Thailand

#### **Poster Presentations**

- Pichanee Watthanasiri, Amornrat Geadkaew Krenc, and Rudi Grams. Morphology and Molecular Characterization of Adult *Fischoederius elongatus* (Poirier, 1883). The 5<sup>th</sup> Graduate Research Conference, 13th–14th December 2014, Faculty of Allied Health Sciences, Rangsit Campus, Thammasat University, Thailand
- 2. <u>Pichanee Watthanasiri</u>, Amornrat Geadkaew Krenc, Peter M. Smooker, and Rudi Grams. *Fischoederius elongatus* (Poirier, 1883), transcriptome and mitochondrial genome of a pouched rumen fluke. Innovation Challenges toward Thailand 4.0: Research Inspiration, Connectivity and Transformation (RGJ-Ph.D. Congress 19), 7<sup>th</sup>–9<sup>th</sup> June 2018, Jomtien Palm Beach Hotel & Resort, Pattaya, Thailand
- 3. <u>Pichanee Watthanasiri</u>, Amornrat Geadkaew Krenc, Peter M. Smooker, and Rudi Grams. *Fischoederius elongatus* (Poirier, 1883), transcriptome and mitochondrial genome of a pouched rumen fluke. The 5<sup>th</sup> Joint Symposium of Thammasat University, BK21 PLUS of CUK and National Defense Medical Center "Biomedical Sciences and Biomechanics for Health", 9<sup>th</sup>–10<sup>th</sup> November 2018, Thammasat University, Rangsit Campus, Pathumthani, Thailand